DESIGN, SYNTHESIS, AND ANTIMICROBIAL EVALUATION OF STRUCTURALLY DIVERSE SHORT PEPTIDE BASED MOLECULES

Thesis submitted in fulfillment of the requirements for the degree of

DOCTOR OF PHILOSOPHY
IN
PHARMACEUTICAL SCIENCES

BY

SANDEEP LOHAN
Enrollment No. 116754

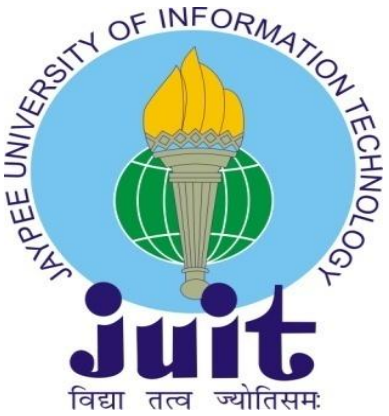

DEPARTMENT OF PHARMACY
JAYPEE UNIVERSITY OF INFORMATION TECHNOLOGY
WAKNAGHAT, SOLAN-173234, HP, INDIA

AUGUST 2015

DECLARATION

I hereby declare that the work contained in the present PhD thesis entitled **"Design, synthesis, and antimicrobial evaluation of structurally diverse short peptide based molecules"** submitted at **Jaypee University of Information Technology, Waknaghat, India,** is an authentic record of my original research work, carried out under the supervision of **Dr. Gopal Singh Bisht**. This work has not been submitted in part or full for the award of any other degree or diploma in any other university/ Institute.

Signature of the Candidate

Sandeep Lohan

Enrolment No.:116754

Department of Pharmacy,

Jaypee University of Information Technology,

Waknaghat, Solan-173234, HP, INDIA

Date:

Place:

CERTIFICATE

This is to certify that the thesis entitled, **"Design, synthesis, and antimicrobial evaluation of structurally diverse short peptide based molecules"** submitted by **Sandeep Lohan** to the **Jaypee University of Information Technology, Waknaghat, India** for the award of degree of **Doctor of Philosophy in Pharmaceutical sciences** is a record of the candidate's own work, carried out by him under our supervision. This work has not been submitted in part or full to any other University or Institute for the award of this or any other degree or diploma.

Supervisor

Dr. Gopal Singh Bisht

Assistant Professor

Department of Pharmacy

Jaypee University of Information Technology

Waknaghat, Solan-173234, HP, INDIA

Email: bishtchem2005@gmail.com

Acknowledgements

With high regards and profound respect, first and foremost, I wish to express my deep sense of gratitude and indebtedness to my supervisor Dr. Gopal Singh Bisht who has been so generous with his time and advice throughout my PhD. I am indebted to him for giving me the opportunity to work on such an excellent project. It has been absorbing from start to finish and I have been blessed to learn from a dedicated and enthusiastic chemist with such an excellent knowledge of organic and peptide chemistry. His encouraging support, endeavour inspiration, perseverance and suggestion constantly motivated me to put everything to achieve the target without being disappointed by failure. I will always cherish my association with him.

I would like to express my sincere gratitude to Jaypee University of Information Technology (JUIT) for giving me the opportunity to do my doctoral study in such a wonderful place. I acknowledge the Department of Science and Technology (DST), New Delhi, India for providing funds to carry out this research work.

I take pleasure to express my sincere thanks to Dr. S.K. Kak (Vice Chancellor, JUIT), Dr. Y. Medury (Ex COO, Jaypee education system), Brigadier (Retd.) Balbir Singh (Director, JUIT), Dr. T.S. Lamba (Dean Academics, JUIT) and Dr. R.S. Chauhan (HOD of BT, BI & Pharmacy) for their helping hands and providing me with necessary facilities to carry out my research work. I extend my gratitude to Dr. Chanderdeep Tondon, Dr. Simran Tondon, and Dr. Manu Sharma and all the faculty members of the Department of Pharmacy and BT & BI for their helping attitudes and backing me with moral support.

It is with great pleasure and profound sense of reverence that I express my gratitude and thanks to Dr. Neeraj Mahindroo (Professor-cum-dean, Shoolini University, Solan, India) for giving me superb guidance, positive attitude, sustained encouragement when I got stuck.

It is my profound privilege to express my heartfelt gratitude to Dr. Sidhartha Sankar Kar and Dr. Jitender Monga, who always showed concern and helped whenever required. I affectionately acknowledge the moral support received from my colleague Mr. Varun Gupta, who has always helped me in numerous ways. The time spent with him will be cherished throughout my life. I cannot forget the assistance of my juniors in particular Arnish Kalanta. I wish them all success for their future endeavors.

I would also like to thank Technical staff Mr. Baleshwar, Mr. Ravikant, Mrs. Somlata Sharma, Mrs. Mamta, Mr. Ismile, and Mr. Kamlesh for helping me to carry out my research work.

Finally, I want to express my deepest love to my parents and brother. Even though, I was staying far away from them, I used to stumble upon them during my tough time to get encouragement and moral support. I would like to acknowledge Saras Jyoti for her unconditional support. Success is something which you will share with someone who is closest to your heart. My family has been my strength and without them I would not be where I am now.

Above all, I offer my humble obeisance to the Almighty, who provided me endurance and eventually rewarded me with the successful completion of my work.

Sandeep Lohan

TABLE OF CONTENTS

LIST OF TABLES

LIST OF FIGURES

Abbreviations

aq.	aqueous
Boc	tert-butoxycarbonyl
BSA	bovine serum albumin
CFU	Colony forming unit
d	doublet
EDTA	Ethylenediaminetetraacetic acid
eq.	equivalent
EtOH	ethanol
Fmoc-Cl	9-Fluorenylmethoxycarbonyl chloride
h	hour
HMDS	Hexamethyldisilazane
HPLC	High-performance liquid chromatography
hRBCs	Human red blood cells
J	coupling constant (NMR)
LDH	Lactate dehydrogenase
m	Multiplet
MDR	Multi-drug resistant
MHA	Mueller-Hinton agar
MHB	Mueller-Hinton broth
min.	minute
mol	mole
MS	Mass Spectroscopy
MTT	3-(4,5-dimethylthiazol-2-yl)-2,5-diphenyltetrazolium bromide
NMR	Nuclear Magnetic Resonance
PBS	Phosphate buffered saline
PDR	Pen drug resistant
Ph	phenyl
Phe	Phenylalanine
PI	Propidium iodide
RP-HPLC	Reverse phase high performance liquid chromatography
s	singlet

SCAMP	Small cationic antimicrobial peptide
t	triplet
TLC	Thin layer chromatography
TFA	Trifluoro acetic acid
Trp	Tryptophan
tPMPs	Thrombin-induced platelet microbicidal proteins
WHO	World Health Organization

Abstract

The near-explosive increased occurrence in multi-drug resistant pathogens is recognized as a severe threat to public health in nations around the globe. AMPs are being considered as a potential source of novel peptide based antibiotics because of their numerous advantages such as broad-spectrum activity, lower tendency to induce resistance, immunomodulatory response and especially their unique mode of action. In spite of these striking features, AMPs are not ideal drug candidates due to unfavorable pharmacokinetics owing to proteolytic degradation, potential immunogenicity and toxicity. Furthermore, AMPs have high production cost as amino acids are expensive building blocks. This may also severely restrict their commercial production as peptide based antibiotic. To address these problems associated with AMPs the research work described here is aimed to develop novel peptide based biocompatible antimicrobial agents.

We have rationally designed and successfully synthesized a library of short abiotic lipopeptides by varying both cationic charge and hydrophobic content with aim to identify the minimum structural requirements for antimicrobial activity. Most of the synthesized lipopeptides displayed broad activity spectrum against susceptible as well as antibiotic resistant clinical isolates of bacteria and fungi. The most potent lipopeptide (LP16) has MICs in the range of 1.5-6.25 μg/mL against all tested Gram-positive, Gram-negative bacterial strains. Maximum antifungal activity was observed for LP24 with MICs in the range of 1.5-4.5 μg/mL. The hemolytic and MTT assay results revealed the lower cytotoxicity of lipopeptides toward mammalian cells. By systematic analysis of the activity results of lipopeptides, we found that three ornithine residues conjugated with myristic acid is minimum requirement for a compound to be an antimicrobial agent. Results of calcein dye leakage experiments suggests the membranolytic effect of lipopeptides, which was further confirmed by visualizing bacterial damage via electron microscopy tool (SEM and TEM). Moreover, stability in human blood plasma and no sign of resistance development against clinical isolates of *Escherichia coli* and *Staphylococcus aureus* were observed for lead lipopeptides. These results demonstrate the potential of short lipopeptides as a novel class of anti-infectives.

In addition, with an objective to probe essential properties of natural antimicrobial peptides (AMPs) in a small structural framework, we carried out the synthesis of small cationic peptidomimetics by incorporating 3-amino benzoic acid (3-ABA) as peptidomimetic element. The new design approach resulted into improvement of activity and selectivity as

compared to linear peptides and allowed us to better understand the influence of structural amphipathicity on biological activity. Lead peptidomimetics (**4g** and **4l**) displayed antibacterial activities against resistant pathogens (MRSA and MRSE). A calcein dye leakage experiment revealed a membranolytic effect of **4g** and **4l** which was further confirmed by fluorescence microscopy. In addition, proteolytic stability and no sign of resistance development against *Staphylococcus aureus* and MRSA demonstrate their potential for further development as novel antimicrobial therapeutics.

CHAPTER 1.
INTRODUCTION

Ever since the discovery of antibiotics, they have been our most reliable weapons in fighting off numerous pathogens that cause potentially fatal infections. In the last few decade resistance development is an unavoidable consequence associated with the use of conventionally available antibiotics. In fact, quite soon after the introduction of antimicrobial drugs, bacteria began to exhibit an accelerated evolution towards resistant strains and the ability to transfer resistance mechanism amongst species [1,2]. In this way, the therapeutic potential of most of the available antibiotics is rather compromised. Moreover, the problem is complicated by the nonappropriate and intensive use of the antibiotics, the increase of immunosuppressed individuals and the spreading of resistant strains by transcontinental travels in modern society [3].

Earlier, infections caused by multi-drug resistant bacterial strains were mostly limited to the nosocomial environment but community acquired resistant strains are now rising in prevalence [4]. Notably, methicillin-resistant *S. aureus* (MRSA) appears to have reached its high point of resistance and has become increasingly difficult to treat in an impressively short time [5]. It is estimated to cause ~19,000 deaths per year in the United States. Apart from their high mortality rate, MRSA infections lead to an estimated $3 billion to $4 billion of additional health care costs per year [6]. In addition, the infections caused by MDR and PDR Gram-negative bacteria are recognized as a severe menace to public health in nations around the globe [7]. The strains of *Acinetobacter baumannii*, *Escherichia coli*, *Klebsiella pneumoniae*, and *Pseudomonas aeruginosa* are found to be resistant to most of the antibiotic currently on the market [8]. In particular, *E. coli* garner increasing attention due to their rapid spread of resistance, leaving limited empirical treatment options [9]. Recently, plasmid associated New Delhi metallo-β-lactamase 1 (NDM-1) gene was identified in Gram-negative bacteria, which may be easily transferred to other bacteria through horizontal gene transfer that confers resistance to a number of antimicrobial drugs, such as fluoroquinolones, aminoglycosides, carbapenems and all β-lactams [10].

The phenomenon of resistance is also extended to other kinds of pathogens; fungi, viruses, and parasites. In the past few years, there has been a remarkable increase in the rate of fatal infections caused by opportunistic fungal strains [11]. Systemic fungal infections spread

primarily among the people who are having impaired immune systems resulting from AIDS [12], cancer chemotherapy [13] and organ transplantation [14]. The fungal cells are eukaryotic in nature [15], which further potentiates the difficulties associated with the development of selective antifungal therapeutics. At present, the available antifungal therapies include polyenes and azoles acting through fungal membrane disruption and inhibit biosynthesis of sterol, respectively [16]. However, the high toxicity of polyenes and the development of resistance against azole [17] have intensified the search of new potential antifungal agents with different modes of action.

Simultaneous marked decline in the development of novel anti-infective agents is one of the greatest negative aspects of modern medicine [18]. Only a handful of new antimicrobial drugs has entered the clinic during last few decades [19]. At present, only a small number of the major pharmaceutical companies have R&D programs on anti-infective agents, and the low interest has been defended based on simple economics [20]. In addition, development of new anti-infective agents is associated with high risks of inducing bacterial resistance within a few years, as shown by history, or to be restricted for use as a drug of last resort [21,22].

These trends have emphasized to discover new class of antimicrobial agents possessing novel mode of action as well as different cellular targets compared to existing antibiotics in order to decrease the likelihood of development of resistance. It is now widely recognized that the native antimicrobial peptides could play a promising role in the development of novel anti-infective agents because of their broad spectrum activity and minimal propensity for resistance development [23-25].

1.1. Antimicrobial peptides (AMPs)

AMPs are an abundant group of molecules that are found in virtually all classes of life across the phylogenetic spectrum [25,26]. AMPs are the main elements of the innate immune defense system; a weapons that all multicellular organisms are ‘‘born with’’ to ward off pathogenic microbes in order to survive and thrive on this planet [27,28]. Importantly, peptide mediated innate immunity is recognized as the first host protective barrier. Most of these gene encoded peptides are mobilized shortly after microbial infection and act rapidly to neutralize a broad range of microbes [29]. AMPs were discovered some 30 years ago, initially isolated from insect lymph, the skin of frogs and mammalian neutrophils. Since then, thousands of cationic peptides have been reported from numerous species, isolated from numerous organs and tissues such as eyes, pancreas, oral mucosa and epithelium of respiratory and

gastrointestinal tract in mammalian species [30,31]. In mammals the two major families of AMPs are defensins and cathelicidins [32,33].

Structurally, AMPs were classified in four major classes: (1) α-helix, (2) β-sheet stabilized by two or three disulfide bridges, (3) extended structures with one or more predominant residues (like tryptophan and proline rich) and (4) loop due to the presence of a single disulfide bridge [31,34]. Among these the first two classes being the most abundant in nature [35]. Most of the AMPs exhibit a relatively unstructured conformation in solution, and fold into amphipathic arrangement with hydrophobic and hydrophilic moieties segregating into distinct patches on the molecular surface when interacting with the unique environment of biological membranes [36]. Generally, AMPs are composed of 12 to 50 amino acid residues. Due to the frequent occurrence of lysine and arginine residues in their amino acid sequence, they usually possess a net positive charge (generally +2 to +9) at physiological pH; although a few negatively charged AMPs have also been found [37]. Such peptides have broad spectra of activity that can encompass bacteria, fungi, viruses and parasites [25]. The potential pharmacologic application and toxicity profile of antimicrobial peptides is mainly determined by their selectivity i.e. the degree to which they differentiate between microbial targets and normal host cells.

1.1.1. Selectivity

The selectivity of antimicrobial peptides is due to fundamental differences, between microbial cells and mammalian host cells and also the microenvironments in which these counterparts convene [38]. The eukaryotic membranes contain zwitterionic components like phosphatidylcholine (PC), phosphatidylethanolamine (PE), sphingomyelin (SM) and sterols such as cholesterol and ergosterol. In contrast, prokaryotic architecture which mainly comprises negatively charged components namely hydroxylated phospholipids, phosphatidylglycerol (PG), cardiolipin (CL) and phosphatidylserine (PS) [39]. Electrostatic interactions between the positively charged AMPs and the negatively charged bacterial phospholipids provide an initial mode of interaction, whereas hydrophobic interactions allow the peptides to penetrate the cell membrane [38,39].

1.1.2. Mode of Action

The mode of action of AMPs is of particular interest, as it is thought to be nonspecific unlike traditional antibiotic drugs (usually directed against a precise cellular receptor) thus, not deriving the development of resistance [40,41]. The mechanism for lytic activity of AMPs

is varied and some significant questions remain still unanswered [42]. The initial contact between the AMPs and the external leaflet of target microorganism would be electrostatic, as most bacterial surfaces are anionic [38, 43]. The linear AMPs re-organize and assume an optimal amphipathic conformation in close proximity of biomembranes. The hydrophilic face interacts with the phospholipid head groups whereas their hydrophobic face is inserted in the bilayer core [43]. Such interactions can lead to structural distortion of the membrane architecture by various possible mechanisms. Three models have been proposed to describe the process of microbial membrane permeation by membrane-active peptides, the carpet model, the barrel-stave model and the toroidal pore model. The details of these models are as follows:

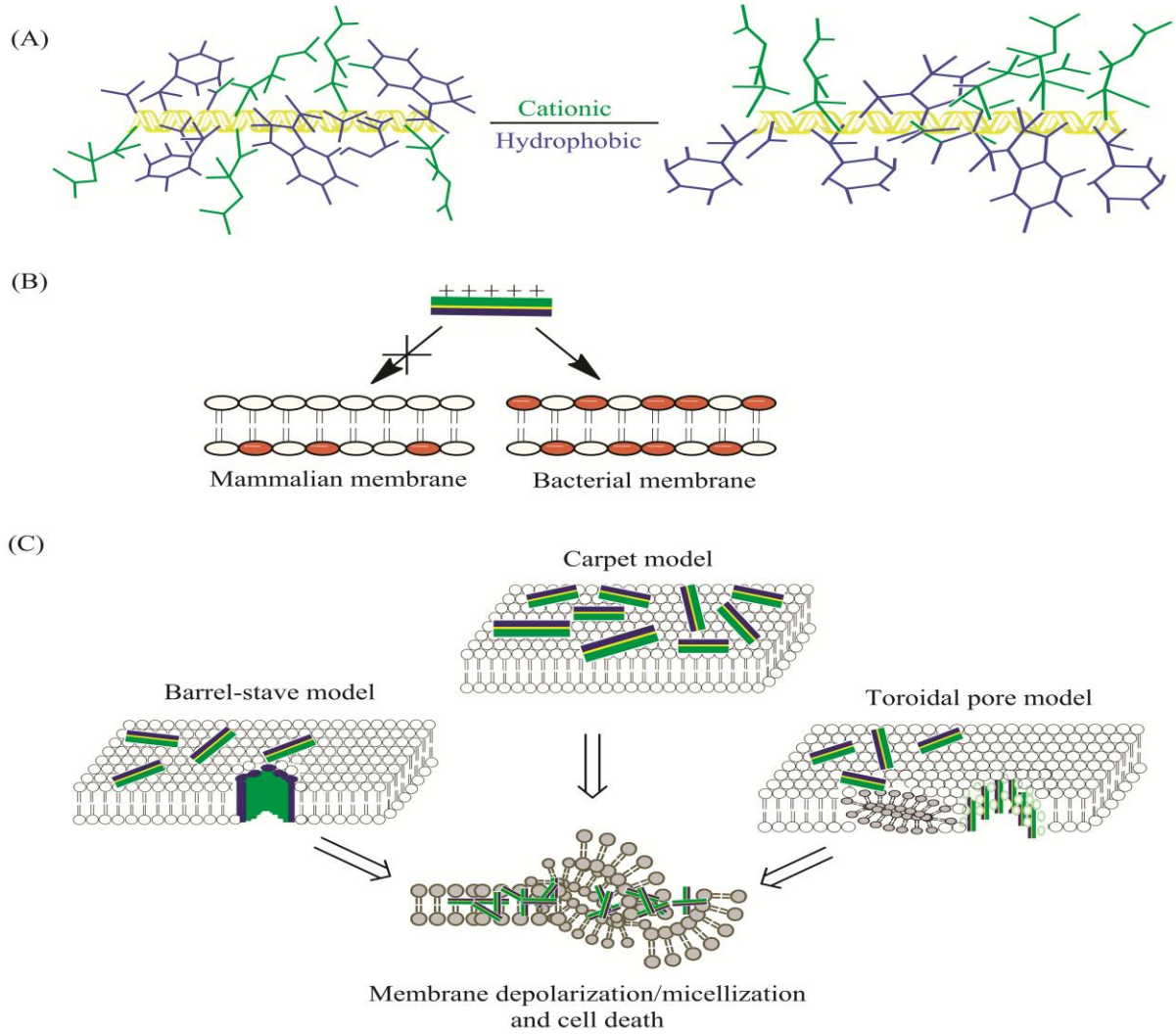

Figure 1.1: Schematic representation of the action of AMPs leading toward bacterial membrane permeation and disruption. (A) AMPs adopt amphiphatic conformation in the close proximity of biological membrane. (B) Representation of the selectivity of AMPs to bacteria over mammalian cells based on electrostatic attraction. (C) Proposed membrane permeabilization models

1.1.2.1. The carpet model

According to the carpet model, AMPs first bind onto the surface of the target microbial cell membrane and subsequently cover it in a carpet-like manner (Figure 1.1C). The initial interaction between the AMPs and the external leaflet of target microorganism would be electrostatic, as most bacterial surfaces are anionic [44]. In the second step, AMPs reorient themselves such that their hydrophobic face points toward the membrane lipids, and the hydrophilic face toward the phospholipid head-groups. After a threshold concentration has been reached, AMPs cause membrane permeation. It affects the membrane in a detergent-like manner, resulting in the collapse of the membrane packing into fragments with physical dissolution of the cell wall [45]. High local concentration on the surface of the membrane depends upon the type of the target membrane and can occur either after all the surface of the membrane is covered with peptide monomers, or alternatively, antimicrobial peptides that associate on the surface of the membrane can form a local carpet [45,46].

The carpet model describes a situation in which AMPs are in contact with the phospholipid head group throughout the entire process of membrane permeation. The presence of negatively charged lipids in the target membrane architecture is essential for the accumulation of AMPs to form carpet-like structures, as they help to reduce the repulsive electrostatic forces between positively charged peptides. AMPs exerting their antimicrobial action via this mechanism do not require a specific structure, length, or specific amino acids sequence [47]. The carpet model was proposed for the first time to describe the mode of action of dermaseptin S [48], and later on was used to describe the mode of action of other antimicrobial peptides, such as dermaseptin natural analogues [49], cecropins [50], and the human antimicrobial peptide LL-37 [51].

1.1.2.2. The barrel-stave model

The term ‘barrel-stave’ describes the overall topology of a membrane channels/pores formed by the aggregation of AMPs through membrane core (Figure 1.1C). In this model, AMPs are self-associate either in solution prior to binding and insertion into the membrane or alternatively, bind to the membrane followed by peptide oligomerization and insertion. During oligomerization, AMPs orient themselves in such a way that the hydrophobic surfaces of AMPs face outward, toward the acyl chains of the membrane, whereas the hydrophilic surfaces constitute the pore lining [52]. The AMP binding at the outer surface of target membrane, most likely as monomers, is considered as the initiation of this membrane

permeabilization mechanism. AMPs with a large number of cationic charged residues (lysine or arginine) spread along the peptide chain cannot form a transmembrane pore unless its charges become neutralized. This suggests that AMPs acting via this mechanism do not have a high net positive charge. Therefore, in this model the peptide interaction toward phospholipid bilayer is driven predominantly by hydrophobic interactions. As a consequence of these properties the peptides bind to phospholipid membranes irrespective of the membrane charge, and therefore, may be toxic toward both bacterial and mammalian cells [53]. After initial binding on the target membrane, AMPs may undergo a conformational phase transition, forcing displacement of polar-phospholipid head groups which result into localized membrane thinning. It is energetically unfavorable for a single AMP molecule to transverse the membrane as a monomer [52]. Consequently, when membrane bound AMPs reaches a threshold concentration, peptide monomers self-aggregate and insert deeper into the hydrophobic membrane core. Progressive recruitment of additional AMP monomers leads to a further expansion of the membrane pore. Leakage of intracellular components through these pores subsequently causes cell death [45].

1.1.2.3. The toroidal pore model

This model describes the well characterized peptide-membrane interactions. Same as that of barrel-stave model in this model also AMPs exert their antimicrobial action by traverse through the membrane core. The only difference between the toroidal pore and barrel-stave models is that in the former, membrane polar-phospholipid head groups are intercalated in between the AMP molecules in the transmembrane channel (Figure 1.1C) [54]. The aggregation of AMPs through membrane core constitutes a membrane-spanning pore, which is referred as a supramolecular complex. AMPs orient themselves through membrane core in such a way that hydrophobic residues face towards hydrophobic membrane core and polar peptide surfaces as well as phospholipid head groups constitutes the pore lining [55]. The formation of so-called wormholes or toroidal pores was proposed to describe the mode of action of magainin [54,55], protegrin [56], and melittin [57].

1.1.2.4. Alternative mode of action

The barrel stave, the carpet and the toroidal models predict that the killing activity of AMPs occurs due to perturbation of membrane integrity. However, several studies indicate that permeabilization is necessary but may not be enough to explain antimicrobial activity. Several studies investigated the relationship between microbial membrane permeabilization

and cell death revealing that cell killing may proceed with relatively little membrane disruption and suggesting that AMPs may interact with key intracellular targets [58]. Xiong and coworkers reported that *S. aureus* cells remained viable long after rapid membrane permeabilization induced by tPMPs. These outcomes suggested that non-membranolytic mechanisms are responsible for cell death. tPMPs exert their microbial killing effect by direct inhibition of nucleic acid synthesis and the relatively strong negative charge of nucleic acids is consistent with the hypothesis that cationic peptides bind to and inhibit these molecules [59]. Kragol *et al.* reported that insect antibacterial peptides (pyrrhocoricin, drosocin, and apidaecin) inhibit the bacterial heat shock protein DnaK, and inhibition of this protein is associated with cell death [60]. Likewise, buforin II has been reported to penetrate microbial cell membranes and interfere with intracellular functions [58]. It is also believed that the antimicrobial peptide, microcin B17, specifically target DNA gyrase within *E. coli* and subsequently resulted into inhibition of DNA replication. Indolicidin was proposed to inhibit DNA synthesis leading to filamentation in *Escherichia coli* [61]. Some AMPs were found to interfere with the metabolic processes of microbes; an example is the glycine-rich attacins that were shown to block the transcription of the *omp* gene in *E. coli* [62], whereas magainins and cecropins induce selective transcription of its stress-related genes *micF* and *osmY* at non-bactericidal concentrations [63]. The above observations suggest that AMPs mediated cell death may occur as a result of several independent mechanisms of action. Furthermore, peptides may kill the same species via more than one mechanism of action, depending on individual factors such as growth phase, tissue localization, and the presence or absence of other immune mechanisms or synergistic exogenous antimicrobial agents. From these perspectives, AMPs may have multiple and complementary mechanisms of action necessary to inhibit or kill a wide variety of pathogens in diverse physiologic settings and simultaneously suppressing the ability of the pathogen to develop resistance.

1.1.3. Resistance to AMPs

Most of the bacteria differ in their intrinsic susceptibility to AMPs, and the relative resistance of some pathogens to these defense molecules is considered as a part of their phenotype. The natural mechanisms of resistance development to AMPs are termed as constructive mechanisms [64]. Though the ability to resist AMP killing appears to be a formidable challenge for microbial evolution, AMP resistance is increasingly recognized as a discriminating feature of some important human pathogens. Several bacterial species possess

resistance to AMPs through constructive mechanisms. For example *Serratia*, *Proteus*, *Providencia*, and *Pseudomonas* species due to unusual composition of their membrane can be inherently resistant to AMPs [64,65]. In addition to the constructive mechanisms bacteria have developed inducible mode of resistance in response to the stress generated by AMPs [65]. Similar to pharmaceutical antibiotics, it appears that bacteria exposed to human AMPs have evolved under selective pressure to develop mechanisms of resistance [66]. Diverse inducible mechanisms of bacterial resistance to AMP have been identified which mainly includes altered cell surface charge, active efflux, production of proteases or trapping proteins, and modification of host cellular processes. However, even though these selective pressures have existed for countless centuries, human AMPs still possess a broad spectrum of potent activity against a diverse array of Gram-positive and Gram-negative bacterial species, fungi, as well as certain protozoan parasites and enveloped viruses [65,66].

1.1.4. Therapeutic potential of AMPs

AMPs constitute an attractive class of therapeutic agents having broad antimicrobial spectrum and are effective against pathogens resistant to the conventional antibiotics [35,53]. Moreover, AMPs can complement conventional antibiotic therapy probably by facilitating access into the bacterial cell resulting in a synergistic effect [67]. AMPs may initiate adaptive immune responses by acting as chemokines and/or induce chemokine production, inhibiting lipopolysaccharide (LPS)-induced pro-inflammatory cytokine production and recruiting antigen-presenting cells [68]. AMPs may also possess immunomodulatory activity when involved in the clearance of infection, including the promotion of wound healing [69]. Because of these properties, the term “host defense peptides” has been proposed for AMPs which indicates the real role played by them in the intended bioenvironment [53]. AMPs having non-specific modes of action might indeed decrease pathogens ability to develop resistance [70,71] and consequently boost up their therapeutic potential. In addition, it has been demonstrated that amphiphilic peptides retain their antimicrobial activity when they are covalently bond to a water-insoluble resin [72]. This behavior suggested their use in therapeutic medical devices such as intravenous catheters [35]. The attractive therapeutic features associated with AMPs greatly motivated the researchers to develop them as ideal drug candidates against pathogenic microbes.

1.2. Lipopeptides

Lipopeptides are another class of native antimicrobial agents produced non-ribosomally in the bacteria and fungi during cultivation on various carbon sources [73-74]. They are composed of an aliphatic acid attached to the N-terminus of short cationic or anionic peptidic moiety of six to seven amino acids. Most native lipopeptides have complex cyclic structures [75,76]. The mode of lytic action of some of them is via perturbation of the cell membrane by unknown mechanisms [77-81]. Similarly to that of AMPs, electrostatic interaction between cationic lipopeptides and negatively charged lipopolysaccharide (LPS) of Gram-negative bacteria or lipoteichoic acid of Gram-positive bacteria is the initial step of their bactericidal activity. Further, lipopeptides traverse into the inner core and destabilize the membrane architecture [76,78]. In the fungi lipopeptides bind to the negatively charged membrane phosphatidylinositol (PI) and to the negatively charged terminal sialic acid moieties [82-84]. In addition to this, lipopeptides display broad-spectrum antimicrobial activity against multi-drug resistant bacteria as well as fungi. These clinical features associated with lipopeptides encourage us to develop them as new generation of antibiotics. Conversely, native lipopeptides are non-cell selective and therefore toxic to mammalian cells [81]. Despite this toxicity profile several members of this novel class of antimicrobials including daptomycin (active only toward Gram-positive bacteria) [85], polymyxin B (active only toward Gram-negative bacteria) [86], and echinocandins (β-1,3-D-glucan synthase inhibitors; active only toward fungi) [87] were approved by the Food and Drug Administration (FDA).

CHAPTER 2.
REVIEW OF LITERATURE

2.1. Short Lipopeptides

Several studies have revealed that mimicking of natural lipopeptide antibiotics by the attachment of suitable length aliphatic chain to the N-terminus of native or synthetic short peptides can result into potentially winning approach to the development of potent antimicrobial agents [81,88,89]. Earlier, Shai *et al*. have shown that the conjugation of fatty acids to the potent native antibacterial peptide magainin endowed it with antifungal activity [90]. In their further studies Shai *et al*. chose inactive diastereomers of magainin containing four D-amino acids ([D]-4-magainin) [90] as well as weakly active diastereomeric lytic peptide containing Leu and Lys ([D]-L_6K_6) [91] to determine whether an antibacterial peptide scaffold is essential for antifungal activity of these conjugate molecules. The outcomes revealed that lipopeptides composed of short aliphatic tail (10 and 12 carbons atoms) are non-hemolytic and active towards both bacteria and fungi. On the other hand, lipopeptides having 14 or 16 carbon atoms long aliphatic tail are found to be good antifungal agents. They are hemolytic only at concentrations above their MIC values [91]. The advantage of using diastereomers versus all L-amino acid peptides for designing of fatty acid conjugates, paves the way for a new group of potent antifungal lipopeptides urgently needed to combat opportunistic fungal infection.

Further studies have been conducted to design small lipopeptide molecules by cutting down the length of peptide sequence. The research team led by Yechiel Shai made efforts in the same direction and came up with ultra-short (di, tri and tetramer) cationic lipopeptides that composed of fatty acid attached to all L- and D,L amino acids showed activity against both bacteria and fungi [86]. The interesting finding of this study was that the attachment of aliphatic acids to ultra-short cationic peptides can compensate for the length of hydrophobicity of the peptidic chain and endow the resulting lipopeptides with antimicrobial activity that is similar to the activity of longer antimicrobial peptides and lipopeptides. Lipopeptide molecule with single lysine residue attached to a palmitic acid resulted in complete loss of activity reveals that the activity of these lipopeptides is not dictated solely by the hydrophobic fatty acid chain but also requires a specific sequence. This is further supported by the finding that C16-KLLK is not active at all in comparison to the lipopeptide

composed of four lysine residues (C16-KKKK; Figure 2.1) [86]. On the basis of these results, one can speculate that further substitutions with different amino acids might result in lipopeptides with additional spectra of activities.

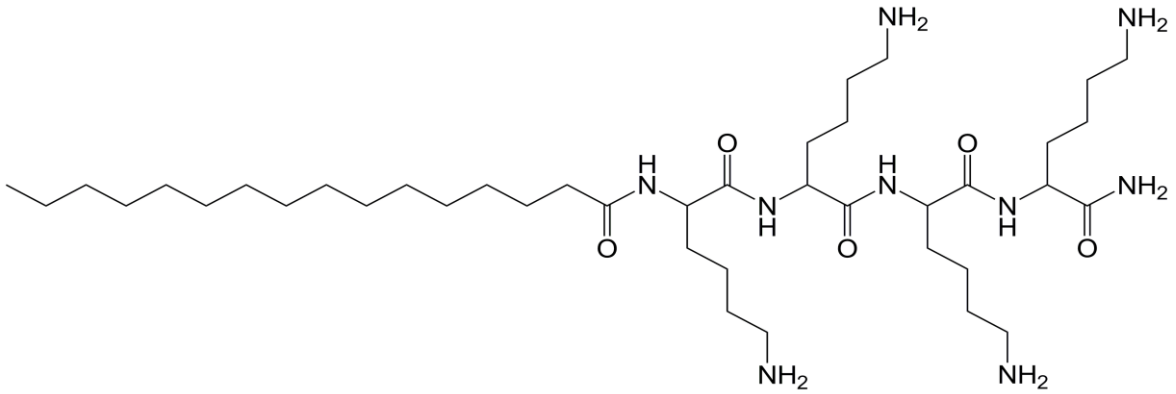

C16-KKKK

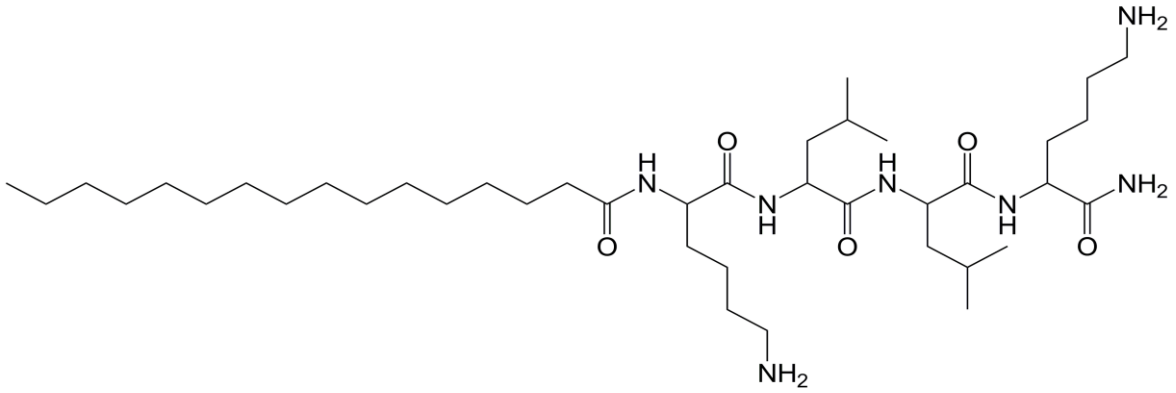

C16-KLLK

Figure 2.1: Chemical structure of ultrashort lipopeptides C16-KKKK and C16-KLLK

Recently, lipophilic modifications with structured hydrophobic biomolecules, such as vitamin E and cholesterol resulted into *de novo* lipopeptides molecules VitE-KGG**K** and Cholesterol-KGG**K** (Figure 2.2) respectively. These bioconjugates were exclusively active against fungi and observed to cause membrane perturbation same as that of native AMPs. Moreover, these ultrashort bioconjugates exhibited a larger therapeutic window, giving higher LC_{50}/MIC ratios than the fatty acid-conjugates and synergize with cyclodextrin and amphotericin B [92].

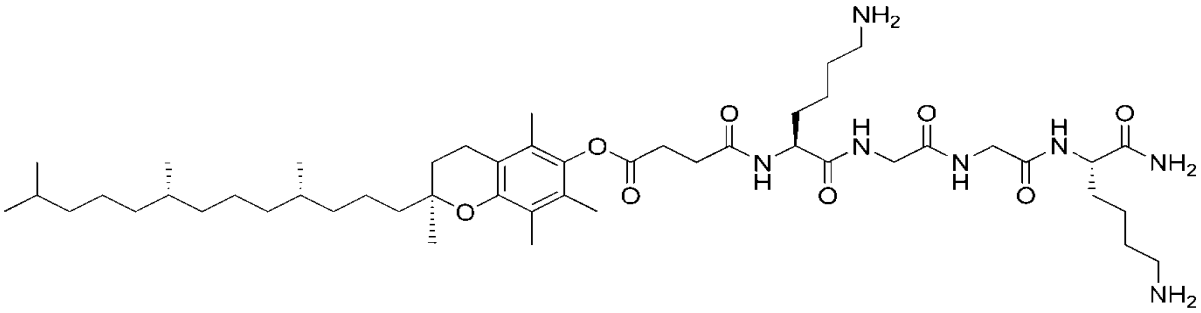

Vit E-KGG**K**

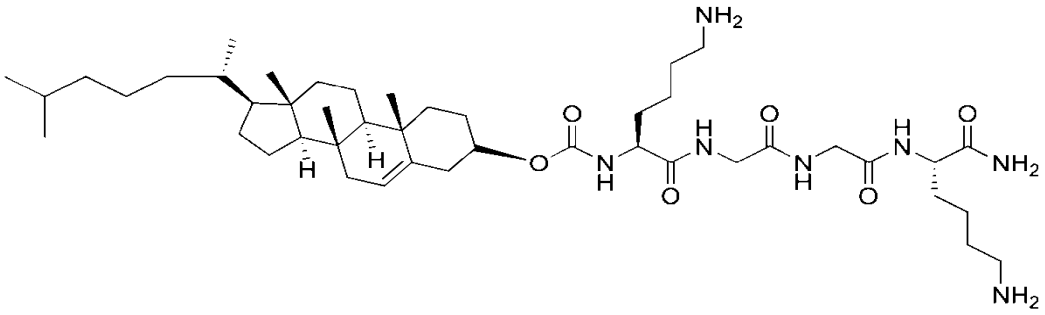

Cholestrol-KGG**K**

Figure 2.2: Chemical Structure of Ultrashort lipopeptides designed by conjugation of Vitamin E succinate (Vit E-KGG**K**) and cholesteryl carbonic acid (Cholesterol-KGG**K**)

Arnusch *et al*. recently designed pH dependent trivalent lipopeptides (Figure 2.3) consisting of multiple ultrashort histidine lipopeptides on a triazacyclophane scaffold. The trimeric molecule with monomer unit composed of myristic acid attached on N-terminal of dipeptide (His-His) showed high activity toward *Aspergillus fumigates* (3.2 μM) and *Cryptococcus neoformans* (3.2 μM) at acidic pH, without any toxic effect [93].

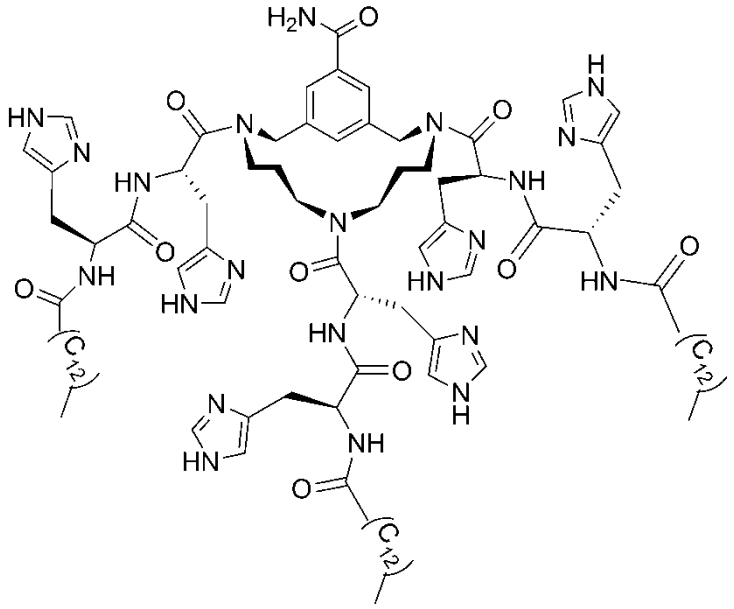

Figure 2.3: Chemical structure of trivalent lipopeptide

Laverty *et al.* reported a series of ultrashort cationic antimicrobial lipopeptides based on N-terminal modification of tetrapeptide amide H-Orn-Orn-Trp-Trp-NH_2 with saturated fatty acid. Most of the synthesized lipopeptides displayed excellent antimicrobial activity. In particular, C_{12}-Orn-Orn-Trp-Trp-NH_2 (Figure 2.4) exhibits broad activity spectrum against bacteria as well as fungi [94]. It indicates that aliphatic tail is a key determinant of antimicrobial activity of lipopeptides.

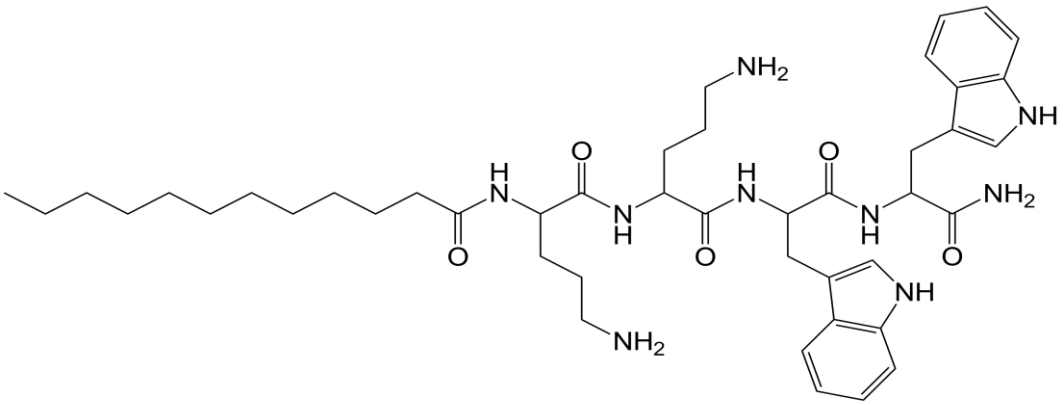

$CH_3(CH_2)_{10}CO$-NH-Orn-Orn-Trp-Trp-NH_2

Figure 2.4: Chemical structure of $CH_3(CH_2)_{10}CO$-NH-Orn-Orn-Trp-Trp-NH_2

2.2. Small cationic peptidomimetics

In the last decade, a number of research groups have systematically investigated the minimum pharmacophore of cationic antimicrobial peptides regarding charge and lipophilicity/bulk [95,96]. This provides a new direction to peptide based antibiotic research and opens the opportunity for the development of cost effective short antimicrobial peptidomimetics for systemic use.

Svendsen *et al*. studied a 15-residue fragment, FKCRRWQWRMKKLGA of bovine lactoferricin (LFB) in search of key amino acids responsible for antibacterial activity of native peptide scaffolds [97,98]. In this truncated sequence, the two tryptophan (Trp) residues were found to be essential for antibacterial activity, as replacement of any one or both Trp residues with another hydrophobic natural amino acid like Phenylalanine, resulted in complete loss of activity [99]. It was also reported that the introduction of one extra Trp in human, goat and porcine lactoferricins increases the antibacterial activity of these peptides up to six-fold [100]. Bikshapathy *et al*. have shown the importance of Trp in peptide PKLLTKFLKSWIG, where the introduction of one and/or two Trp residues resulted in increased antibacterial and hemolytic activity [101]. Incorporation of Trp in cyclic bactenecin, a cationic antimicrobial

peptide from bovine neutrophils, also resulted in a substantial increase of antibacterial activity [102]. The high content of Trp in several antibacterial peptides such as tritrpticin [103] and indolicidine [104] suggest a crucial role of Trp in the interaction with bacterial membrane. The indole nucleus was suggested to be inserted into the membrane, with the hydrophobic part interacting with the hydrophobic portion of the bilayer, and the amine function interacting more closely with the polar head-groups in the proximity of the outside of membrane [105]. Possibly, these membrane perturbation properties of Trp make it favorable among the other natural hydrophobic amino acids.

In another study of the antimicrobial peptide Bac2A (RLARIVVIRVAR-NH_2), it was found that the antibacterial profile of peptides generally increased in the presence of four amino acids: cysteine, lysine, arginine and tryptophan. Arginine and lysine were found most fruitful when complemented with tryptophan substitutions [106]. Recently, Hancock and Cherkasov reconfirmed the strong preference for tryptophan residues by *in silico* analysis of over 100,000 nonameric peptides [107].

To further reduce the length of AMPs in agreement with findings discussed above Strøm *et al.* chose arginine and tryptophan to represent the charged moiety and lipophilic bulk respectively [96]. A series of peptides was designed with balance content of charged and bulky/lipophilic groups. Outcomes of this study reveal that, peptides were effective antibacterial agents irrespective of their amino acid order and smaller peptides (tetra- and tripeptides) showed no antibacterial activity in contrast to larger peptides (hexa- and pentapeptides). However, it is interesting to note that a tripeptide (Trp-Arg-Trp-NH_2) displayed activity against *S. aureus*, albeit weakly with a MIC value of 100μg/mL. Esterification of the C-terminal carboxylic acid moiety and stereoisomeric replacement of monomer unit has been resulted in to increased antimicrobial activity [96].

The amino acid sequence of AMPs provides a large space for structural modification by incorporation of non-proteogenic amino acids and C- and N-terminal capping with bulky aromatic residues [95]. The introduction of bulky unnatural amino acids in the small pharmacophore model of AMPs expand the range of hydrophobicity beyond what can be obtained by native amino acids like tryptophan and phenylalanine [108]. In last few years, different research groups have studied the effect of these structural modifications on bactericidal activity of native peptide sequence and reported number of structurally diverse active scaffolds.

Gime´nez *et al*. studied the hydrophobic effect of fluorine atom by using fluorine and trifluoromethyl substituted phenylalanine analogues fF and tfF respectively. Peptide sequences with fluorinated phenylalanine (SCAMP-I and SCAMP-II; Figure 2.5) showed antibacterial activity comparable to peptide scaffolds having same number of tryptophan residues [109]. These outcomes suggest that fluorine substituted phenylalanine residue have hydrophobic bulk almost equivalent to tryptophan. All the synthesized peptide molecules with fluorinated amino acids were reported to be non-hemolytic at 250 μg/mL [109].

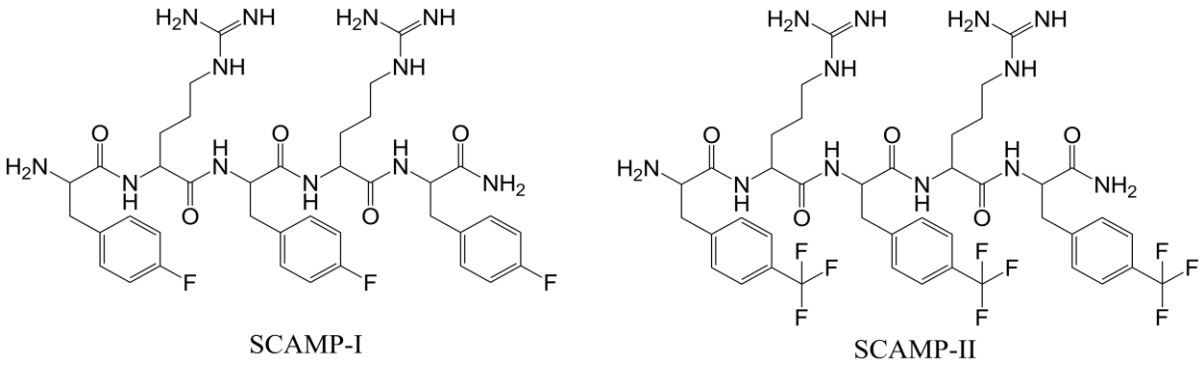

Figure 2.5: Chemical structure of SCAMP-I and SCAMP-II

Another attempt was made by Sharma *et al*. in the same direction by using aliphatic group substituted histidine derivatives in place of native histidine amino acid residue. In the search of novel structurally diverse active scaffolds, synthetic analogues of histidine were incorporated in dipeptide molecules based on Trp-His (SCAMP-III) and His-Arg (SCAMP-IV) structural frameworks (Figure 2.6). These small synthetic dipeptide molecules are active against several Gram-negative and Gram-positive bacterial strains with MIC in the range of 5-20 μg/mL and were not found to be cytotoxic up to 200 μg/mL [110].

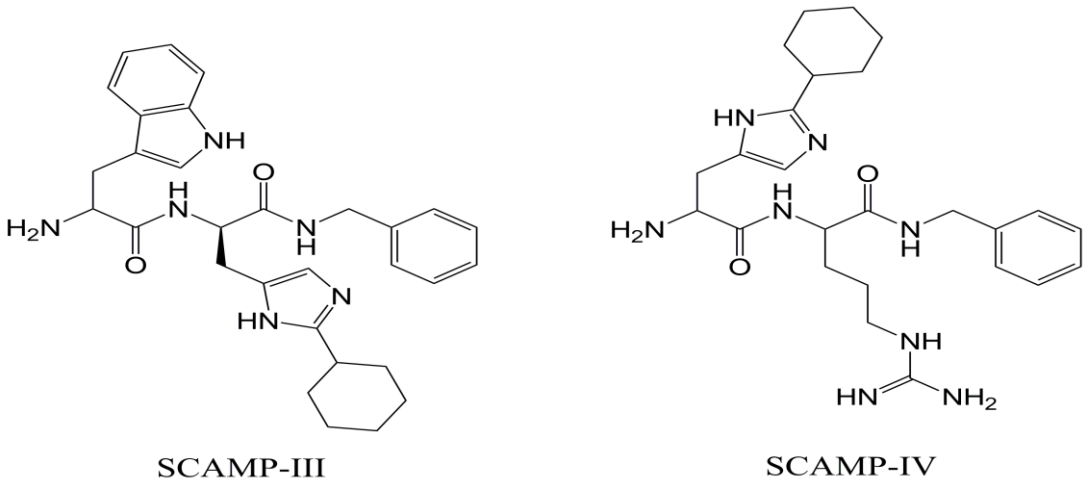

Figure 2.6: Chemical structure of SCAMP-III and SCAMP-IV

Svenson *et al*. designed several structurally diverse libraries of SCAMPs by introducing hydrophobic C-terminal amide modifications and likewise bulky synthetic side chains on the central amino acid of tripeptide scaffold (Arg-Trp-Arg-NHBn) in order to explore an effective way to increase biological activity and stability in the intended bioenvironment [111]. Peptides (SCAMP-V to SCAMP-VIII),which were designed by replacing central Trp residue with different bulky unnatural amino acids, showed improved antibacterial activity and proteolytic stability (Figure 2.7).

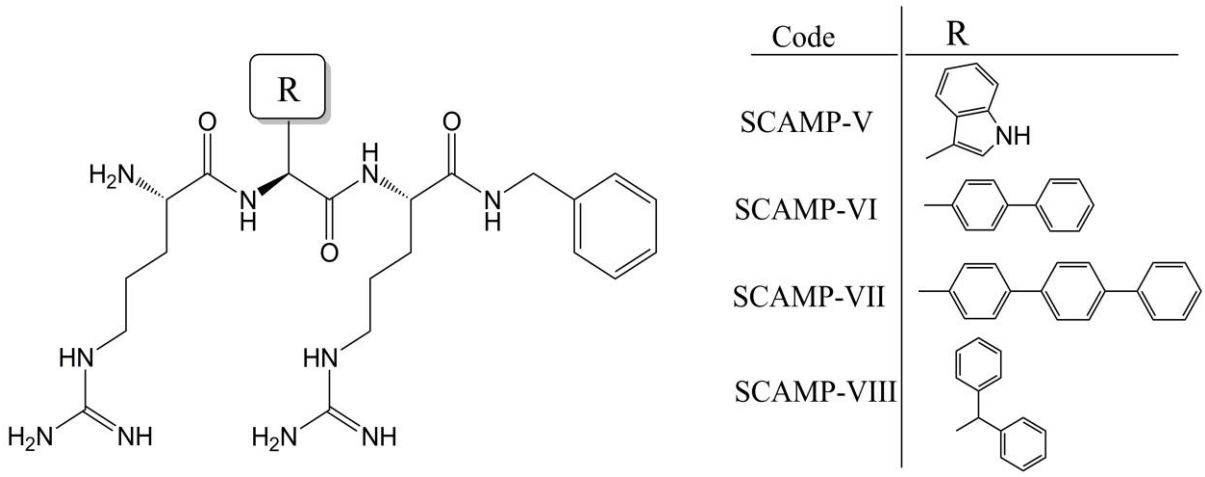

Figure 2.7: Chemical structure of SCAMP-V to SCAMP-VIII

To study the influence of the C-terminal capping moiety on the biological activity and tryptic stability, another library of SCAMPs was designed by introducing both N-monosubstituted amides and N,N-disubstituted amides on the C-terminal of tripeptide molecule (Arg-Trp-Arg-NHBn; Figure 2.8). The structural modification by C-terminal capping resulted in improvement of antibacterial activity. The compounds with N, N-disubstituted amide (SCAMP-XII and SCAMP-XIII) were stable against tryptic degradation whereas, the closely resemble analogues N-monosubstituted amides (SCAMP-IX to SCAMP-XI) were degraded by trypsin. On the basis of stability studies of N-monosubstituted amides, it was concluded that stability was increased when the phenyl group of the C-capping moiety was two carbon atoms away from the amide nitrogen (SCAMP-X), compared to the analogues with one (SCAMP-IX) or three (SCAMP-XI) carbon atoms between the amide nitrogen atom and the phenyl group [111].

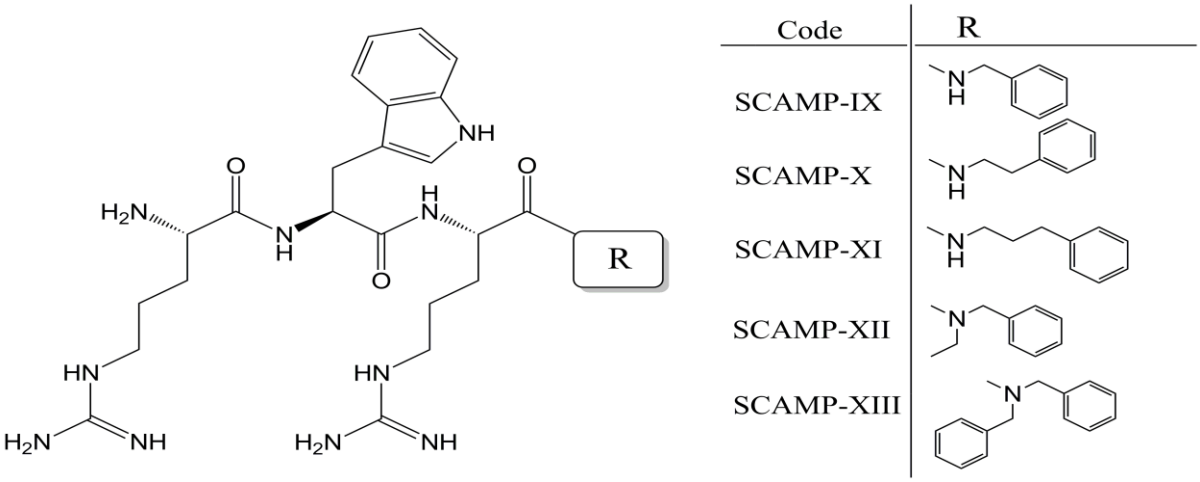

Figure 2.8: Chemical structure of SCAMP-IX to SCAMP-XIII

Later on several design principles were suggested by Karstad *et al*., to circumvent the enzymatic degradation catalyzed by chymotrypsin [112]. Thus, the indole nucleus of tryptophan in the tripeptide molecule (Arg-Trp-Arg-NH_2) was replaced with different hydrophobic moieties (Phe, Bip and Dip). The resulting SCAMPs with non-natural amino acids showed improved antibacterial activity as well as chymotryptic stability. Later on Karstad *et al*. designed SCAMPs by altering cationic charge unit and side chain length of arginine residue of tripeptide molecule (Arg-Trp-Arg-NHBn; Figure 2.9). Substitution of guanidine with amino group decreases the potency of the resultant peptide (SCAMP-XVIII) but simultaneously increase proteolytic stability against chymotryptic degradation [112]. Another mode of lead modification was performed by direct conjugation of cationic charged unit of arginine with backbone of peptide (SCAMP-XV). The side chain modification of cationic amino acid (Arg) favorably increased the antibacterial potency but there was no improvement in proteolytic stability [112].

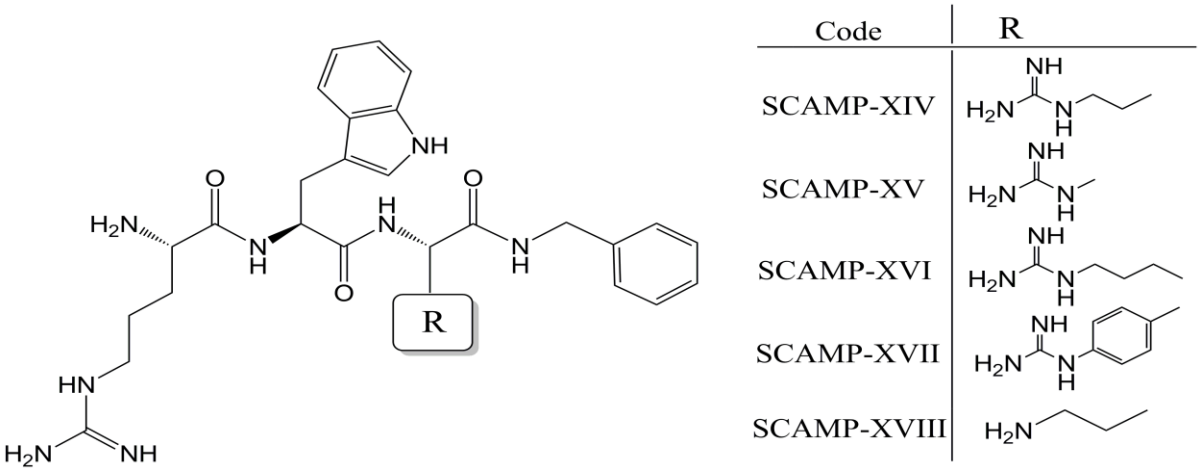

Figure 2.9: Chemical structure of SCAMP-XIV to SCAMP-XVIII

Haug *et al*. made a successful effort by replacing tryptophan residue of tripeptide molecule (Arg-Trp-Arg-NH_2) with 2,5,7-tri(tert-butyl) tryptophan (tbW) resulted into a potent tripeptide molecule (SCAMP-XIX; Figure 11) [108]. Later on, C-terminal capping of SCAMP-XIX by ethyl phenyl group resulted in most active molecule LTX 109 (Lytix Biopharma) of this class. LTX 109 (SCAMP-XX; Figure 2.10) is one among the synthetic antimicrobial peptidomimetic molecule, currently in clinical phase II trials for topical treatment of infections caused by multidrug resistant strains [113].

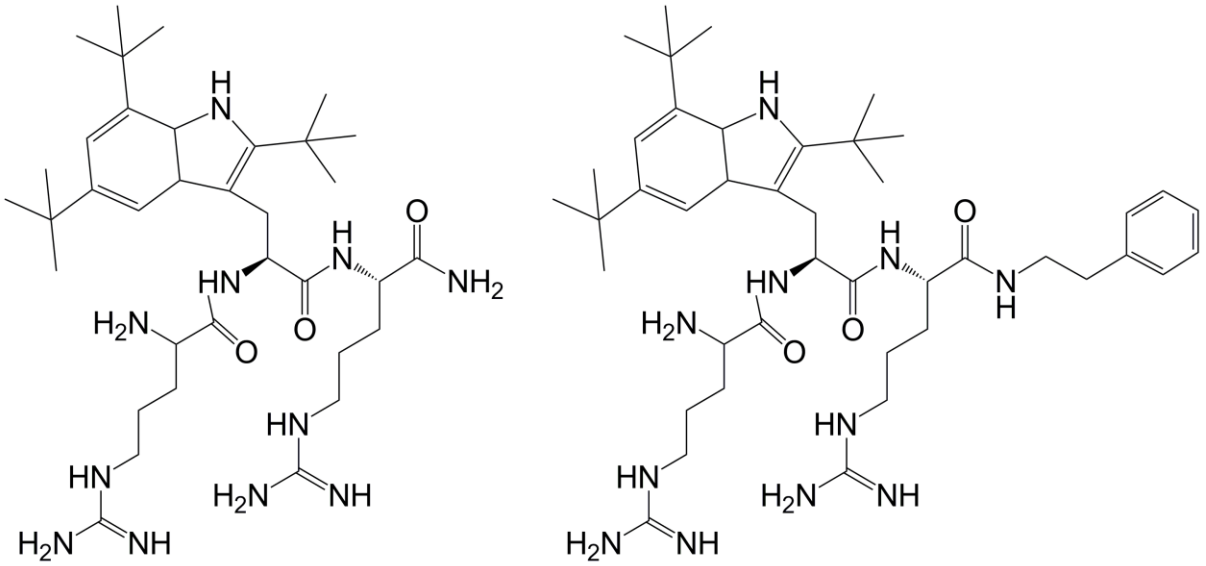

Figure 2.10: Chemical structure of SCAMP-XIX to SCAMP-XX

Bisht *et al*. systematically investigated the effect of N-terminal capping by taking ornithine and tryptophan based small cationic antimicrobial peptide. A series of tetrapeptide was synthesized by conjugating different synthetic moieties on the N-terminus of the peptide sequence. Amino modified peptides with N-terminal cinnamic acid (SCAMP-XXI), *p*-Hydroxycinnamic acid (SCAMP-XXII) and 3-(4-hydroxyphenyl) propionic acid (SCAMP-XXIII; Figure 2.11), exhibit potent activity against different bacterial strains with no hemolytic activity even at high dose level (1000 µg/mL) [114].

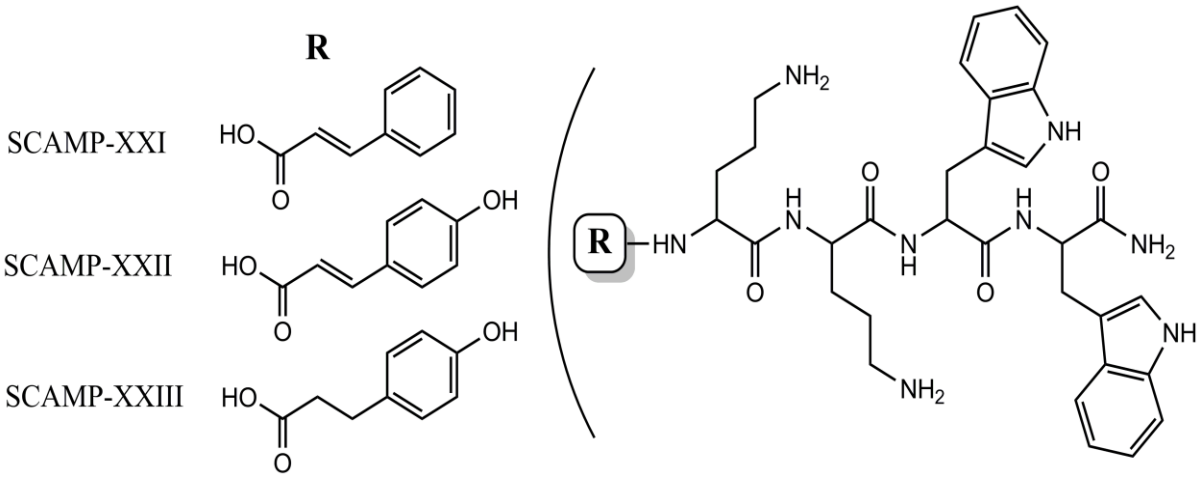

Figure 2.11: Chemical structure of SCAMP-XXI to SCAMP-XXIII

The aromatic γ-amino acid 3-ABA has been incorporated in peptide sequences to provide a specific turn like conformation. 3-ABA has a constrained structural framework due to the presence of two principal dihedral angles θ1 (C2-C3) and θ2 (C1-C2), sandwiched between φ (N-C3) and ψ (C1-CO). They have a fixed dihedral angle of about 180^{o}. Possibly, it may attribute to its β-sheet like structure (Figure 2.12) [115].

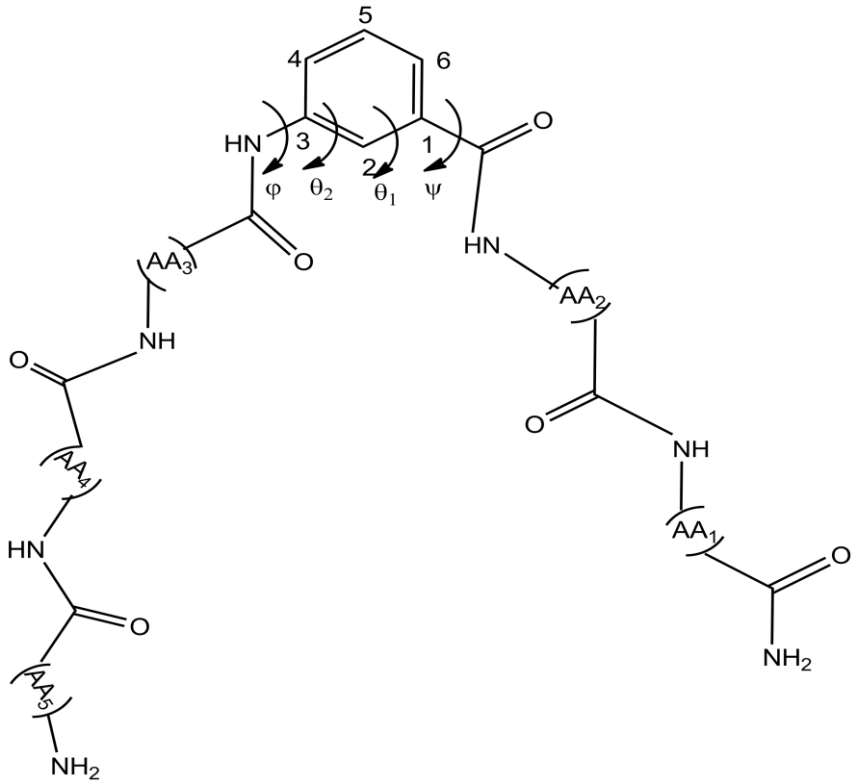

Figure 2.12: Structural overview of the small peptide sequence having 3-ABA as a peptidomimetic element with bond angles present in the structural framework of 3-ABA

Rao *et al.* have incorporated 3-ABA in β-hairpin loop as a turn inducing motif and demonstrated that it results in very stable secondary structures [116]. Lundy *et al.* reported synthetic analogues of α-defensin (HNP-1) synthesized by incorporating constrained aromatic amino benzoic acids as β-turn motif exhibit broad-spectrum antibacterial activity [117]. Recently, Lengyel *et al.* reported that incorporation of 3-ABA in the peptide sequence improved the stability of folded conformation in aqueous medium without effecting the arrangement of side chain residues [118].

Coming to the challenges posed in further development of short peptide based antimicrobial agents, it is useful to evaluate key desirable attributes for a new lead in terms of therapeutic potential and safety. These include optimum bioavailability, acceptable stability against proteolytic degradation, appropriate avoidance of toxicities and lack of resistance development. These are the characteristics that one should pursue for the next generation peptide antibiotics.

CHAPTER 3.
PURPOSE OF THE WORK

3.1. Motivation

Looking into the WHO report-2013, there is no ambiguity that development of antibiotic resistance needs urgent attention from researchers to discover novel anti-infective agents which can combat the infections caused by multi-drug resistant strains.

From the review of literature, it is clear that most of the lipopeptides and synthetically designed small cationic antimicrobial peptidomimetics exert their antimicrobial action through membrane binding and disruption, followed by aggregation, poration, and insertion into the membrane. Therefore, it could be extremely difficult for microbes to develop resistance against them by counteract all killing mechanisms at once. Generally, pathogens are unable to develop resistance against membrane active agents, which recommend their therapeutic application in other critical diseased conditions where the growing resistance to chemotherapeutic agents is a major concern. Moreover, peptide based antibiotics in particular lipopeptides display broad-spectrum antimicrobial activity against multi-drug resistant bacteria as well as fungi, which makes them suitable candidates for the development of new generation antibiotics.

Lipo-antibiotics available in the market are from natural origin which includes polymyxin B, daptomycin, and caspofungin not all but just for mention. However, literature reports highlight toxicity toward mammalian cells as their major drawback. Structurally, these native lipo-antibiotics have a somewhat complex structural framework which might be responsible for their non-cell selectivity. Proteolytic degradation is another drawback associated with peptide based therapeutics which renders them considerably inactive in intended bioenvironment. Although there are many reports published which underscores the better therapeutic potential of short lipopeptides and small cationic peptidomimetics but to our knowledge improvement of their druggability has so far escaped from serious attention of researchers.

3.2. Objectives

The research program described here, aimed at rationally structure based design, synthesis and biological evaluation of novel short lipopeptides and small cationic peptidomimetics. The specific objectives are illustrated below:

- To design and synthesize structurally small peptide based molecules.
- To evaluate the antimicrobial activity and therapeutic index of synthesized molecules.
- To examine proteolytic stability and pathogens ability to develop resistance against lead molecules.
- To study the mechanism involved in antimicrobial activity of lead molecules.

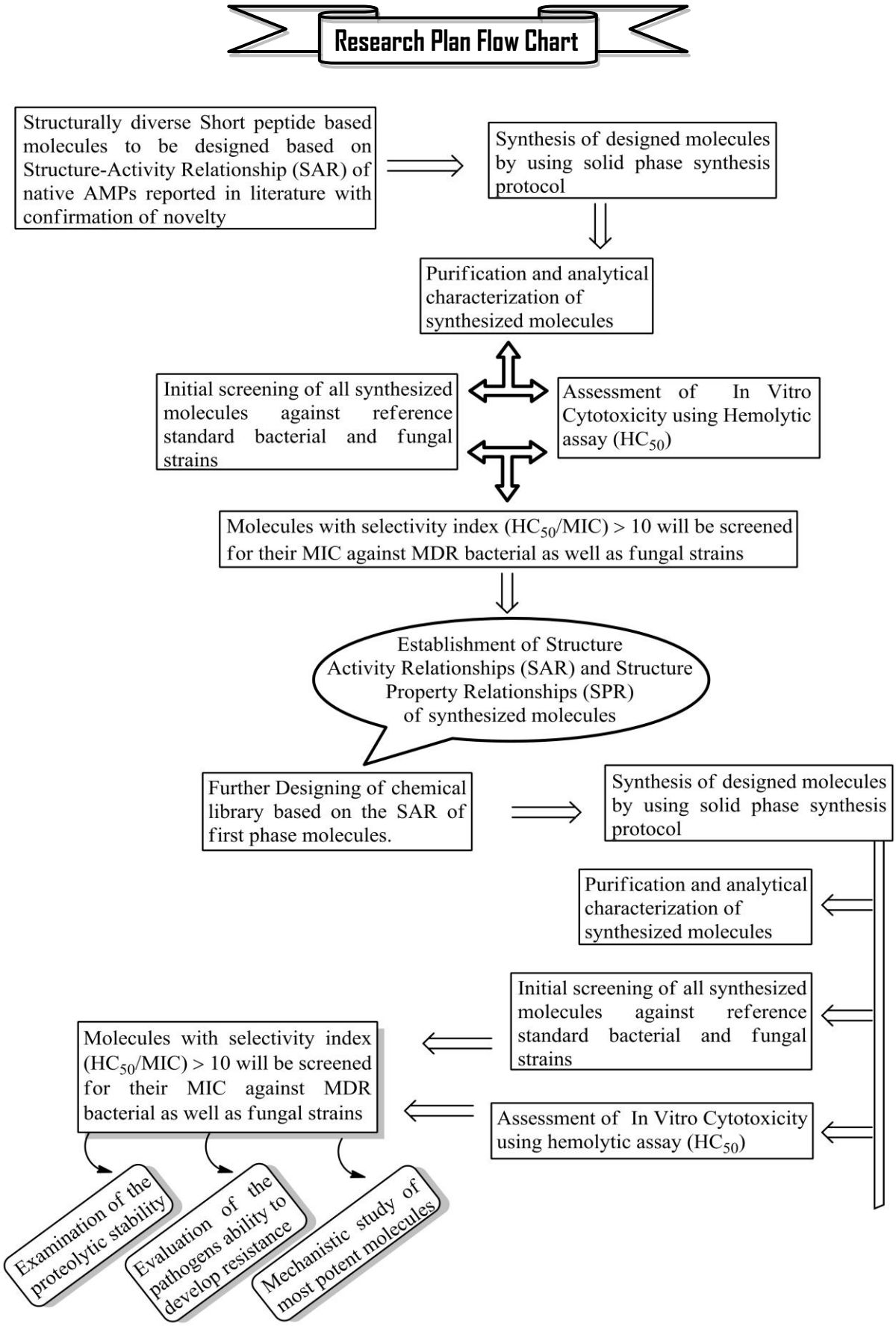
Research Plan Flow Chart
Structurally diverse Short peptide based molecules to be designed based on Structure-Activity Relationship (SAR) of native AMPs reported in literature with confirmation of novelty
Synthesis of designed molecules by using solid phase synthesis protocol
Purification and analytical characterization of synthesized molecules
Initial screening of all synthesized molecules against reference standard bacterial and fungal strains
Assessment of In Vitro Cytotoxicity using Hemolytic assay (HC_{50})
Molecules with selectivity index (HC_{50}/MIC) > 10 will be screened for their MIC against MDR bacterial as well as fungal strains
Establishment of Structure Activity Relationships (SAR) and Structure Property Relationships (SPR) of synthesized molecules
Further Designing of chemical library based on the SAR of first phase molecules.
Synthesis of designed molecules by using solid phase synthesis protocol
Purification and analytical characterization of synthesized molecules
Initial screening of all synthesized molecules against reference standard bacterial and fungal strains
Assessment of In Vitro Cytotoxicity using hemolytic assay (HC_{50})
Molecules with selectivity index (HC_{50}/MIC) > 10 will be screened for their MIC against MDR bacterial as well as fungal strains
Examination of the proteolytic stability
Evaluation of the pathogens ability to develop resistance
Mechanistic study of most potent molecules

CHAPTER 4.
MATERIALS AND METHOD

4.1. Chemicals and reagents

Rink amide MBHA resin and protected amino acids Fmoc-Arg(Pbf)-OH, Fmoc-Trp(Boc)-OH, Fmoc-Phe-OH and Fmoc-Orn(Boc)-OH were purchased from Novabiochem (Mumbai, India). Aromatic amino acid 3-amino benzoic acid and Fmoc-Cl were obtained from Spectrochem (Mumbai, India). Fatty acids capric acid, caprylic acid, lauric acid, myristic acid, palmitic acid, and stearic acid used for lipopeptide synthesis were procured from Fluka. Other reagents used for the solid phase synthesis of lipopeptides and peptidomimetic molecules included N-hydroxybenzotriazole (HOBt), N,N'-diisopropylcarbodiimide (DIC), Piperidine, N,N-dimethylformamide (DMF) (Spectrochem, Mumbai, India), Dimethyl sulphoxide (DMSO), Dichloromethane (DCM), Diethyl ether, 1,2-Ethanedithiol (Merck, Mumbai, India), and Trifluoro acetic acid (TFA; Loba Chemie, Mumbai, India). Membrane bilayer mimicking phospholipids dipalmitoylphosphatidylcholine (DPPC), dipalmitoylphosphatidylglycerol (DPPG), phosphatidylcholine (PC), phosphatidylethanolamine (PE), phosphatidylinositol (PI), phosphatidylglycerol (PG), cholesterol, and ergosterol were purchased from Avanti Polar Lipids (New Delhi, India). Calcein, propidium iodide, DAPI and buffer material were purchased from Sigma-Aldrich (Mumbai, India). Dulbecco's modified Eagle's medium (DMEM), 3-(4,5-dimethylthiazol-2-yl)-2,5-diphenyltetrazolium bromide (MTT), were obtained from Sigma Chemical Co. (St Louis, MO, USA). The lactate dehydrogenase (LDH) assay kit was purchased from Promega (Madison, WI, USA). All the solvents used for purification were of HPLC grade and obtained from Merck (Mumbai, India). Buffers were prepared in double-distilled water.

4.2. Synthesis and characterization

4.2.1. Method for the synthesis of short lipopeptides

Scheme-1[a]

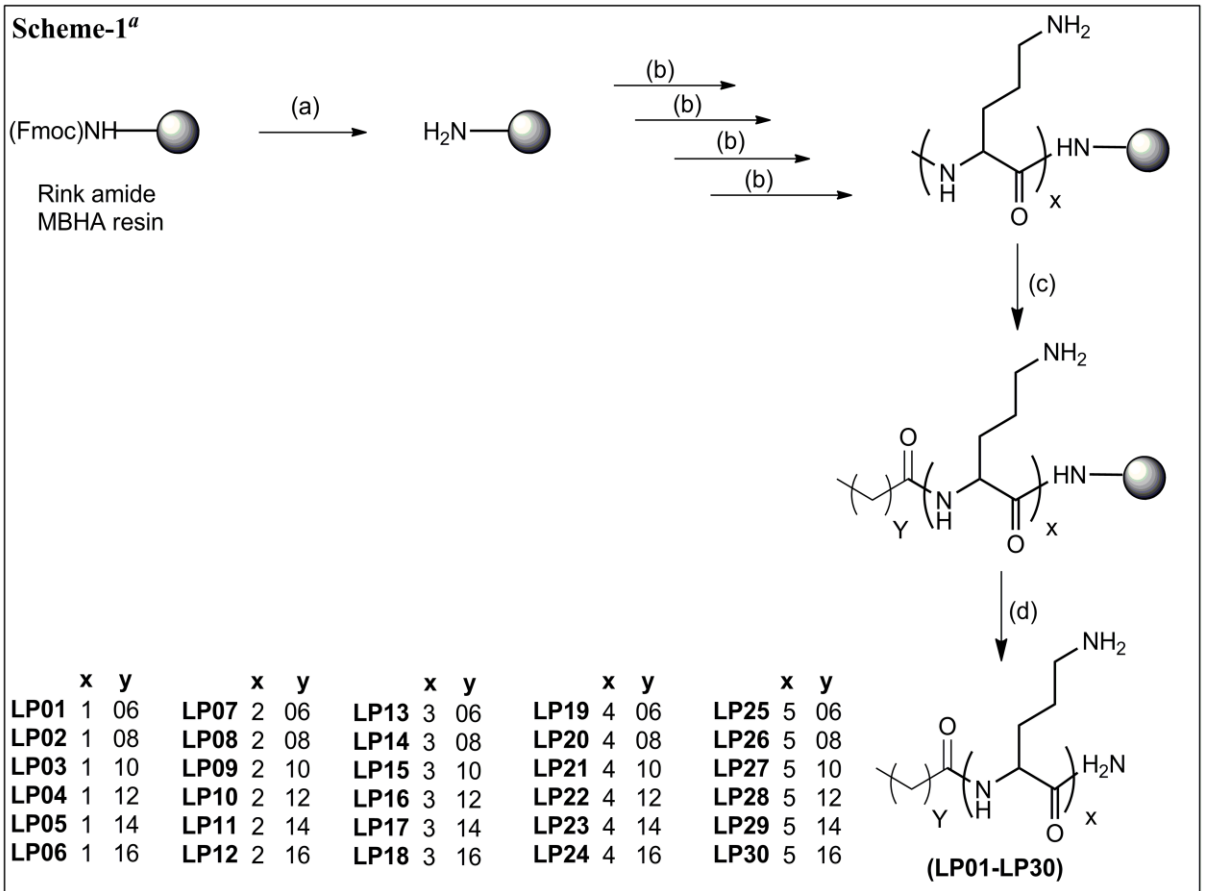

	x	y		x	y		x	y		x	y		x	y
LP01	1	06	**LP07**	2	06	**LP13**	3	06	**LP19**	4	06	**LP25**	5	06
LP02	1	08	**LP08**	2	08	**LP14**	3	08	**LP20**	4	08	**LP26**	5	08
LP03	1	10	**LP09**	2	10	**LP15**	3	10	**LP21**	4	10	**LP27**	5	10
LP04	1	12	**LP10**	2	12	**LP16**	3	12	**LP22**	4	12	**LP28**	5	12
LP05	1	14	**LP11**	2	14	**LP17**	3	14	**LP23**	4	14	**LP29**	5	14
LP06	1	16	**LP12**	2	16	**LP18**	3	16	**LP24**	4	16	**LP30**	5	16

[a]**Reagents and reaction conditions** (a) Deprotection; 20% piperidine. (b) Coupling; Fmoc-Orn(Boc)-OH, HOBt, DIC, DMF. Deprotection; 20% piperidine. (c) Acylation; Capric acid, Caprylic acid, Lauric acid, Myristic acid, Palmitic acid, Stearic acid, HOBt, DIC, DMF. Deprotection; 20% piperidine. (d) Cleavage; TFA : 1, 2-Ethanedithiol : H_2O (95:2.5:2.5).

General method for solid phase synthesis of short lipopeptide (LP01-LP30)

Lipopeptides were synthesized manually following standard Fmoc solid phase protocols using Rink amide-4-methylbenzhydrylamine hydrochloride salt (MBHA) resin (loading 0.56 mmol/g) as solid support [119]. Each coupling cycle included an Fmoc deprotection using 20% piperidine in DMF and 3 h coupling of 4 eq. of Fmoc-Orn(Boc)-OH onto resin in the presence 2 eq. of DIC/HOBt in DMF. The acylation was accomplished by reacting fatty acid (capric acid, caprylic acid, lauric acid, myristic acid, palmitic acid, or oleic acid) with the N-terminus of resin bound peptide using DIC/HOBt as activation agents. After the desired sequences were assembled, the lipopeptides were cleaved from solid support (Scheme 1).

All crude lipopeptides were analyzed on RP-HPLC using a C18 waters column (Spherisorb®, ODS2, 5 µm, 4.6 mm × 250 mm) at room temperature. A linear gradient of 0.5-60% solvent B (0.05% TFA in acetonitrile) in solvent A (0.05% TFA in water) over 35 min, followed by 60-0.5% solvent B over 10 min was used at a flow rate of 0.5 mL/min. Preparative RP-HPLC was then performed on a Waters column (Spherisorb®, ODS2, 5 µm, 20 mm × 250 mm) using 0.5-60% linear gradient of solvent B (0.05% TFA in acetonitrile) in solvent A (0.05% TFA in water) over 35 min, followed by 60-0.5% solvent B over 10 min at a flow rate of 5 mL/min. Purified HPLC fractions were then lyophilized.

$CH_3(CH_2)_6CO$-NH-Orn-NH_2 (LP01)

LCMS (+ESI-m/z): calcd for $C_{29}H_{59}N_7O_4$: 257.21, observed 258.00 $(M+H)^+$; Purity determined by RP-HPLC: 97.30%.

$CH_3(CH_2)_8CO$-NH-Orn-NH_2 (LP02)

LCMS (+ESI-m/z): calcd for $C_{29}H_{59}N_7O_4$: 285.24, observed 286.10 $(M+H)^+$; Purity determined by RP-HPLC: 85.38%.

$CH_3(CH_2)_{10}CO$-NH-Orn-NH_2 (LP03)

LCMS (+ESI-m/z): calcd for $C_{29}H_{59}N_7O_4$: 313.27, observed 314.0 $(M+H)^+$; Purity determined by RP-HPLC: 98.30%.

$CH_3(CH_2)_{12}CO$-NH-Orn-NH_2 (LP04)

LCMS (+ESI-m/z): calcd for $C_{29}H_{59}N_7O_4$: 341.30, observed 342.38 $(M+H)^+$; Purity determined by RP-HPLC: 94.06%.

$CH_3(CH_2)_{14}CO$-NH-Orn-NH_2 (LP05)

LCMS (+ESI-m/z): calcd for $C_{29}H_{59}N_7O_4$: 369.34, observed 370.10 $(M+H)^+$; Purity determined by RP-HPLC: 93.81%.

$CH_3(CH_2)_{16}CO$-NH-Orn-NH_2 (LP06)

LCMS (+ESI-m/z): calcd for $C_{29}H_{59}N_7O_4$: 397.37, observed 398.00 $(M+H)^+$; Purity determined by RP-HPLC: 98.88%.

$CH_3(CH_2)_6CO$-NH-Orn-Orn-NH_2 (LP07)

LCMS (+ESI-m/z): calcd for $C_{29}H_{59}N_7O_4$: 371.29, observed 372.00 $(M+H)^+$; Purity determined by RP-HPLC: 98.87%.

$CH_3(CH_2)_8CO$-NH-Orn-Orn-NH_2 (LP08)

LCMS (+ESI-m/z): calcd for $C_{29}H_{59}N_7O_4$: 399.32, observed 400.41 $(M+H)^+$; Purity determined by RP-HPLC: 89.84%.

$CH_3(CH_2)_{10}CO$-NH-Orn-Orn-NH_2 (LP09)

LCMS (+ESI-m/z): calcd for $C_{29}H_{59}N_7O_4$: 427.35, observed 428.42 $(M+H)^+$; Purity determined by RP-HPLC: 98.62%.

$CH_3(CH_2)_{12}CO$-NH-Orn-Orn-NH_2 (LP10)

LCMS (+ESI-m/z): calcd for $C_{29}H_{59}N_7O_4$: 455.38, observed 456.45 $(M+H)^+$; Purity determined by RP-HPLC: 98.89%.

$CH_3(CH_2)_{14}CO$-NH-Orn-Orn-NH_2 (LP11)

LCMS (+ESI-m/z): calcd for $C_{29}H_{59}N_7O_4$: 483.41, observed 484.54 $(M+H)^+$; Purity determined by RP-HPLC: 97.25%.

$CH_3(CH_2)_{16}CO$-NH-Orn-Orn-NH_2 (LP12)

LCMS (+ESI-m/z): calcd for $C_{29}H_{59}N_7O_4$: 511.45, observed 512.57 $(M+H)^+$; Purity determined by RP-HPLC: 88.19%.

$CH_3(CH_2)_6CO$-NH-Orn-Orn-Orn-NH_2 (LP13)

LCMS (+ESI-m/z): calcd for $C_{29}H_{59}N_7O_4$: 485.37, observed 486.40 $(M+H)^+$; Purity determined by RP-HPLC: 95.87%.

$CH_3(CH_2)_8CO$-NH-Orn-Orn-Orn-NH_2 (LP14)

LCMS (+ESI-m/z): calcd for $C_{29}H_{59}N_7O_4$: 513.40, observed 514.40 $(M+H)^+$; Purity determined by RP-HPLC: 95.39%.

$CH_3(CH_2)_{10}CO$-NH-Orn-Orn-Orn-NH_2 (LP15)

LCMS (+ESI-m/z): calcd for $C_{29}H_{59}N_7O_4$: 541.43, observed 542.40 $(M+H)^+$; Purity determined by RP-HPLC: 98.99%.

$CH_3(CH_2)_{12}CO$-NH-Orn-Orn-Orn-NH_2 (LP16)

^{1}H NMR (400 MHz, DMSO-d_6) δ 7.88 (s, 3H), 7.11 (s, 2H), 4.21 (t, J = 16.0 Hz, 3H), 3.61 (s, 6H), 2.78-2.66 (m, 6H), 2.09 (t, J = 16.0 Hz, 2H), 1.71-144 (m, 15H), 1.43-1.11 (m, 20H), 0.81 (t, J = 8.0 Hz, 3H). LCMS (+ESI-m/z): calcd for $C_{29}H_{59}N_7O_4$: 569.46, observed 570.34 $(M+H)^+$; Purity determined by RP-HPLC: 98.95%.

$CH_3(CH_2)_{14}CO$-NH-Orn-Orn-Orn-NH_2 (LP17)

^{1}H NMR (400 MHz, DMSO-d_6) δ 7.86 (s, 3H), 7.11 (s, 2H), 4.22 (t, J = 20.0 Hz, 3H), 3.43 (s, 6H), 2.73 (m, 6H), 2.10-2.03 (m, 3H), 1.68-145 (m, 13H), 1.42-1.15 (m, 25H), 0.82 (t, J = 12.0 Hz, 3H). LCMS (+ESI-m/z): calcd for $C_{31}H_{63}N_7O_4$: 597.49, observed 598.37 $(M+H)^+$; Purity determined by RP-HPLC: 98.90%.

$CH_3(CH_2)_{16}CO$-NH-Orn-Orn-Orn-NH_2 (LP18)

^{1}H NMR (400 MHz, DMSO-d_6) δ 7.88 (s, 3H), 7.11 (s, 2H), 4.21 (t, J = 16.0 Hz, 3H), 3.61 (s, 6H), 2.84-2.69 (m, 7H), 2.08 (t, J = 8.0 Hz, 2H), 1.71-141 (m, 14H), 1.25-1.10 (m, 28H), 0.79 (t, J = 8.0 Hz, 3H). LCMS (+ESI-m/z): calcd for $C_{33}H_{67}N_7O_4$: 625.53, observed 626.5 $(M+H)^+$; Purity determined by RP-HPLC: 97.99%.

$CH_3(CH_2)_6CO$-NH-Orn-Orn-Orn-Orn-NH_2 (LP19)

LCMS (+ESI-m/z): calcd for $C_{29}H_{59}N_7O_4$: 599.45, observed 600.29 $(M+H)^+$; Purity determined by RP-HPLC: 93.35%.

$CH_3(CH_2)_8CO$-NH-Orn-Orn-Orn-Orn-NH_2 (LP20)

LCMS (+ESI-m/z): calcd for $C_{29}H_{59}N_7O_4$: 627.48, observed 628.32 $(M+H)^+$; Purity determined by RP-HPLC: 93.55%.

$CH_3(CH_2)_{10}CO$-NH-Orn-Orn-Orn-Orn-NH_2 (LP21)

LCMS (+ESI-m/z): calcd for $C_{29}H_{59}N_7O_4$: 655.51, observed 656.42 $(M+H)^+$; Purity determined by RP-HPLC: 87.58%.

$CH_3(CH_2)_{12}CO$-NH-Orn-Orn-Orn-Orn-NH_2 (LP22)

^{1}H NMR (400 MHz, DMSO-d_6) δ 7.88 (s, 4H), 7.12 (s, 2H), 4.25-4.16 (m, 4H), 3.48 (s, 8H), 2.77-2.73 (m, 9H), 2.08 (t, J = 12.0 Hz, 2H), 1.70-151 (m, 18H), 1.25-1.08 (m, 21H), 0.80 (t, J = 4.0 Hz, 3H). LCMS (+ESI-m/z): calcd for $C_{34}H_{69}N_9O_5$: 683.54, observed 684.39 $(M+H)^+$; Purity determined by RP-HPLC: 94.86%.

$CH_3(CH_2)_{14}CO$-NH-Orn-Orn-Orn-Orn-NH_2 (LP23)

^{1}H NMR (400 MHz, DMSO-d_6) δ 7.90 (s, 4H), 7.14 (s, 2H), 4.27-4.16 (m, 4H), 3.46 (s, 8H), 2.77-2.66 (m, 9H), 2.13 (t, J = 16.0 Hz, 2H), 1.70-139 (m, 19H), 1.23-1.09 (m, 24H), 0.81 (t, J = 8.0 Hz, 3H). LCMS (+ESI-m/z): calcd for $C_{36}H_{73}N_9O_5$: 711.57, observed 712.36 $(M+H)^+$; Purity determined by RP-HPLC: 97.25%.

$CH_3(CH_2)_{16}CO$-NH-Orn-Orn-Orn-Orn-NH_2 (LP24)

^{1}H NMR (400 MHz, DMSO-d_6) δ 7.88 (s, 4H), 7.13 (s, 2H), 4.27-4.15 (m, 4H), 3.48 (s, 8H), 2.84-2.67 (m, 9H), 2.09 (t, J = 16.0 Hz, 2H), 1.74-142 (m, 21H), 1.27-1.07 (m, 28H), 0.80 (t, J = 8.0 Hz, 3H). LCMS (+ESI-m/z): calcd for $C_{38}H_{77}N_9O_5$: 739.60, observed 740.53 $(M+H)^+$; Purity determined by RP-HPLC: 96.45%.

$CH_3(CH_2)_6CO$-NH-Orn-Orn-Orn-Orn-Orn-NH_2 (LP25)

LCMS (+ESI-m/z): calcd for $C_{29}H_{59}N_7O_4$: 713.53, observed 714.42 $(M+H)^+$; Purity determined by RP-HPLC: 98.98%.

$CH_3(CH_2)_8CO$-NH-Orn-Orn-Orn-Orn-Orn-NH_2 (LP26)

LCMS (+ESI-m/z): calcd for $C_{29}H_{59}N_7O_4$: 741.56, observed 742.40 $(M+H)^+$; Purity determined by RP-HPLC: 98.65%.

$CH_3(CH_2)_{10}CO$-NH-Orn-Orn-Orn-Orn-Orn-NH_2 (LP27)

LCMS (+ESI-m/z): calcd for $C_{29}H_{59}N_7O_4$: 769.59, observed 770.31 $(M+H)^+$; Purity determined by RP-HPLC: 95.20%.

$CH_3(CH_2)_{12}CO$-NH-Orn-Orn-Orn-Orn-Orn-NH_2 (LP28)

^{1}H NMR (400 MHz, DMSO-d_6) δ 7.89 (s, 5H), 7.13 (s, 2H), 4.27-4.16 (m, 5H), 3.43 (s, 10H), 2.79-2.63 (m, 10H), 2.11-2.01 (m, 2H), 1.72-140 (m, 20H), 1.27-1.07 (m, 22H), 0.80 (t, J = 4.0 Hz, 3H). LCMS (+ESI-m/z): calcd for $C_{39}H_{79}N_{11}O_6$: 797.62, observed 798.48 $(M+H)^+$; Purity determined by RP-HPLC: 98.33%.

$CH_3(CH_2)_{14}CO$-NH-Orn-Orn-Orn-Orn-Orn-NH_2 (LP29)

^{1}H NMR (400 MHz, DMSO-d_6) δ 7.91 (s, 5H), 7.13 (s, 2H), 4.26-4.21 (m, 5H), 3.59 (s, 10H), 2.76-2.72 (m, 10H), 2.13-2.03 (m, 2H), 1.73-142 (m, 20H), 1.26-1.11 (m, 26H), 0.80 (t, J = 8.0 Hz, 3H). LCMS (+ESI-m/z): calcd for $C_{41}H_{83}N_{11}O_6$: 825.65, observed 826.52 $(M+H)^+$; Purity determined by RP-HPLC: 98.72%.

$CH_3(CH_2)_{16}CO$-NH-Orn-Orn-Orn-Orn-Orn-NH_2 (LP30)

^{1}H NMR (400 MHz, DMSO-d_6) δ 7.87 (s, 5H), 7.13 (s, 2H), 4.25-4.17 (m, 5H), 3.39 (s, 10H), 2.77-2.71 (m, 10H), 2.10-2.03 (m, 3H), 1.73-143 (m, 20H), 1.23-1.11 (m, 30H), 0.81 (t, J = 12.0 Hz, 3H). LCMS (+ESI-m/z): calcd for $C_{43}H_{87}N_{11}O_6$: 853.68, observed 854.50 $(M+H)^+$; Purity determined by RP-HPLC: 96.10%.

4.2.2. Spectra

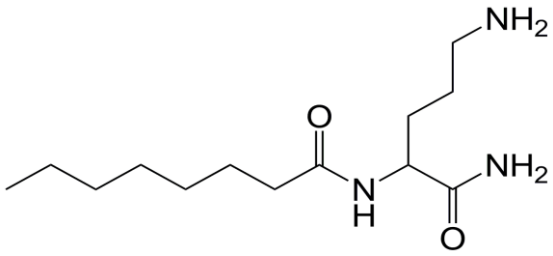

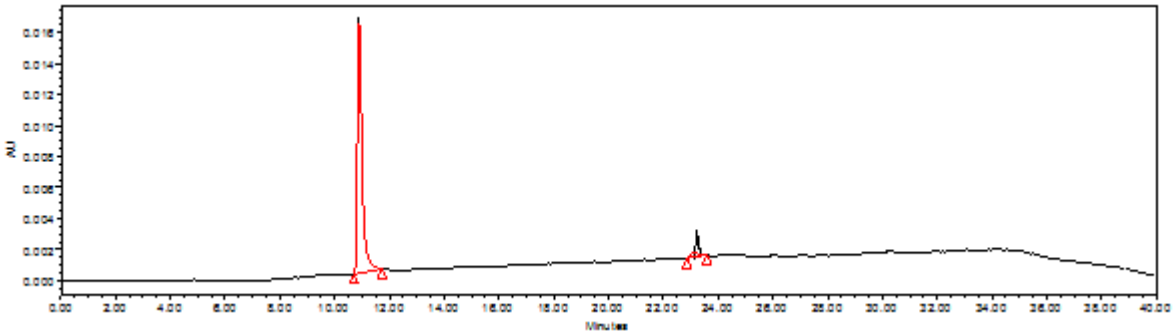

	Name	Retention Time	Area	% Area	Height	RT Ratio
1		11.08	2402725	98.97	186217	
2		23.812	4215	1.03	1533	

Molecular Weight: 257.21

LCMS (+ESI, m/z): 258.03 $(M+H)^+$

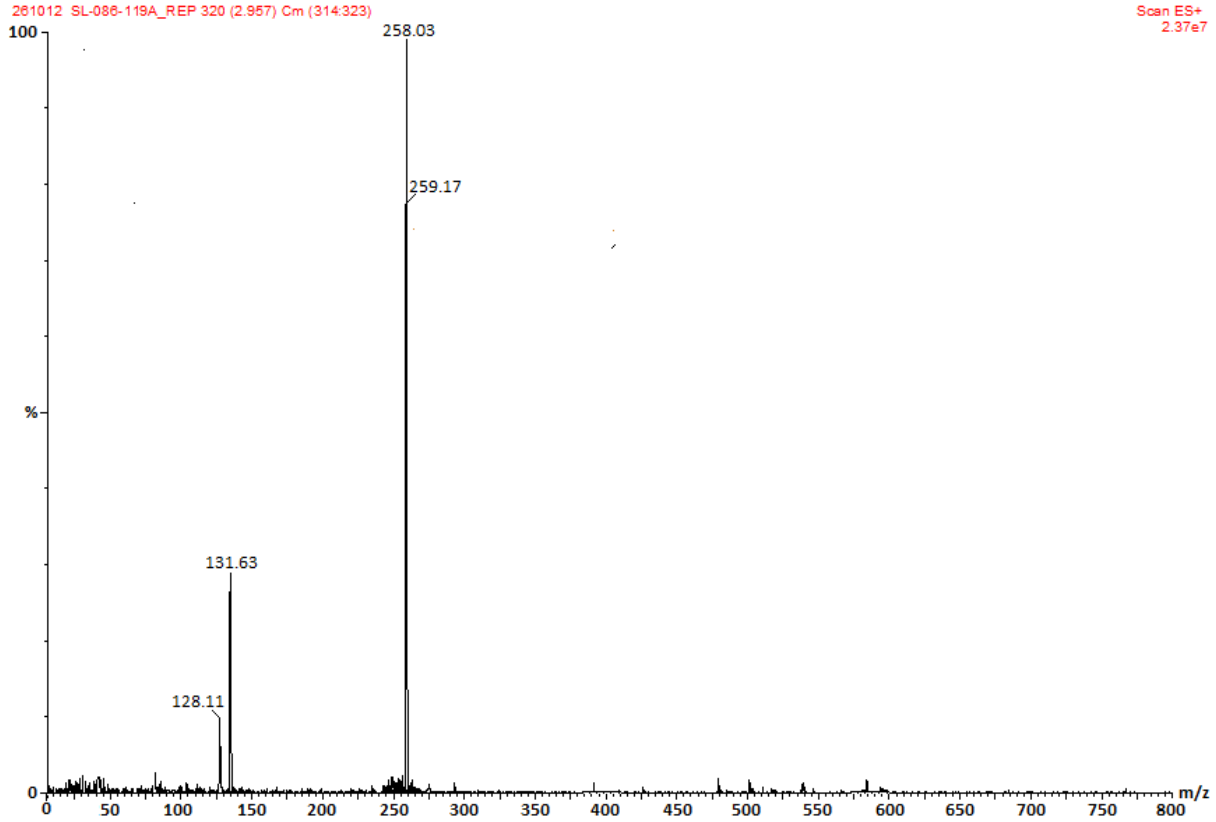

Figure 4.1: Chemical structure, HPLC chromatogram and Mass spectra of **LP01**

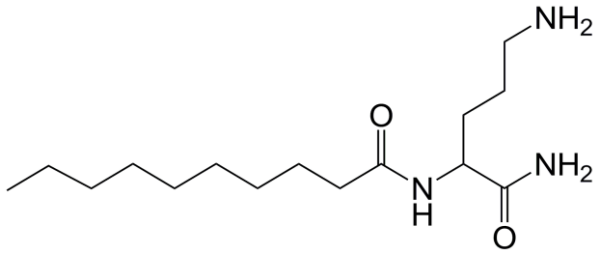

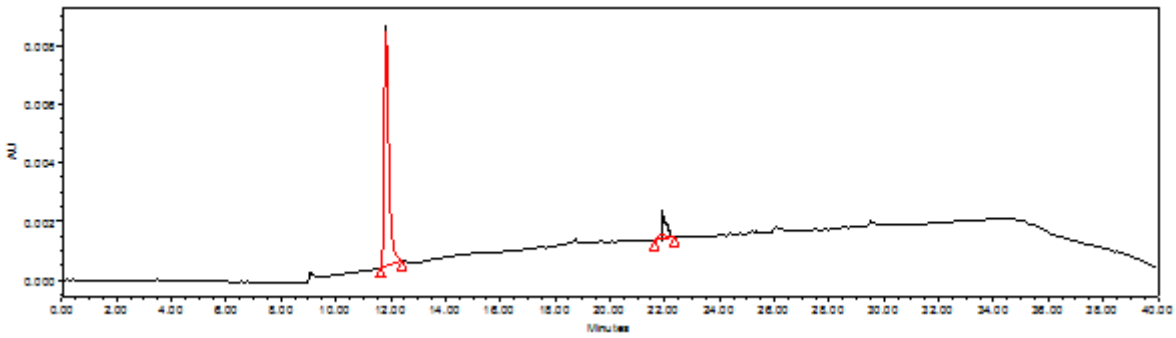

	Name	Retention Time	Area	% Area	Height	RT Ratio
1		11.90	2721899	97.81	96543	
2		22.05	4215	2.19	1124	

Molecular Weight: 285.24

LCMS (+ESI, m/z): 286.10 $(M+H)^+$

Figure 4.2: Chemical structure, HPLC chromatogram and Mass spectra of **LP02**

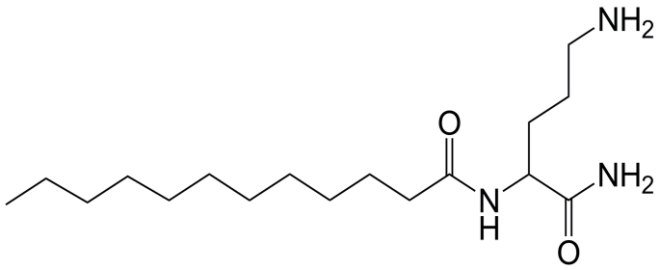

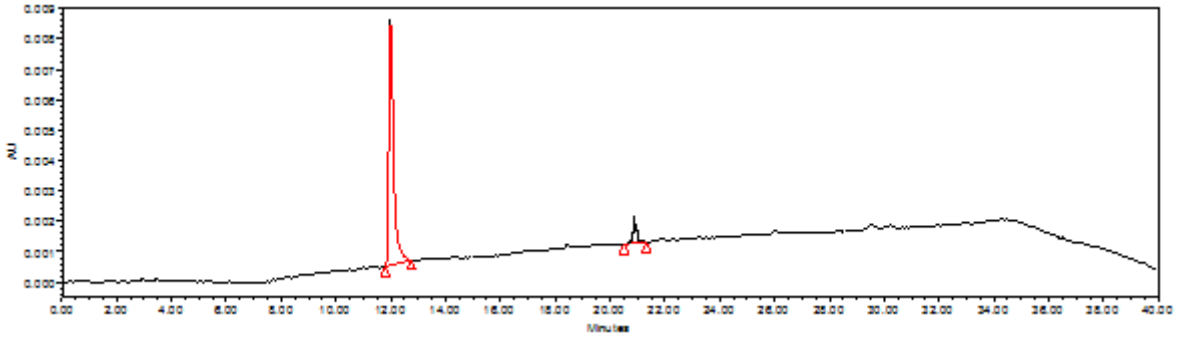

	Name	Retention Time	Area	% Area	Height	RT Ratio
1		12.31	3155780	98.31	137890	
2		20.86	4215	1.69	1419	

Molecular Weight: 313.27

LCMS (+ESI, m/z): 314.12 $(M+H)^+$

Figure 4.3: Chemical structure, HPLC chromatogram and Mass spectra of **LP03**

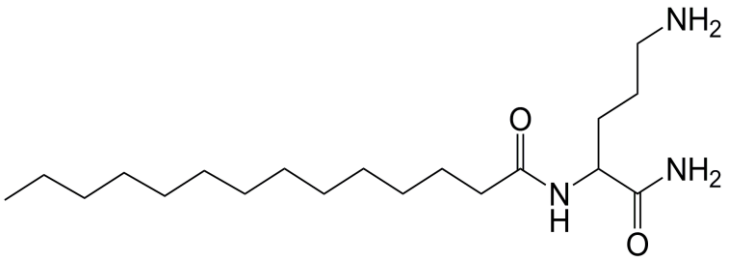

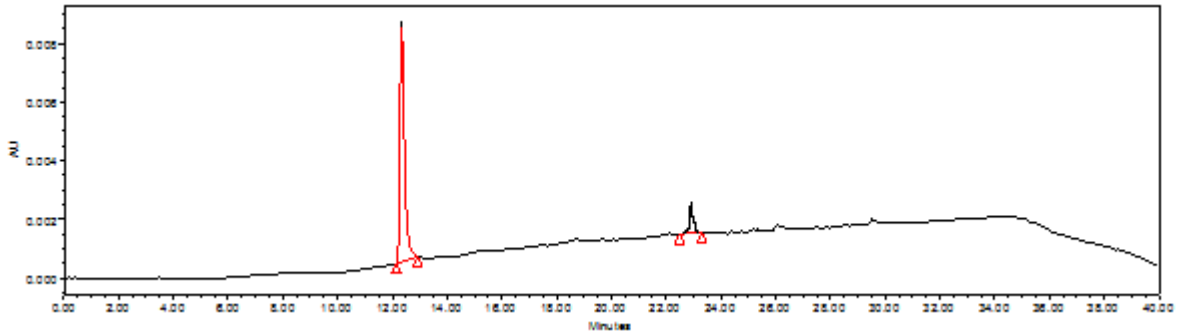

	Name	Retention Time	Area	% Area	Height	RT Ratio
1		12.53	2991528	98.45	159754	
2		22.86	3221	1.55	1533	

Molecular Weight: 341.30

LCMS (+ESI, m/z): 342.38 $(M+H)^+$

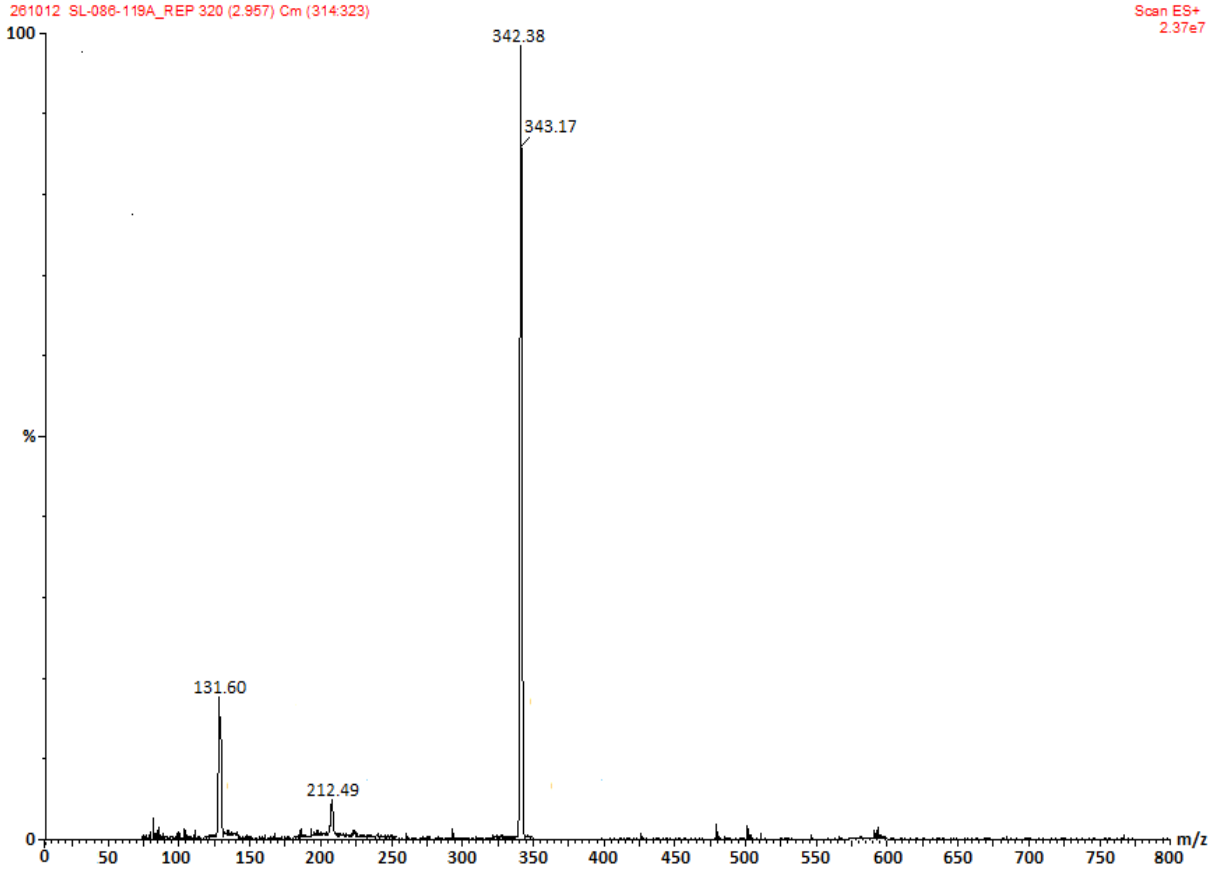

Figure 4.4: Chemical structure, HPLC chromatogram and Mass spectra of **LP04**

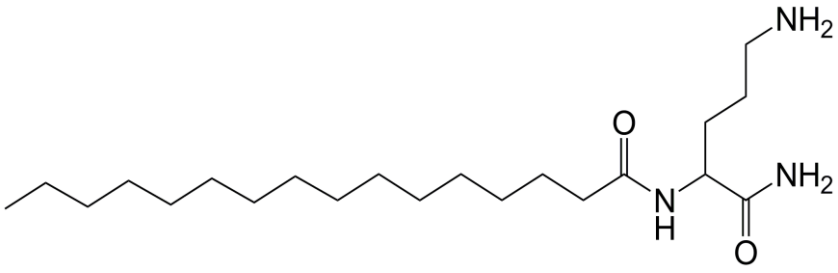

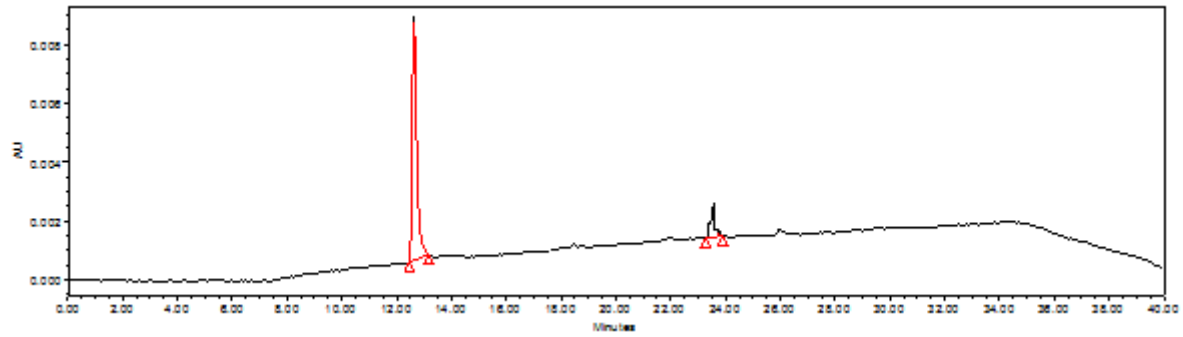

	Name	Retention Time	Area	% Area	Height	RT Ratio
1		12.72	3378945	97.11	91561	
2		23.49	5423	2.89	1267	

Molecular Weight: 369.34

LCMS (+ESI, m/z): 370.10 $(M+H)^+$

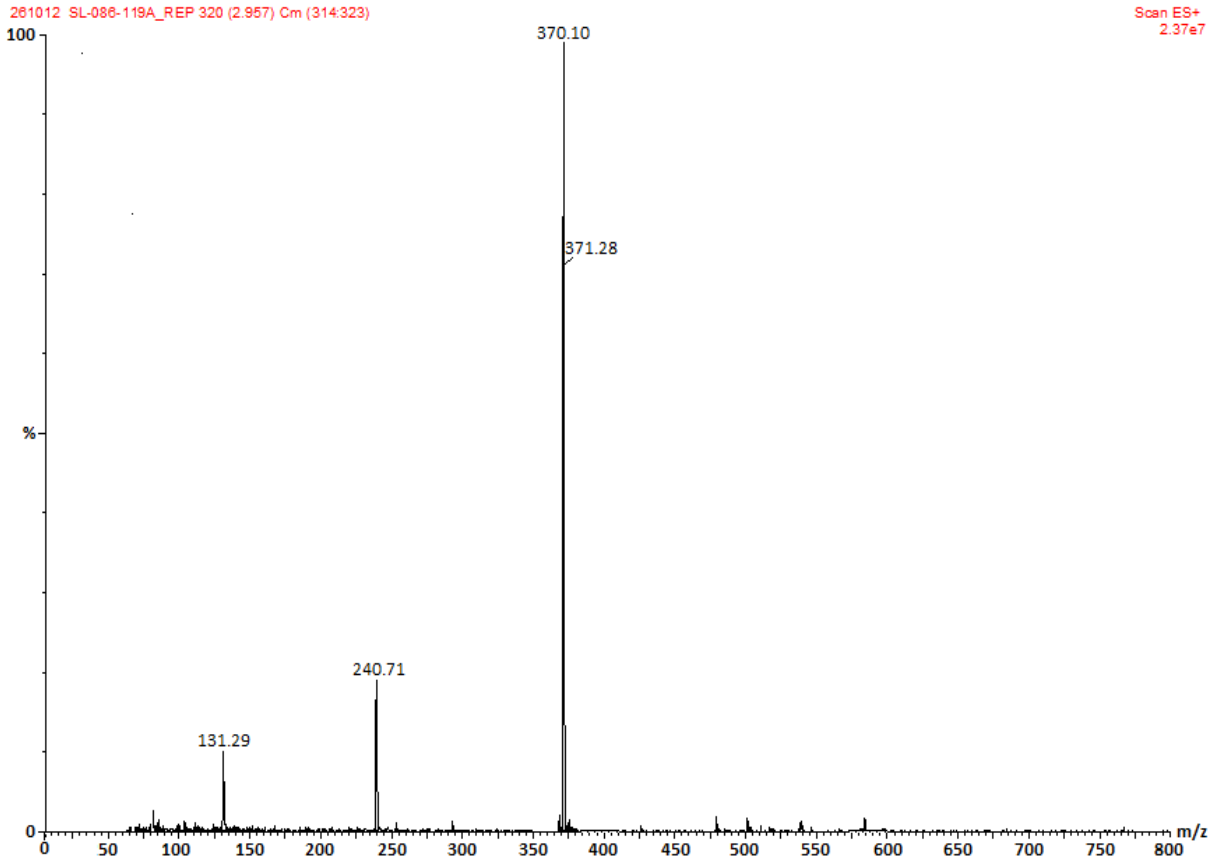

Figure 4.5: Chemical structure, HPLC chromatogram and Mass spectra of **LP05**

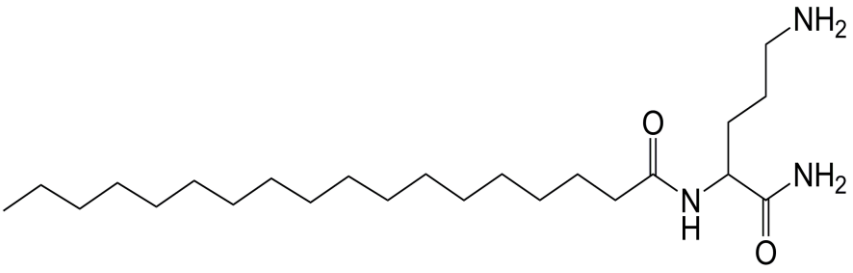

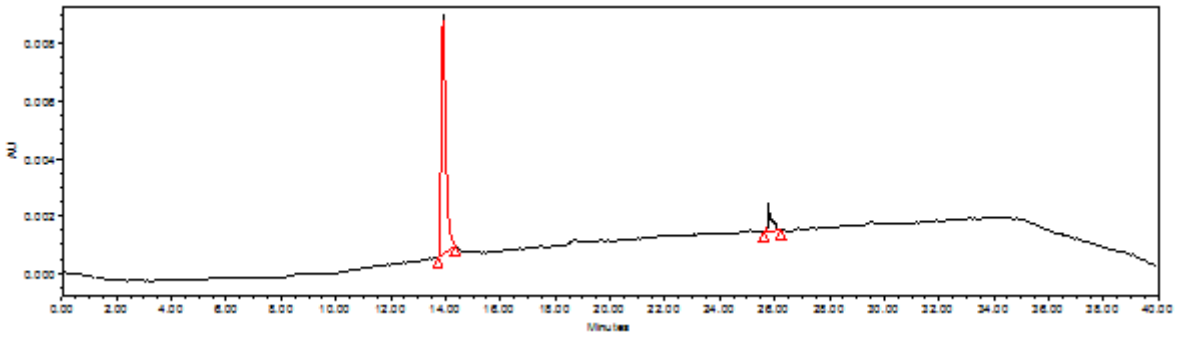

	Name	Retention Time	Area	% Area	Height	RT Ratio
1		13.98	2289756	98.10	90744	
2		27.81	6788	1.90	1120	

Molecular Weight: 397.37

LCMS (+ESI, m/z): 398.07 $(M+H)^+$

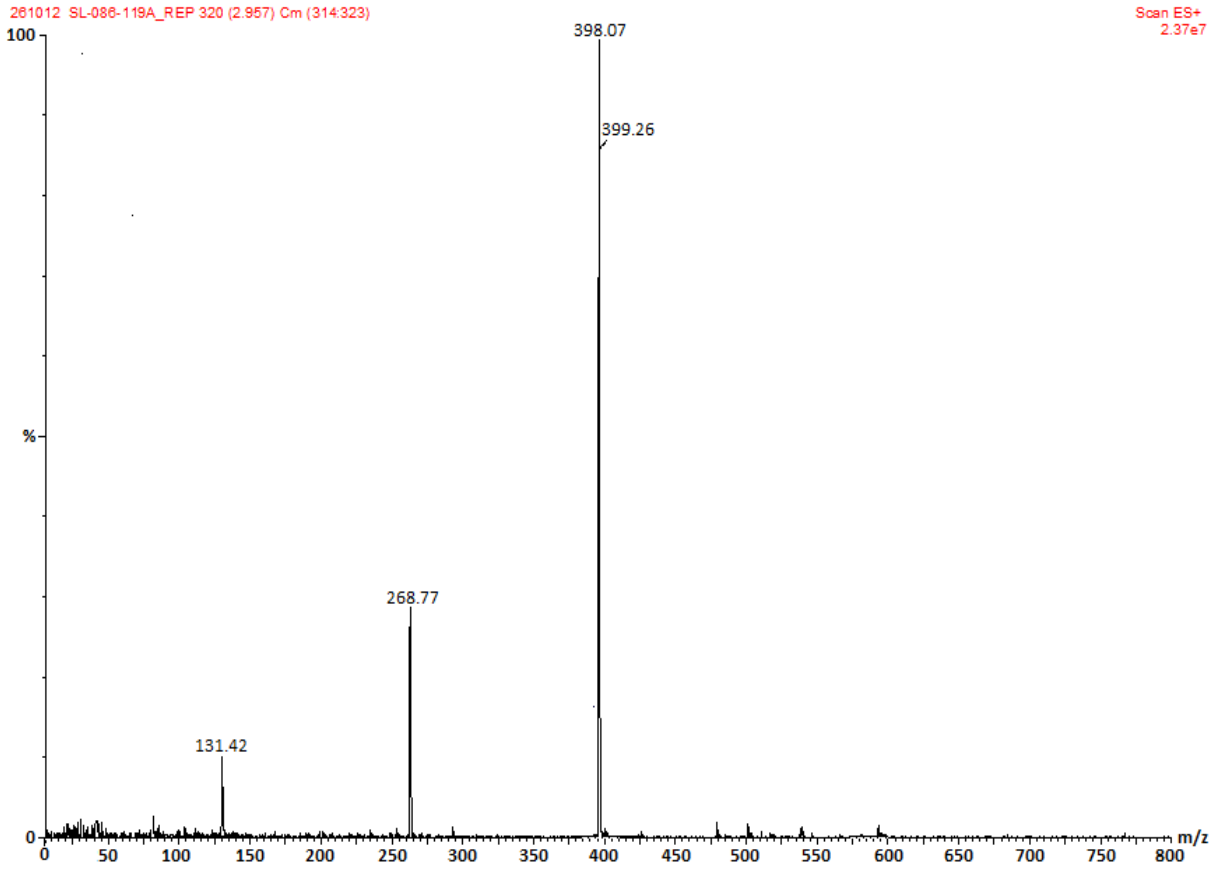

Figure 4.6: Chemical structure, HPLC chromatogram and Mass spectra of **LP06**

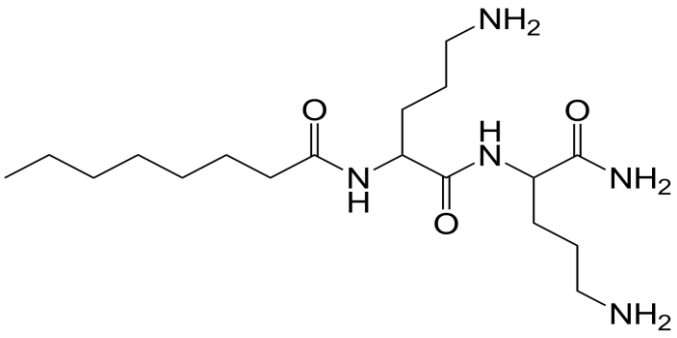

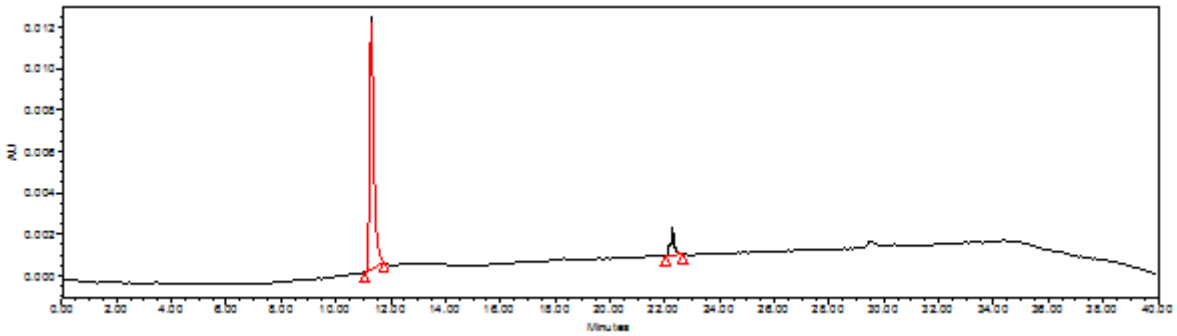

	Name	Retention Time	Area	% Area	Height	RT Ratio
1		11.40	3167890	97.90	170661	
2		22.28	5670	2.10	1139	

Molecular Weight: 371.29

LCMS (+ESI, m/z): 372.10 $(M+H)^+$

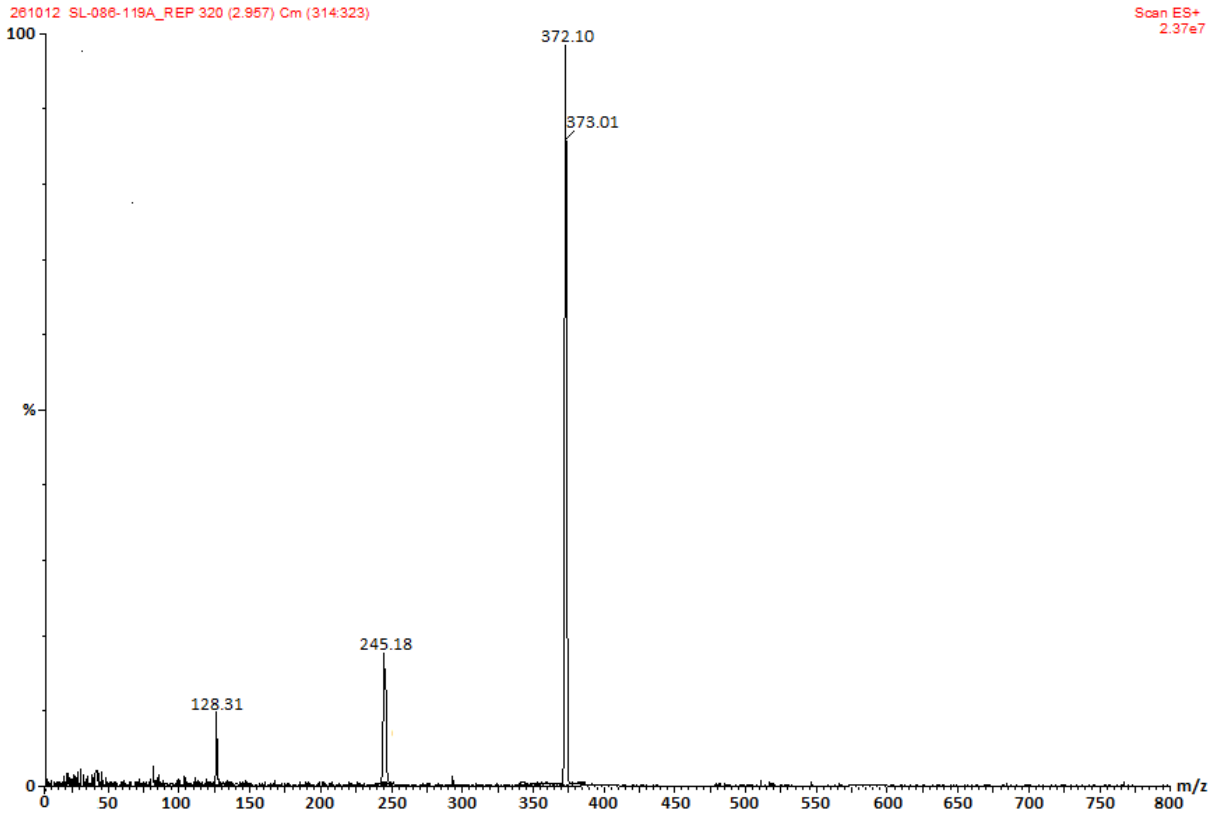

Figure 4.7: Chemical structure, HPLC chromatogram and Mass spectra of **LP07**

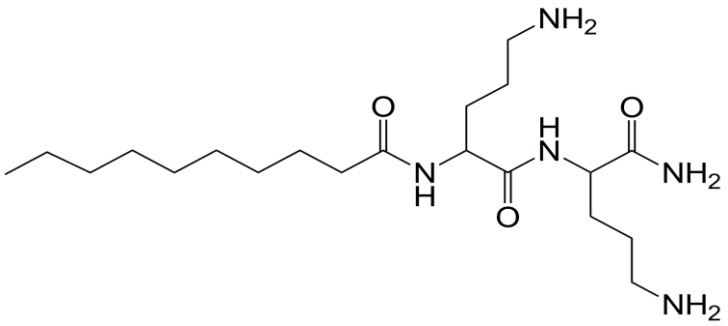

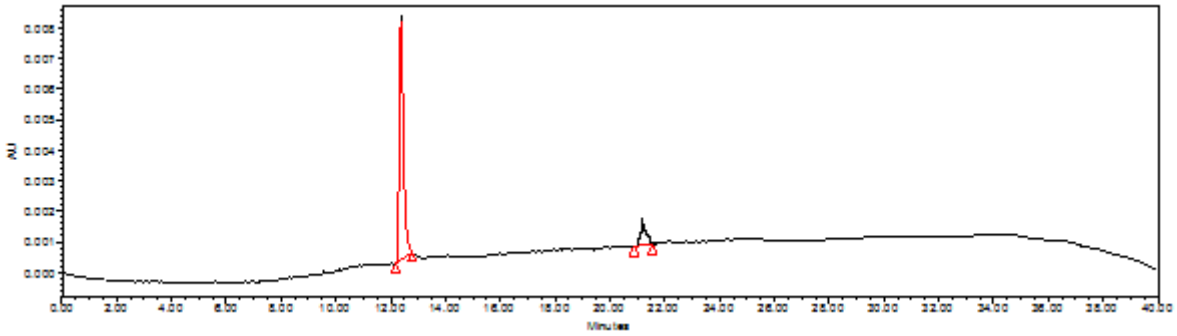

	Name	Retention Time	Area	% Area	Height	RT Ratio
1		12.55	3976981	97.30	163488	
2		21.19	9746	2.70	1951	

Molecular Weight: 399.32

LCMS (+ESI, m/z): 400.41 $(M+H)^+$

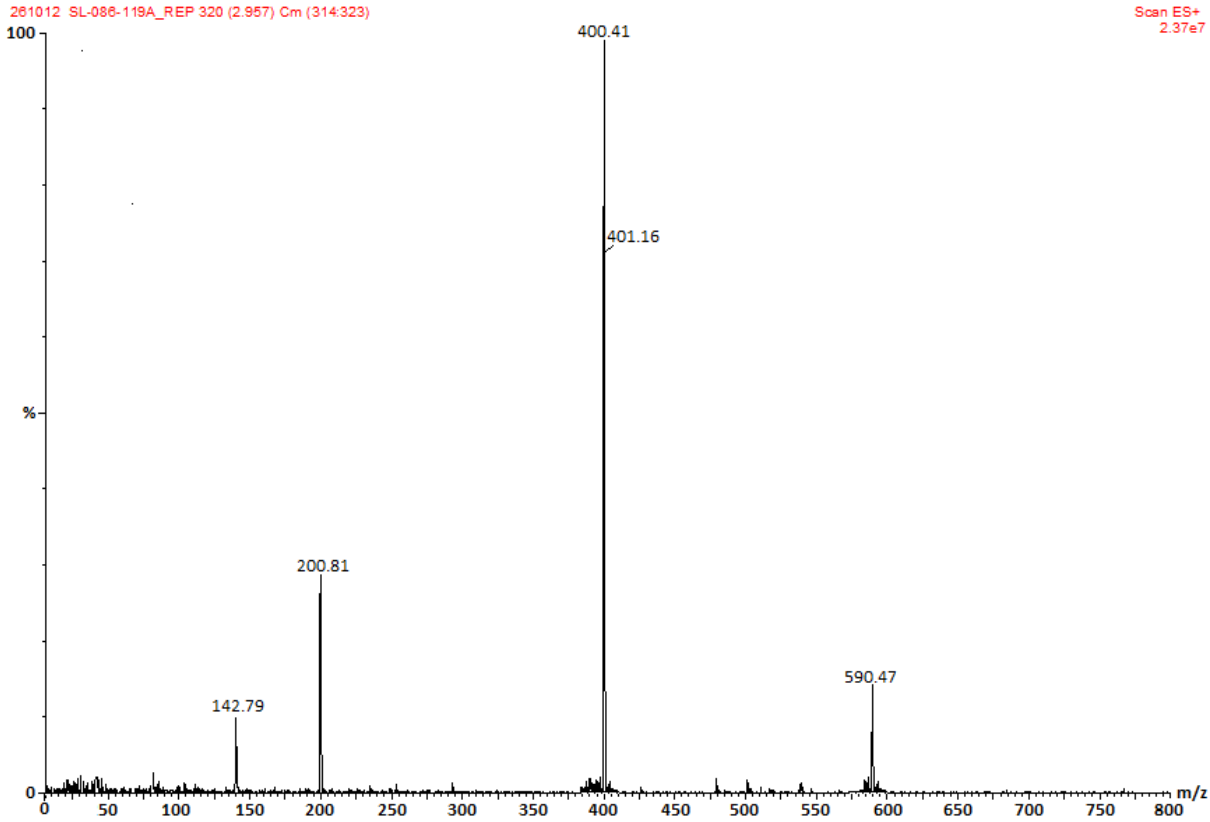

Figure 4.8: Chemical structure, HPLC chromatogram and Mass spectra of **LP08**

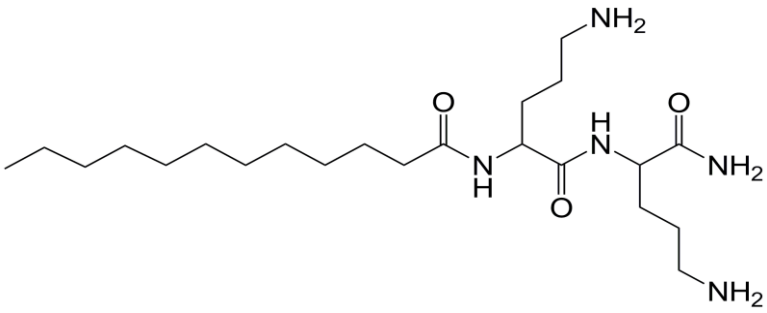

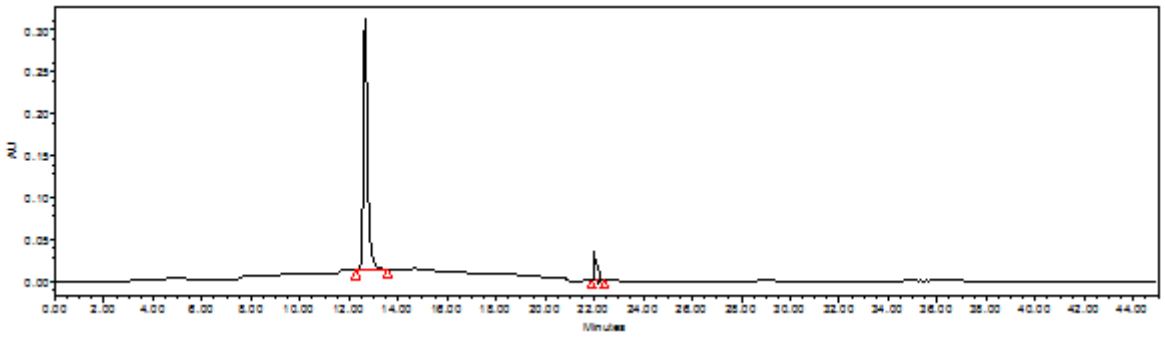

	Name	Retention Time	Area	% Area	Height	RT Ratio
1		12.61	4389956	98.09	172534	
2		22.25	6543	1.91	1785	

Molecular Weight: 427.35

LCMS (+ESI, m/z): 428.42 $(M+H)^+$

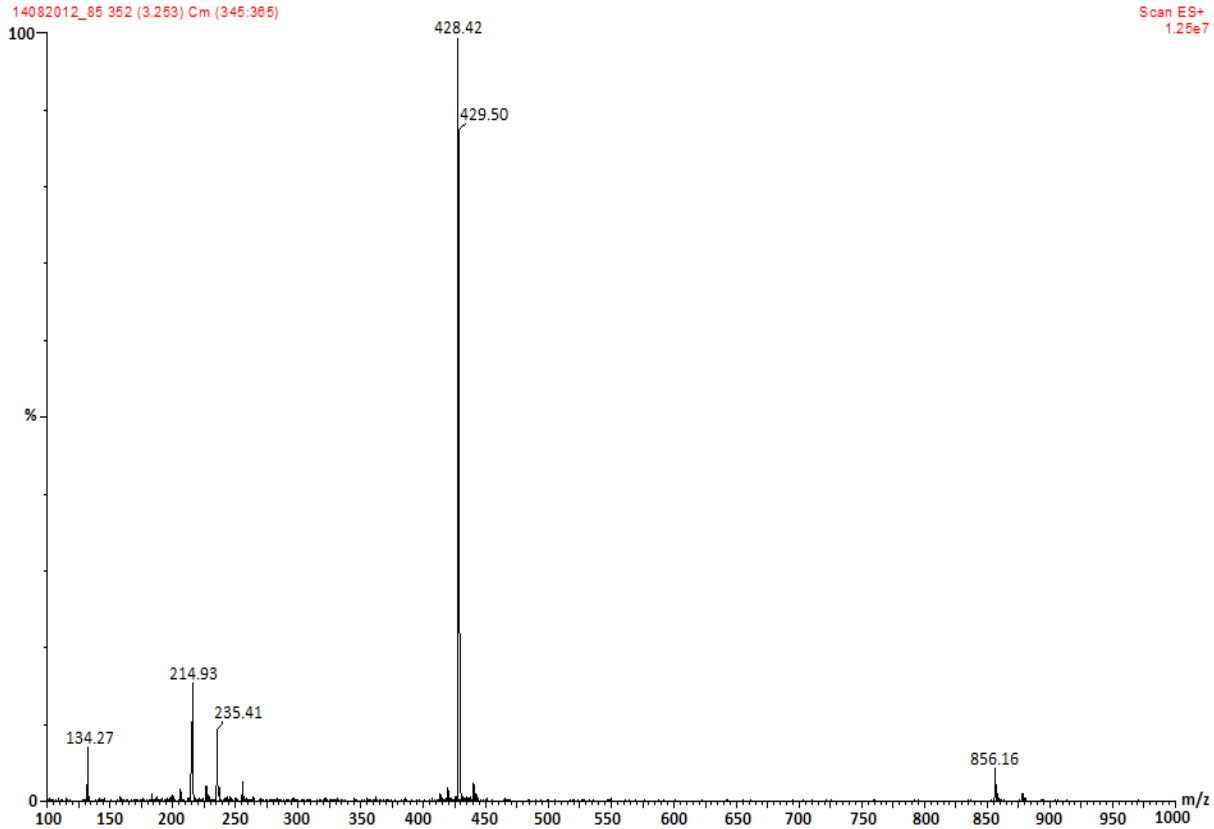

Figure 4.9: Chemical structure, HPLC chromatogram and Mass spectra of **LP09**

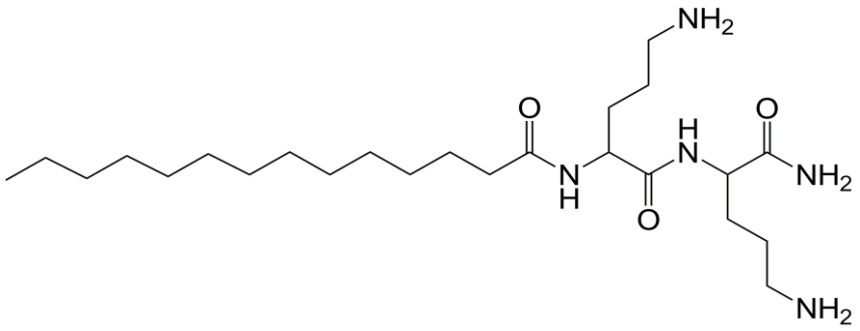

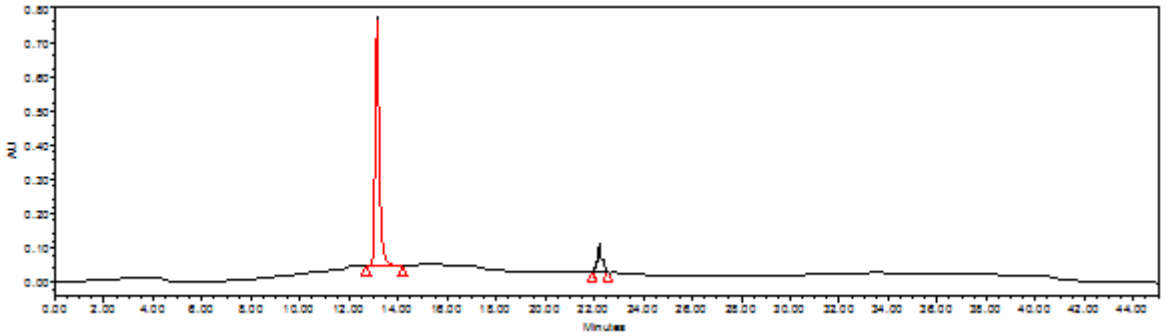

	Name	Retention Time	Area	% Area	Height	RT Ratio
1		13.27	4074561	96.89	101765	
2		22.31	11874	3.11	1284	

Molecular Weight: 455.38

LCMS (+ESI, m/z): 456.45 $(M+H)^+$

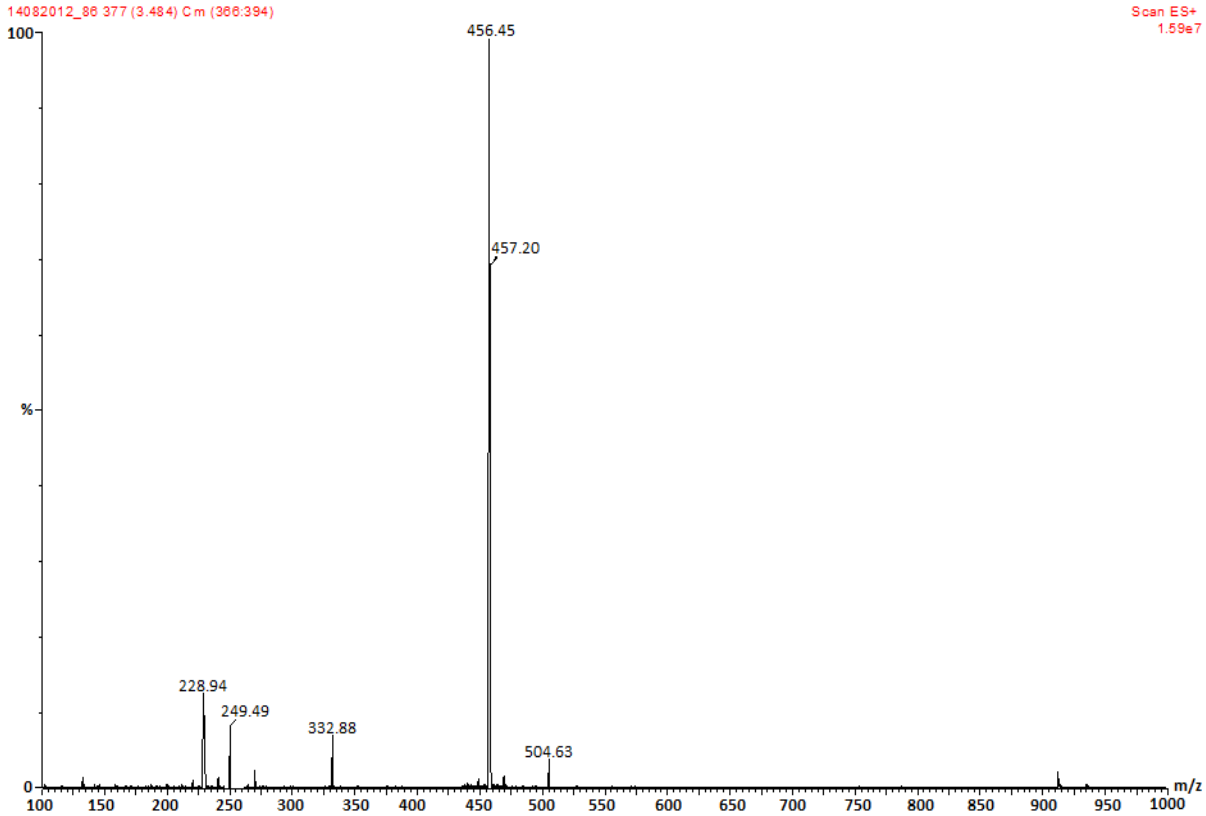

Figure 4.10: Chemical structure, HPLC chromatogram and Mass spectra of **LP10**

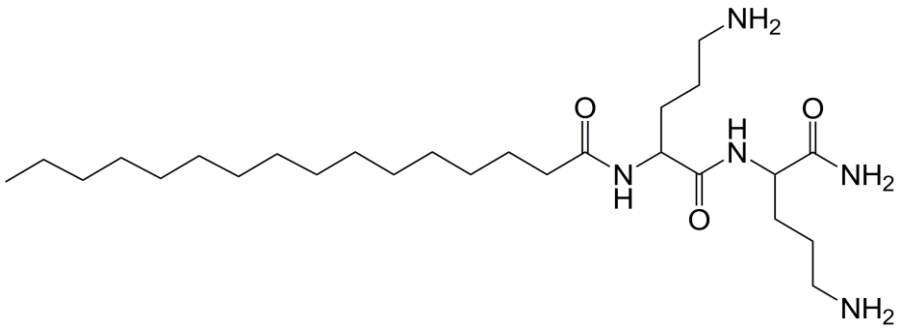

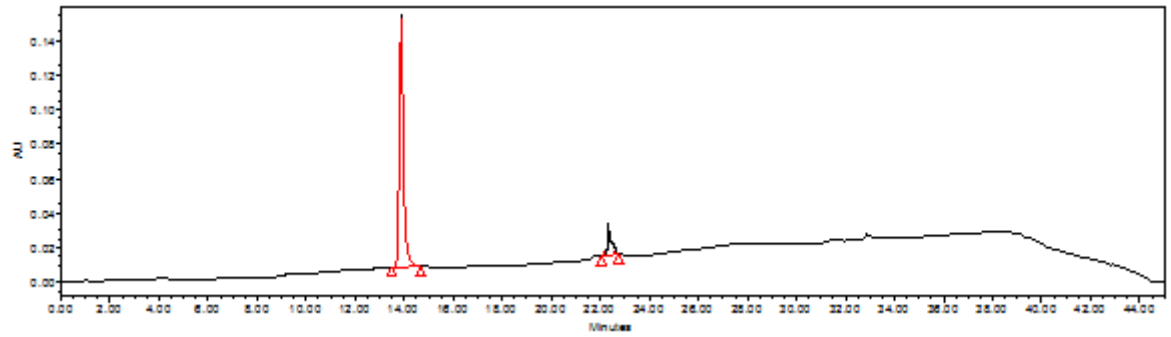

	Name	Retention Time	Area	% Area	Height	RT Ratio
1		14.05	2402725	97.29	163450	
2		22.46	5034215	2.71	1663	

Molecular Weight: 483.41

LCMS (+ESI, m/z): 484.54 $(M+H)^+$

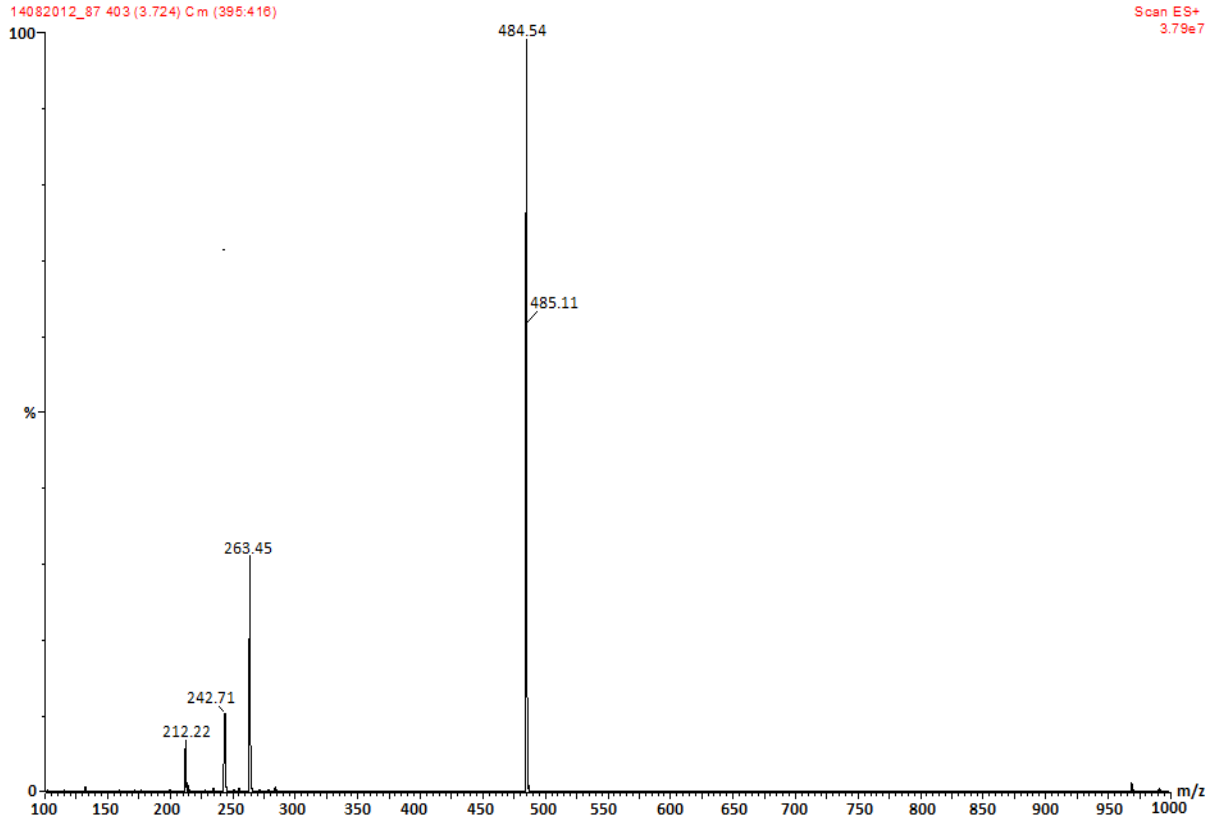

Figure 4.11: Chemical structure, HPLC chromatogram and Mass spectra of **LP11**

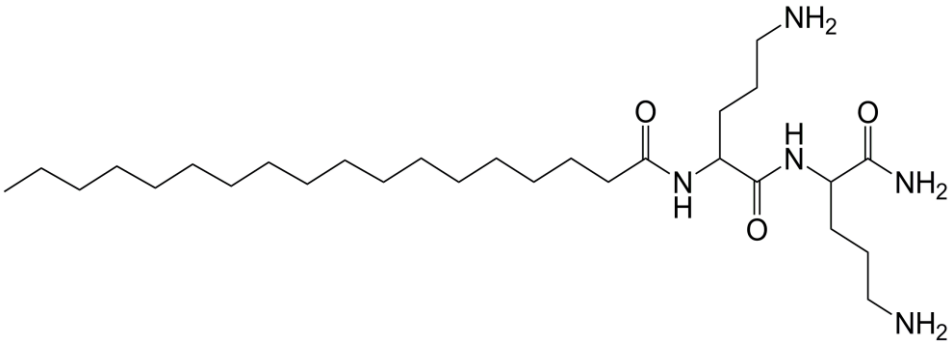

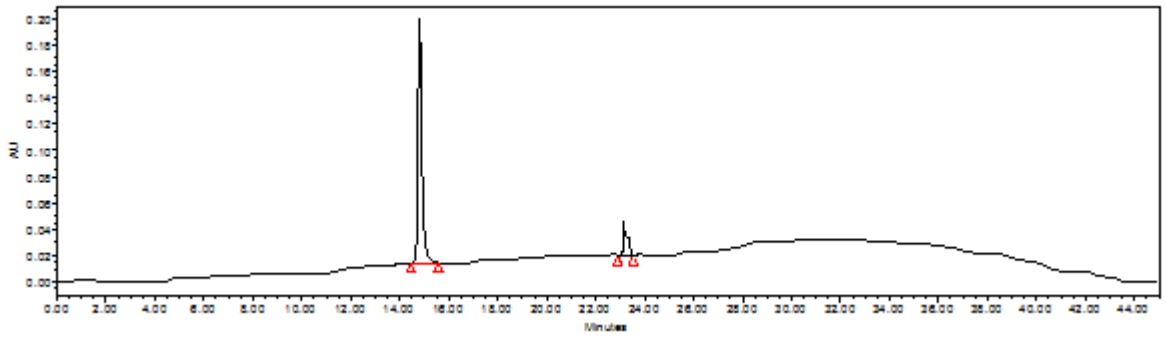

	Name	Retention Time	Area	% Area	Height	RT Ratio
1		14.93	3398117	96.94	190872	
2		23.812	10567	3.06	3099	

Molecular Weight: 511.45

LCMS (+ESI, m/z): 512.57 $(M+H)^+$

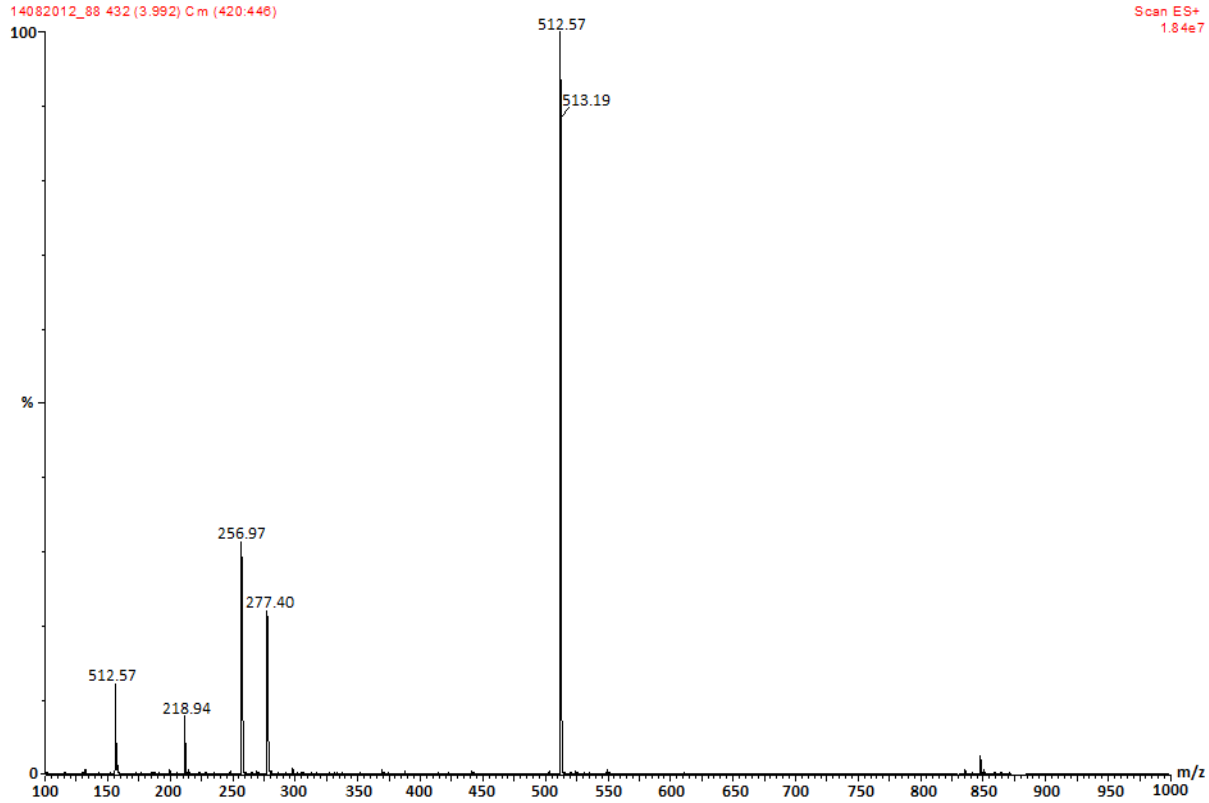

Figure 4.12: Chemical structure, HPLC chromatogram and Mass spectra of **LP12**

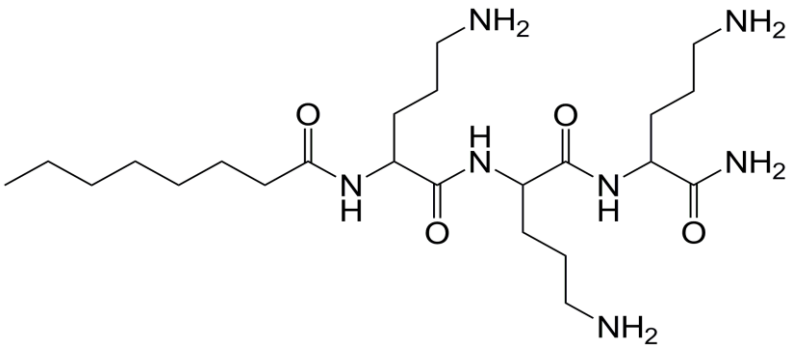

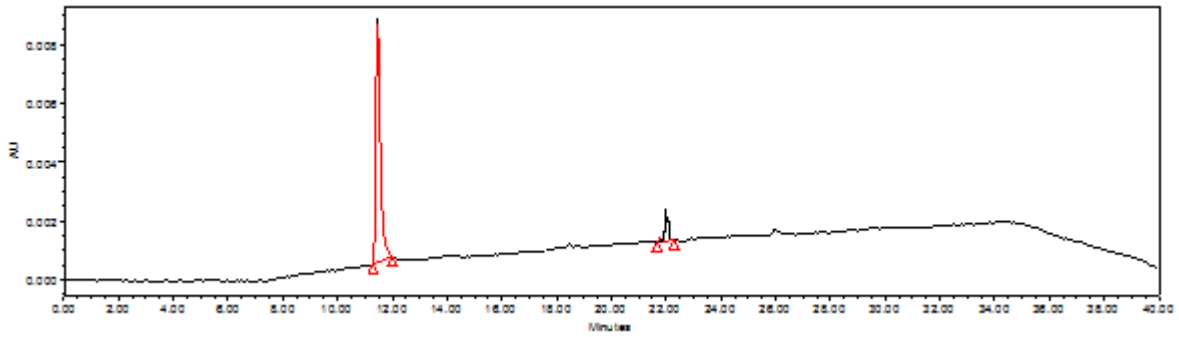

	Name	Retention Time	Area	% Area	Height	RT Ratio
1		11.59	2175890	98.17	206753	
2		22.08	4215	1.83	1253	

Molecular Weight: 485.37

LCMS (+ESI, m/z): 486.40 $(M+H)^+$

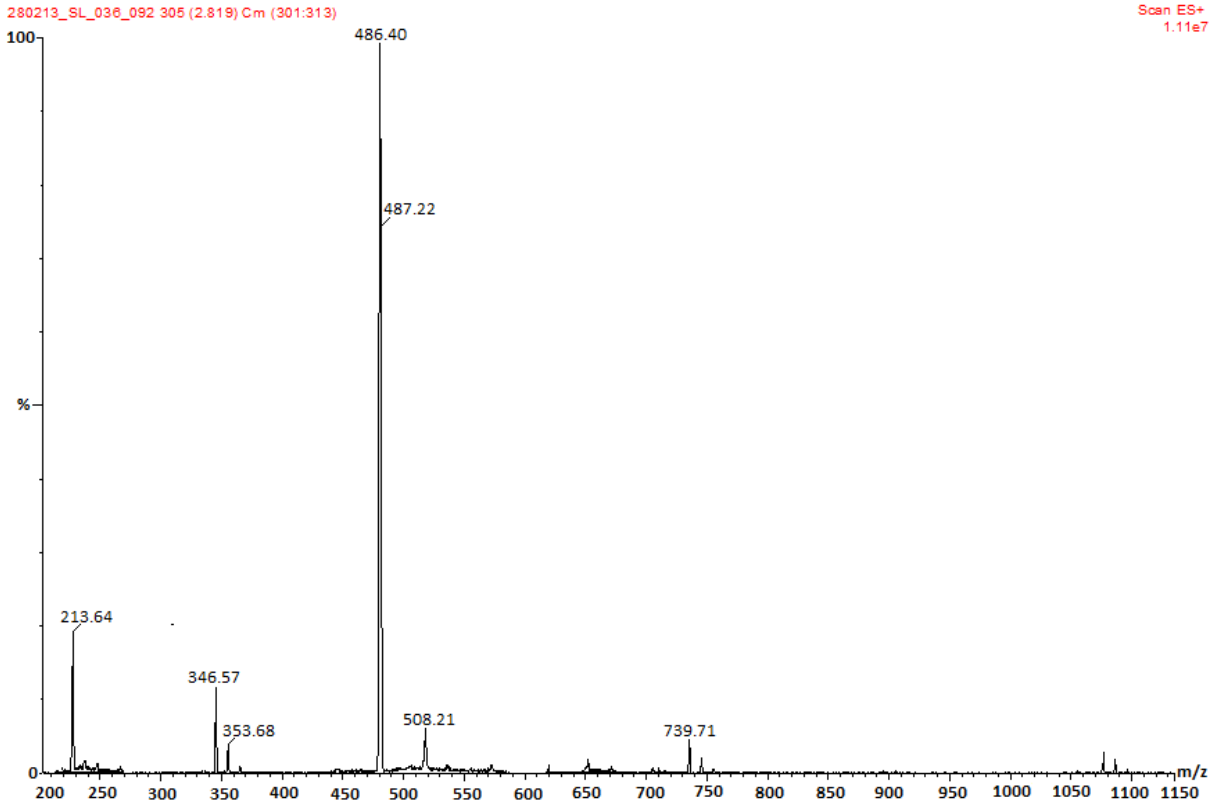

Figure 4.13: Chemical structure, HPLC chromatogram and Mass spectra of **LP13**

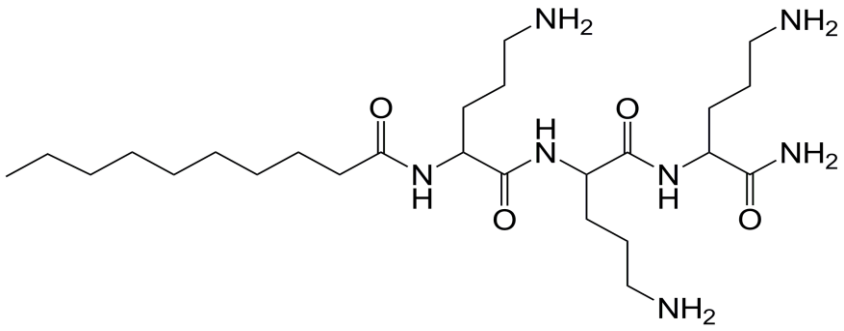

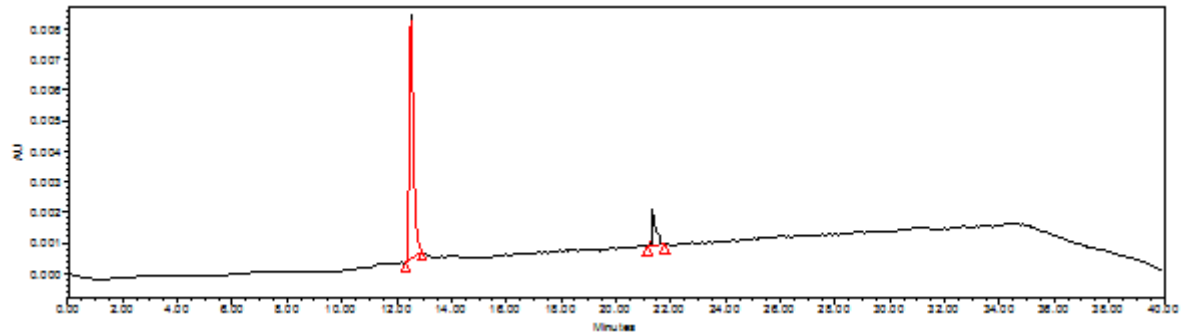

	Name	Retention Time	Area	% Area	Height	RT Ratio
1		12.58	3956761	97.73	187642	
2		21.47	9788	2.27	1419	

Molecular Weight: 513.40

LCMS (+ESI, m/z): 514.40 $(M+H)^+$

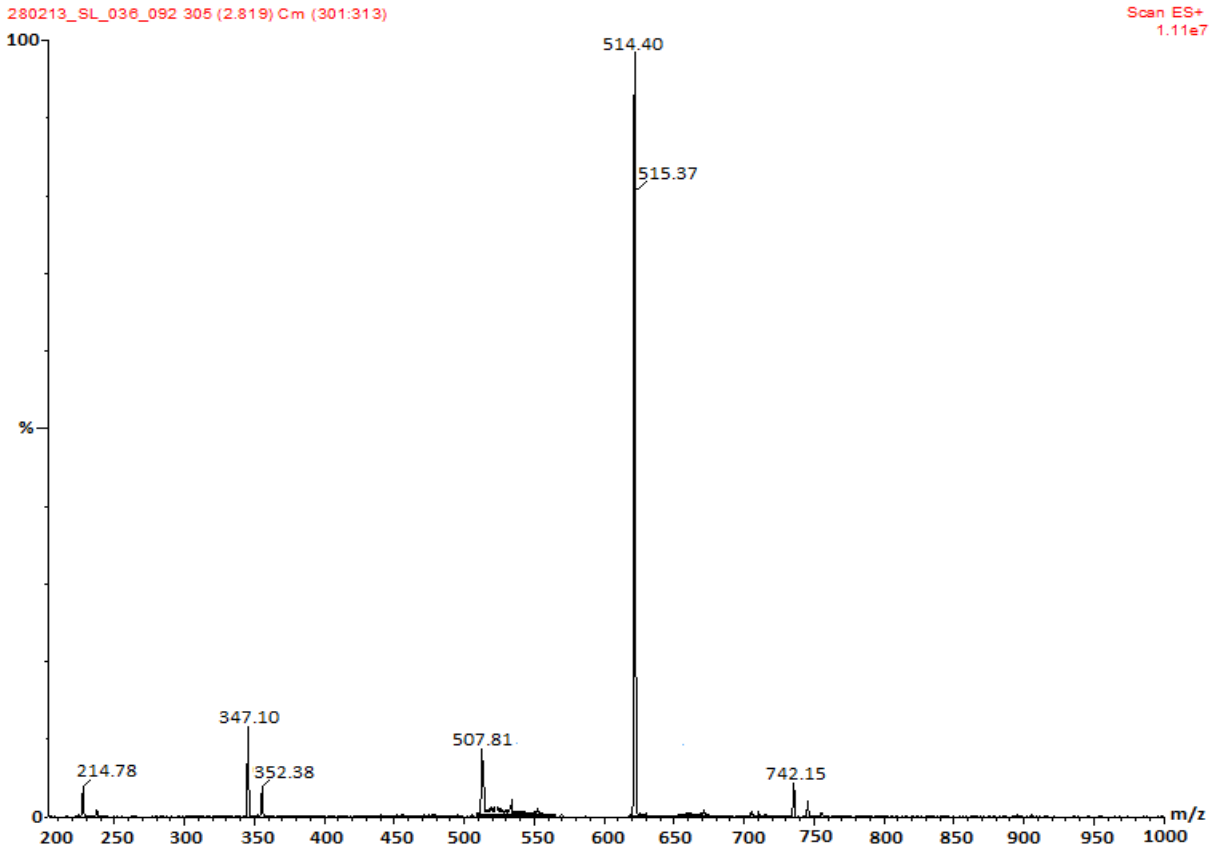

Figure 4.14: Chemical structure, HPLC chromatogram and Mass spectra of **LP14**

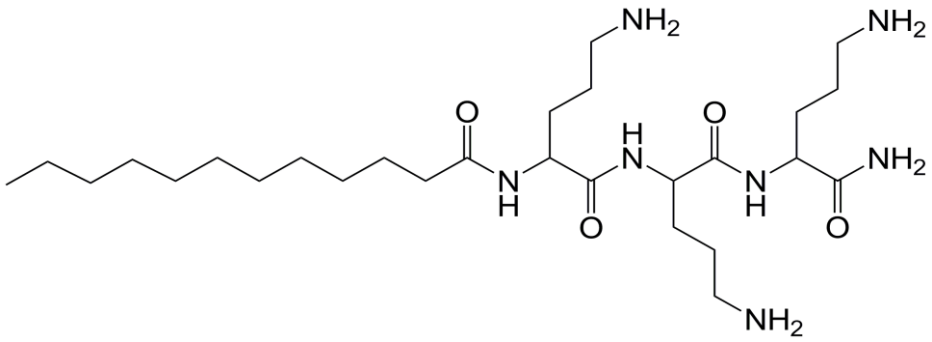

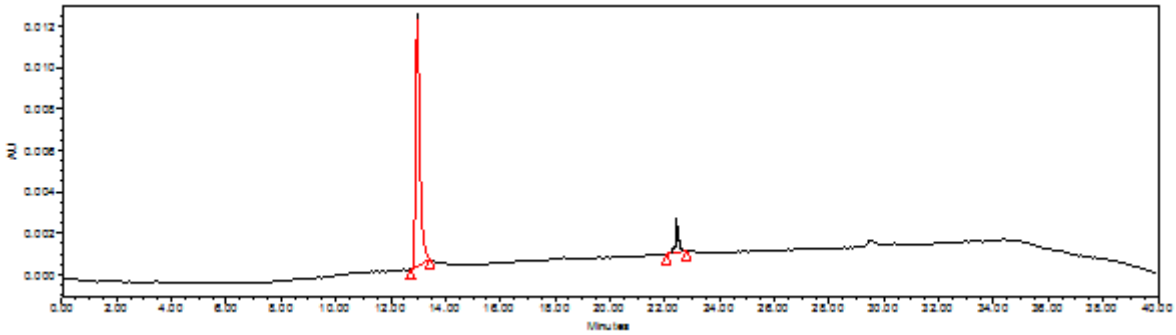

	Name	Retention Time	Area	% Area	Height	RT Ratio
1		13.24	3788641	99.08	186217	
2		22.40	7522	0.92	1671	

Molecular Weight: 541.43

LCMS (+ESI, m/z): 542.40 $(M+H)^+$

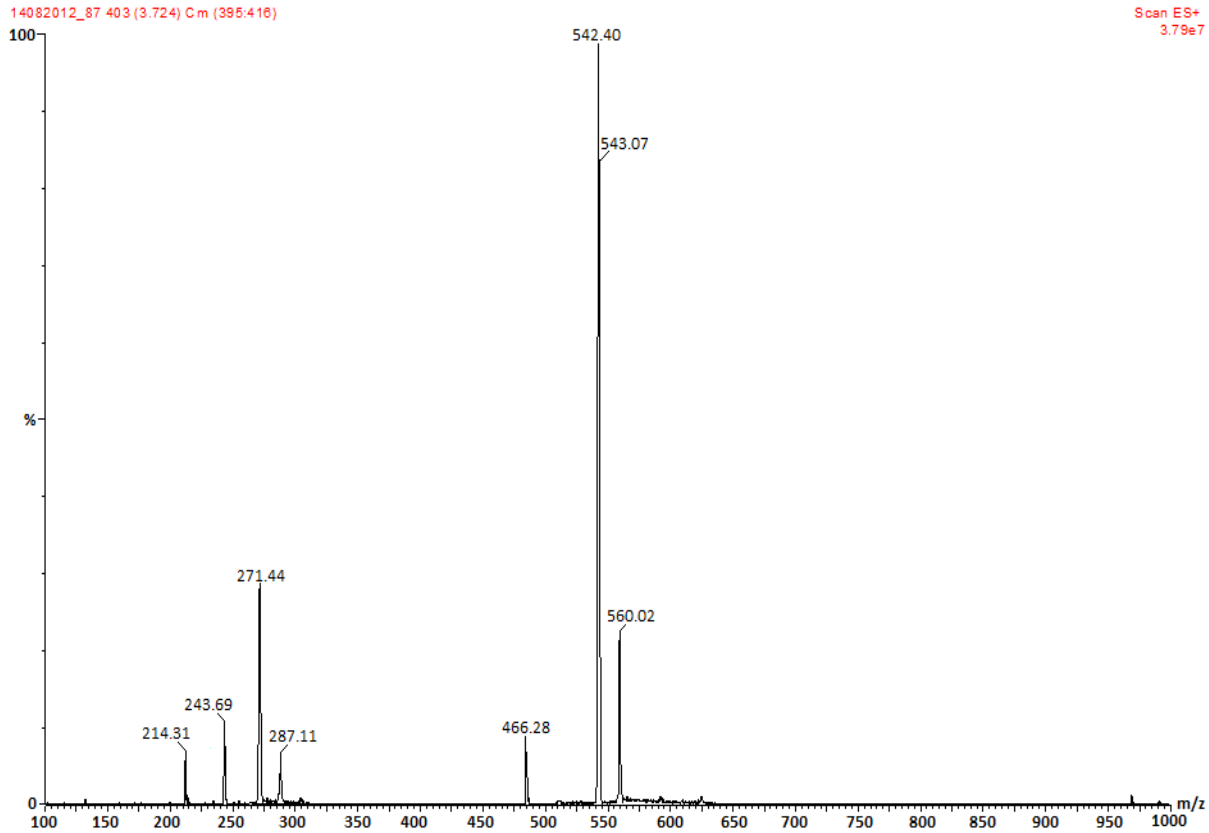

Figure 4.15: Chemical structure, HPLC chromatogram and Mass spectra of **LP15**

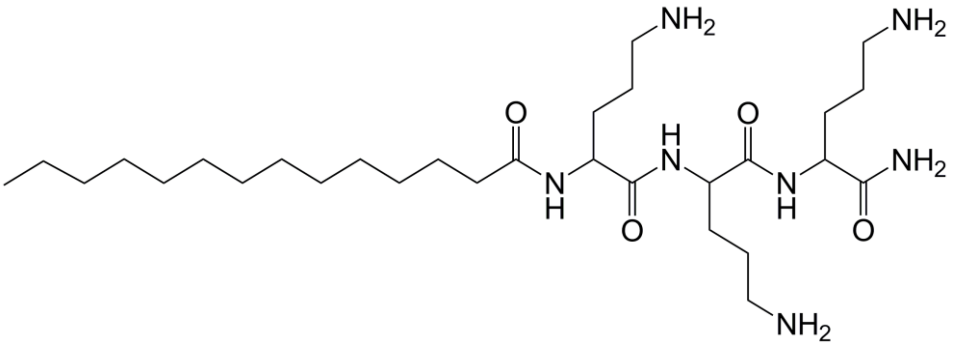

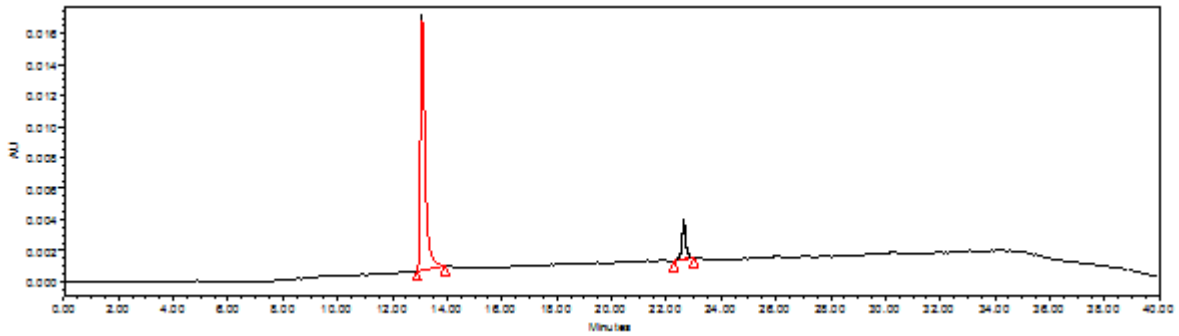

	Name	Retention Time	Area	% Area	Height	RT Ratio
1		13.44	5178930	97.54	93566	
2		22.73	21537	2.46	2190	

Molecular Weight: 569.46

LCMS (+ESI, m/z): 570.34 $(M+H)^+$

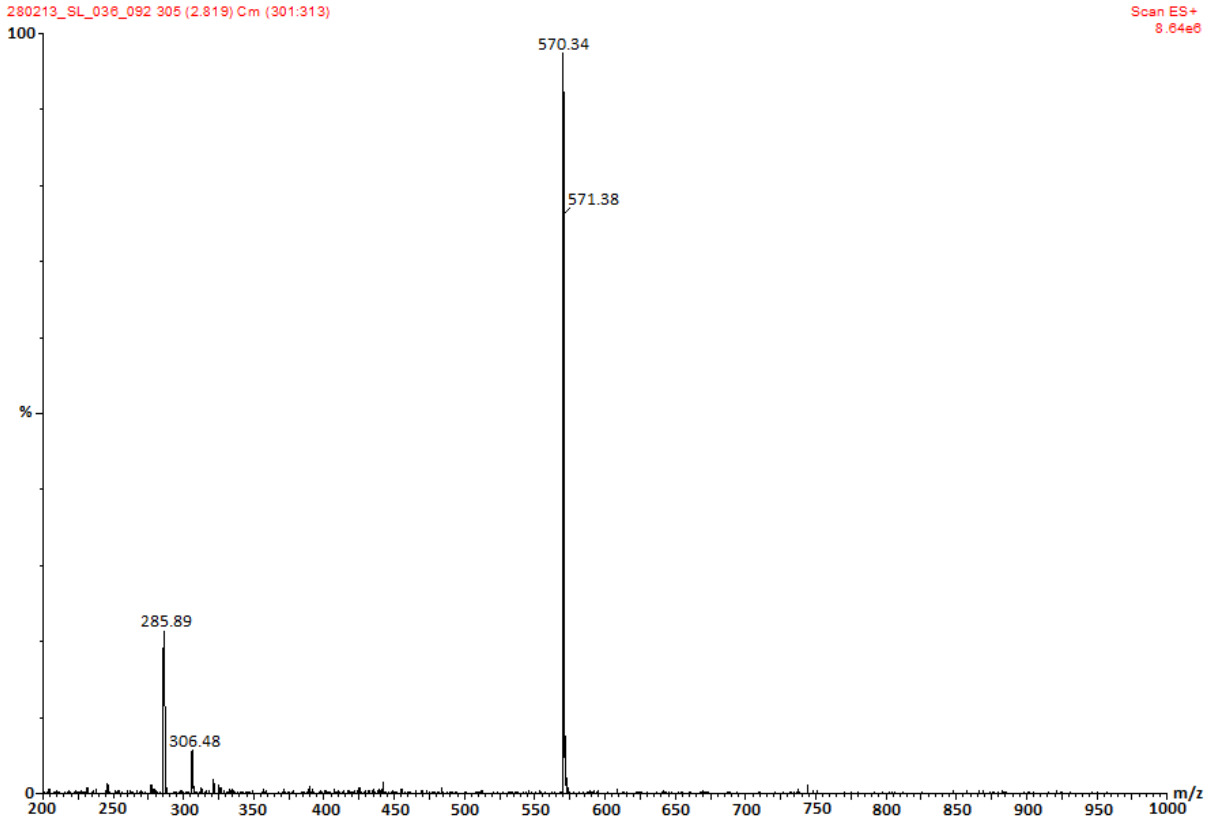

Figure 4.16: Chemical structure, HPLC chromatogram and Mass spectra of **LP16**

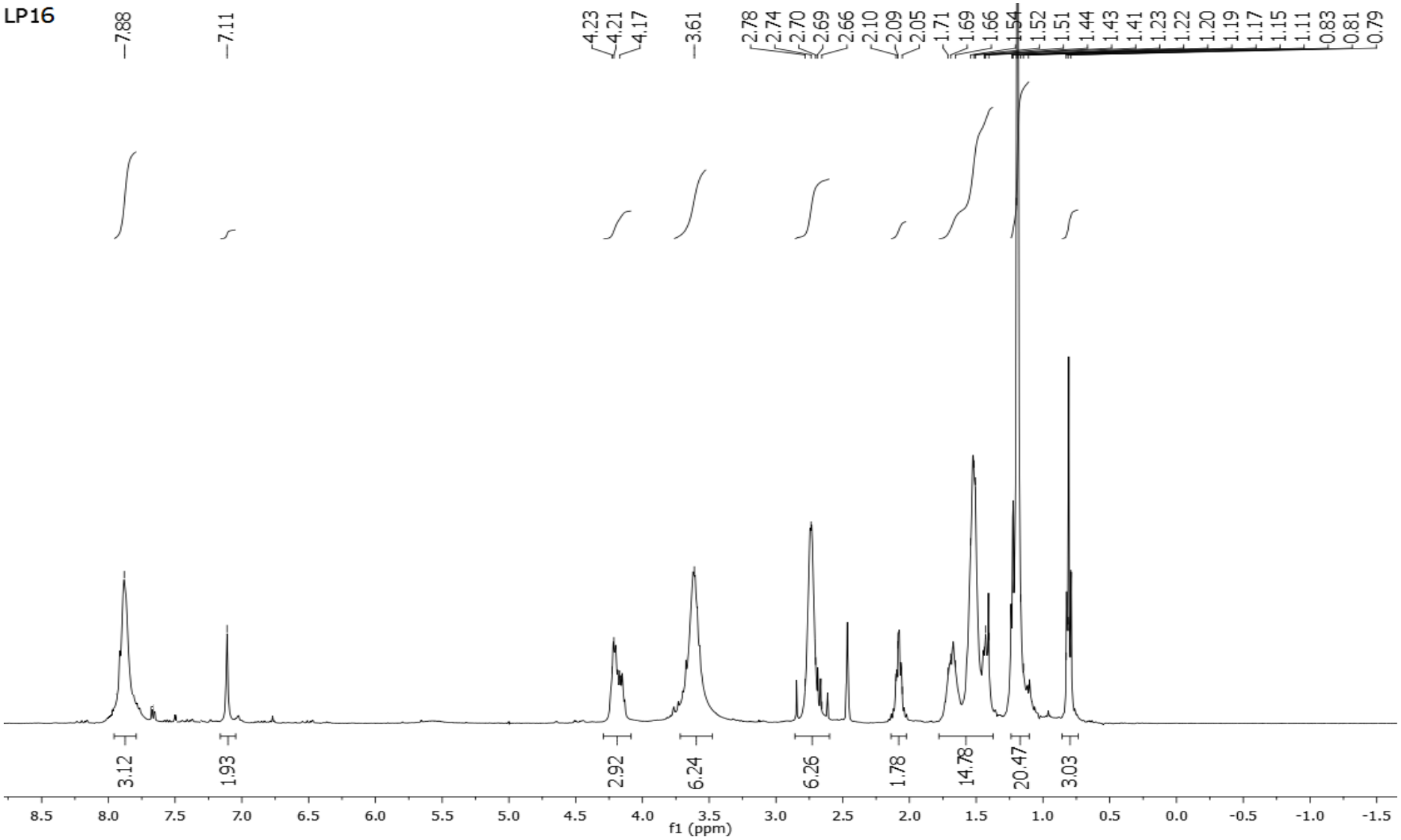

Figure 4.17: ^{1}H NMR (400 MHz, DMSO d_6) spectra of lipopeptide molecule **LP16**

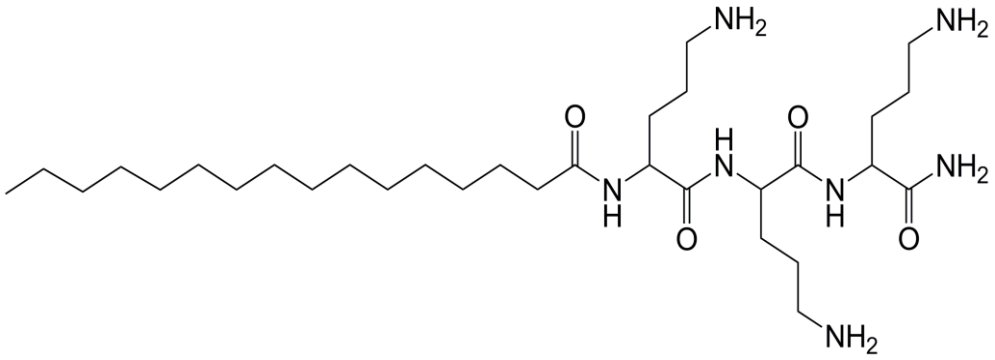

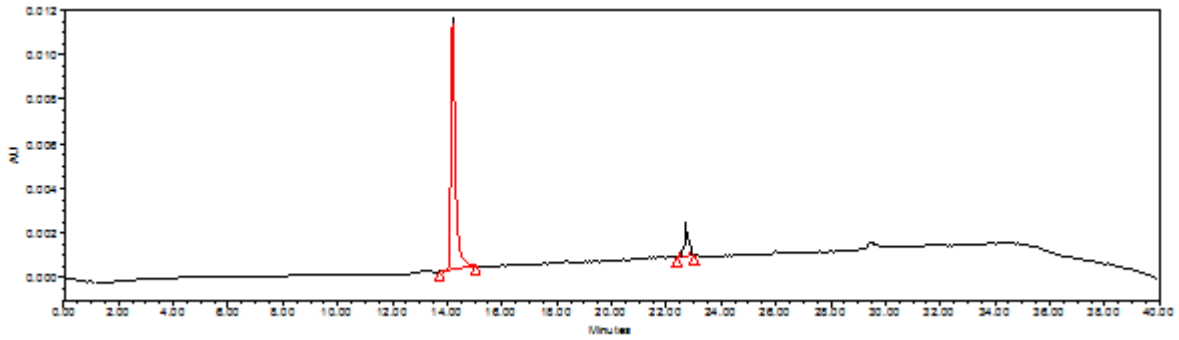

	Name	Retention Time	Area	% Area	Height	RT Ratio
1		14.36	4756980	96.97	191427	
2		22.90	17435	3.03	1780	

Molecular Weight: 597.49

LCMS (+ESI, m/z): 598.37 $(M+H)^+$

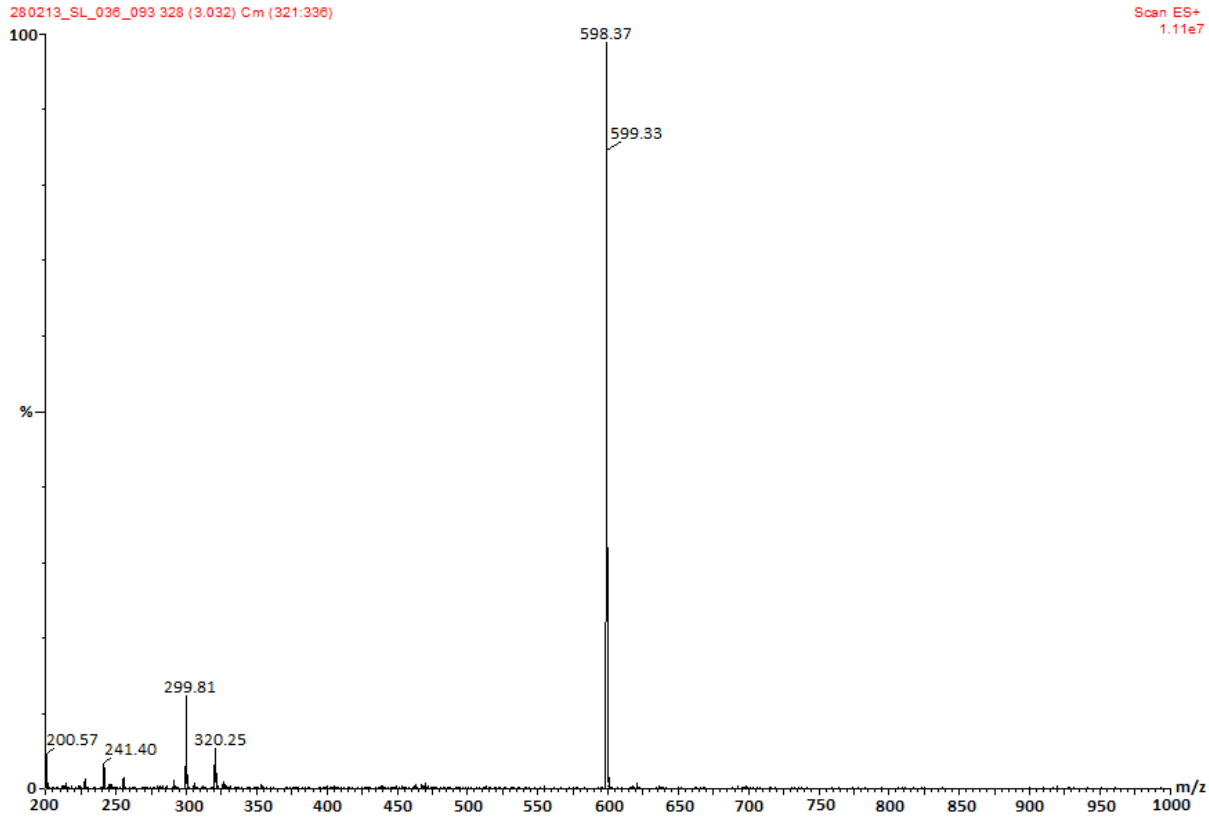

Figure 4.18: Chemical structure, HPLC chromatogram and Mass spectra of **LP17**

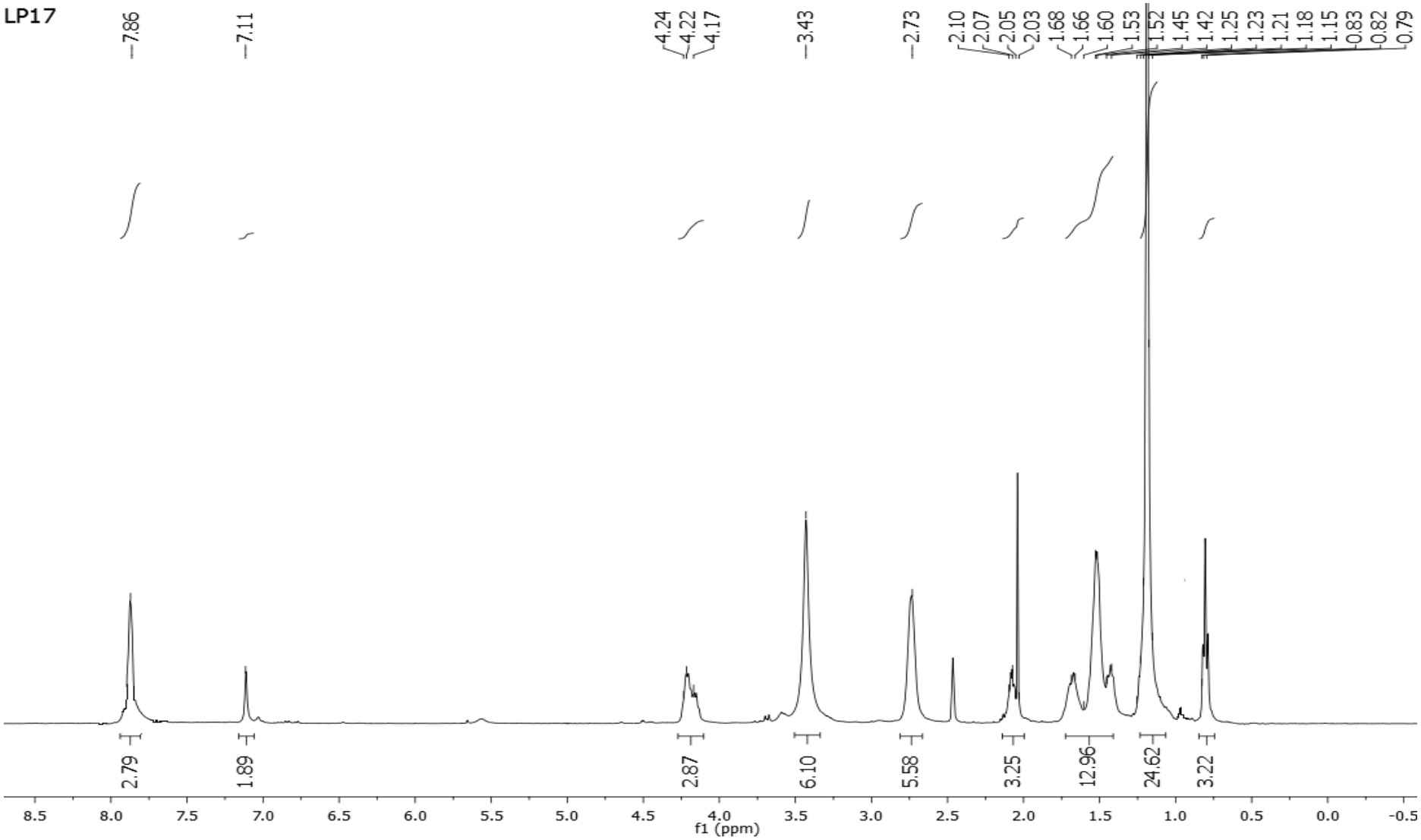

Figure 4.19: ^{1}H NMR (400 MHz, DMSO d_6) spectra of lipopeptide molecule **LP17**

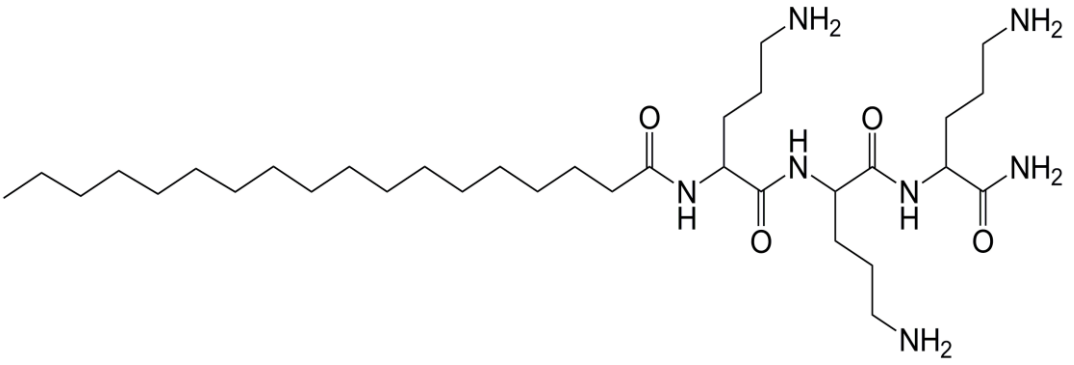

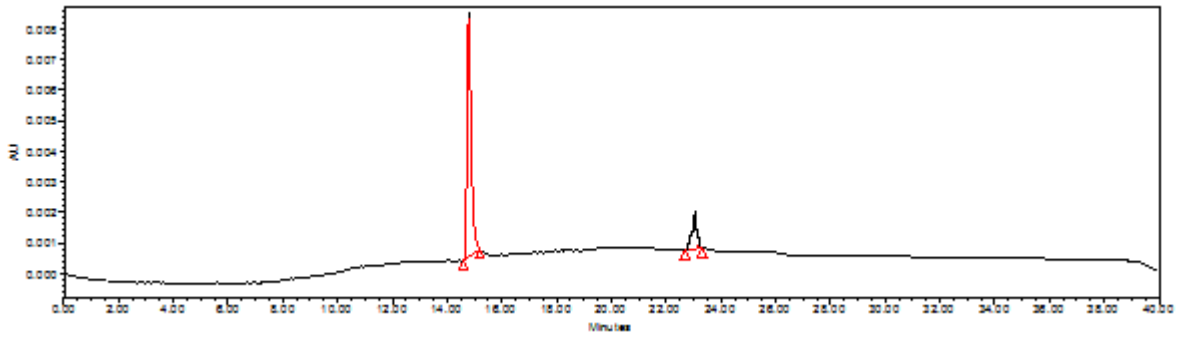

	Name	Retention Time	Area	% Area	Height	RT Ratio
1		15.11	4865781	96.63	198762	
2		23.18	20357	3.37	2241	

Molecular Weight: 625.53

LCMS (+ESI, m/z): 626.50 $(M+H)^+$

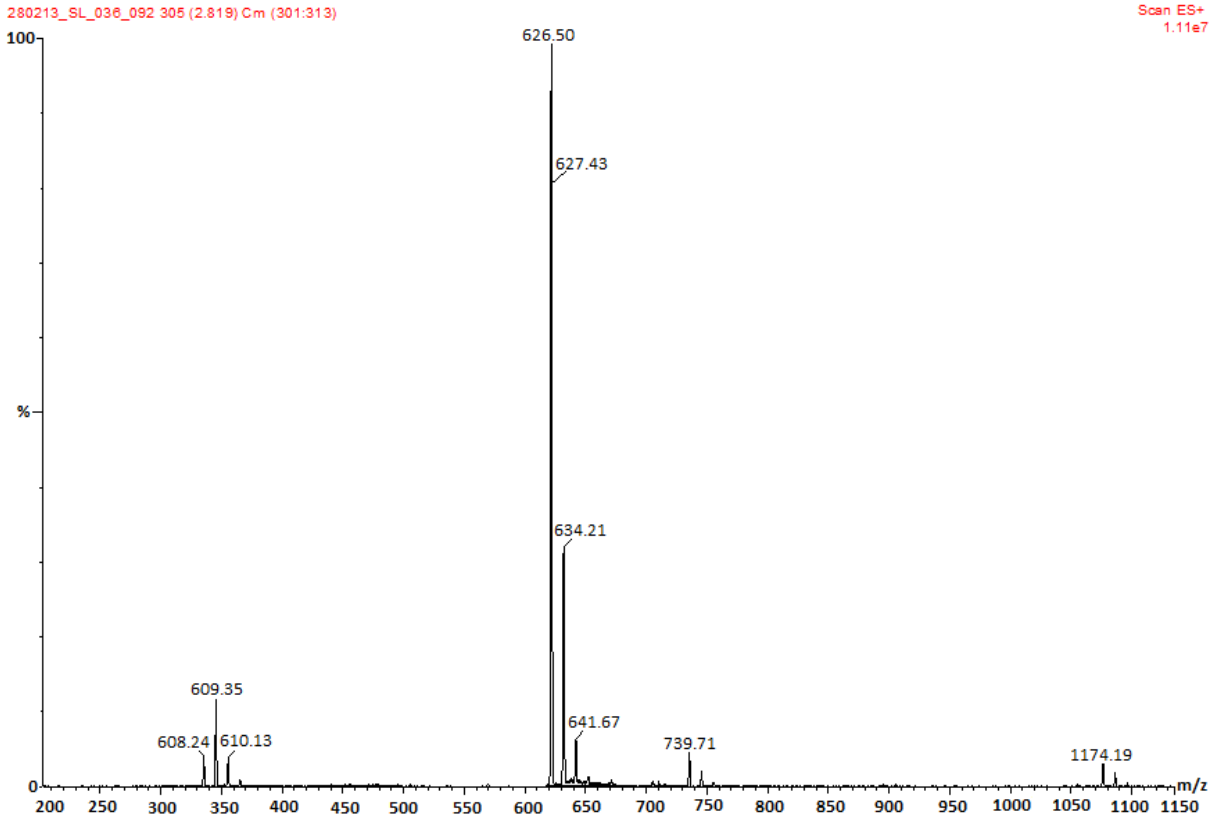

Figure 4.20: Chemical structure, HPLC chromatogram and Mass spectra of **LP18**

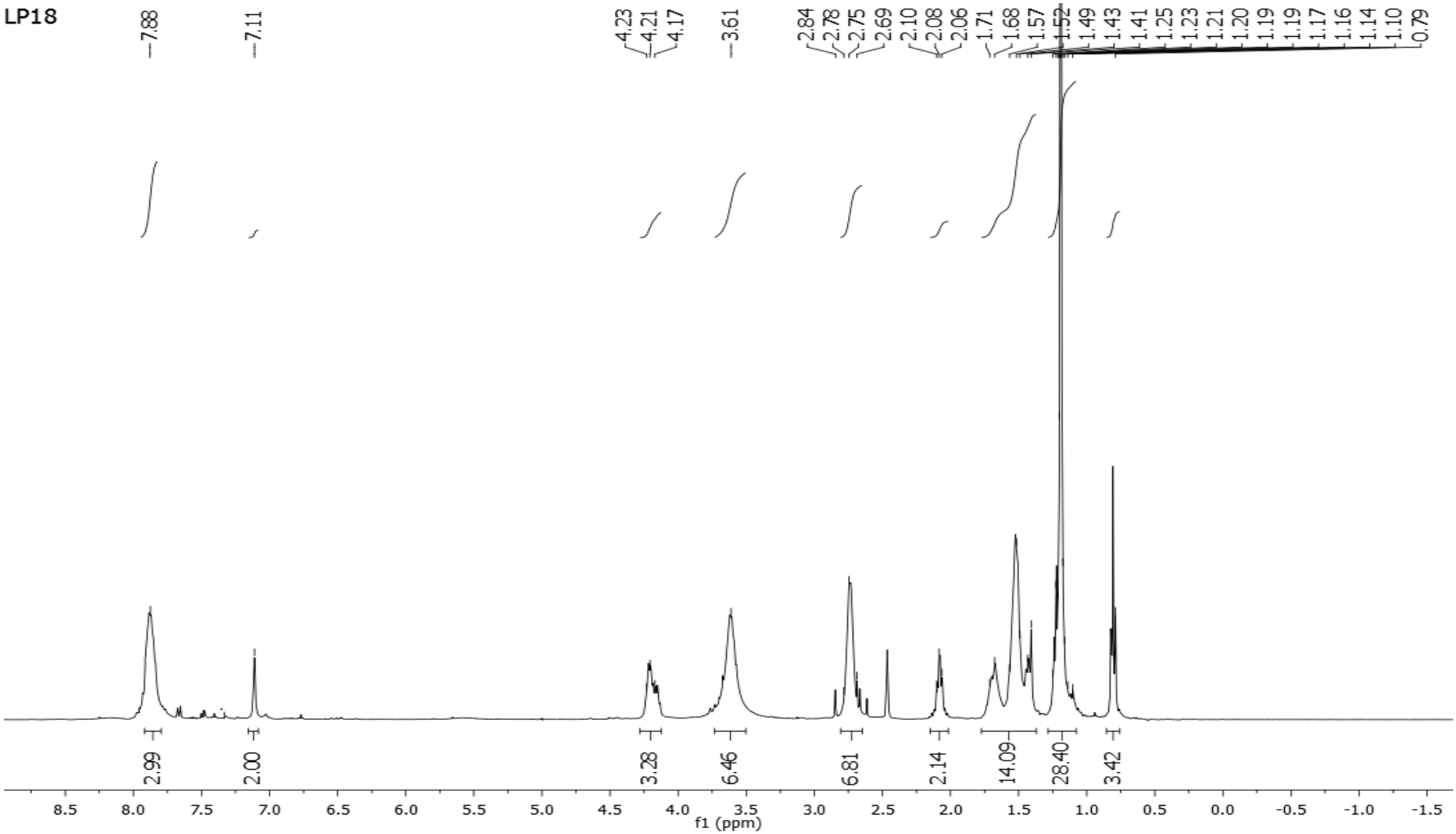

Figure 4.21: ^{1}H NMR (400 MHz, DMSO d_6) spectra of lipopeptide molecule **LP18**

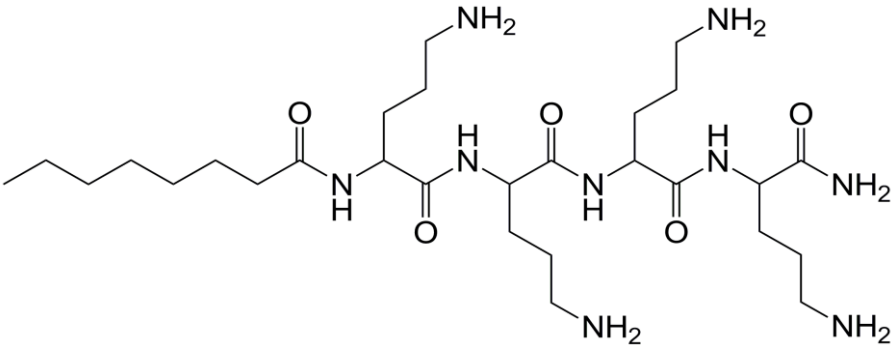

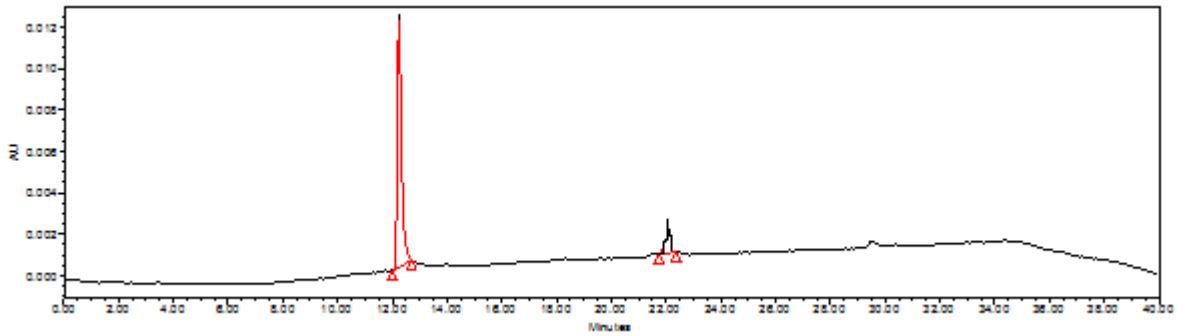

	Name	Retention Time	Area	% Area	Height	RT Ratio
1		12.20	4456892	97.36	178330	
2		22.04	12751	2.64	1980	

Molecular Weight: 599.45

LCMS (+ESI, m/z): 600.29 $(M+H)^+$

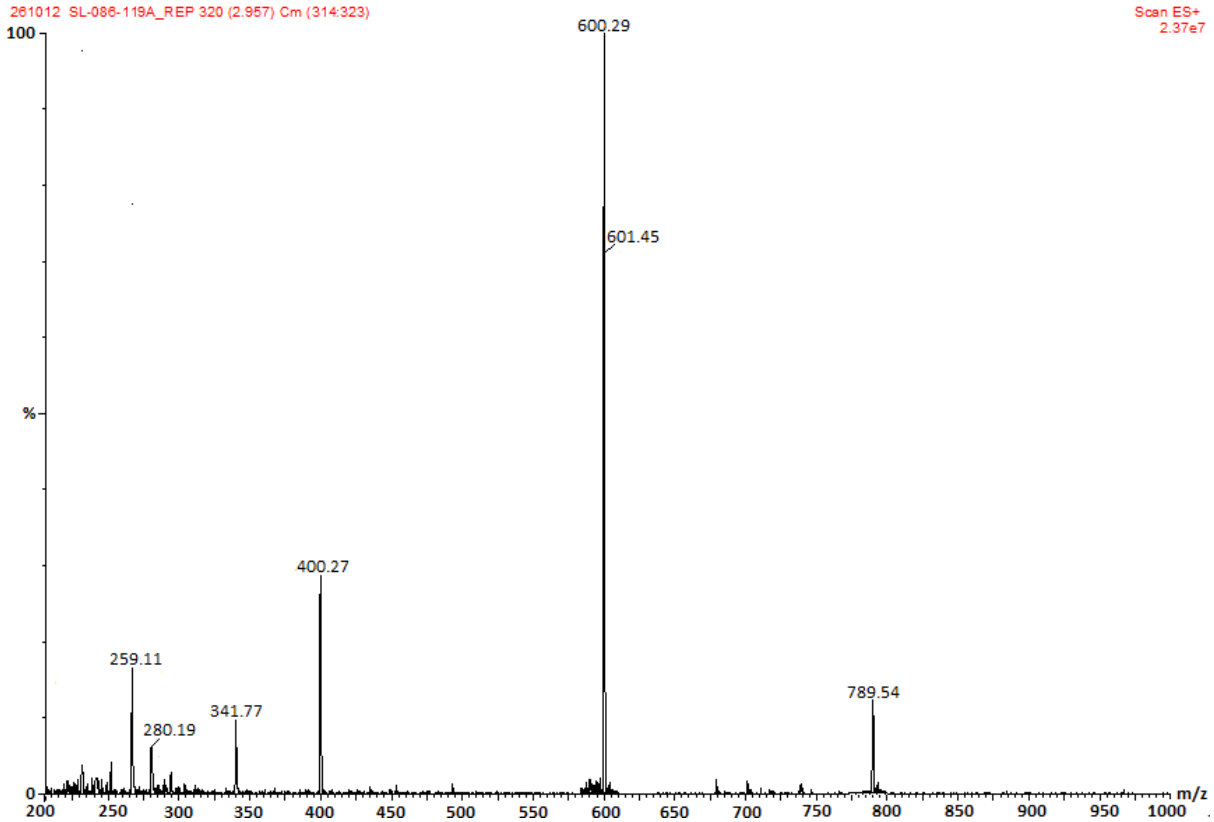

Figure 4.22: Chemical structure, HPLC chromatogram and Mass spectra of **LP19**

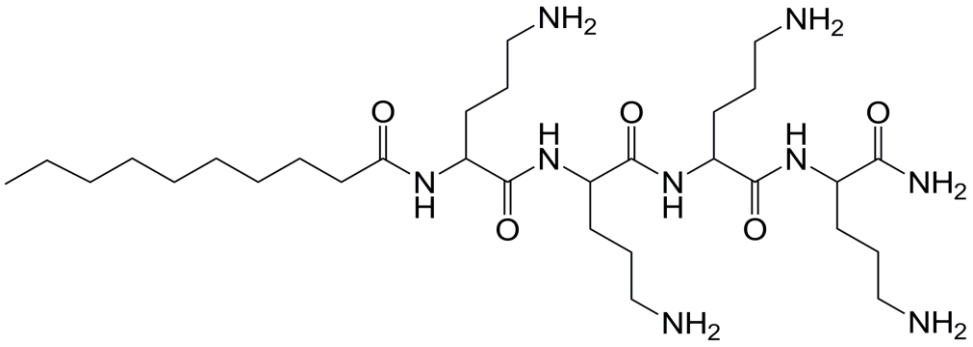

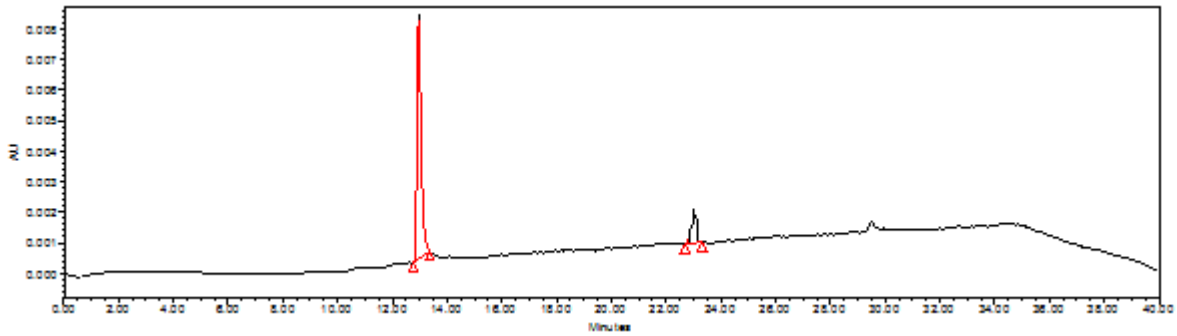

	Name	Retention Time	Area	% Area	Height	RT Ratio
1		13.09	3879199	96.20	207889	
2		23.10	16782	3.80	1533	

Molecular Weight: 627.48

LCMS (+ESI, m/z): 628.32 $(M+H)^+$

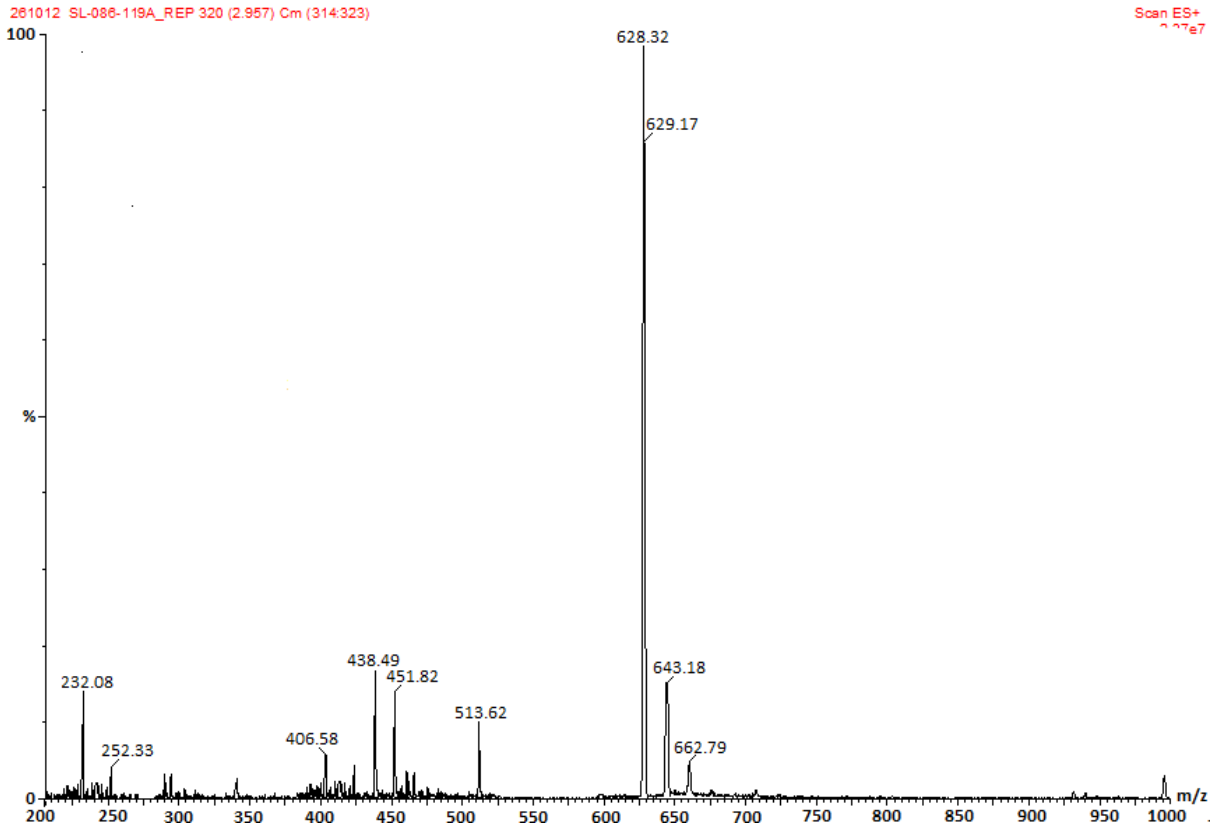

Figure 4.23: Chemical structure, HPLC chromatogram and Mass spectra of **LP20**

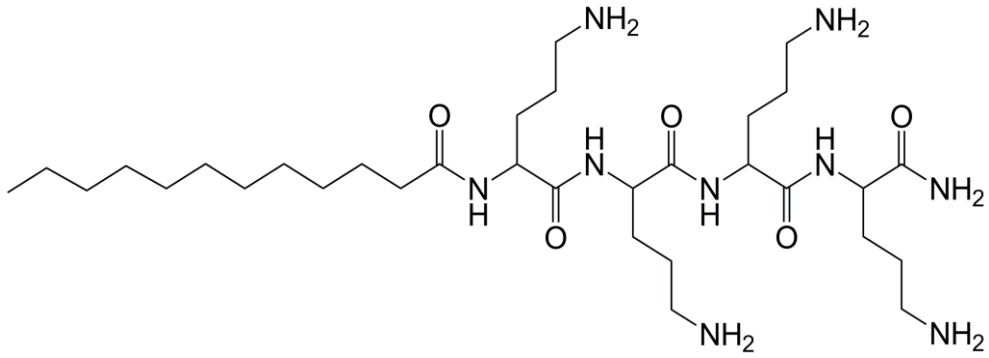

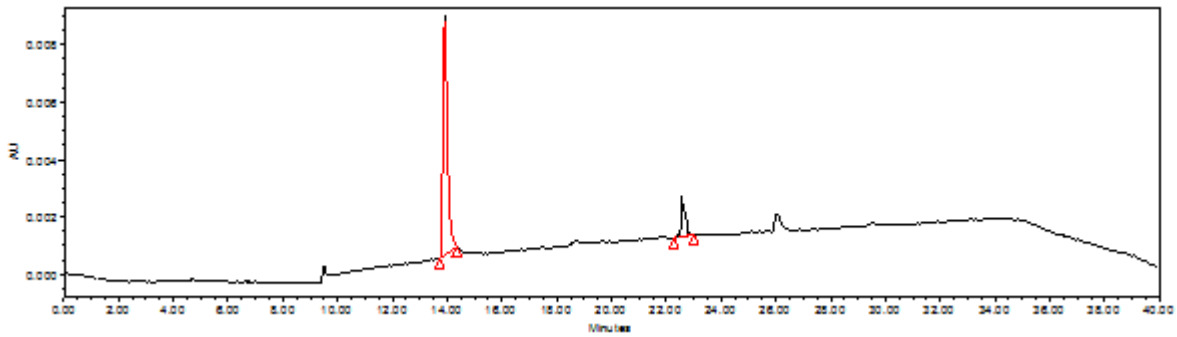

	Name	Retention Time	Area	% Area	Height	RT Ratio
1		14.11	3176410	96.89	284533	
2		22.79	14376	3.11	2067	

Molecular Weight: 655.51

LCMS (+ESI, m/z): 656.42 $(M+H)^+$

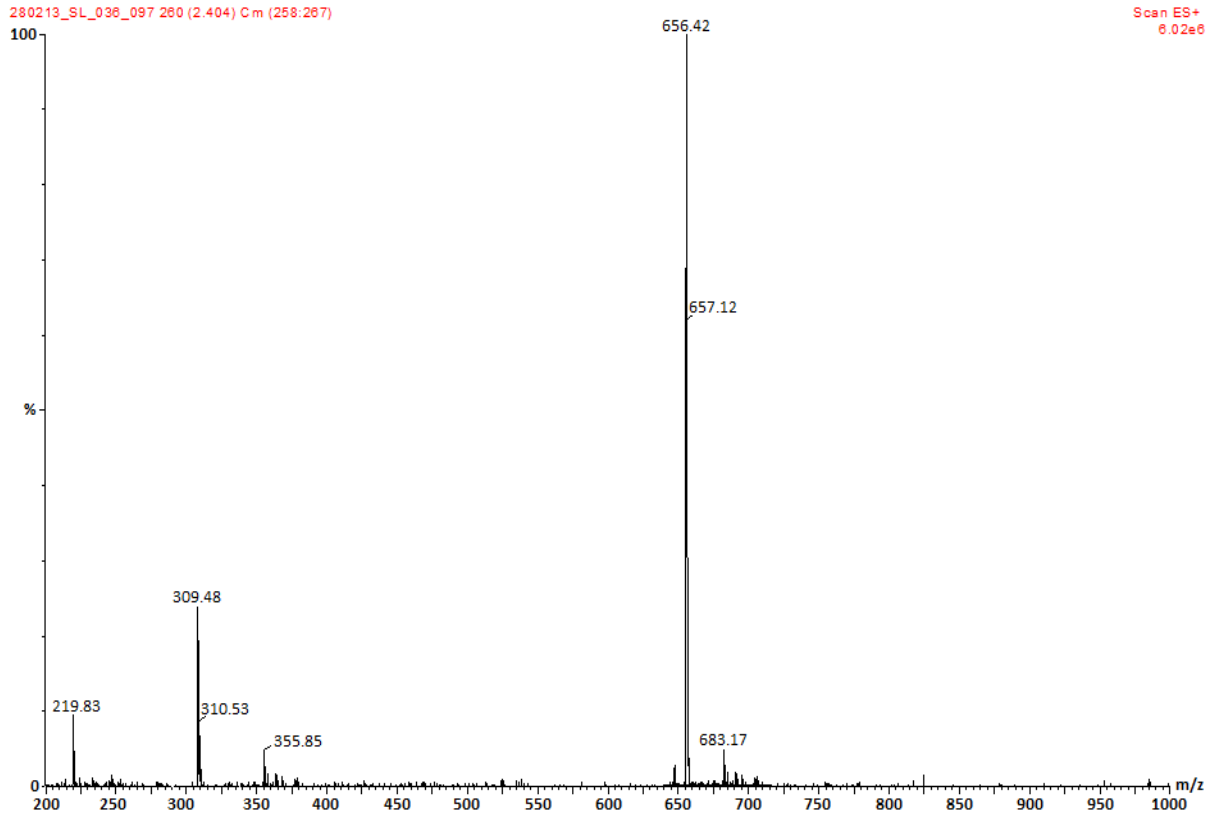

Figure 4.24: Chemical structure, HPLC chromatogram and Mass spectra of **LP21**

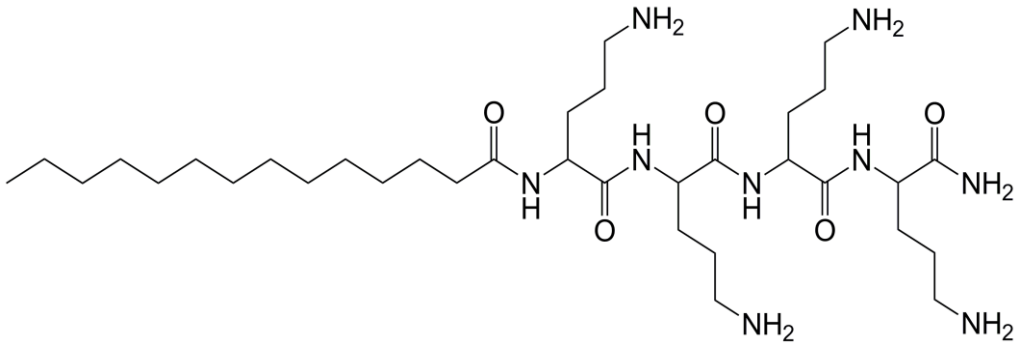

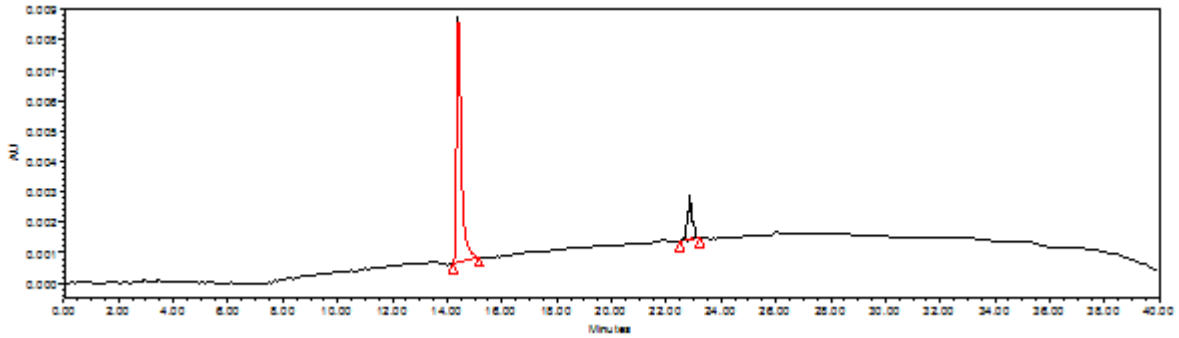

	Name	Retention Time	Area	% Area	Height	RT Ratio
1		14.52	4655780	95.12	98750	
2		22.81	23450	4.88	1099	

Molecular Weight: 683.54

LCMS (+ESI, m/z): 684.39 $(M+H)^+$

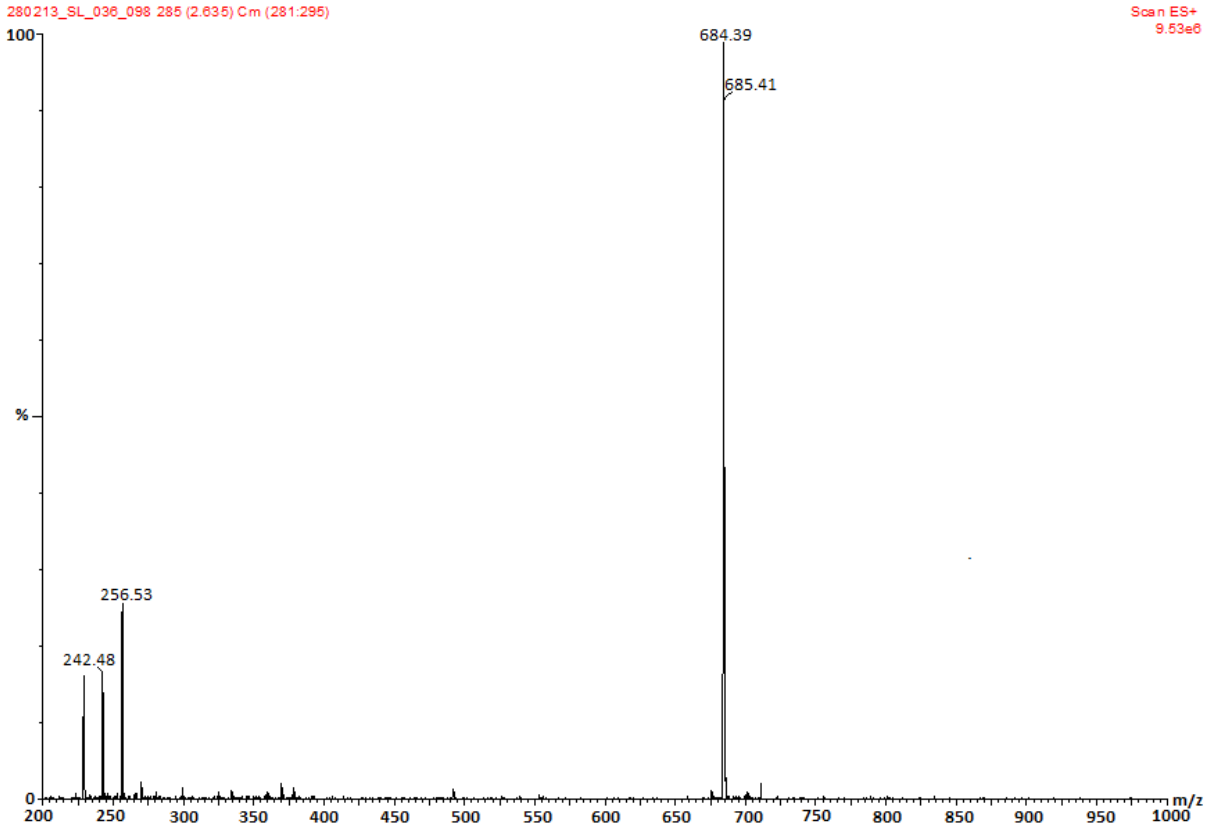

Figure 4.25: Chemical structure, HPLC chromatogram and Mass spectra of **LP22**

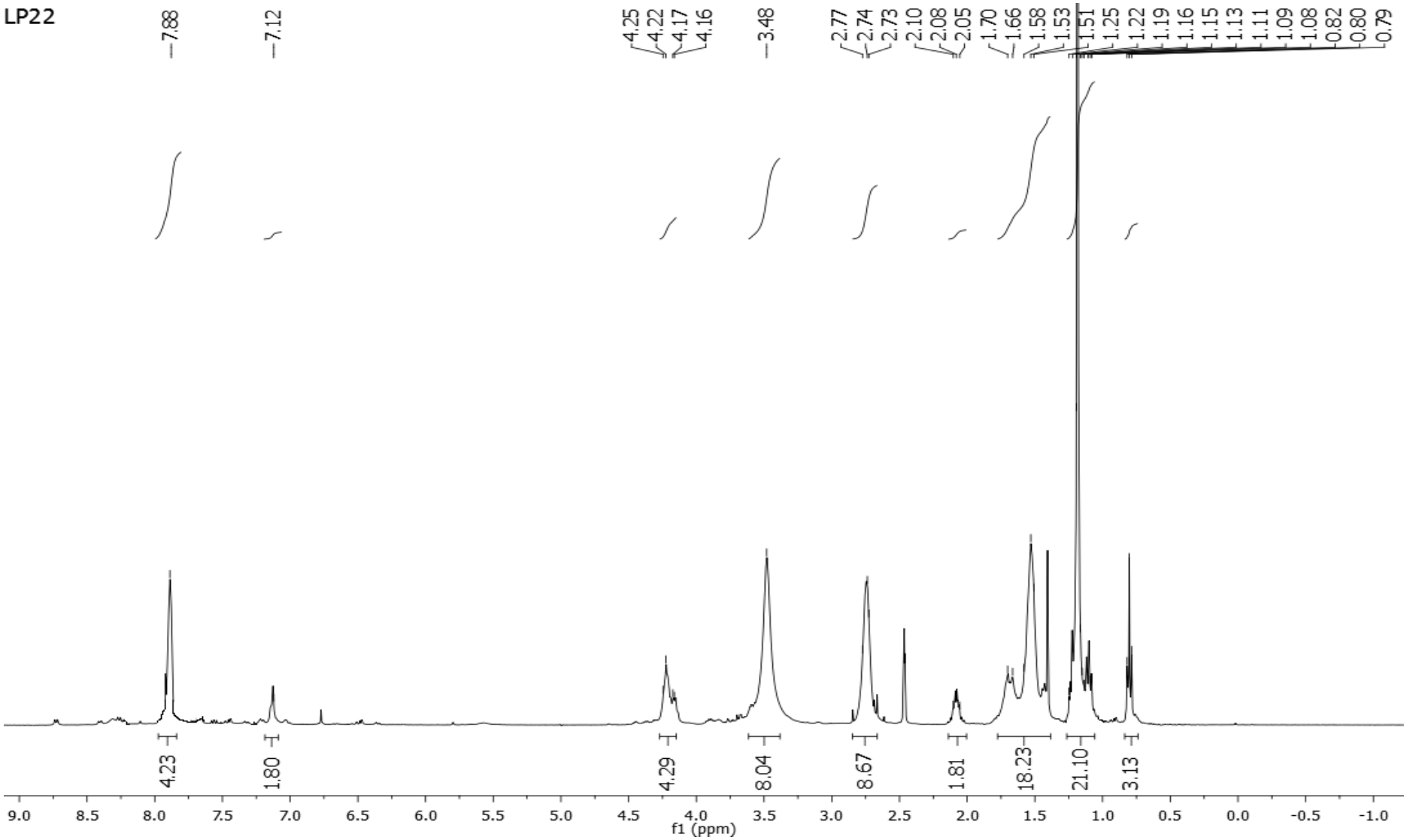

Figure 4.26: ^{1}H NMR (400 MHz, DMSO d_6) spectra of lipopeptide molecule **LP22**

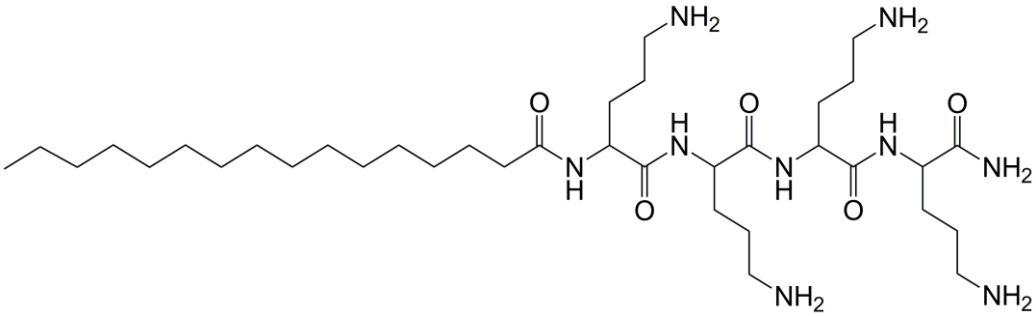

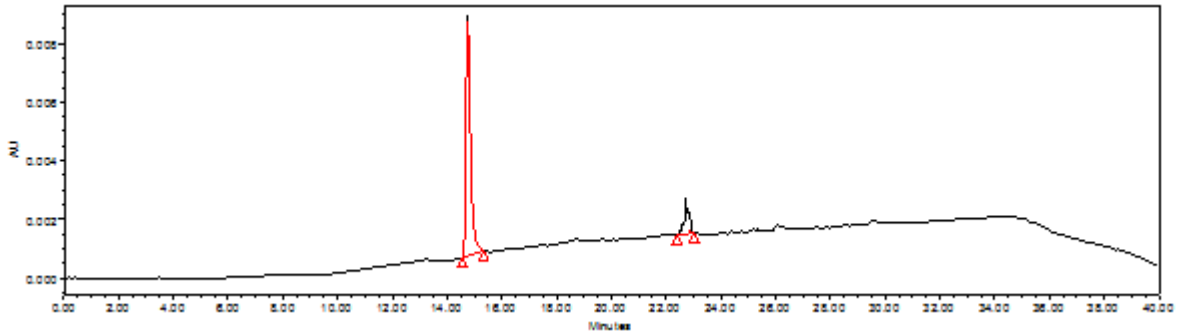

	Name	Retention Time	Area	% Area	Height	RT Ratio
1		15.02	3129832	96.27	170652	
2		22.90	13249	3.73	1976	

Molecular Weight: 711.57

LCMS (+ESI, m/z): 712.36 $(M+H)^+$

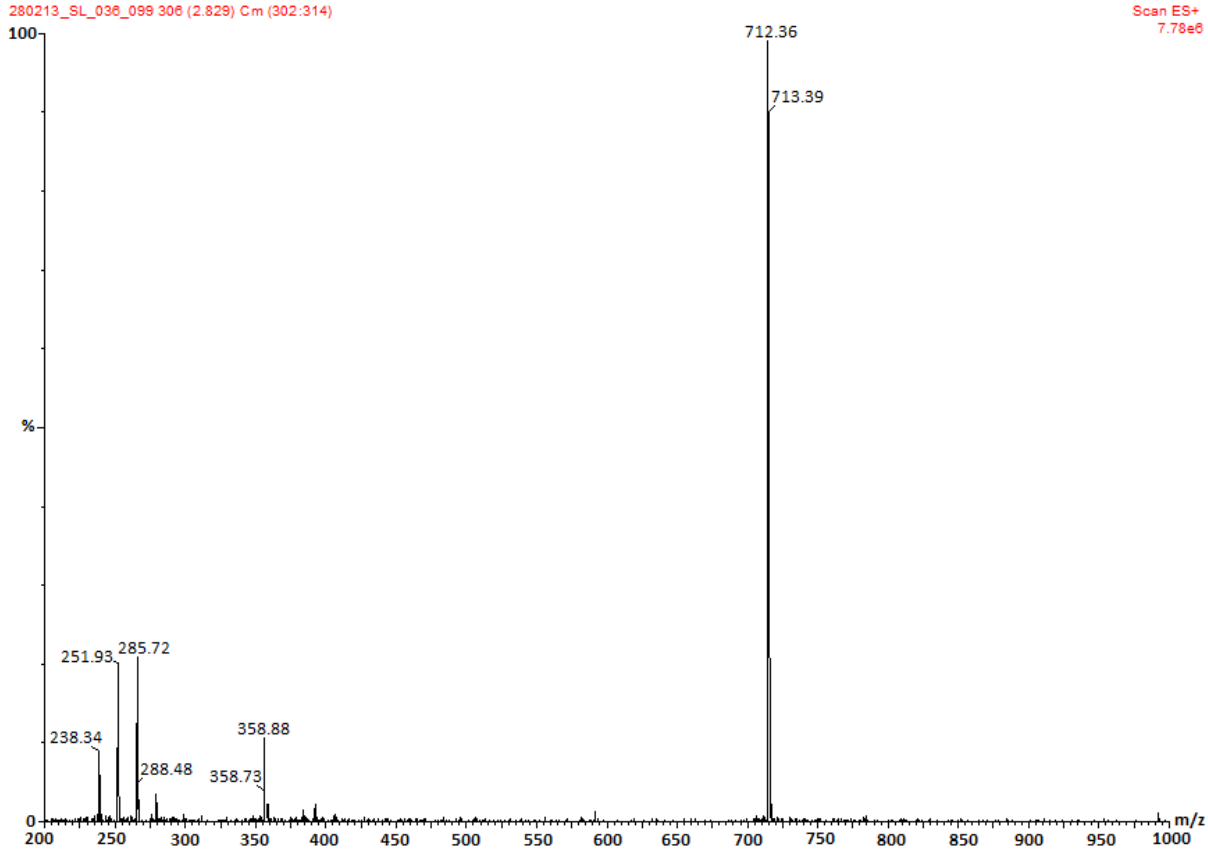

Figure 4.27: Chemical structure, HPLC chromatogram and Mass spectra of **LP23**

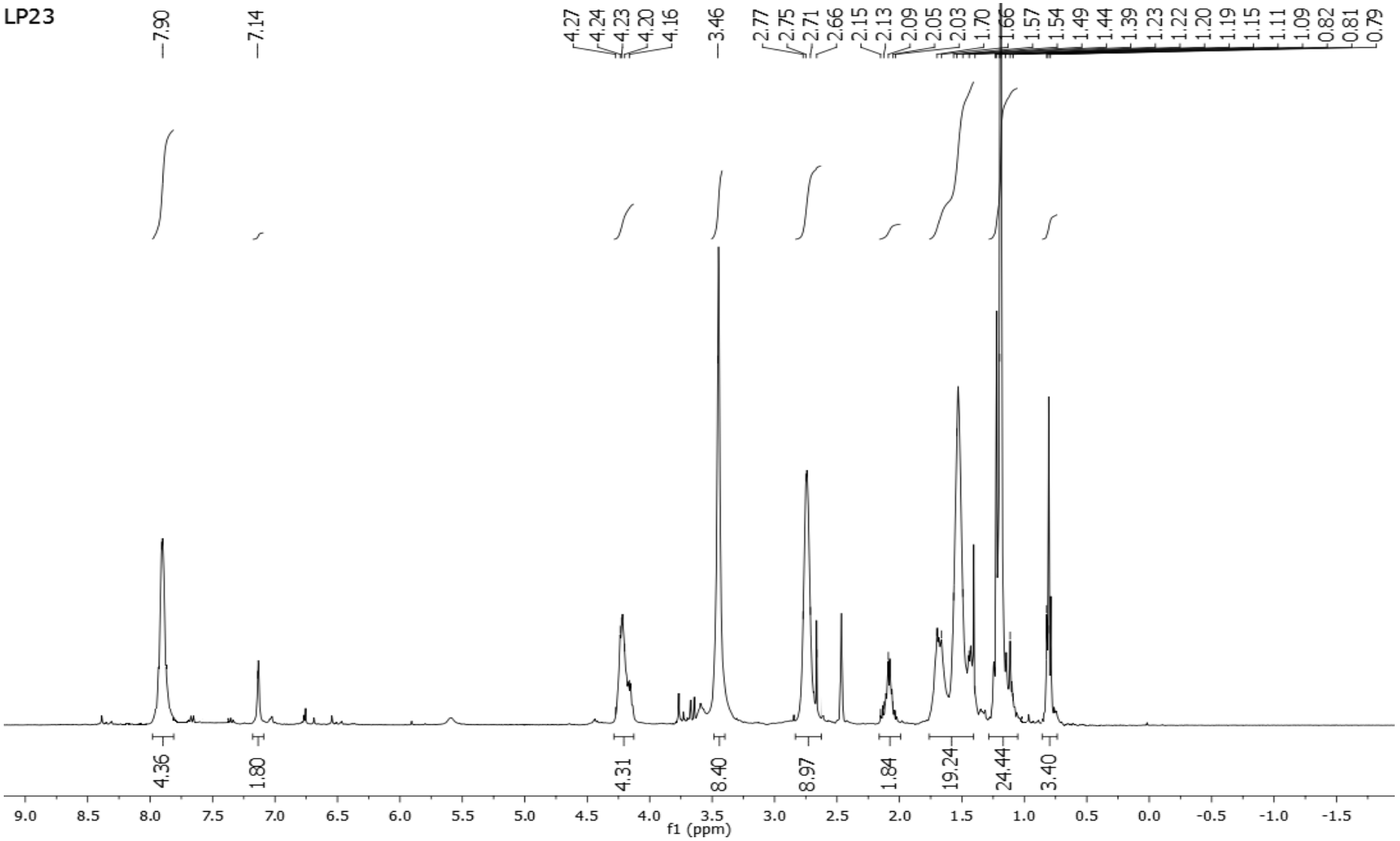

Figure 4.28: ^{1}H NMR (400 MHz, DMSO d_6) spectra of lipopeptide molecule **LP23**

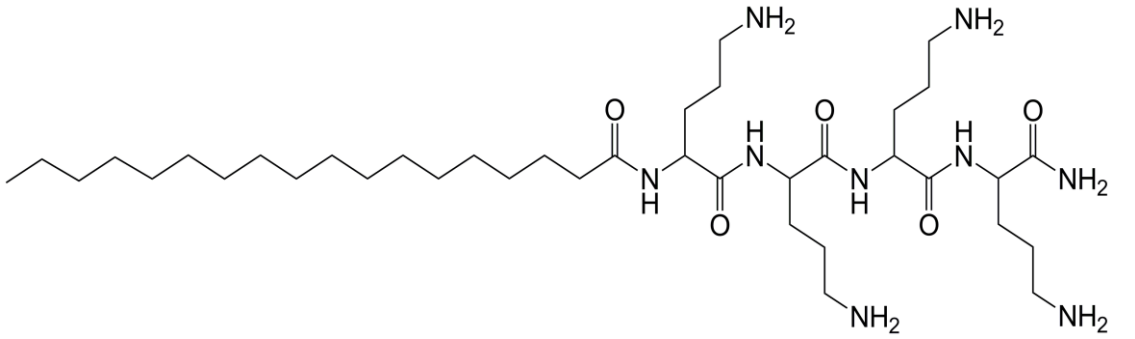

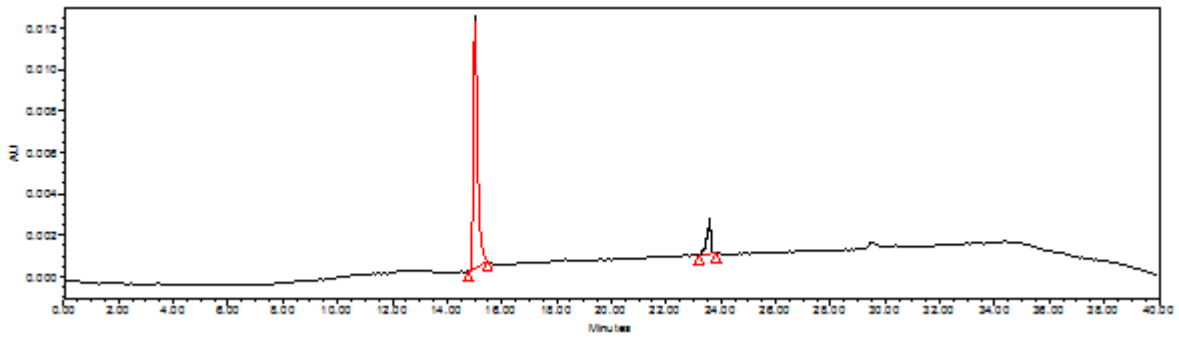

	Name	Retention Time	Area	% Area	Height	RT Ratio
1		15.22	4178932	96.91	165890	
2		23.80	17899	3.09	2278	

Molecular Weight: 739.60

LCMS (+ESI, m/z): 740.53 $(M+H)^+$

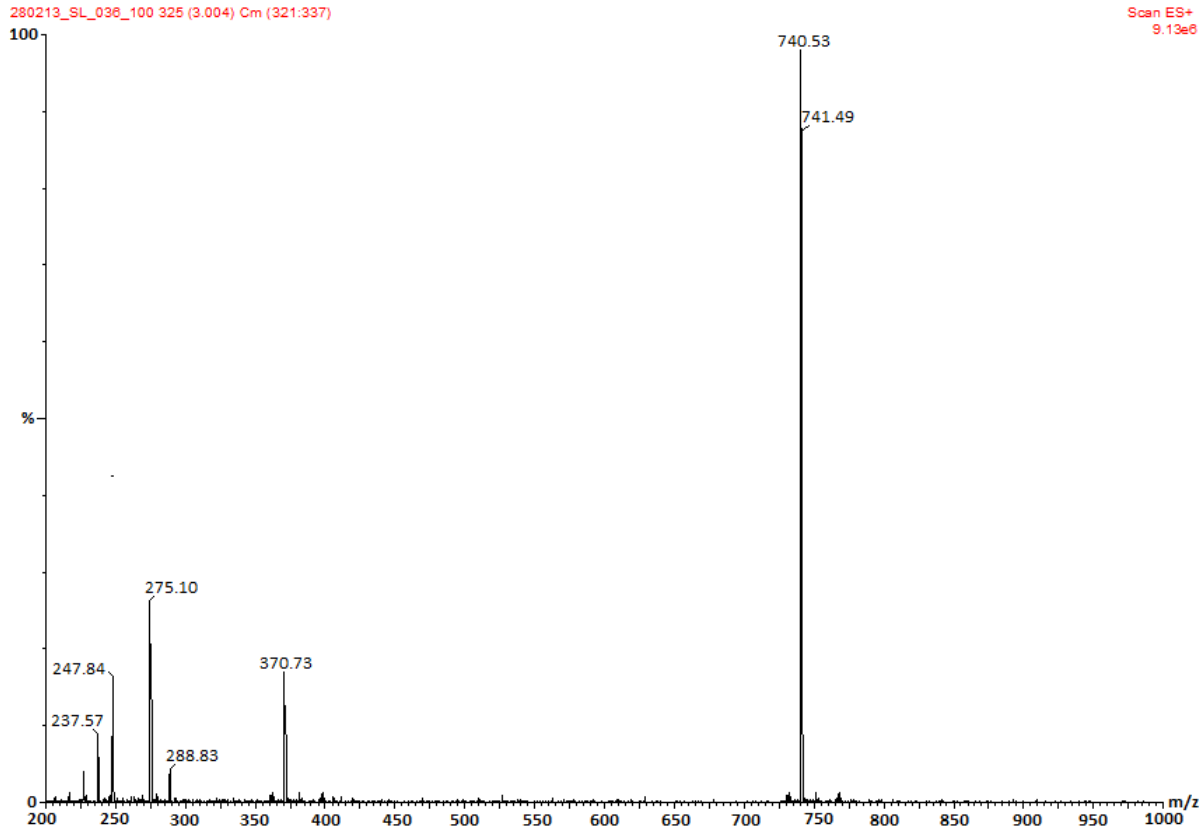

Figure 4.29: Chemical structure, HPLC chromatogram and Mass spectra of **LP24**

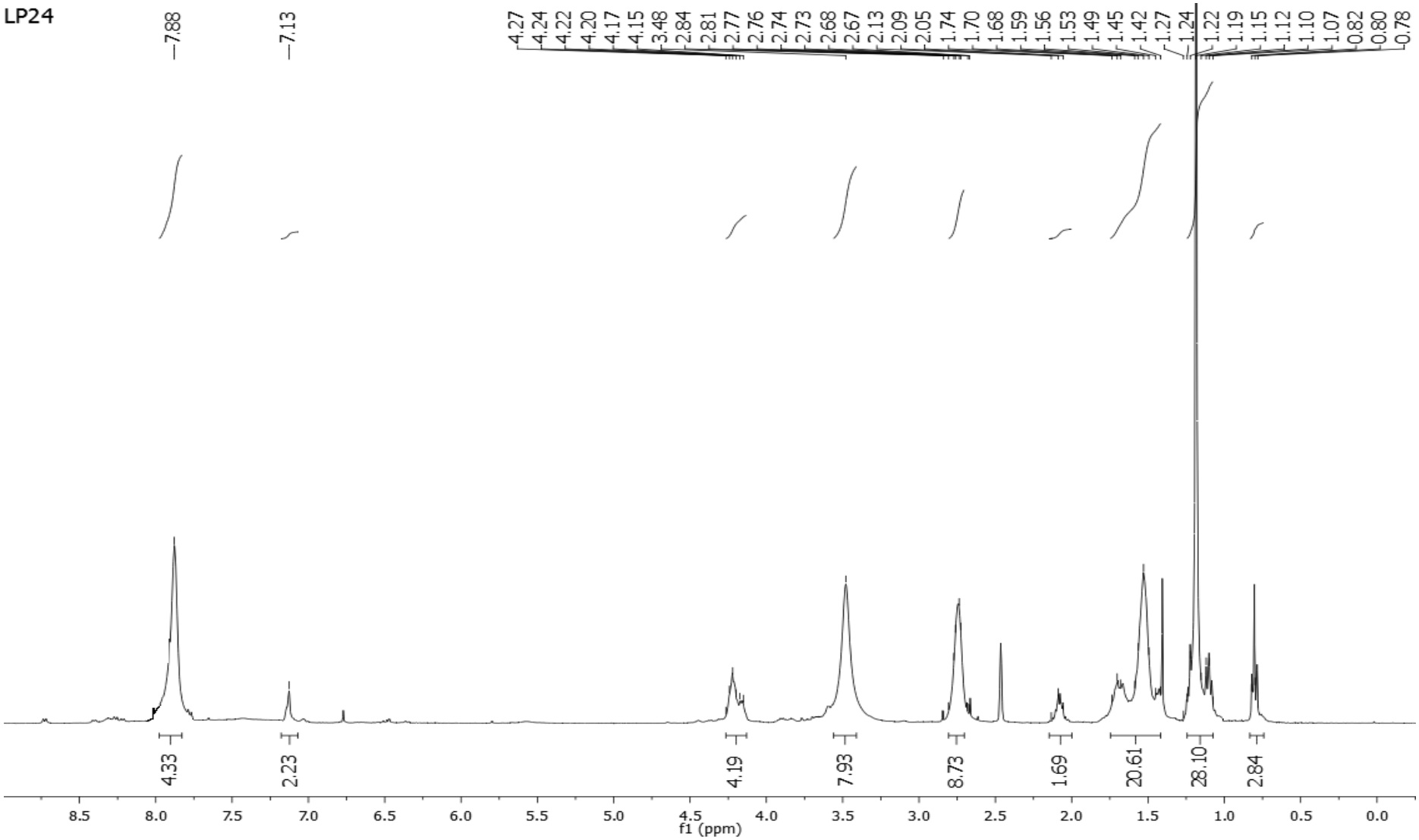

Figure 4.30: ^{1}H NMR (400 MHz, DMSO d_6) spectra of lipopeptide molecule **LP24**

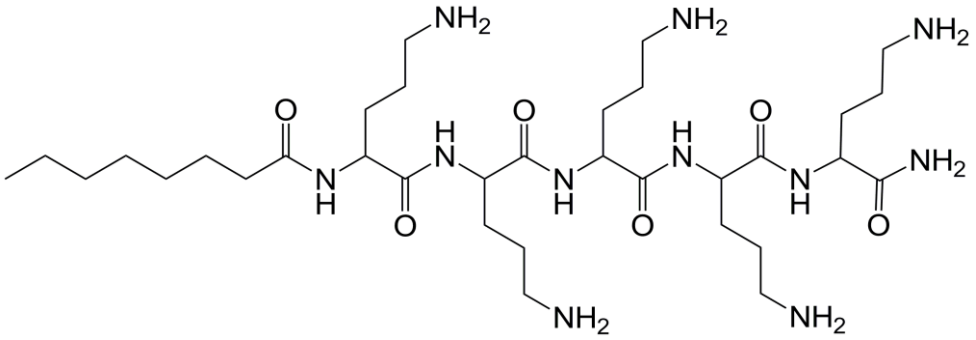

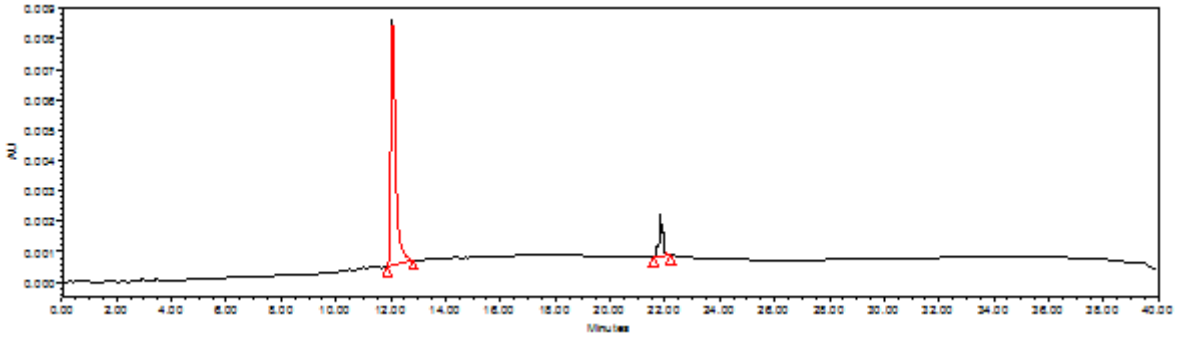

	Name	Retention Time	Area	% Area	Height	RT Ratio
1		12.19	3378991	97.26	190674	
2		21.87	18764	2.74	2378	

Molecular Weight: 713.53

LCMS (+ESI, m/z): 714.42 $(M+H)^+$

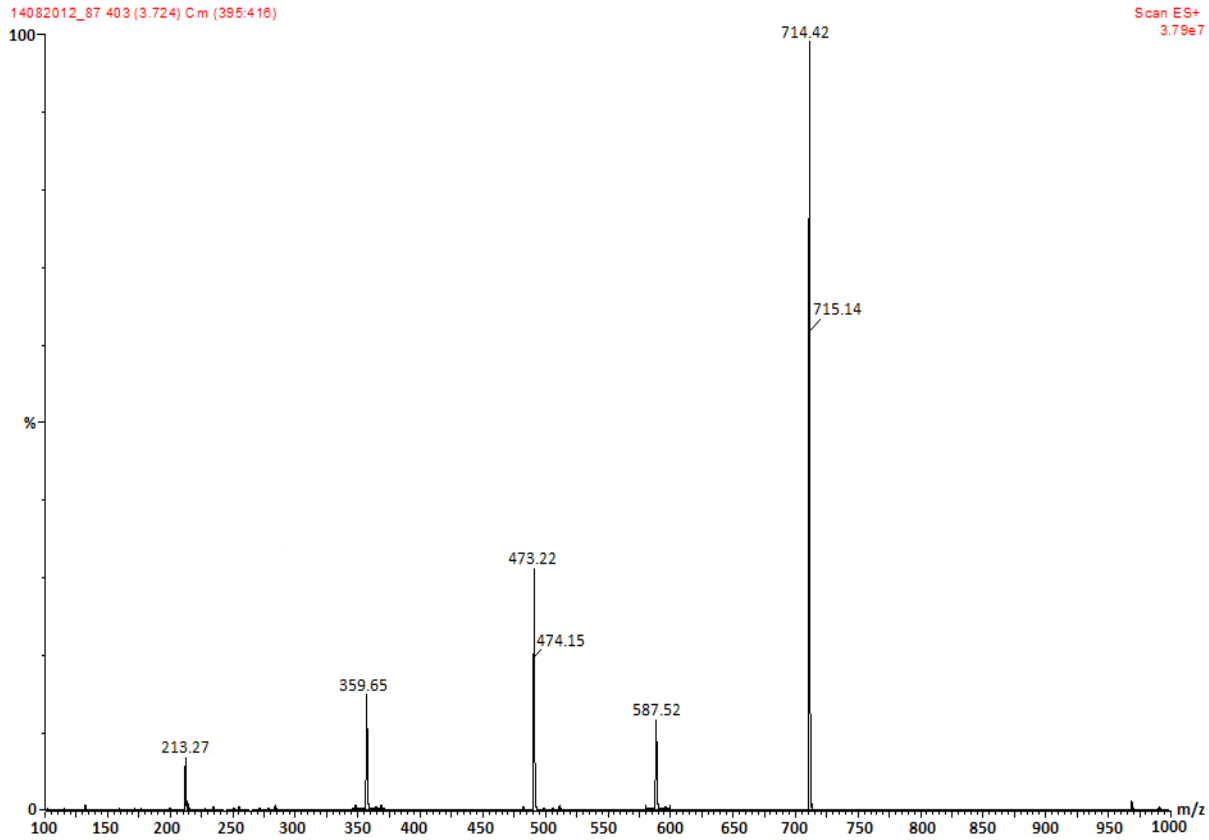

Figure 4.31: Chemical structure, HPLC chromatogram and Mass spectra of **LP25**

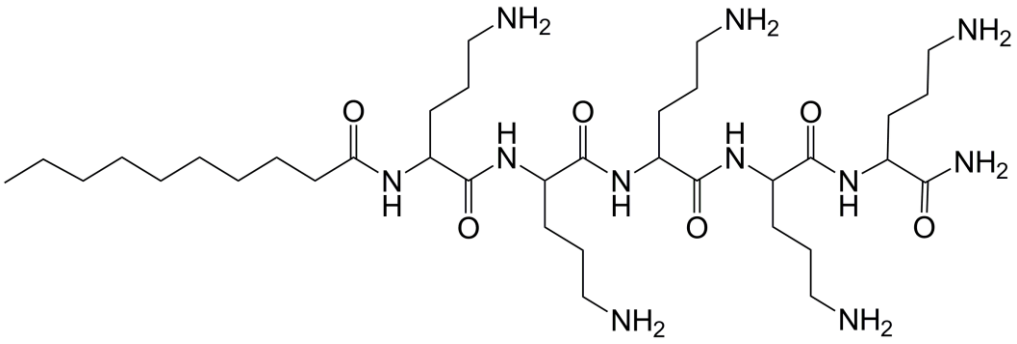

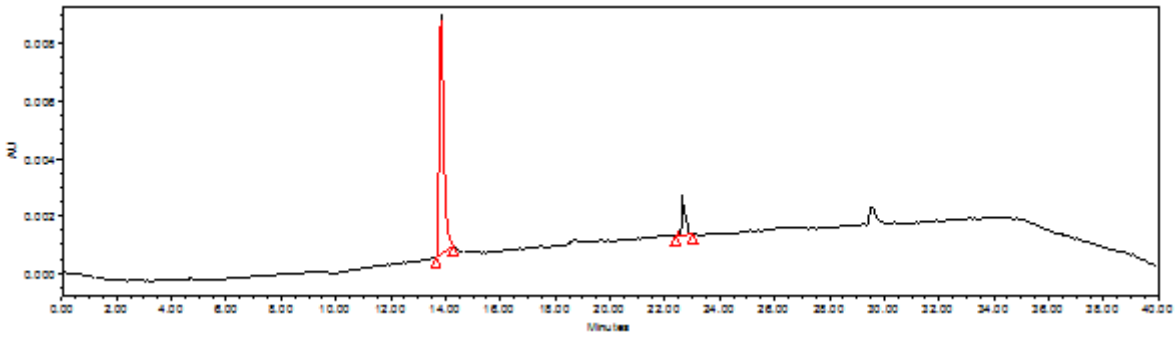

	Name	Retention Time	Area	% Area	Height	RT Ratio
1		14.03	4388762	97.52	188520	
2		22.71	13781	2.48	1427	

Molecular Weight: 741.56

LCMS (+ESI, m/z): 742.40 $(M+H)^+$

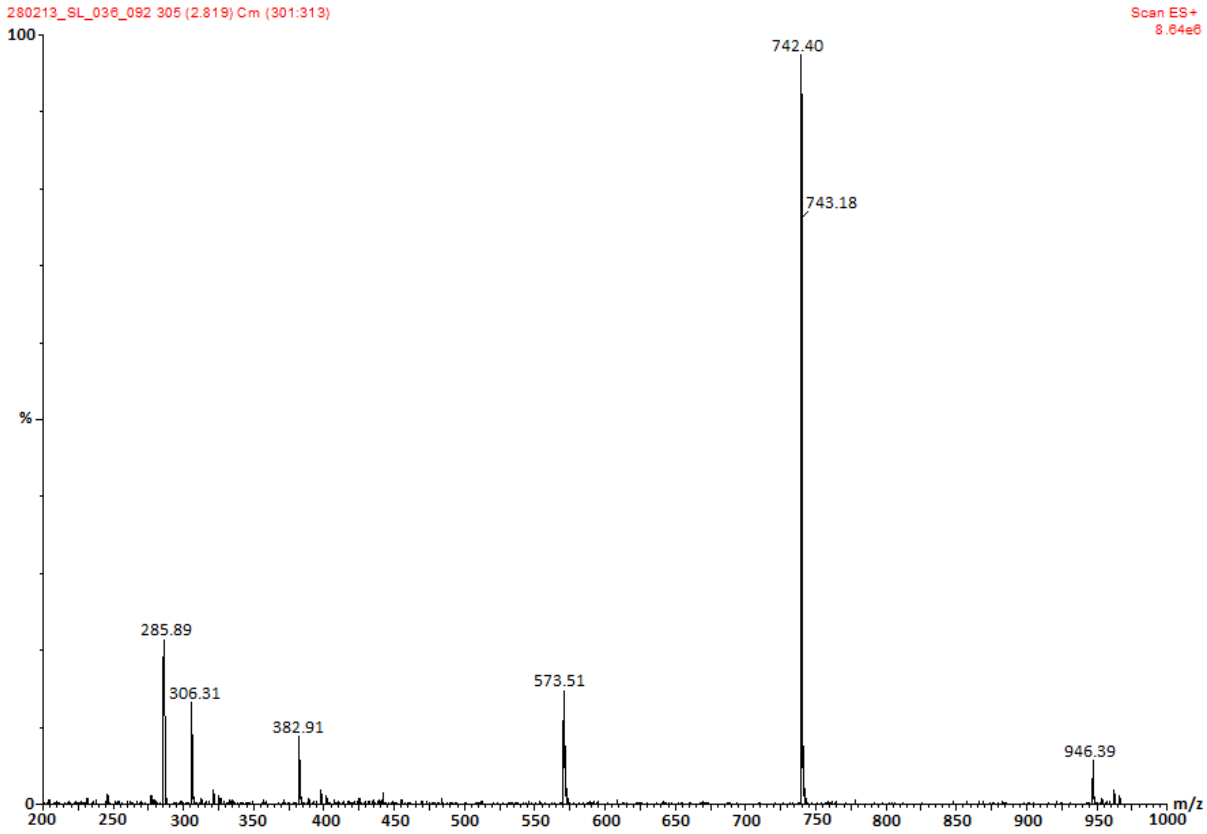

Figure 4.32: Chemical structure, HPLC chromatogram and Mass spectra of **LP26**

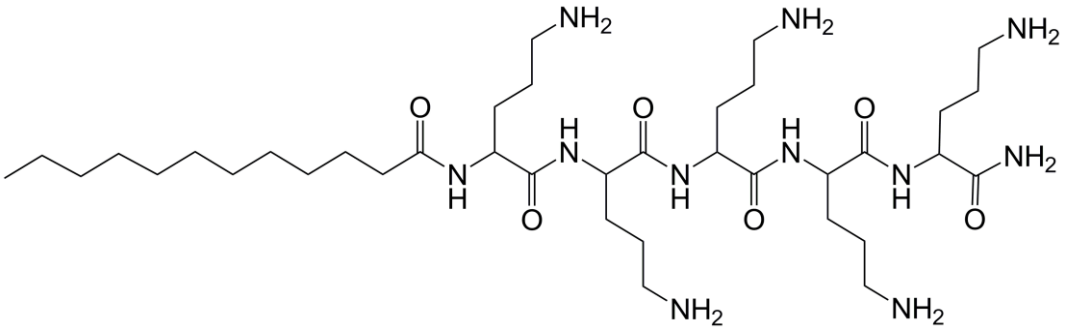

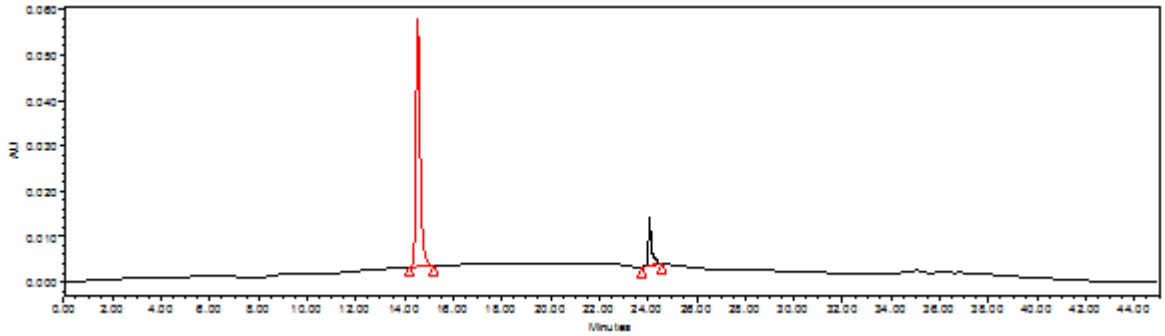

	Name	Retention Time	Area	% Area	Height	RT Ratio
1		14.57	4198721	96.93	153890	
2		24.30	14899	3.07	1345	

Molecular Weight: 769.59

LCMS (+ESI, m/z): 770.31 $(M+H)^+$

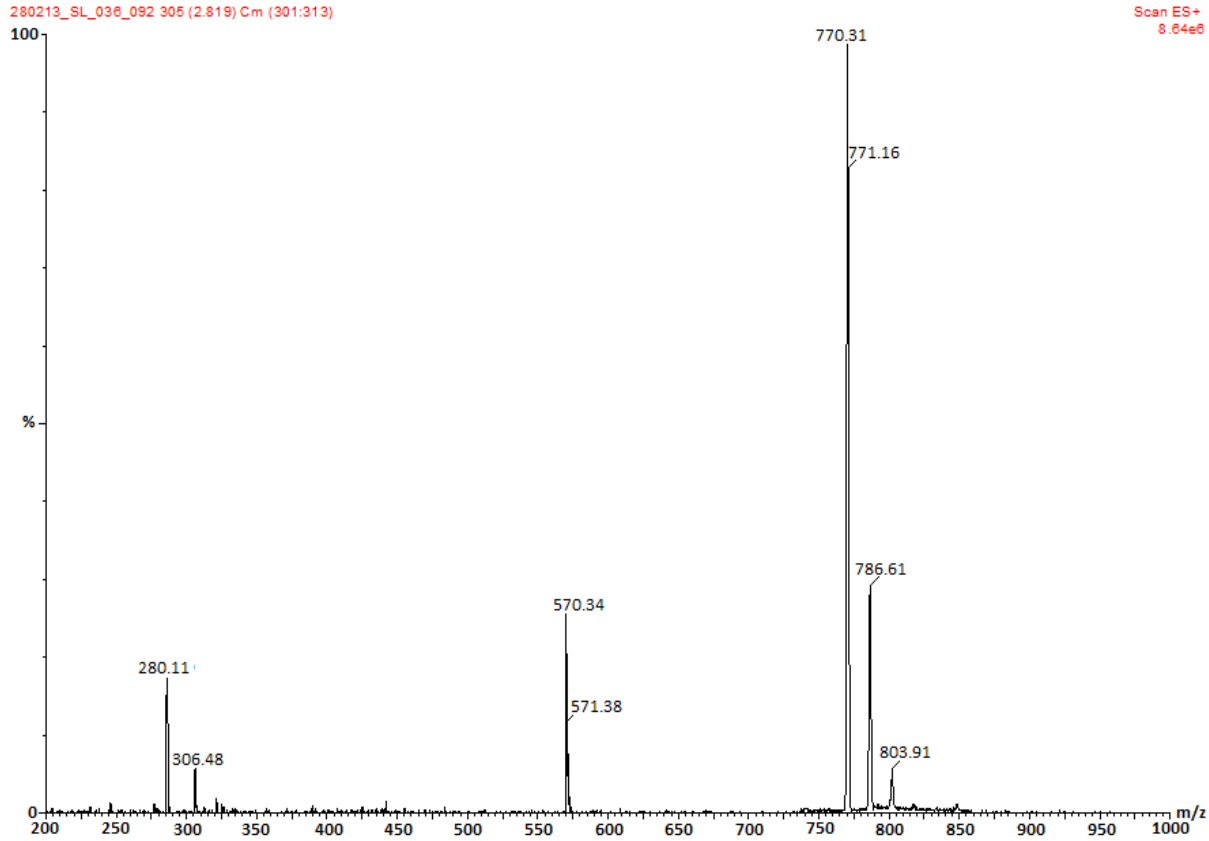

Figure 4.33: Chemical structure, HPLC chromatogram and Mass spectra of **LP27**

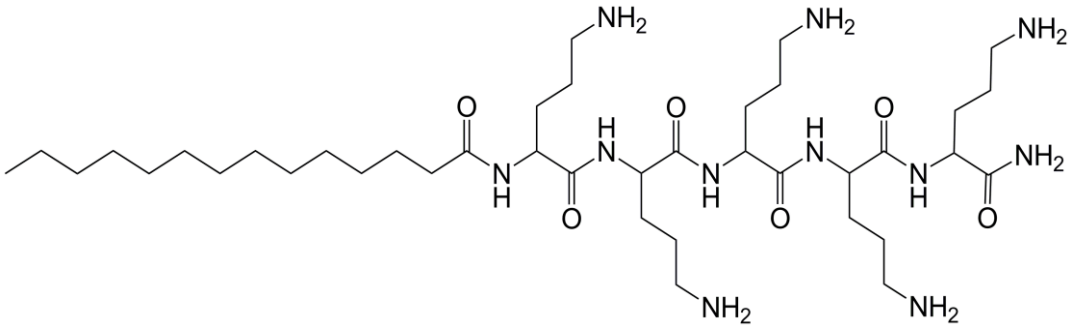

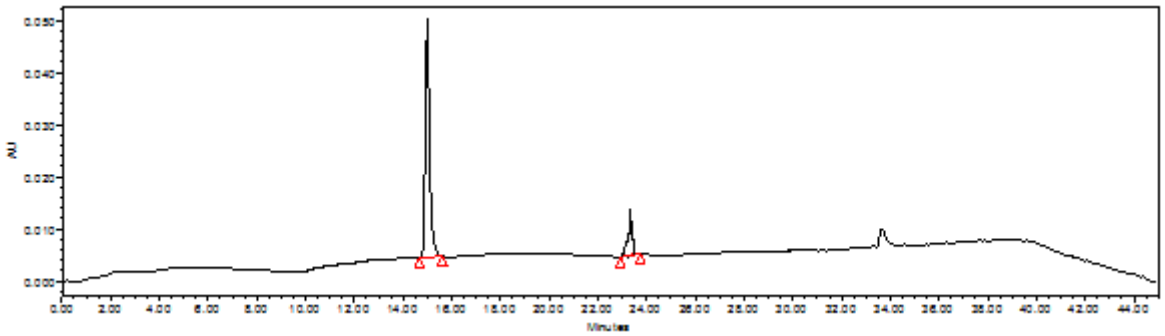

	Name	Retention Time	Area	% Area	Height	RT Ratio
1		15.31	3897643	95.53	171390	
2		23.37	11677	4.47	2075	

Molecular Weight: 797.62

LCMS (+ESI, m/z): 798.48 $(M+H)^+$

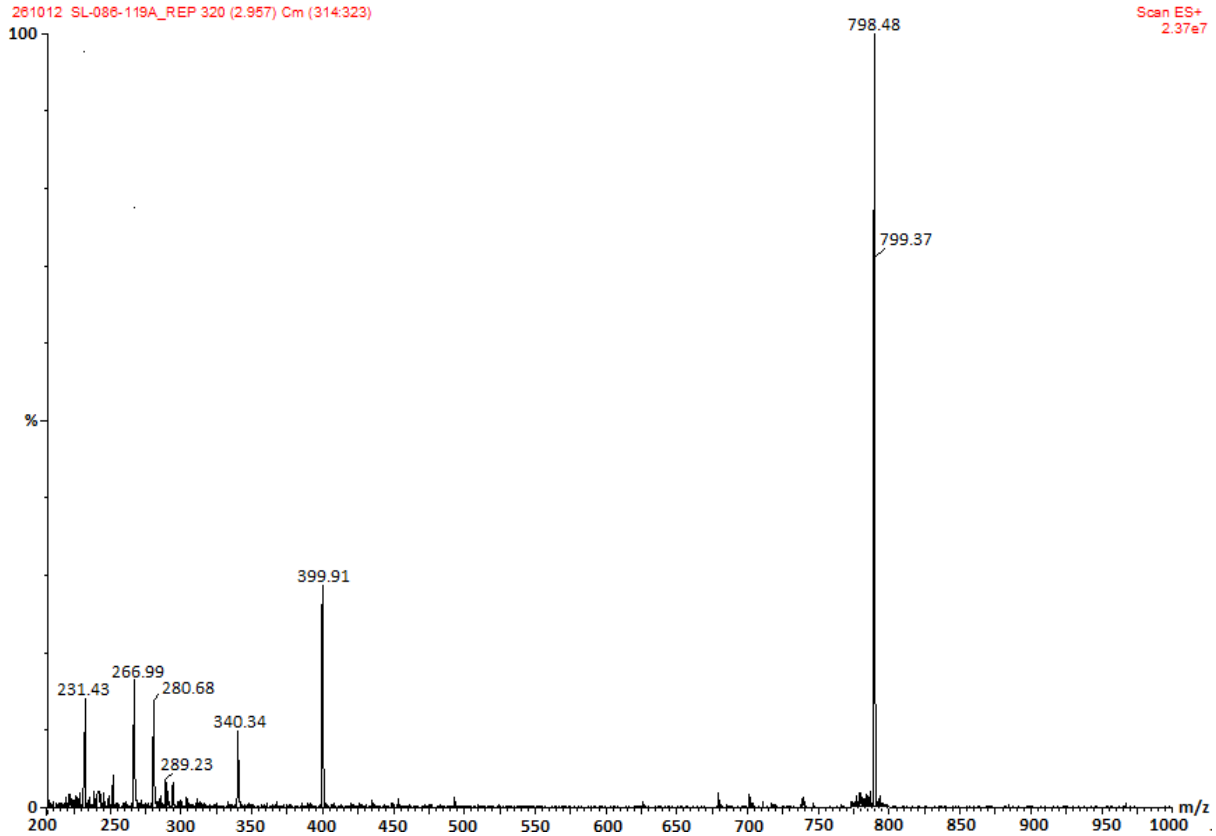

Figure 4.34: Chemical structure, HPLC chromatogram and Mass spectra of **LP28**

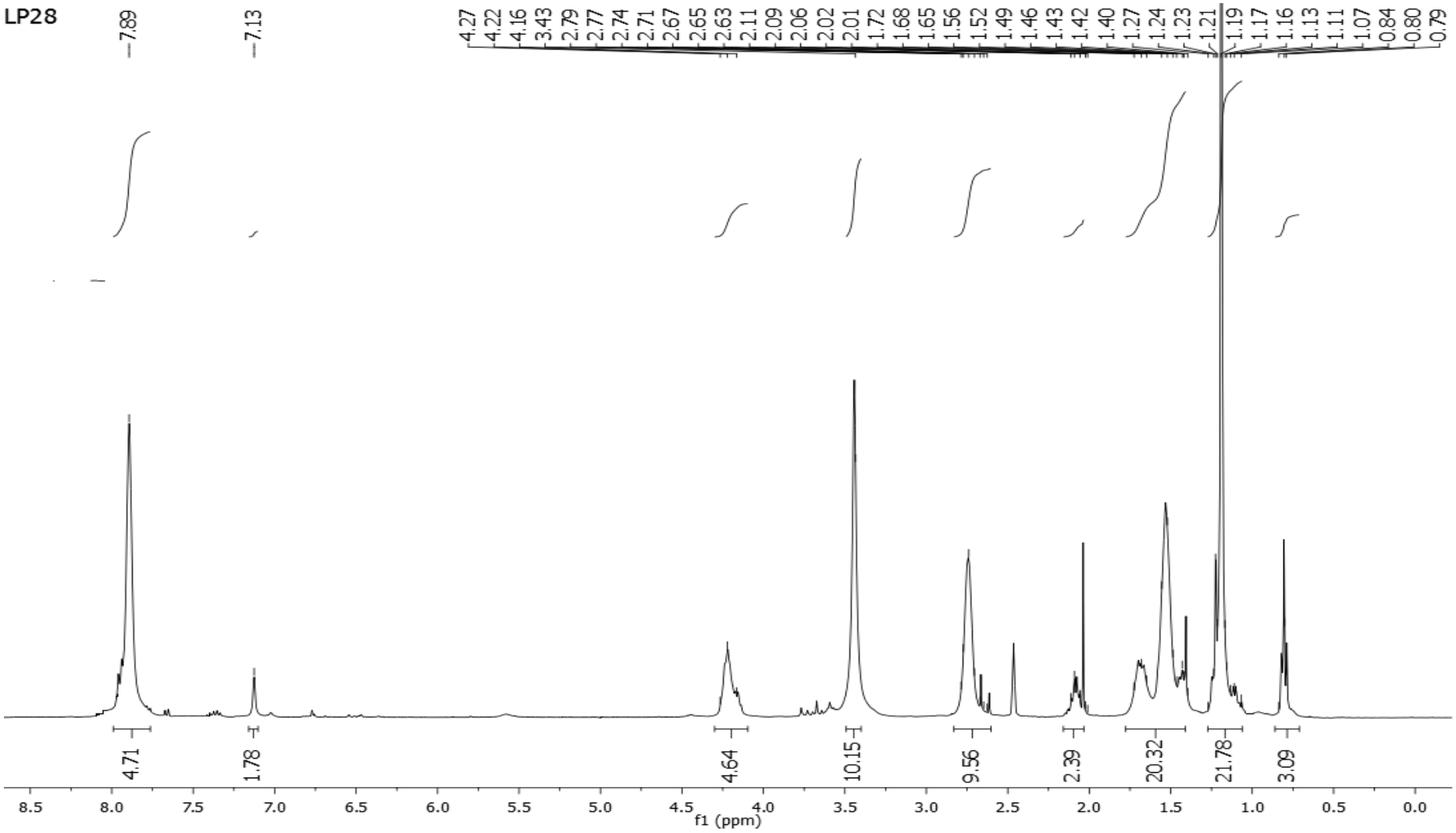

Figure 4.35: ^{1}H NMR (400 MHz, DMSO d_6) spectra of lipopeptide molecule **LP28**

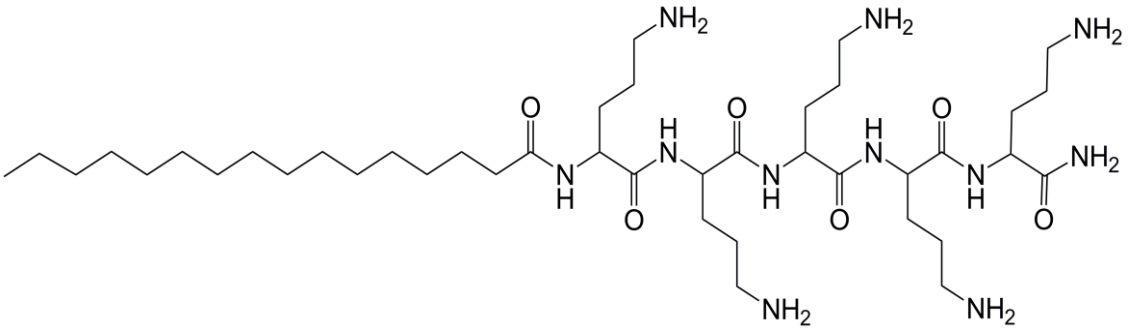

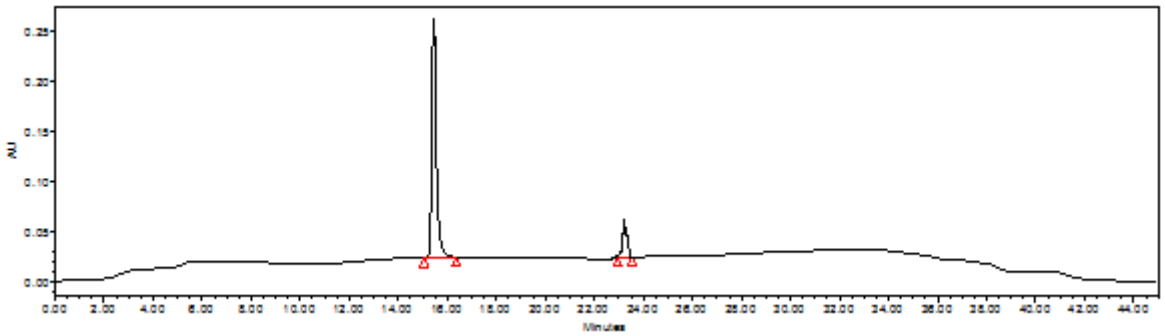

	Name	Retention Time	Area	% Area	Height	RT Ratio
1		15.92	2678956	96.12	192783	
2		23.60	17891	3.88	1822	

Molecular Weight: 825.65

LCMS (+ESI, m/z): 826.52 $(M+H)^+$

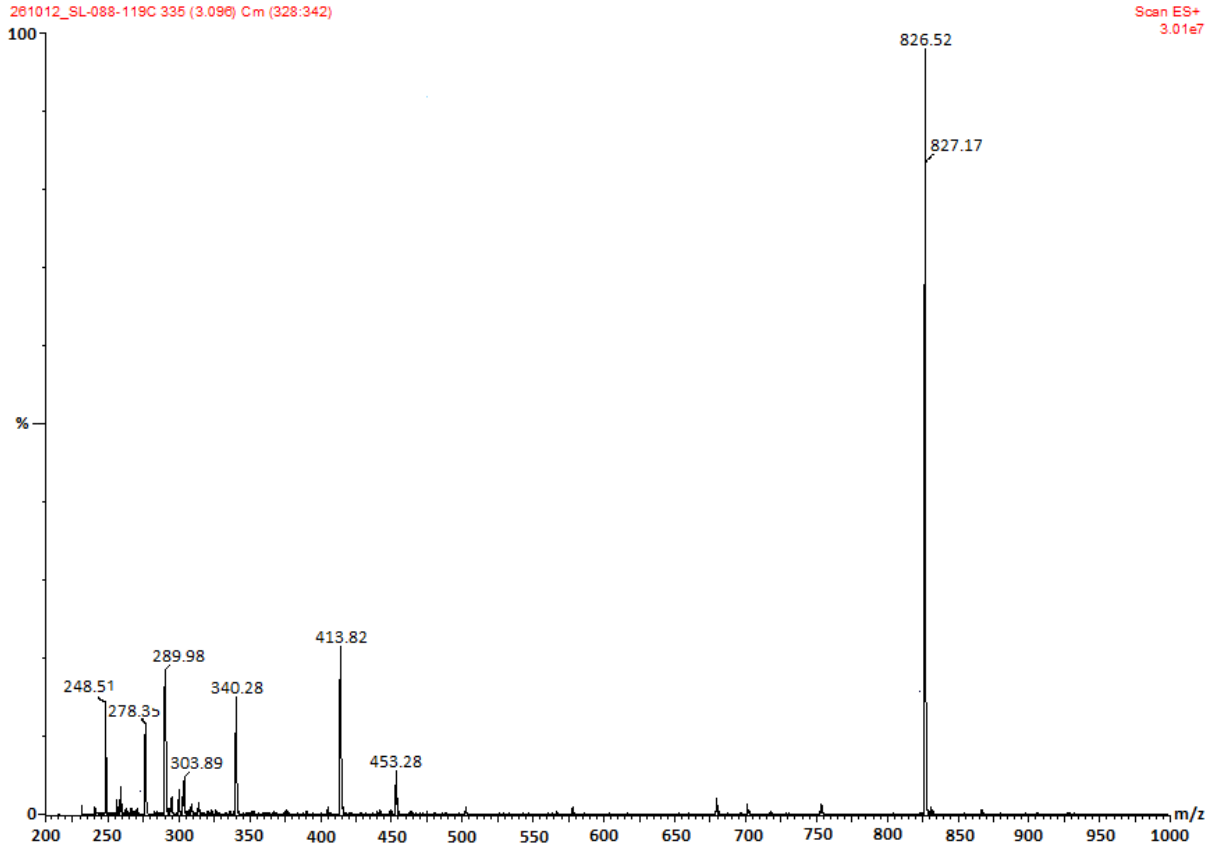

Figure 4.36: Chemical structure, HPLC chromatogram and Mass spectra of **LP29**

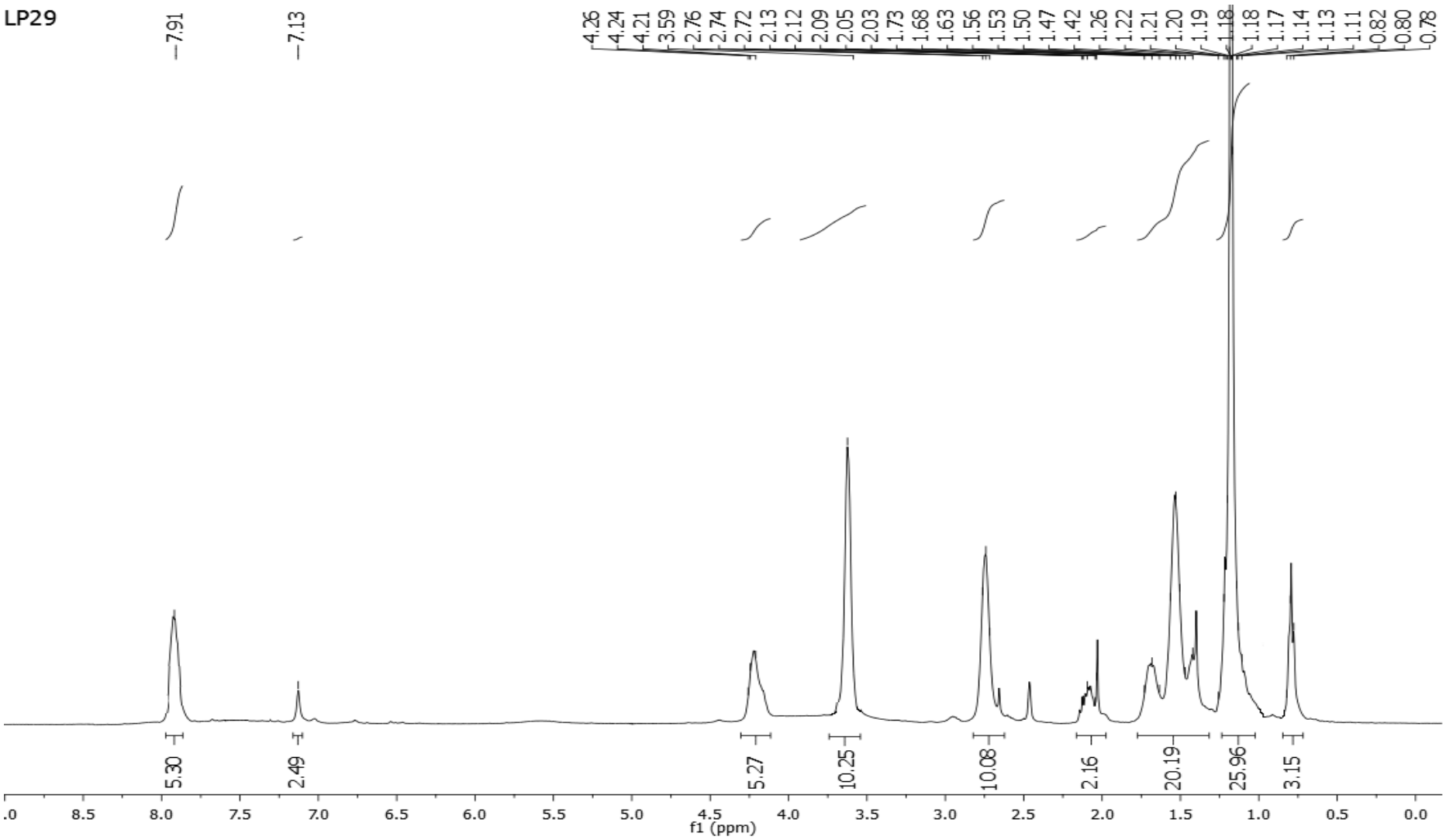

Figure 4.37: ^{1}H NMR (400 MHz, DMSO d_6) spectra of lipopeptide molecule **LP29**

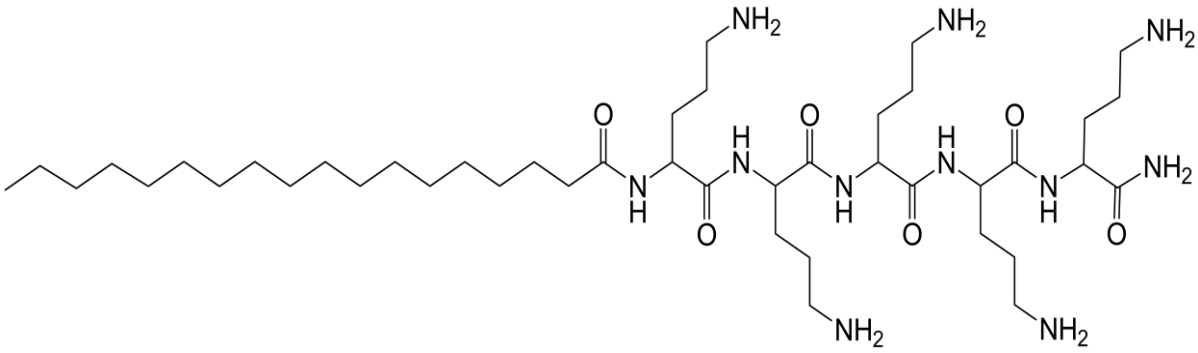

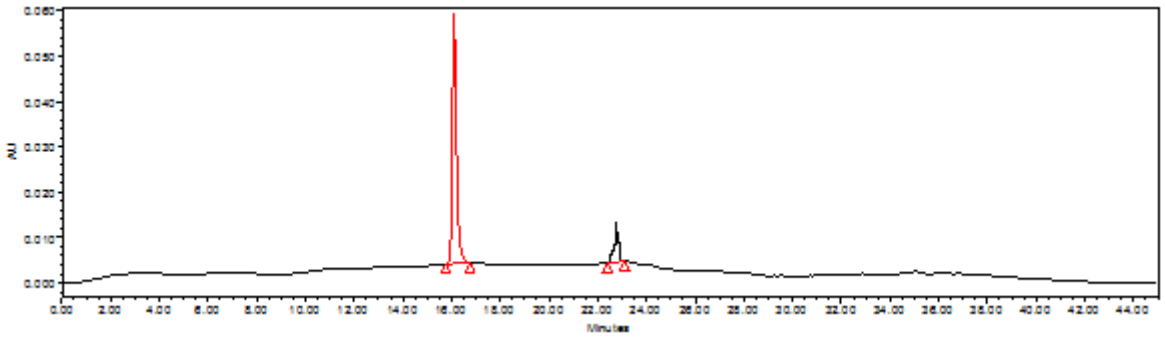

	Name	Retention Time	Area	% Area	Height	RT Ratio
1		16.27	3276580	96.01	181903	
2		22.83	19655	3.99	1273	

Molecular Weight: 853.68

LCMS (+ESI, m/z): 854.50 $(M+H)^+$

Figure 4.38: Chemical structure, HPLC chromatogram and Mass spectra of **LP30**

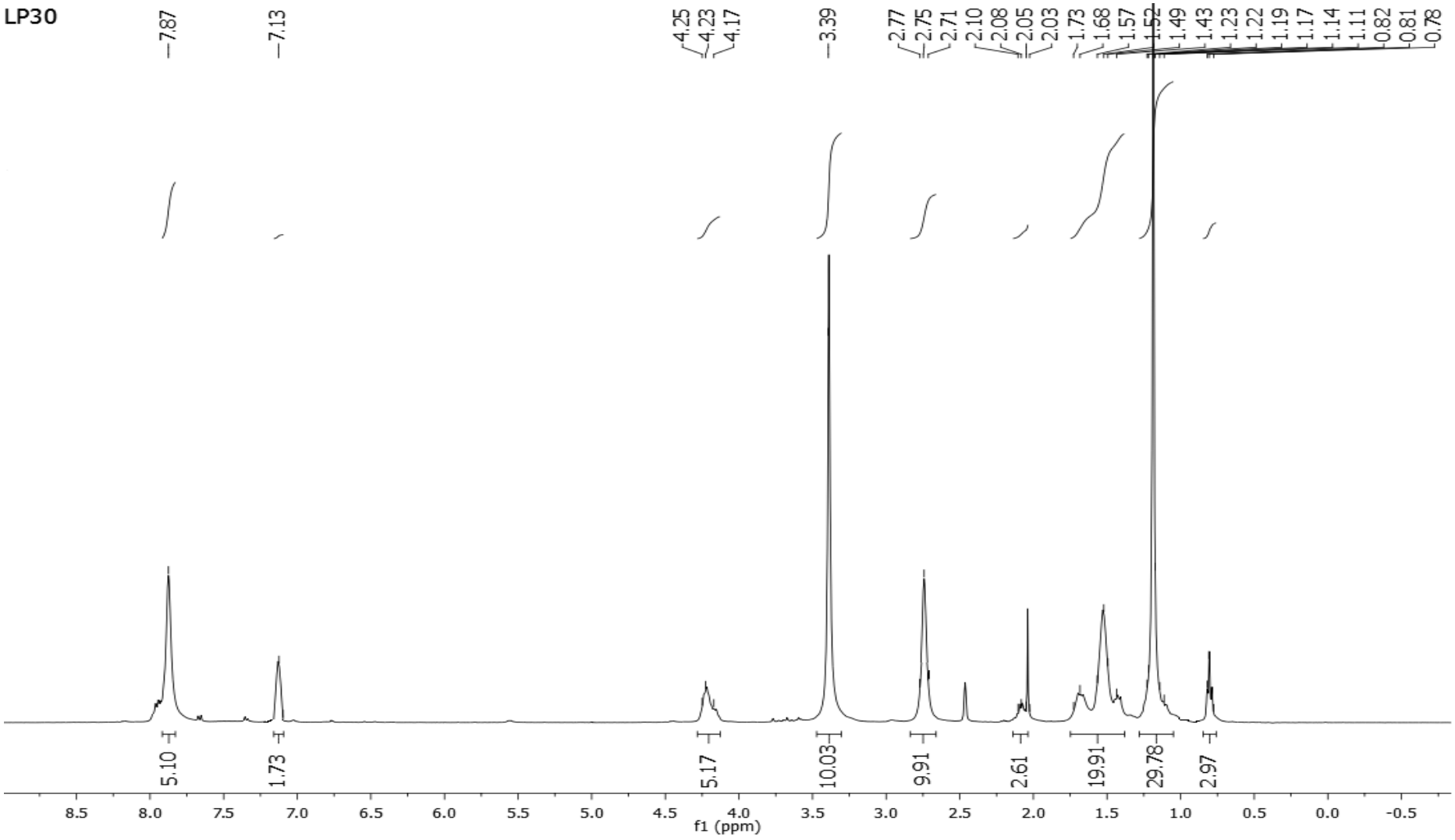

Figure 4.39: ^{1}H NMR (400 MHz, DMSO d_6) spectra of lipopeptide molecule **LP30**

4.2.3. Method for the synthesis of 3-ABA based peptidomimetics using Arginine and Tryptophan

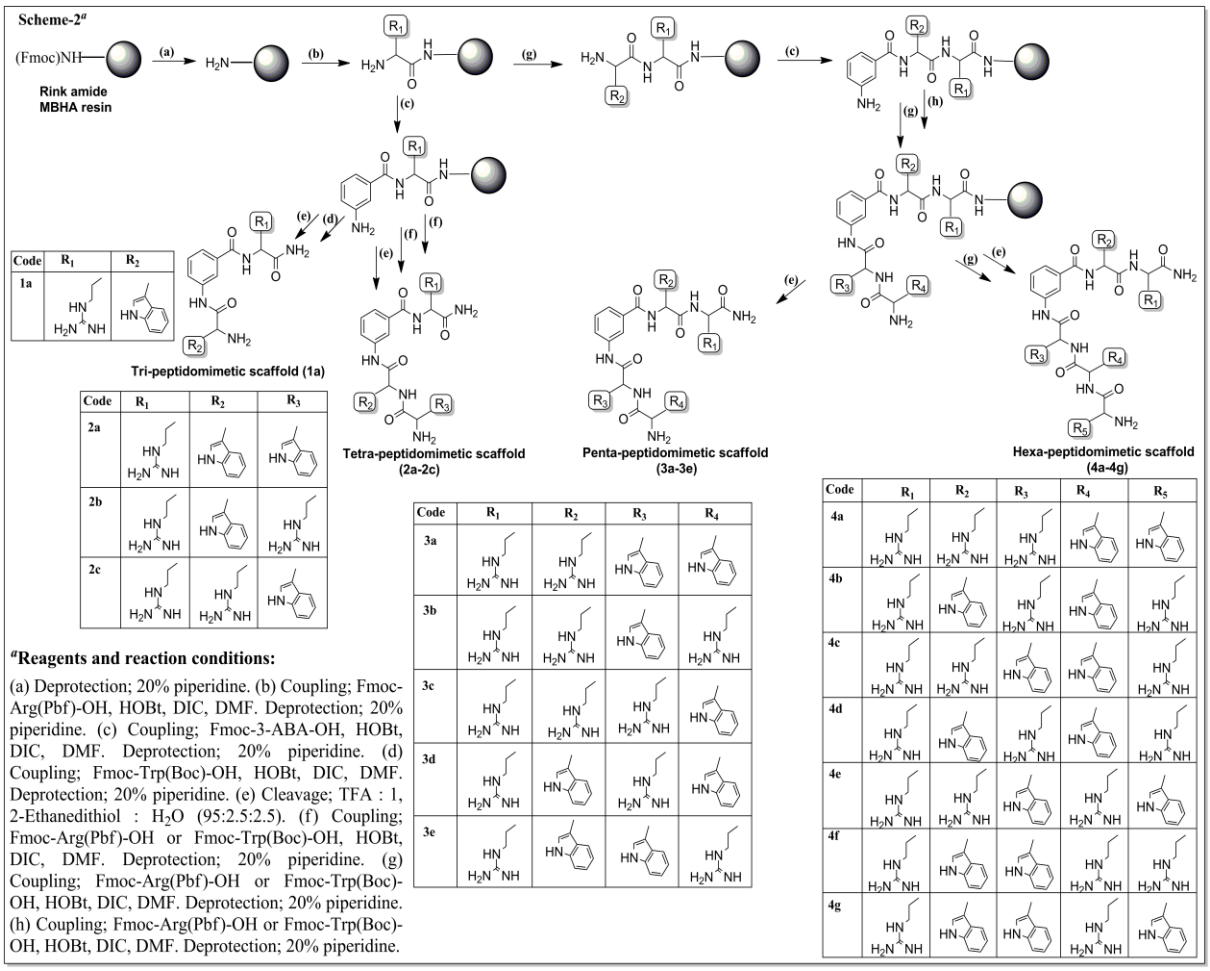

General method for the Fmoc protection of 3-amino benzoic acid

To a solution of 3-amino benzoic acid (1.37 g, 10 mmol) in water (35 mL), was added sodium hydrogen carbonate (2.52 g, 30 mmol), and the resulting mixture was cooled to 5 °C and it was slowly added with Fmoc-Cl (3.87 g, 15 mmol) as a solution in *p*-dioxane. The resulting mixture was stirred at 0 °C for 1 h and allowed to warm to room temperature overnight. Completion of the reaction was monitored by precoated TLC plate. After the completion of reaction water was added to the reaction mixture and the aq. layer was extracted with ethyl acetate. Then the organic layer was extracted twice with a saturated aq. solution of sodium bicarbonate. The combined aq. layers were acidified to a pH of 2 with 10% HCl, and then extracted three times with ethyl acetate. The combined organic layers were removed under reduced pressure to isolate the title compound. The crude material was used without any further purification.

Fmoc-3-ABA

^{1}H NMR (400 MHz, DMSO d_6) δ: 12.21 (s, 1H), 9.81 (s, 1H), 7.91 - 7.66 (m, 6H), 7.52 - 7.27 (m, 6H), 4.47 - 4.45 (d, J = 8Hz, 2H), 4.26 - 4.23 (t, J = 12Hz, 1H). MALDI-TOF (+ESI-m/z): calcd for $C_{22}H_{17}NO_4$: 359.12, observed 360.39$(M+H)^+$.

General method for solid phase synthesis of peptidomimetics (1a, 2a-2c, 3a-3e, 4a-4g)

Peptidomimetic molecules were synthesized manually following standard Fmoc solid phase synthesis method using Rink amide-4-methylbenzhydrylamine hydrochloride salt (MBHA) resin (loading 0.79 mmol/g) as solid support [119]. Rink amide resin (150 mg) was washed with CH_2Cl_2 (3 × 2 mL), followed by swelling in DMF (3.5 mL) for 25 min. The Fmoc protecting group of resin was removed by treating with piperidine/DMF (20% v/v) mixture for 10 min, followed by extensive washes with DMF (5 × 2 mL). The deprotection step was performed twice. Each amino acid coupling step included an Fmoc deprotection and 3 h coupling of 4 eq. of Fmoc protected amino acid (Fmoc-Arg(Pbf)-OH or Fmoc-Trp(Boc)-OH or Fmoc-3-ABA-OH) onto resin in the presence 2 eq. of DIC/HOBt in DMF. After the desired sequences were assembled, the peptidomimetic molecules were cleaved with a solution of TFA/H_2O/1,2-Ethanedithiol (95:2.5:2.5) from solid support (Scheme 2).

All crude peptidomimetics were analyzed on RP-HPLC using a C18 waters column (Spherisorb®, ODS2, 5 µm, 4.6 mm × 250 mm) at room temperature. A linear gradient of 0.5-60% solvent B (0.05% TFA in acetonitrile) in solvent A (0.05% TFA in water) over 35 min, followed by 60-0.5% solvent B over 10 min was used at a flow rate of 0.5 mL/min. Preparative RP-HPLC was then performed on a Waters column (Spherisorb®, ODS2, 5 µm, 20 mm × 250 mm) using 0.5-60% linear gradient of solvent B (0.05% TFA in acetonitrile) in solvent A (0.05% TFA in water) over 35 min, followed by 60-0.5% solvent B over 10 min at a flow rate of 5 mL/min. Mass spectra were obtained on a Agilent MALDI-TOF mass spectrometer. Purified HPLC fractions were than lyophilized.

H-Trp-3ABA-Arg-NH_2 (1a)

^{1}H NMR (400 MHz, DMSO d_6) δ: 10.98 (s, 1H), 10.91 (s, 2H), 10. 80 (s, 1H),10.76 (s, 2H), 9.42 (s, 2H), 8.80 (s, 1H), 8.16 - 8.15 (d, J = 4Hz, 2H), 7.33 - 6.97 (m, 8H), 4.67 - 4.64 (t, J = 12Hz, 1H), 4.22 - 4.19 (t, J = 12Hz, 1H), 3.19 - 3.18 (d, J = 4Hz, 5H), 2.84 (s, 1H), 2.46 - 2.45 (t, J = 4Hz, 3H), 1.25 - 1.22 (m, 2H), 1.12 - 1.11 (m, 2H). MALDI-TOF (+ESI-m/z): calcd for $C_{24}H_{30}N_8O_3$: 478.24, observed 479.24$(M+H)^+$; Purity determined by RP-HPLC: 99.61%.

H-Trp-Trp-3ABA-Arg-NH_2 (2a)

^{1}H NMR (400 MHz, DMSO d_6) δ: 11.19 (s, 2H), 10.90 (s, 1H), 10.82 (s, 1H), 10. 76 (s, 2H), 10.34 (s, 2H), 9.37 (s, 1H),8.63 (s, 2H), 7.90 - 7.89 (d, *J* = 4Hz, 2H), 7.30 - 6.97 (m, 12H), 4.67 - 4.65 (m, 2H), 4.39 - 4.38 (t, *J* = 4Hz, 1H), 3.19 - 3.18 (d, *J* = 4Hz, 5H), 2.84 (s, 1H), 2.47 - 2.45 (m, 3H), 1.25 - 1.11 (m, 4H). MALDI-TOF (+ESI-m/z): calcd for $C_{35}H_{40}N_{10}O_4$: 664.32, observed 665.12$(M+H)^+$; Purity determined by RP-HPLC: 98.77%.

H-Arg-Trp-3ABA-Arg-NH_2 (2b)

^{1}H NMR (400 MHz, DMSO d_6) δ: 11.12 (s, 1H), 10.86 (s, 2H), 10.80 (s, 2H), 10. 32 (s, 1H), 10.14 (s, 2H), 9.19 (s, 2H), 8.44 (s, 2H), 7.93 - 7.91 (d, *J* = 8Hz, 2H), 7.31 - 7.01 (m, 7H), 4.62 - 4.57 (m, 2H), 4.37 - 4.35 (t, *J* = 8Hz, 1H), 3.21 - 3.20 (d, *J* = 4Hz, 2H), 2.81 (s, 2H), 2.43 - 2.40 (m, 4H), 1.27 - 1.12 (m, 8H). MALDI-TOF (+ESI-m/z): calcd for $C_{30}H_{42}N_{12}O_4$: 634.35, observed 635.44$(M+H)^+$; Purity determined by RP-HPLC: 98.66%.

H-Trp-Arg-3ABA-Arg-NH_2 (2c)

^{1}H NMR (400 MHz, DMSO d_6) δ: 11.09 (s, 1H), 10.81 (s, 2H), 10.79 (s, 2H), 10. 41 (s, 1H), 10.02 (s, 2H), 8.97 (s, 2H), 8.29 (s, 2H), 7.87 - 7.85 (d, *J* = 8Hz, 2H), 7.35 - 7.07 (m, 7H), 4.71 - 4.66 (m, 2H), 4.32 - 4.31 (t, *J* = 4Hz, 1H), 3.19 - 3.17 (d, *J* = 8Hz, 2H), 2.81 (s, 2H), 2.49 - 2.45 (m, 4H), 1.28 - 1.14 (m, 8H). MALDI-TOF (+ESI-m/z): calcd for $C_{30}H_{42}N_{12}O_4$: 634.35, observed 635.39$(M+H)^+$; Purity determined by RP-HPLC: 98.57%.

H-Trp-Trp-3ABA-Arg-Arg-NH_2 (3a)

^{1}H NMR (400 MHz, DMSO d_6) δ: 11.14 (s, 2H), 10.80 (s, 2H), 10.76 (s, 2H), 10. 29 (s, 2H), 9.91 (s, 4H), 8.90 (s, 2H), 8.22 (s, 2H), 7.74 - 7.71 (d, *J* = 12Hz, 2H), 7.29 - 6.98 (m, 12H), 4.82 - 4.77 (m, 3H), 4.30 - 4.29 (t, *J* = 4Hz, 1H), 3.18 - 3.16 (d, *J* = 8Hz, 4H), 2.80 (s, 2H), 2.51 - 2.46 (m, 4H), 1.29 - 1.13 (m, 8H). MALDI-TOF (+ESI-m/z): calcd for $C_{41}H_{52}N_{14}O_5$: 820.42, observed 821.19$(M+H)^+$; Purity determined by RP-HPLC: 96.62%.

H-Arg-Trp-3ABA-Arg-Arg-NH_2 (3b)

^{1}H NMR (400 MHz, DMSO d_6) δ: 11.04 (s, 1H), 10.78 (s, 6H), 10.71 (s, 2H), 10. 27 (s, 2H), 9.93 (s, 4H), 8.88 (s, 3H), 8.20 (s, 2H), 7.71 - 7.69 (d, *J* = 8Hz, 2H), 7.28 - 7.09 (m, 8H), 4.80 - 4.74 (m, 3H), 4.29 - 4.27 (t, *J* = 8Hz, 1H), 3.16 - 3.15 (d, *J* = 4Hz, 2H), 2.81 (s, 3H), 2.50 - 2.43 (m, 6H), 1.26 - 1.11 (m, 13H). MALDI-TOF (+ESI-m/z): calcd for $C_{36}H_{54}N_{16}O_5$: 790.45, observed 791.44$(M+H)^+$; Purity determined by RP-HPLC: 97.66%.

H-Trp-Arg-3ABA-Arg-Arg-NH_2 (3c)

^{1}H NMR (400 MHz, DMSO d_6) δ: 11.07 (s, 1H), 10.81 (s, 6H), 10.70 (s, 2H), 10. 29 (s, 2H), 9.71 (s, 4H), 8.81 (s, 3H), 8.25 (s, 2H), 7.71 - 7.69 (d, *J* = 8Hz, 2H), 7.31 - 7.11 (m, 8H), 4.82

- 4.74 (m, 3H), 4.30 - 4.27 (t, *J* = 12Hz, 1H), 3.18 - 3.16 (d, *J* = 8Hz, 2H), 2.83 (s, 3H), 2.51 - 2.46 (m, 6H), 1.21 - 1.10 (m, 13H). MALDI-TOF (+ESI-m/z): calcd for $C_{36}H_{54}N_{16}O_5$: 790.45, observed 791.41$(M+H)^+$; Purity determined by RP-HPLC: 96.95%.

H-Trp-Arg-3ABA-Trp-Arg-NH_2 (3d)

^{1}H NMR (400 MHz, DMSO d_6) δ: 11.10 (s, 2H), 10.87 (s, 2H), 10.70 (s, 2H), 10. 12 (s, 2H), 9.84 (s, 4H), 8.79 (s, 2H), 8.23 (s, 2H), 7.65 - 7.63 (d, *J* = 8Hz, 2H), 7.36 - 7.02 (m, 13H), 4.79 - 4.73 (m, 3H), 4.29 - 4.27 (t, *J* = 8Hz, 1H), 3.20 - 3.17 (d, *J* = 12Hz, 5H), 2.84 (s, 2H), 2.53 - 2.44 (m, 4H), 1.26 - 1.11 (m, 9H). MALDI-TOF (+ESI-m/z): calcd for $C_{41}H_{52}N_{14}O_5$: 820.42, observed 821.33$(M+H)^+$; Purity determined by RP-HPLC: 97.46%.

H-Arg-Trp-3ABA-Trp-Arg-NH_2 (3e)

^{1}H NMR (400 MHz, DMSO d_6) δ: 11.12 (s, 2H), 10.81 (s, 2H), 10.78 (s, 2H), 10. 23 (s, 2H), 9.86 (s, 4H), 8.94 (s, 2H), 8.19 (s, 2H), 7.72 - 7.70 (d, *J* = 8Hz, 2H), 7.33 - 6.99 (m, 14H), 4.86 - 4.81 (m, 3H), 4.33 - 4.31 (t, *J* = 8Hz, 1H), 3.20 - 3.18 (d, *J* = 8Hz, 4H), 2.84 (s, 2H), 2.56 - 2.49 (m, 4H), 1.27 - 1.13 (m, 8H). MALDI-TOF (+ESI-m/z): calcd for $C_{41}H_{52}N_{14}O_5$: 820.42, observed 821.41$(M+H)^+$; Purity determined by RP-HPLC: 97.42%.

H-Trp-Trp-Arg-3ABA-Arg-Arg-NH_2 (4a)

^{1}H NMR (400 MHz, DMSO d_6) δ: 10.96 (s, 1H), 10.90 (s, 3H), 10.82 (s, 2H),10. 76 (s, 4H), 10.35 (s, 2H), 9.37 (s, 6H), 8.51 (s, 2H), 7.94 - 7.93 (d, *J* = 4Hz, 2H), 7.75 - 7.57 (m, 4H), 7.48 - 6.96 (m, 8H), 4.70 - 4.65 (m, 3H), 4.21 - 4.19 (t, *J* = 8Hz, 2H), 3.14 - 3.12 (d, *J* = 8Hz, 8H), 2.83 (s, 3H), 2.47 - 2.45 (m, 6H), 1.24 - 1.08 (m, 14H). MALDI-TOF (+ESI-m/z): calcd for $C_{47}H_{64}N_{18}O_6$: 976.53, observed 977.23$(M+H)^+$; Purity determined by RP-HPLC: 97.59%.

H-Arg-Trp-Arg-3ABA-Trp-Arg-NH_2 (4b)

^{1}H NMR (400 MHz, DMSO d_6) δ: 10.98 (s, 1H), 10.88 (s, 3H), 10.80 (s, 2H), 10. 77 (s, 4H), 10.32 (s, 2H), 9.34 (s, 6H), 8.52 (s, 2H), 7.95 - 7.94 (d, *J* = 4Hz, 2H), 7.71 - 7.53 (m, 4H), 7.44 - 6.90 (m, 8H), 4.68 - 4.61 (m, 3H), 4.24 - 4.22 (t, *J* = 8Hz, 2H), 3.13 - 3.11 (d, *J* = 8Hz, 8H), 2.84 (s, 3H), 2.47 - 2.44 (m, 6H), 1.25 - 1.07 (m, 14H). MALDI-TOF (+ESI-m/z): calcd for $C_{47}H_{64}N_{18}O_6$: 976.53, observed 977.29$(M+H)^+$; Purity determined by RP-HPLC: 97.19%.

H-Arg-Trp-Trp-3ABA-Arg-Arg-NH_2 (4c)

^{1}H NMR (400 MHz, DMSO d_6) δ: 10.98 (s, 1H), 10.89 (s, 3H), 10.81 (s, 2H), 10. 76 (s, 4H), 10.36 (s, 2H), 9.39 (s, 6H), 8.52 (s, 2H), 7.96 - 7.93 (d, *J* = 12Hz, 2H), 7.71 - 7.58 (m, 4H), 7.44 - 6.91 (m, 8H), 4.69 - 4.64 (m, 3H), 4.22 - 4.20 (t, *J* = 8Hz, 2H), 3.13 - 3.11 (d, *J* = 8Hz, 8H), 2.82 (s, 3H), 2.46 - 2.43 (m, 6H), 1.25 - 1.08 (m, 14H). MALDI-TOF (+ESI-m/z): calcd for $C_{47}H_{64}N_{18}O_6$: 976.53, observed 977.19$(M+H)^+$; Purity determined by RP-HPLC: 98.34%.

H-Trp-Arg-Arg-3ABA-Trp-Arg-NH_2 (4d)

^{1}H NMR (400 MHz, DMSO d_6) δ: 10.97 (s, 1H), 10.89 (s, 3H), 10.82 (s, 2H), 10. 76 (s, 4H), 10.35 (s, 2H), 9.39 (s, 6H), 8.52 (s, 2H), 7.95 - 7.93 (d, *J* = 8Hz, 2H), 7.72 - 7.54 (m, 4H), 7.40 - 6.90 (m, 8H), 4.70 - 4.64 (m, 3H), 4.22 - 4.20 (t, *J* = 8Hz, 2H), 3.13 - 3.12 (d, *J* = 4Hz, 8H), 2.84 (s, 3H), 2.47 - 2.45 (m, 6H), 1.24 - 1.08 (m, 14H). MALDI-TOF (+ESI-m/z): calcd for $C_{47}H_{64}N_{18}O_6$: 976.53, observed 977.27$(M+H)^+$; Purity determined by RP-HPLC: 98.40%.

H-Trp-Arg-Trp-3ABA-Arg-Arg-NH_2 (4e)

^{1}H NMR (400 MHz, DMSO d_6) δ: 10.98 (s, 1H), 10.89 (s, 3H), 10.81 (s, 2H), 10. 76 (s, 4H), 10.36 (s, 2H),9.42 (s, 6H), 8.55 (s, 2H), 7.95 - 7.94 (d, *J* = 4Hz, 2H), 7.72 - 7.54 (m, 4H), 7.43 - 6.91 (m, 8H), 4.70 - 4.64 (m, 3H), 4.22 - 4.20 (t, *J* = 8Hz, 2H), 3.13 - 3.11 (d, *J* = 8Hz, 8H), 2.84 (s, 3H), 2.48 - 2.45 (m, 6H), 1.25 - 1.08 (m, 14H). MALDI-TOF (+ESI-m/z): calcd for $C_{47}H_{64}N_{18}O_6$: 976.53, observed 977.53$(M+H)^+$; Purity determined by RP-HPLC: 97.83 %.

H-Arg-Arg-Trp-3ABA-Trp-Arg-NH_2 (4f)

^{1}H NMR (400 MHz, DMSO d_6) δ: 10.98 (s, 1H), 10.89 (s, 3H), 10.80 (s, 2H), 10. 76 (s, 4H), 10.36 (s, 2H), 9.39 (s, 6H),8.52 (s, 2H), 7.95 - 7.93 (d, *J* = 8Hz, 2H), 7.72 - 7.58 (m, 4H), 7.44 - 6.91 (m, 8H), 4.70 - 4.64 (m, 3H), 4.22 - 4.19 (t, *J* = 12Hz, 2H), 3.13 - 3.12 (d, *J* = 4Hz, 8H), 2.84 (s, 3H), 2.47 - 2.45 (m, 6H), 1.25 - 1.08 (m, 14H). MALDI-TOF (+ESI-m/z): calcd for $C_{47}H_{64}N_{18}O_6$: 976.53, observed 977.39$(M+H)^+$; Purity determined by RP-HPLC: 97.36%.

H-Trp-Arg-Trp-3ABA-Trp-Arg-NH_2 (4g)

^{1}H NMR (400 MHz, DMSO d_6) δ: 10.98 (s, 3H), 10.91 (s, 2H), 10.80 (s, 1H), 10. 76 (s, 4H), 10.36 (s, 3H), 9.31 (s, 5H), 8.51 (s, 2H), 8.16 - 8.15 (d, *J* = 8Hz, 2H), 7.74 - 7.56 (m, 8H), 7.44 - 6.84 (m, 9H), 4.70 - 4.62 (m, 2H), 4.22 - 4.19 (t, *J* = 8Hz, 3H), 3.24 - 3.22 (d, *J* = 8Hz, 8H), 2.84 (s, 2H), 2.47 - 2.45 (m, 4H), 1.25 - 1.22 (m, 4H), 1.13 - 1.07 (m, 4H). MALDI-TOF (+ESI-m/z): calcd for $C_{52}H_{62}N_{16}O_6$: 1006.5, observed 1007.49$(M+H)^+$; Purity determined by RP-HPLC: 97.81%.

4.2.4. Method for the synthesis of 3-ABA based peptidomimetics using Ornithine and Tryptophan

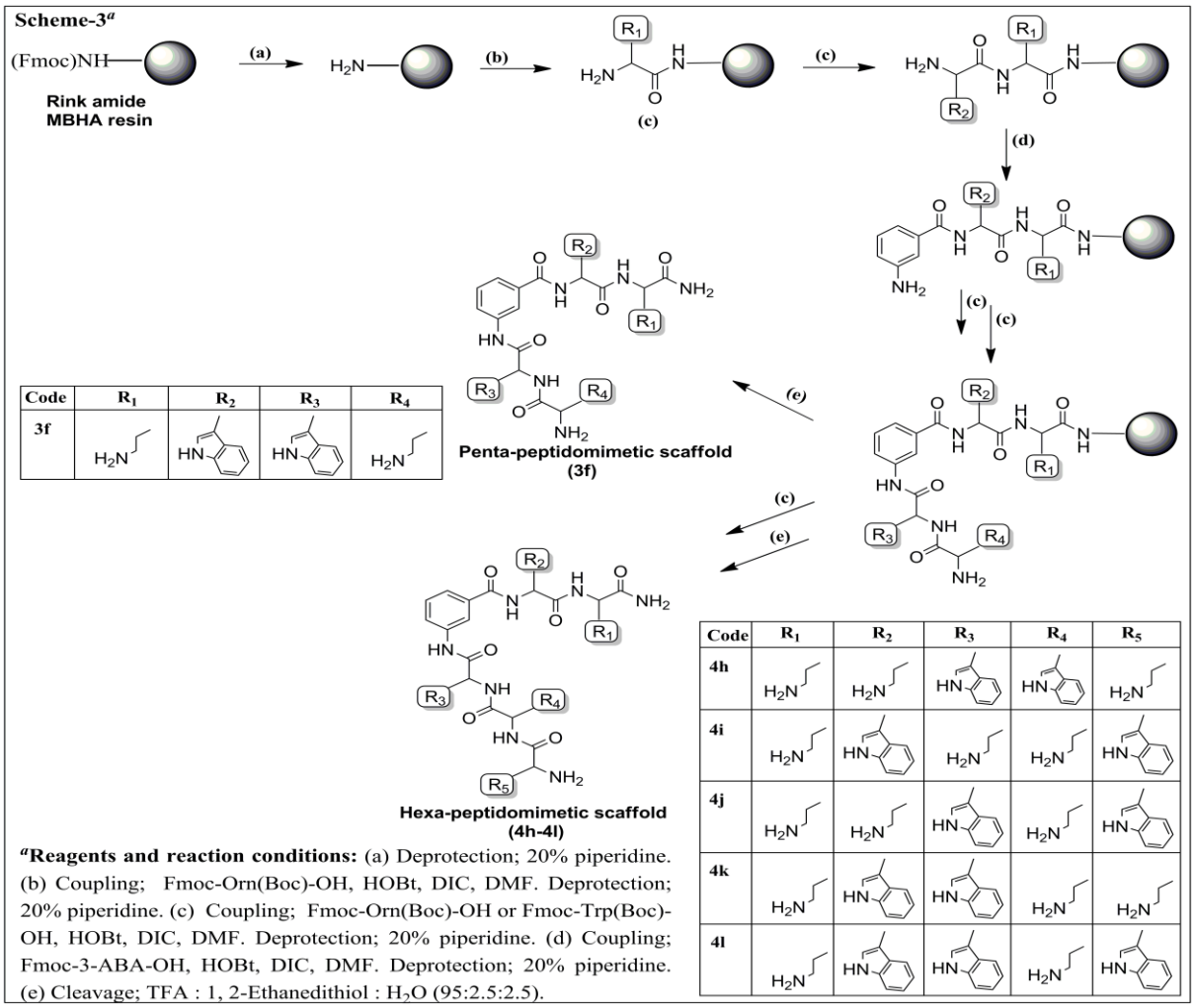

Code	R_1	R_2	R_3	R_4
3f	H_2N	HN	HN	H_2N

Code	R_1	R_2	R_3	R_4	R_5
4h	H_2N	H_2N	HN	HN	H_2N
4i	H_2N	HN	H_2N	H_2N	HN
4j	H_2N	H_2N	HN	H_2N	HN
4k	H_2N	HN	HN	H_2N	H_2N
4l	H_2N	HN	HN	H_2N	HN

[a]**Reagents and reaction conditions:** (a) Deprotection; 20% piperidine. (b) Coupling; Fmoc-Orn(Boc)-OH, HOBt, DIC, DMF. Deprotection; 20% piperidine. (c) Coupling; Fmoc-Orn(Boc)-OH or Fmoc-Trp(Boc)-OH, HOBt, DIC, DMF. Deprotection; 20% piperidine. (d) Coupling; Fmoc-3-ABA-OH, HOBt, DIC, DMF. Deprotection; 20% piperidine. (e) Cleavage; TFA : 1, 2-Ethanedithiol : H_2O (95:2.5:2.5).

General method for solid phase synthesis of peptidomimetics (3f, 4h-4l)

All peptidomimetics were synthesized manually following standard Fmoc solid phase synthesis method using Rink amide-4-methylbenzhydrylamine hydrochloride salt (MBHA) resin (loading 0.79 mmol/g) as solid support [119]. Rink amide resin (150 mg) was washed with CH_2Cl_2 (3 × 2 mL), followed by swelling in DMF (3.5 mL) for 25 min. The Fmoc protecting group of resin was removed by treating with piperidine/DMF (20% v/v) mixture for 10 min, followed by extensive washes with DMF (5 × 2 mL). The deprotection step was performed twice. Each amino acid coupling step included an Fmoc deprotection and 3 h coupling of 4 eq. of Fmoc protected amino acid (Fmoc-Orn(Boc)-OH or Fmoc-Trp(Boc)-OH or Fmoc-3ABA-OH) onto resin in the presence 2 eq. of DIC/HOBt in DMF. After the desired sequences were assembled, the peptidomimetic molecules were cleaved with a solution of TFA/H_2O/1,2-Ethanedithiol (95:2.5:2.5) from solid support (Scheme 3).

All crude peptidomimetics were analyzed on RP-HPLC using a C18 waters column (Spherisorb®, ODS2, 5 µm, 4.6 mm × 250 mm) at room temperature. A linear gradient of 0.5-60% solvent B (0.05% TFA in acetonitrile) in solvent A (0.05% TFA in water) over 35 min, followed by 60-0.5% solvent B over 10 min was used at a flow rate of 0.5 mL/min. Preparative RP-HPLC was then performed on a Waters column (Spherisorb®, ODS2, 5 µm, 20 mm × 250 mm) using 0.5-60% linear gradient of solvent B (0.05% TFA in acetonitrile) in solvent A (0.05% TFA in water) over 35 min, followed by 60-0.5% solvent B over 10 min at a flow rate of 5 mL/min. Mass spectra were obtained on a Agilent MALDI-TOF mass spectrometer. Purified HPLC fractions were than lyophilized.

H-Orn-Trp-3ABA-Trp-Orn-NH_2 (3f)

^{1}H NMR (400 MHz, DMSO d_6) δ: 10.91 (s, 2H), 10.83 (s, 2H), 10.80 (s, 1H), 10. 21 (s, 2H), 9.50 (s, 3H), 8.54 (s, 4H), 8.14 - 8.12 (d, *J* = 8Hz, 2H), 7.83 - 7.44 (m, 12H), 4.67 - 4.58 (m, 3H), 4.23 - 4.21 (t, *J* = 8Hz, 1H), 3.32 - 3.28 (d, *J* = 16Hz, 5H), 2.49 - 2.44 (m, 5H), 1.72 - 1.61 (m, 4H), 1.26 - 1.08 (m, 4H). MALDI-TOF (+ESI-m/z): calcd for $C_{39}H_{48}N_{10}O_5$: 736.38, observed 737.18$(M+H)^+$; Purity determined by RP-HPLC: 98.66%.

H-Orn-Trp-Trp-3ABA-Orn-Orn-NH_2 (4h)

^{1}H NMR (400 MHz, DMSO d_6) δ: 10.97 (s, 2H), 10.85 (s, 2H), 10.78 (s, 2H), 10. 38 (s, 2H), 9.54 (s, 3H), 8.81 (s, 6H), 8.61 - 8.58 (d, *J* = 12Hz, 2H), 8.51 - 8.42 (m, 4H), 8.35 - 7.88 (m, 4H), 7.49 - 6.99 (m, 5H), 4.70 - 4.61 (m, 3H), 4.34 - 4.20 (m, 2H), 3.27 - 3.23 (d, *J* = 16Hz, 5H), 2.83 - 2.68 (m, 5H), 2.47 - 2.45 (m, 2H), 1.72 - 1.55(m, 7H), 1.27 - 1.07 (m, 6H). MALDI-TOF (+ESI-m/z): calcd for $C_{44}H_{58}N_{12}O_6$: 850.46, observed 851.47$(M+H)^+$; Purity determined by RP-HPLC: 96.29%.

H-Trp-Orn-Orn-3ABA-Trp-Orn-NH_2 (4i)

^{1}H NMR (400 MHz, DMSO d_6) δ: 10.98 (s, 2H), 10.84 (s, 1H), 10.81 (s, 2H), 10. 38 (s, 2H), 9.50 (s, 4H), 8.79 (s, 6H), 8.66 - 8.63 (d, *J* = 12Hz, 2H), 8.51 - 8.43 (m, 5H), 8.35 - 7.83 (m, 4H), 7.46 - 6.90 (m, 6H), 4.68 - 4.61 (m, 3H), 4.37 - 4.24 (m, 2H), 3.52 - 3.47 (d, *J* = 20Hz, 5H), 2.83 - 266 (m, 6H), 2.47 - 2.45 (m, 2H), 1.72 - 1.54 (m, 7H), 1.25 - 1.08 (m, 6H). MALDI-TOF (+ESI-m/z): calcd for $C_{44}H_{58}N_{12}O_6$: 850.46, observed 851.37$(M+H)^+$; Purity determined by RP-HPLC: 97.80%.

H-Trp-Orn-Trp-3ABA-Orn-Orn-NH_2 (4j)

^{1}H NMR (400 MHz, DMSO d_6) δ: 10.98 (s, 2H), 10.85 (s, 1H), 10.80 (s, 2H), 10. 41 (s, 2H), 9.52 (s, 4H), 8.79 (s, 6H), 8.64 - 8.61 (d, *J* = 12Hz, 2H), 8.47 - 8.39 (m, 5H), 8.33 - 7.80 (m, 4H), 7.45 - 6.88 (m, 6H), 4.70 - 4.58 (m, 3H), 4.38 - 4.24 (m, 2H), 3.67 - 3.62 (d, *J* = 20Hz,

5H), 2.81 - 265 (m, 6H), 2.46 - 2.45 (m, 2H), 1.71 - 1.54 (m, 7H), 1.26 - 1.07 (m, 6H). MALDI-TOF (+ESI-m/z): calcd for $C_{44}H_{58}N_{12}O_6$: 850.46, observed 851.41$(M+H)^+$; Purity determined by RP-HPLC: 98.69%.

H-Orn-Orn-Trp-3ABA-Trp-Orn-NH_2 (4k)

^{1}H NMR (400 MHz, DMSO d_6) δ: 10.98 (s, 2H), 10.85 (s, 1H), 10.81 (s, 1H), 10. 38 (s, 2H), 9.50 (s, 5H), 8.79 (s, 6H), 8.64 - 8.62 (d, *J* = 8Hz, 2H), 8.49 - 8.42 (m, 5H), 8.34 - 7.83 (m, 4H), 7.46 - 6.90 (m, 6H), 4.69 - 4.61 (m, 3H), 4.37 - 4.21 (m, 2H), 3.68 - 3.60 (d, *J* = 32Hz, 5H), 2.84 - 266 (m, 6H), 2.47 - 2.45 (m, 2H), 1.72 - 1.54 (m, 7H), 1.25 - 1.07 (m, 6H). MALDI-TOF (+ESI-m/z): calcd for $C_{44}H_{58}N_{12}O_6$: 850.46, observed 851.34$(M+H)^+$; Purity determined by RP-HPLC: 98.97%.

H-Trp-Orn-Trp-3ABA-Trp-Orn-NH_2 (4l)

^{1}H NMR (400 MHz, DMSO d_6) δ: 10.98 (s, 3H), 10.87 (s, 1H), 10.82 (s, 1H), 10. 30 (s, 1H), 9.59 (s, 3H), 8.86 (s, 5H), 8.44 - 8.38 (d, *J* = 24Hz, 2H), 7.65 - 7.26 (m, 8H), 7.02 - 6.83 (m, 11H), 4.72 - 4.68 (m, 3H), 4.45 - 4.22 (m, 2H), 3.21 - 3.17 (d, *J* = 16Hz, 6H), 2.84 - 264 (m, 5H), 2.47 - 2.45 (m, 2H), 1.71 - 1.54 (m, 6H), 1.23 - 1.06 (m, 4H). MALDI-TOF (+ESI-m/z): calcd for $C_{50}H_{58}N_{12}O_6$: 922.46, observed 923.29$(M+H)^+$; Purity determined by RP-HPLC: 98.10%.

4.2.5. Method for the synthesis of 3-ABA based peptidomimetics by replacing Tryptophan with Phenylalanine

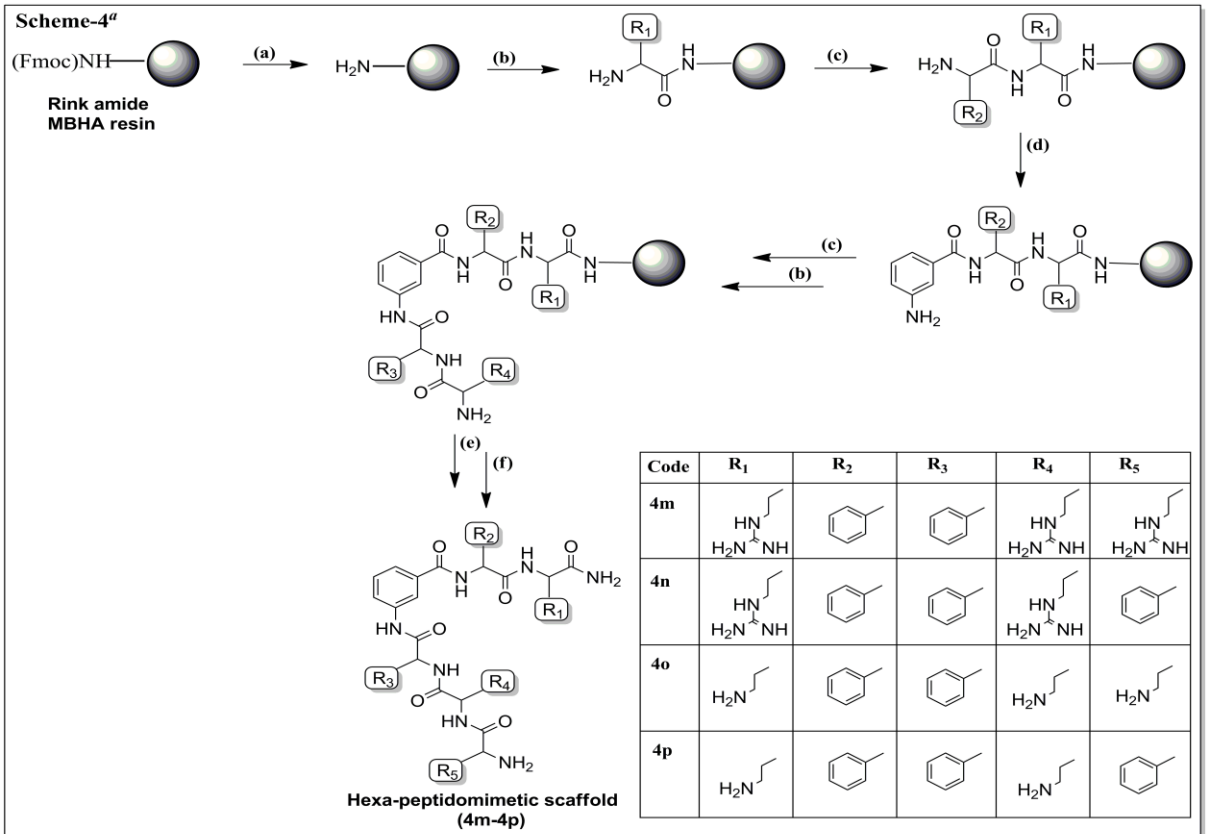

Code	R_1	R_2	R_3	R_4	R_5
4m					
4n					
4o					
4p					

[a]Reagents and reaction conditions: (a) Deprotection; 20% piperidine. (b) Coupling; Fmoc-Arg(pbf)-OH or Fmoc-Orn(Boc)-OH, HOBt, DIC, DMF. Deprotection; 20% piperidine. (c) Coupling; Fmoc-Phe-OH, HOBt, DIC, DMF. Deprotection; 20% piperidine. (d) Coupling; Fmoc-3-ABA-OH, HOBt, DIC, DMF. Deprotection; 20% piperidine. (e) Coupling; Fmoc-Arg(pbf)-OH or Fmoc-Orn(Boc)-OH or Fmoc-Phe-OH, HOBt, DIC, DMF. Deprotection; 20% piperidine. (f) Cleavage; TFA : 1, 2-Ethanedithiol : H_2O (95:2.5:2.5).

General method for solid phase synthesis of small cationic peptidomimetics (4m-4p)

All peptidomimetics were synthesized manually following standard Fmoc solid phase protocols using Rink amide-4-methylbenzhydrylamine hydrochloride salt (MBHA) resin (loading 0.79 mmol/g) as solid support [119]. Rink amide resin (150 mg) was washed with CH_2Cl_2 (3 × 2 mL), which is followed by swelling in DMF (3.5 mL) for 25 min. The Fmoc protecting group of resin was removed by treating with piperidine/DMF (20% v/v) mixture for 10 min, followed by extensive washes with DMF (5 × 2 mL). The deprotection step was performed twice. Each amino acid coupling step included an Fmoc deprotection and 3 h coupling of 4 eq. of Fmoc protected amino acid (Fmoc-Arg(Pbf)-OH or Fmoc-Orn-(Boc)-OH or Fmoc-3-ABA-OH or Fmoc-Phe-OH)onto resin in the presence 2 eq. of DIC/HOBt in DMF. After the desired sequences were assembled, the peptidomimetic molecules were cleaved with a solution of TFA/H_2O/1,2-Ethanedithiol (95:2.5:2.5) from solid support (Scheme 4).

All crude peptidomimetics were analyzed on RP-HPLC using a C18 waters column (Spherisorb®, ODS2, 5 µm, 4.6 mm × 250 mm) at room temperature. A linear gradient of 0.5-60% solvent B (0.05% TFA in acetonitrile) in solvent A (0.05% TFA in water) over 35 min, followed by 60-0.5% solvent B over 10 min was used at a flow rate of 0.5 mL/min. Preparative RP-HPLC was then performed on a Waters column (Spherisorb®, ODS2, 5 µm, 20 mm × 250 mm) using 0.5-60% linear gradient of solvent B (0.05% TFA in acetonitrile) in solvent A (0.05% TFA in water) over 35 min, followed by 60-0.5% solvent B over 10 min at a flow rate of 5 mL/min. Mass spectra were obtained on a Agilent MALDI-TOF mass spectrometer. Purified HPLC fractions were than lyophilized.

H-Arg-Arg-Phe-3ABA-Phe-Arg-NH_2 (4m)

^{1}H NMR (400 MHz, DMSO d_6) δ: 10.90 (s, 2H), 10.82 (s, 3H), 10. 77 (s, 3H), 10.35 (s, 6H), 9.39 (s, 2H), 8.51 (s, 2H), 7.58 - 7.56 (d, *J* = 8Hz, 2H), 7.49 - 7.02 (m, 13H), 4.61 - 4.54 (m, 3H), 4.17 - 4.16 (t, *J* = 4Hz, 2H), 3.11 - 3.10 (d, *J* = 4Hz, 6H), 2.83 (s, 3H), 2.47 - 2.45 (m, 6H), 1.24 - 1.07 (m, 13H). MALDI-TOF (+ESI-m/z): calcd for $C_{43}H_{62}N_{16}O_6$: 898.5, observed 899.39$(M+H)^+$; Purity determined by RP-HPLC: 97.38%.

H-Phe-Arg-Phe-3ABA-Phe-Arg-NH_2 (4n)

^{1}H NMR (400 MHz, DMSO d_6) δ: 10.89 (s, 2H), 10.80 (s, 3H), 10. 76 (s, 2H), 10.36 (s, 4H), 9.38 (s, 2H), 8.52 (s, 2H), 7.58 - 7.57 (d, *J* = 4Hz, 2H), 7.52 - 7.21 (m, 11H), 7.14 - 6.98 (m, 8H), 4.60 - 4.54 (m, 3H), 4.17 - 4.15 (t, *J* = 8Hz, 2H), 3.11 - 3.9 (d, *J* = 8Hz, 7H), 2.84 (s, 2H), 2.48 - 2.45 (m, 5H), 1.25 - 1.07 (m, 9H). MALDI-TOF (+ESI-m/z): calcd for $C_{46}H_{59}N_{13}O_6$: 889.47, observed 890.33$(M+H)^+$; Purity determined by RP-HPLC: 98.06%.

H-Orn-Orn-Phe-3ABA-Phe-Orn-NH_2 (4o):

^{1}H NMR (400 MHz, DMSO d_6) δ: 10.90 (s, 2H), 10.83 (s, 3H), 10.36 (s, 6H), 9.41 (s, 2H), 8.50 (s, 2H), 7.58 - 7.56 (d, *J* = 8Hz, 2H), 7.50 - 7.02 (m, 14H), 4.61 - 4.54 (m, 3H), 4.17 - 4.15 (t, *J* = 8Hz, 2H), 3.12 - 3.10 (d, *J* = 8Hz, 5H), 2.47 - 2.45 (m, 6H), 1.24 - 1.07 (m, 14H). MALDI-TOF (+ESI-m/z): calcd for $C_{40}H_{56}N_{10}O_6$: 772.44, observed 773.46$(M+H)^+$; Purity determined by RP-HPLC: 97.87%.

H-Phe-Orn-Phe-3ABA-Phe-Orn-NH_2 (4p)

^{1}H NMR (400 MHz, DMSO d_6) δ: 10.89 (s, 2H), 10.80 (s, 3H), 10.36 (s, 4H), 9.36 (s, 2H), 8.50 (s, 2H), 7.58 - 7.57 (d, *J* = 4Hz, 2H), 7.53 - 7.20 (m, 10H), 7.16 - 6.98 (m, 8H), 4.60 - 4.54 (m, 3H), 4.17 - 4.15 (t, *J* = 8Hz, 2H), 3.11 - 3.9 (d, *J* = 8Hz, 7H), 2.48 - 2.45 (m, 5H), 1.25 - 1.07 (m, 9H). MALDI-TOF (+ESI-m/z): calcd for $C_{44}H_{55}N_9O_6$: 805.43, observed 806.36$(M+H)^+$; Purity determined by RP-HPLC: 98.75%.

4.2.6. Method for the synthesis of linear peptides without incorporating 3-ABA

Scheme-5[a]

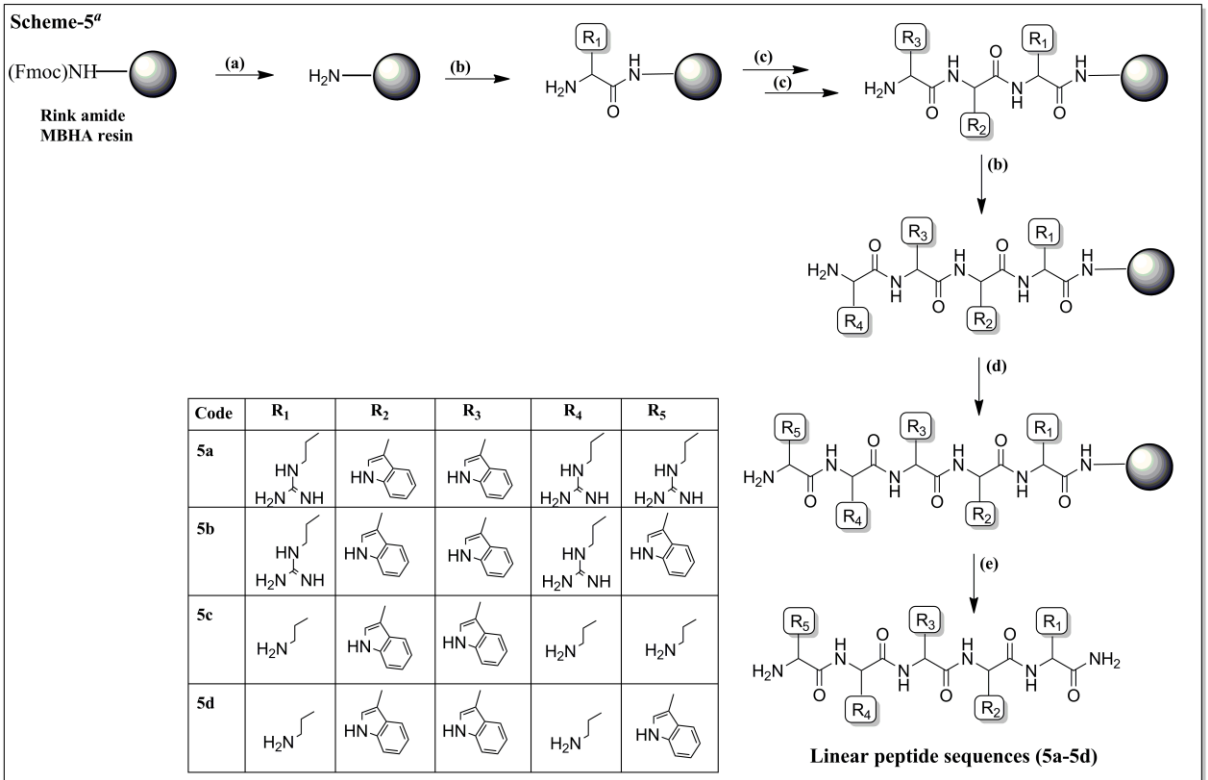

Code	R_1	R_2	R_3	R_4	R_5
5a					
5b					
5c					
5d					

[a]**Reagents and reaction conditions:** (a) Deprotection; 20% piperidine. (b) Coupling; Fmoc-Arg(Pbf)-OH or Fmoc-Orn(Boc)-OH, HOBt, DIC, DMF. Deprotection; 20% piperidine. (c) Coupling; Fmoc-Trp(Boc)-OH, HOBt, DIC, DMF. Deprotection; 20% piperidine. (d) Coupling; Fmoc-Arg(Pbf)-OH or Fmoc-Orn(Boc)-OH or Fmoc-Trp(Boc)-OH, HOBt, DIC, DMF. Deprotection; 20% piperidine. (e) Cleavage; TFA : 1, 2-Ethanedithiol : H_2O (95:2.5:2.5).

General method for solid phase synthesis of linear peptides (5a-5d).

All peptidomimetics were synthesized manually following standard Fmoc solid phase protocols using Rink amide-4-methylbenzhydrylamine hydrochloride salt (MBHA) resin (loading 0.79 mmol/g) as solid support [119]. Rink amide resin (150 mg) was washed with CH_2Cl_2 (3 × 2 mL), which is followed by swelling in DMF (3.5 mL) for 25 min. The Fmoc protecting group of resin was removed by treating with piperidine/DMF (20% v/v) mixture for 10 min, followed by extensive washes with DMF (5 × 2 mL). The deprotection step was performed twice. Each amino acid coupling step included an Fmoc deprotection and 3 h coupling of 4 eq. of Fmoc protected amino acid (Fmoc-Arg(Pbf)-OH or Fmoc-Trp(Boc)-OH) onto resin in the presence 2 eq.of DIC/HOBt in DMF. After the desired sequences were assembled, the peptidomimetic molecules were cleaved with a solution of TFA/H_2O/1,2-Ethanedithiol (95:2.5:2.5) from solid support (Scheme 5).

All crude peptide sequences were analyzed on RP-HPLC using a C18 waters column (Spherisorb®, ODS2, 5 µm, 4.6 mm × 250 mm) at room temperature. A linear gradient of 0.5-60% solvent B (0.05% TFA in acetonitrile) in solvent A (0.05% TFA in water) over 35 min,

followed by 60-0.5% solvent B over 10 min was used at a flow rate of 0.5 mL/min. Preparative RP-HPLC was then performed on a Waters column (Spherisorb®, ODS2, 5 µm, 20 mm × 250 mm) using 0.5-60% linear gradient of solvent B (0.05% TFA in acetonitrile) in solvent A (0.05% TFA in water) over 35 min, followed by 60-0.5% solvent B over 10 min at a flow rate of 5 mL/min. Mass spectra were obtained on a Agilent MALDI-TOF mass spectrometer. Purified HPLC fractions were than lyophilized.

H-Arg-Arg-Trp-Trp-Arg-NH_2 (5a)

MALDI-TOF (+ESI-m/z): calcd for $C_{40}H_{59}N_{17}O_5$: 857.49, observed 858.36$(M+H)^+$; Purity determined by RP-HPLC: 98.56%.

H-Trp-Arg-Trp-Trp-Arg-NH_2 (5b)

MALDI-TOF (+ESI-m/z): calcd for $C_{45}H_{57}N_{15}O_5$: 887.47, observed 888.42$(M+H)^+$; Purity determined by RP-HPLC: 99.01%.

H-Orn-Orn-Trp-Trp-Orn-NH_2 (5c)

MALDI-TOF (+ESI-m/z): calcd for $C_{37}H_{53}N_{11}O_5$: 731.42, observed 732.33$(M+H)^+$; Purity determined by RP-HPLC: 98.74%.

H-Trp-Orn-Trp-Trp-Orn-NH_2 (5d)

MALDI-TOF (+ESI-m/z): calcd for $C_{43}H_{53}N_{11}O_5$: 803.42, observed 804.27$(M+H)^+$; Purity determined by RP-HPLC: 98.61%.

4.2.7. Spectra

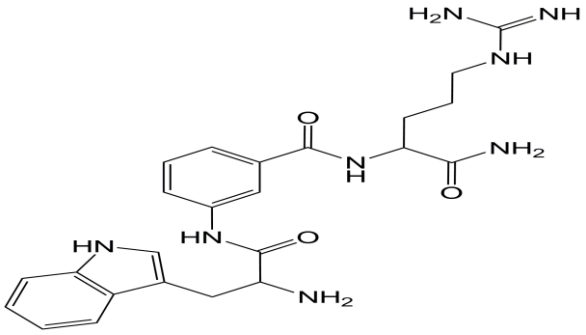

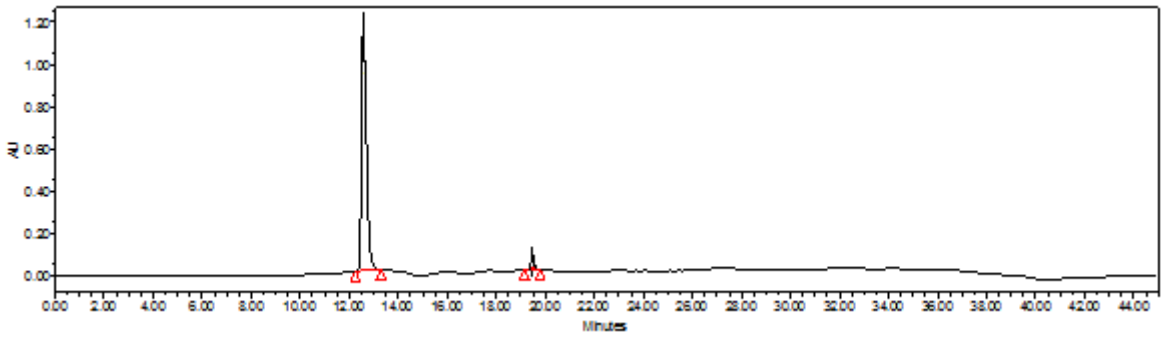

	Name	Retention Time	Area	% Area	Height	RT Ratio
1		12.71	16573026	99.61	1184979	
2		19.47	64616	0.39	5759	

Molecular Weight: 478.24

LCMS (+ESI, m/z): 479.11 $(M+H)^+$

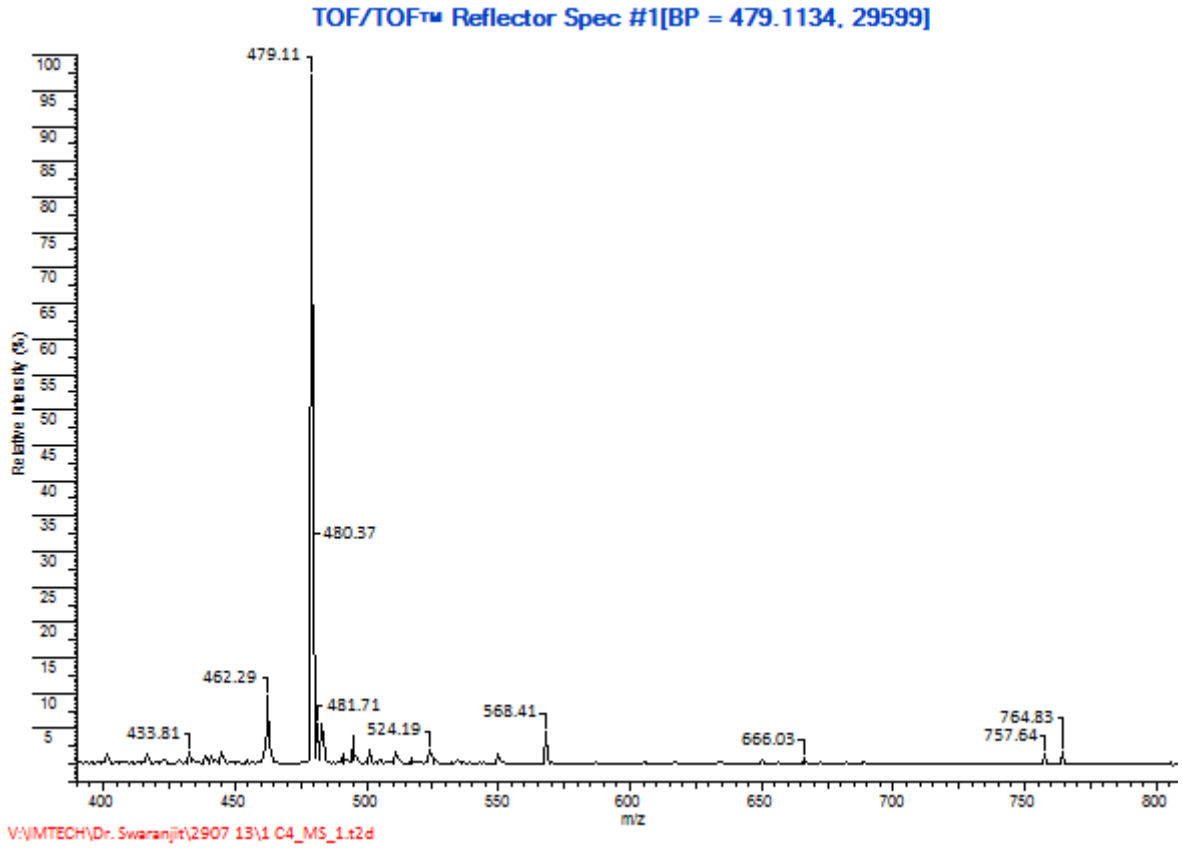

Figure 4.40: Chemical structure, HPLC chromatogram, and Mass spectra of peptidomimetic molecule **1a**

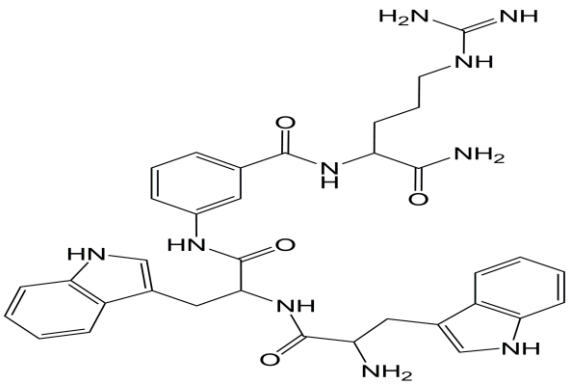

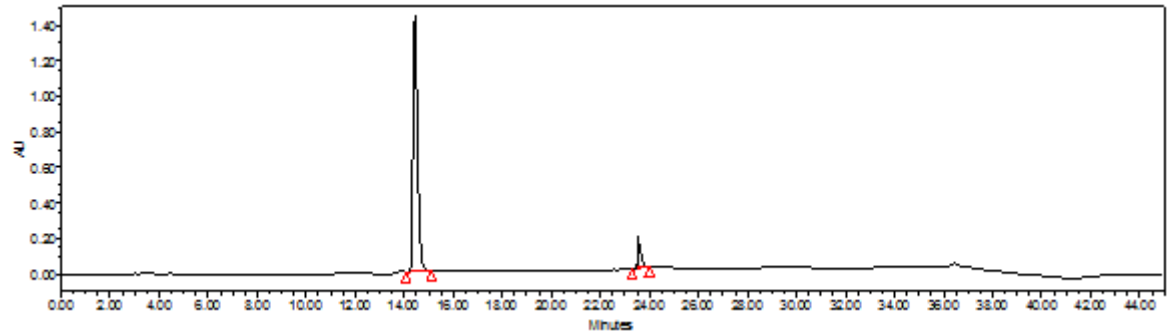

	Name	Retention Time	Area	% Area	Height	RT Ratio
1		14.62	18281342	98.77	1412045	
2		23.76	227484	1.23	8692	

Molecular Weight: 664.32

LCMS (+ESI, m/z): 665.27$(M+H)^+$

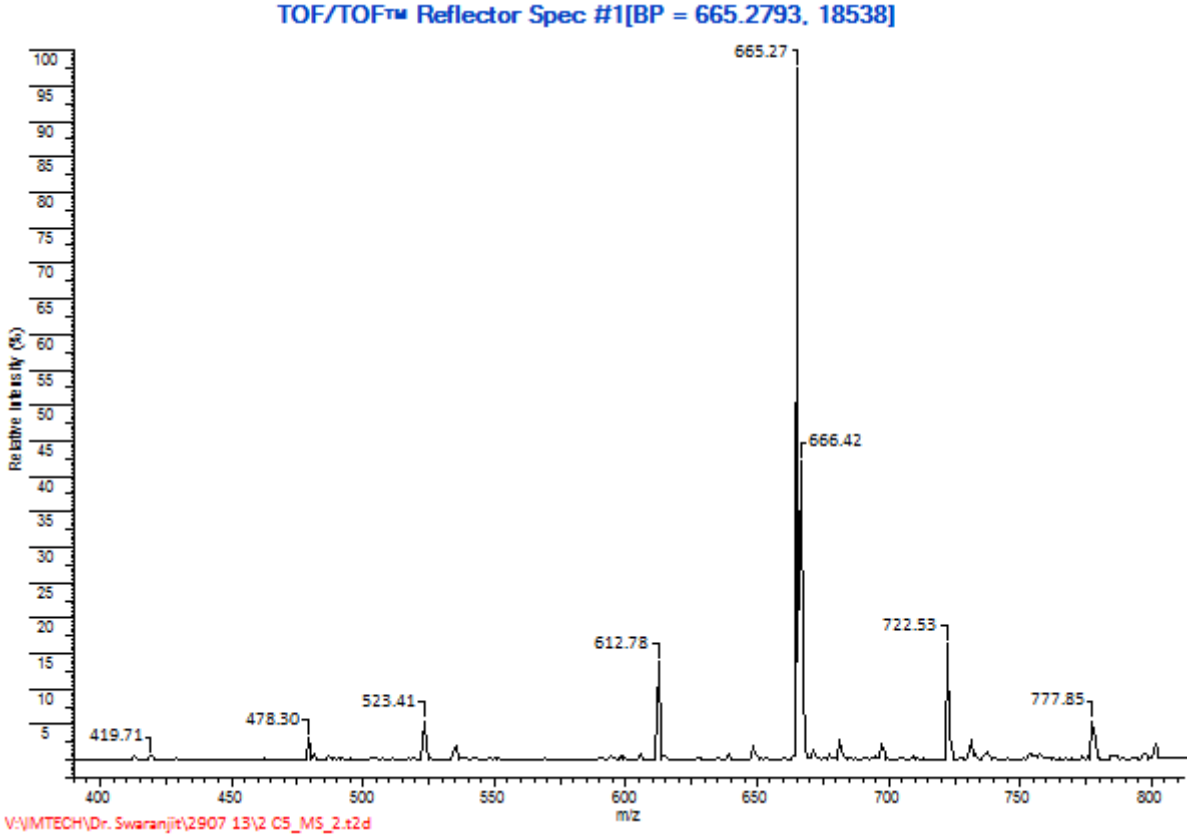

Figure 4.41: Chemical structure, HPLC chromatogram, and Mass spectra of peptidomimetic molecule **2a**

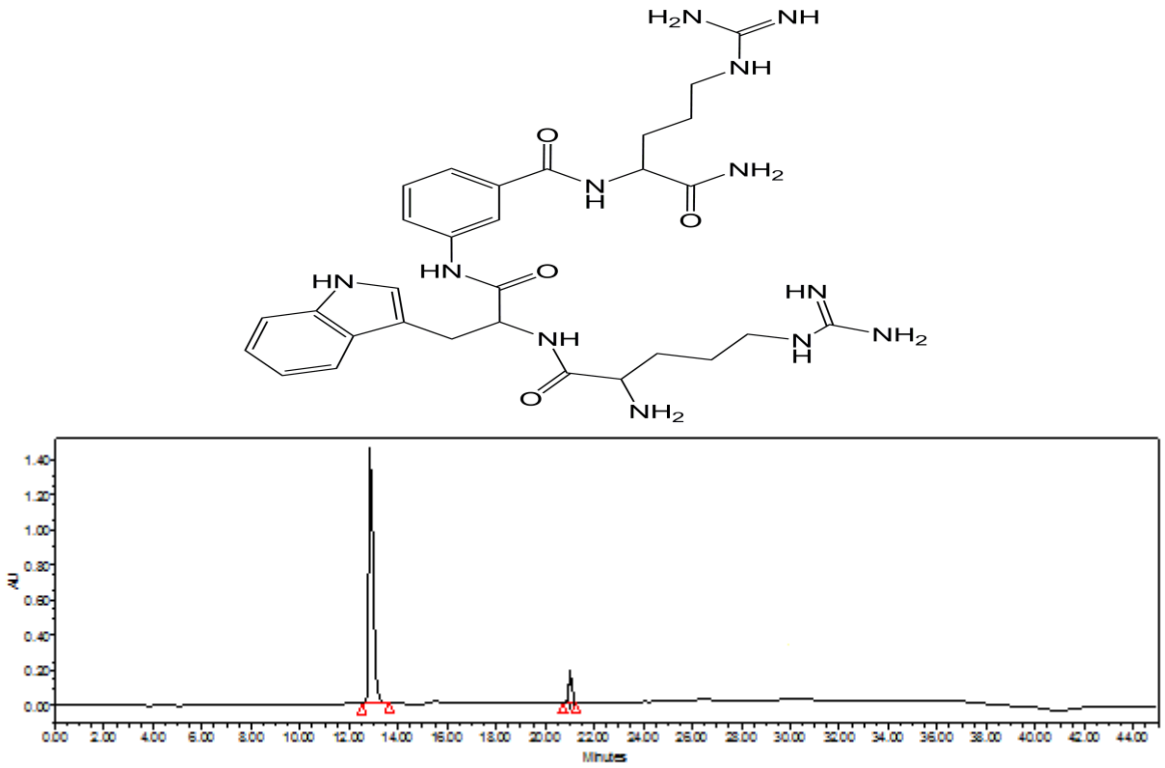

	Name	Retention Time	Area	% Area	Height	RT Ratio
1		13.04	18575158	98.66	1420411	
2		20.98	64223	1.34	6204	

Molecular Weight: 634.35

LCMS (+ESI, m/z): 635.44$(M+H)^+$

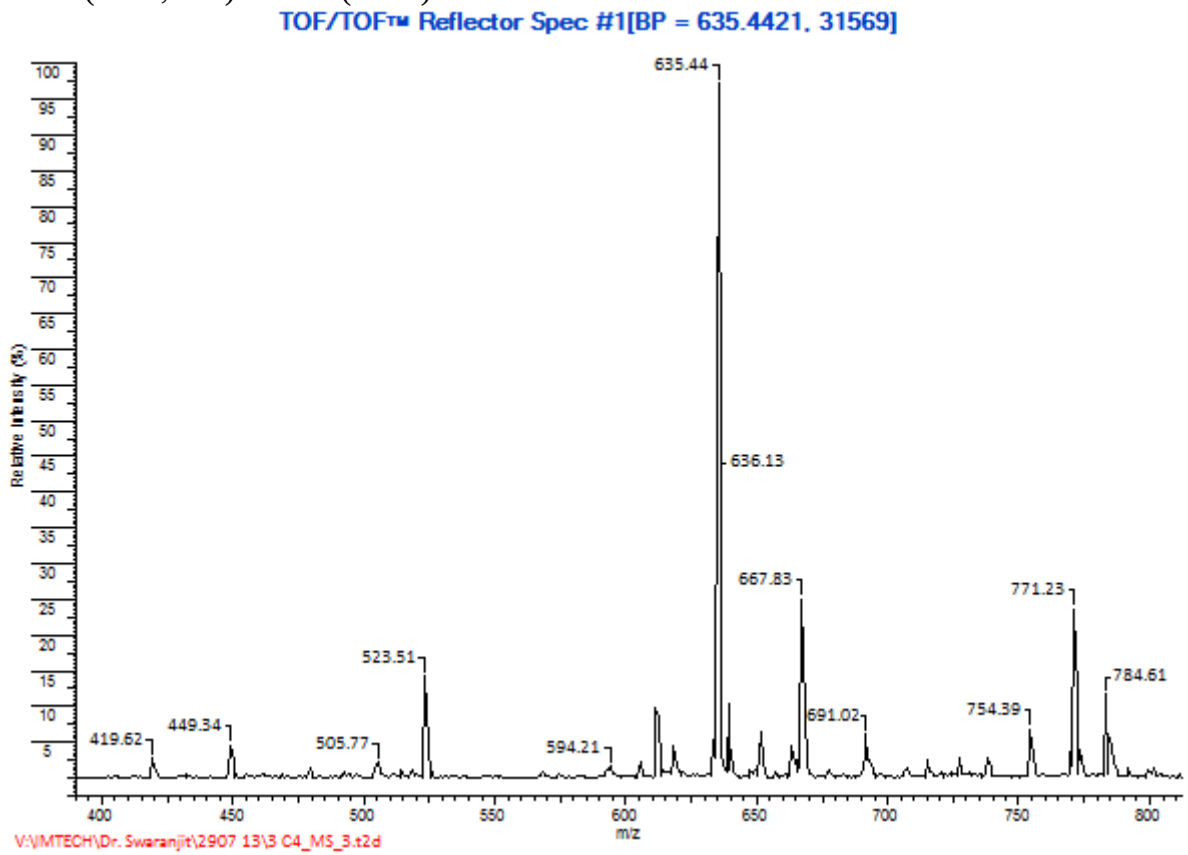

Figure 4.42: Chemical structure, HPLC chromatogram, and Mass spectra of peptidomimetic molecule **2b**

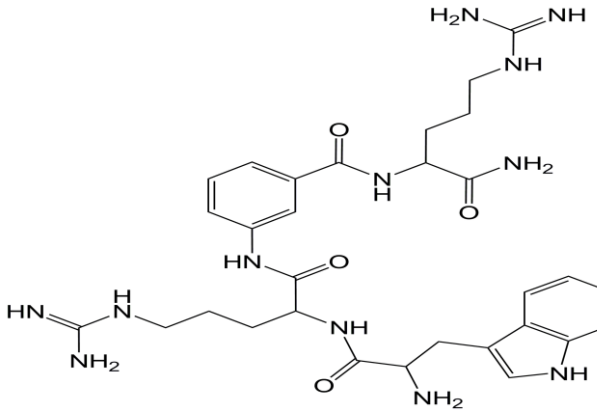

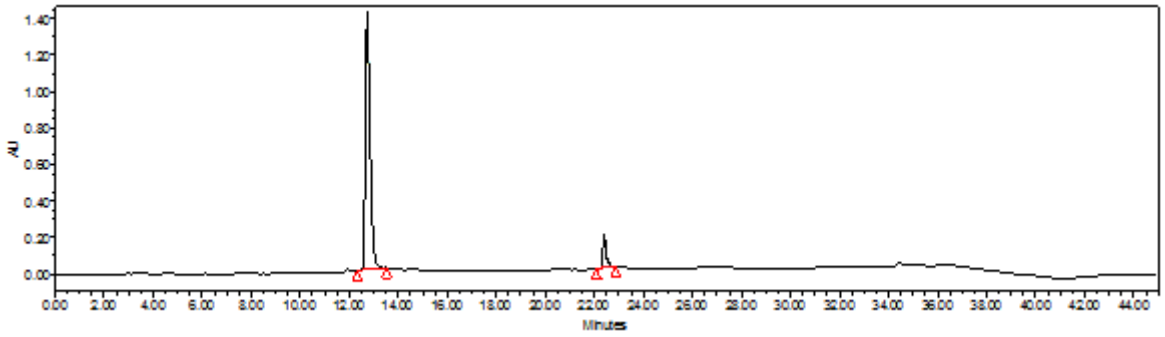

	Name	Retention Time	Area	% Area	Height	RT Ratio
1		12.84	18578390	98.57	1368616	
2		22.49	62016	1.43	6745	

Molecular Weight: 634.35

LCMS (+ESI, m/z): 635.39$(M+H)^+$

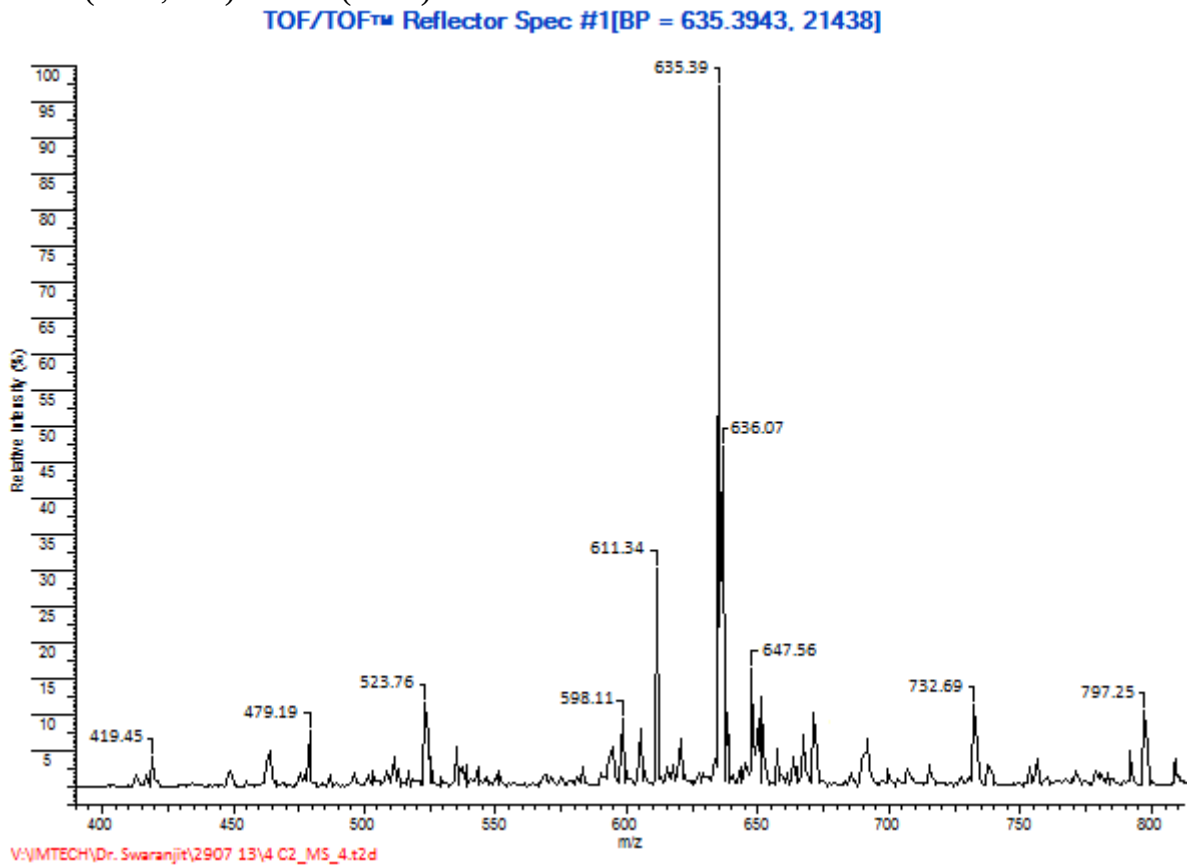

Figure 4.43: Chemical structure, HPLC chromatogram, and Mass spectra of peptidomimetic molecule **2c**

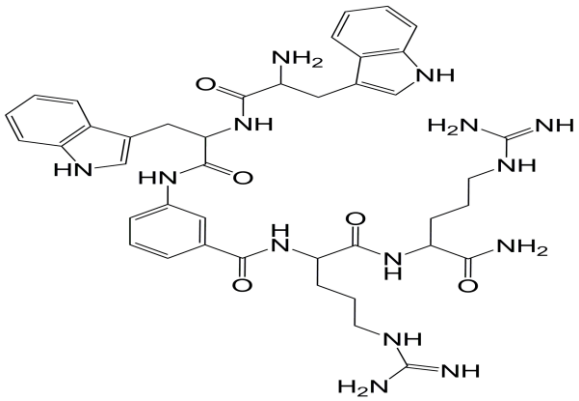

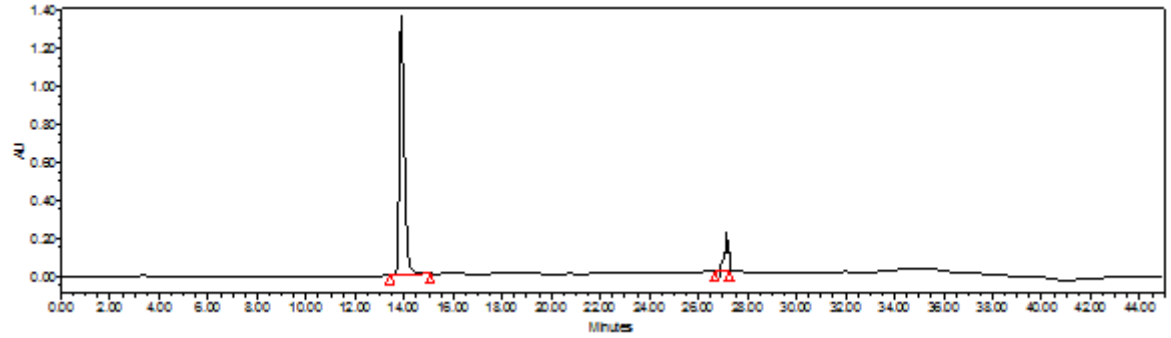

	Name	Retention Time	Area	% Area	Height	RT Ratio
1		14.27	19157909	96.62	1320434	
2		27.01	72229	3.38	6211	

Molecular Weight: 820.42

LCMS (+ESI, m/z): 821.19$(M+H)^+$

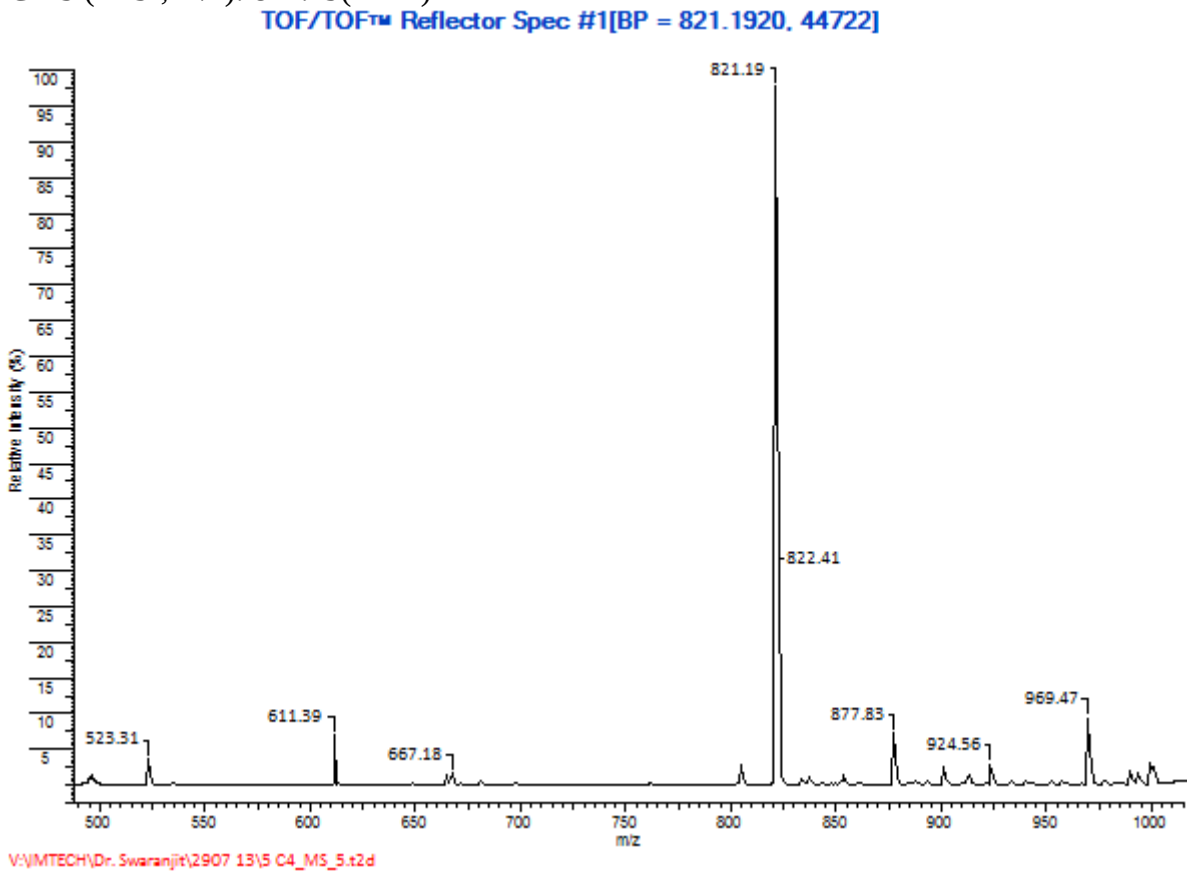

Figure 4.44: Chemical structure, HPLC chromatogram, and Mass spectra of peptidomimetic molecule **3a**

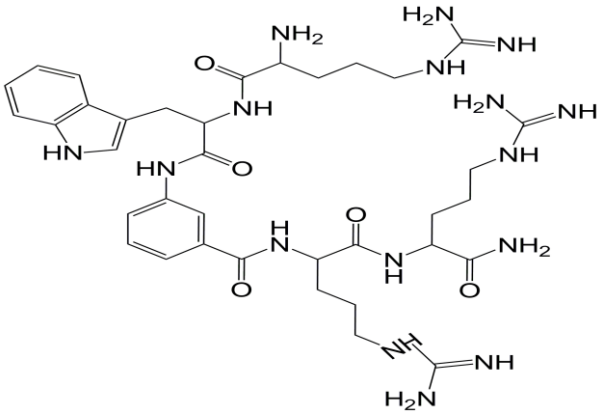

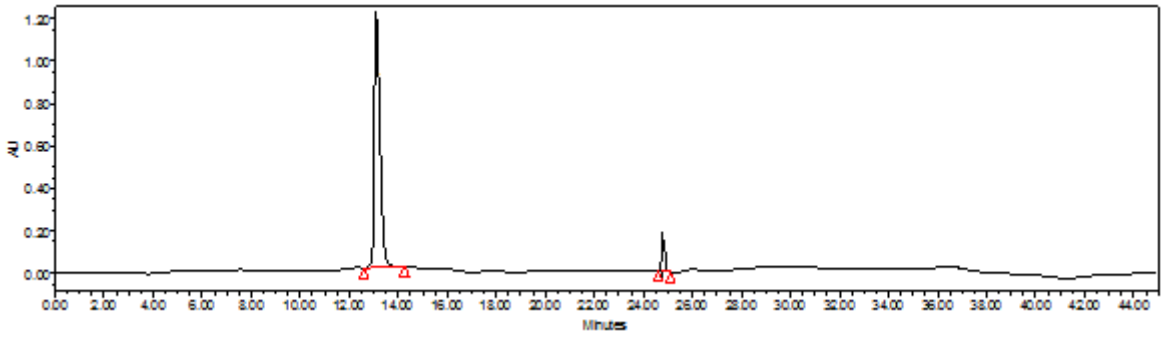

	Name	Retention Time	Area	% Area	Height	RT Ratio
1		13.41	19384992	97.66	1176418	
2		24.83	66234	2.34	5838	

Molecular Weight: 790.45

LCMS (+ESI, m/z): 791.44$(M+H)^+$

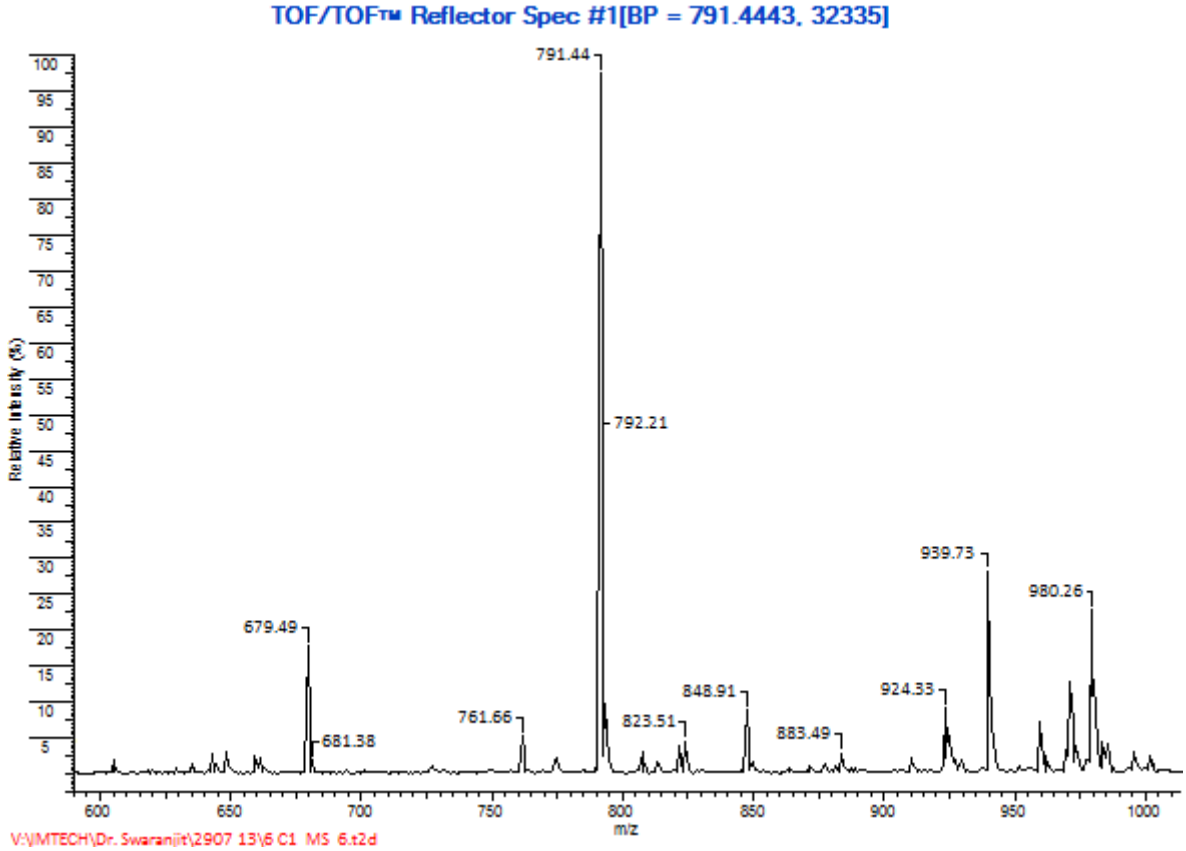

Figure 4.45: Chemical structure, HPLC chromatogram, and Mass spectra of peptidomimetic molecule **3b**

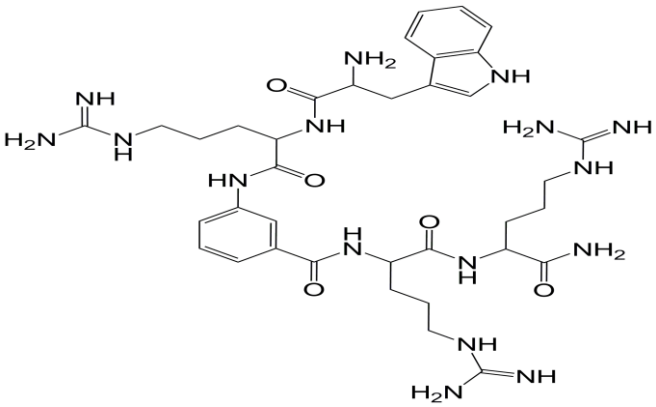

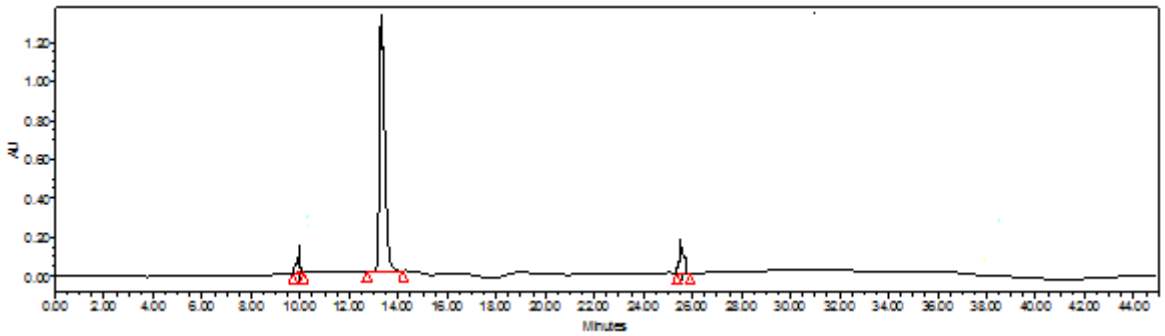

	Name	Retention Time	Area	% Area	Height	RT Ratio
1		9.99	14227	0.86	1119	
2		13.48	19335641	96.95	1294613	
3		25.81	31182	2.16	1908	

Molecular Weight: 790.45

LCMS (+ESI, m/z): 791.41$(M+H)^+$

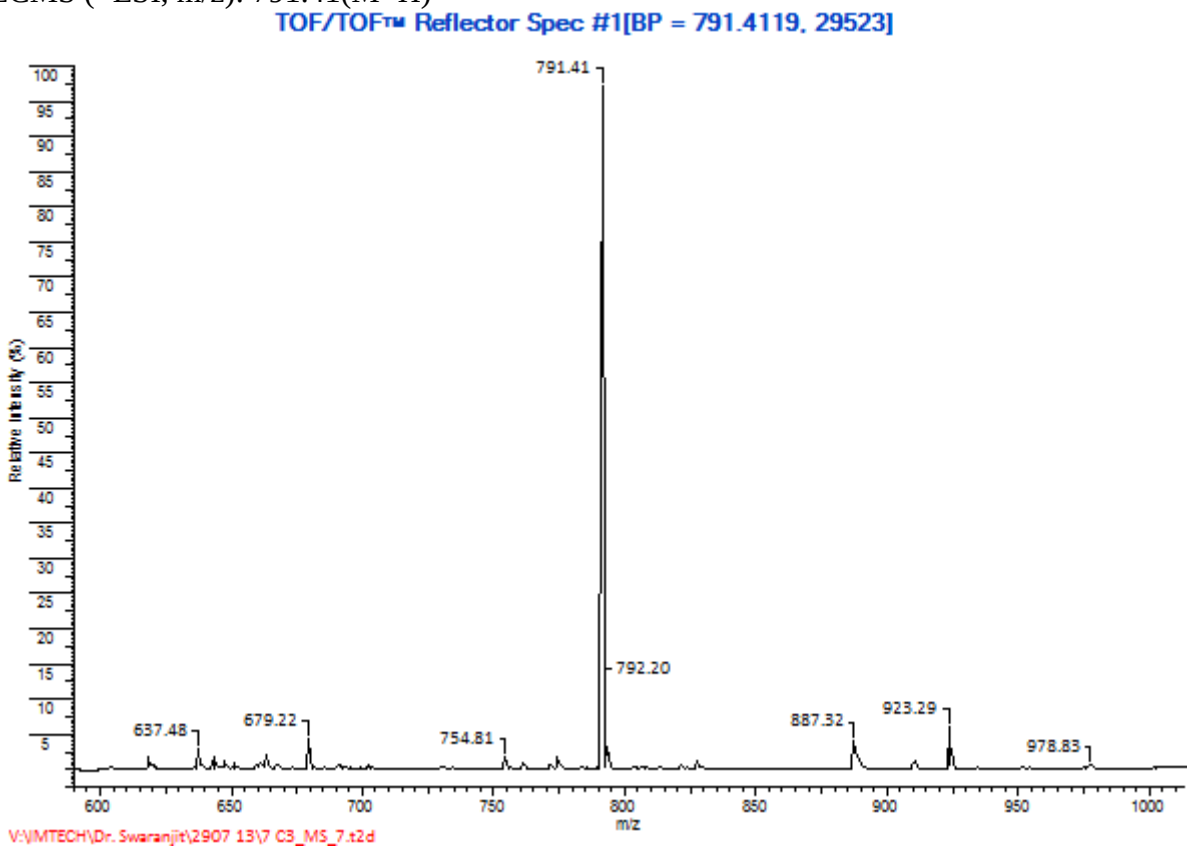

Figure 4.46: Chemical structure, HPLC chromatogram, and Mass spectra of peptidomimetic molecule **3c**

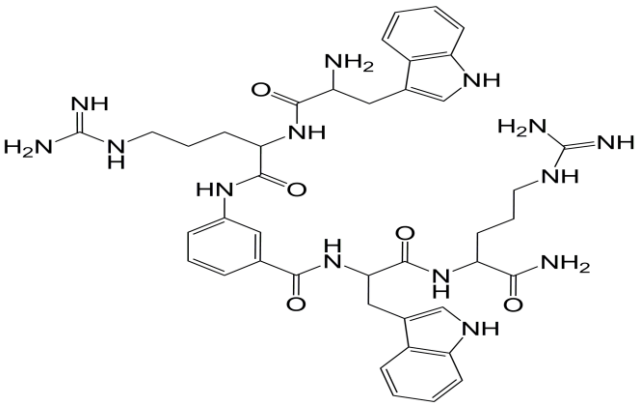

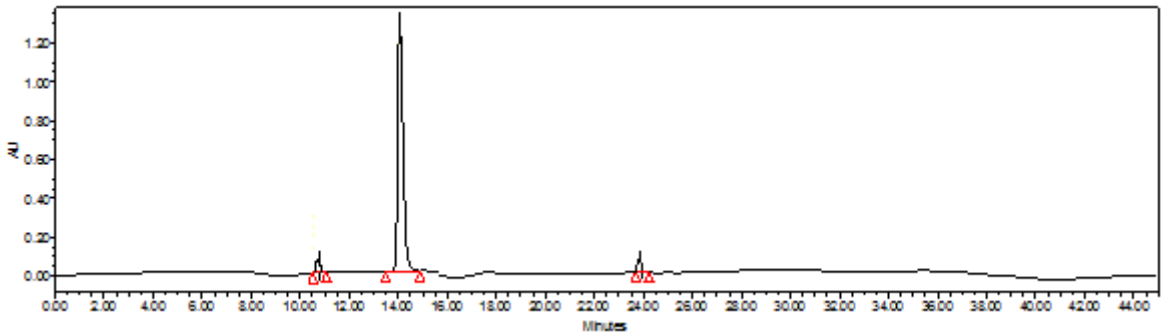

	Name	Retention Time	Area	% Area	Height	RT Ratio
1		10.78	15594	1.19	1317	
2		14.19	19576421	97.46	1300952	
3		23.96	18237	1.35	1956	

Molecular Weight: 820.42

LCMS (+ESI, m/z): 821.33$(M+H)^+$

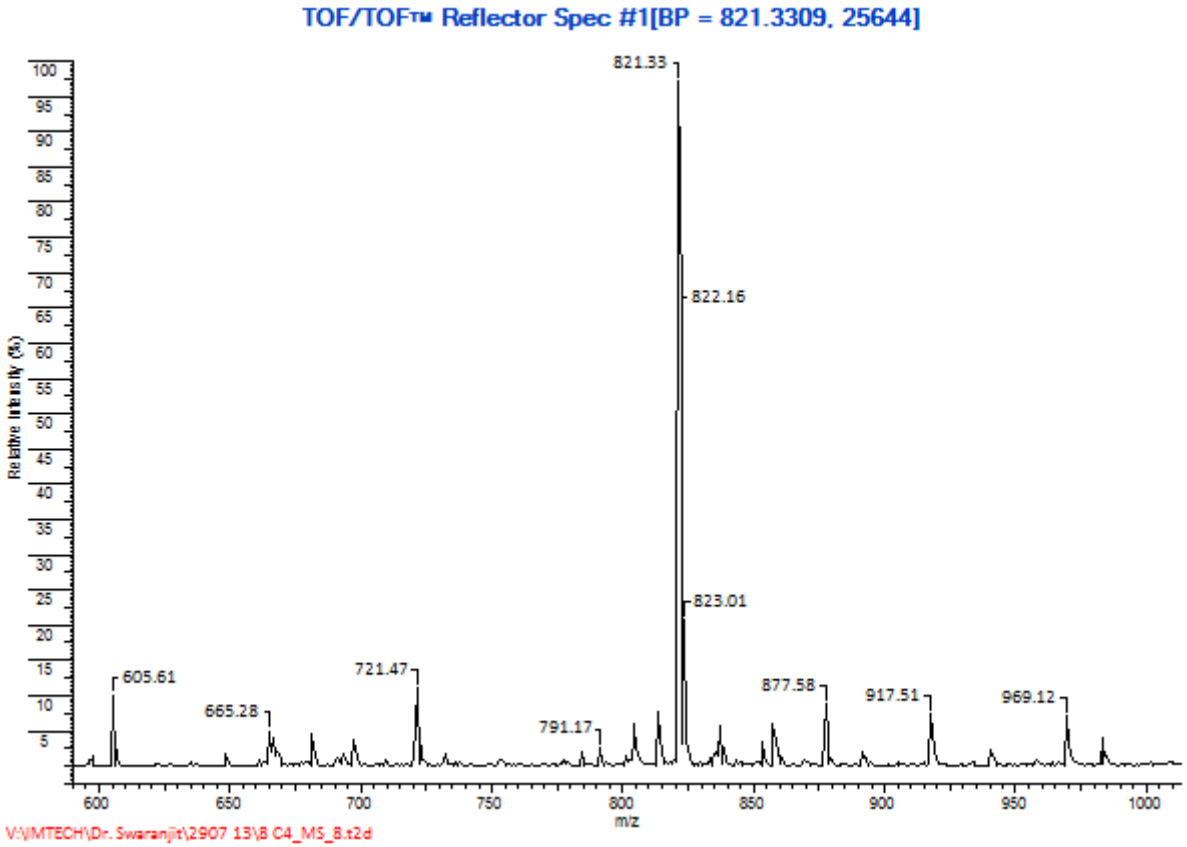

Figure 4.47: Chemical structure, HPLC chromatogram, and Mass spectra of peptidomimetic molecule **3d**

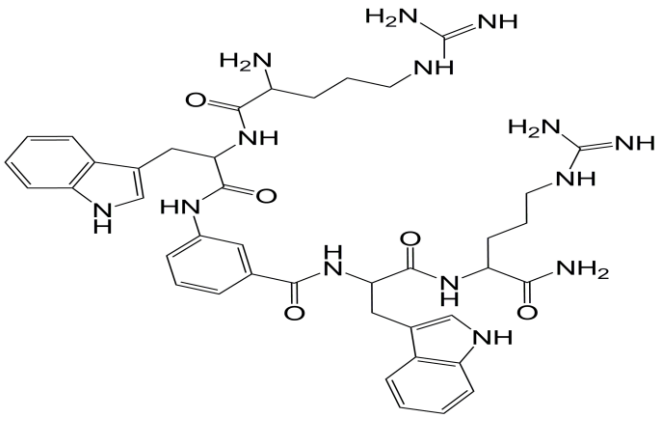

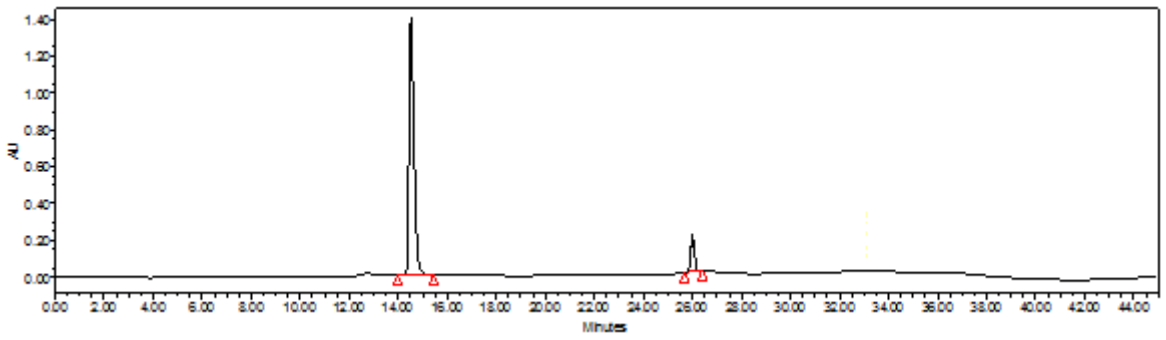

	Name	Retention Time	Area	% Area	Height	RT Ratio
1		14.61	19539837	97.42	1368615	
2		26.07	33654	2.58	9573	

Molecular Weight: 820.42

LCMS (+ESI, m/z): 821.13$(M+H)^+$

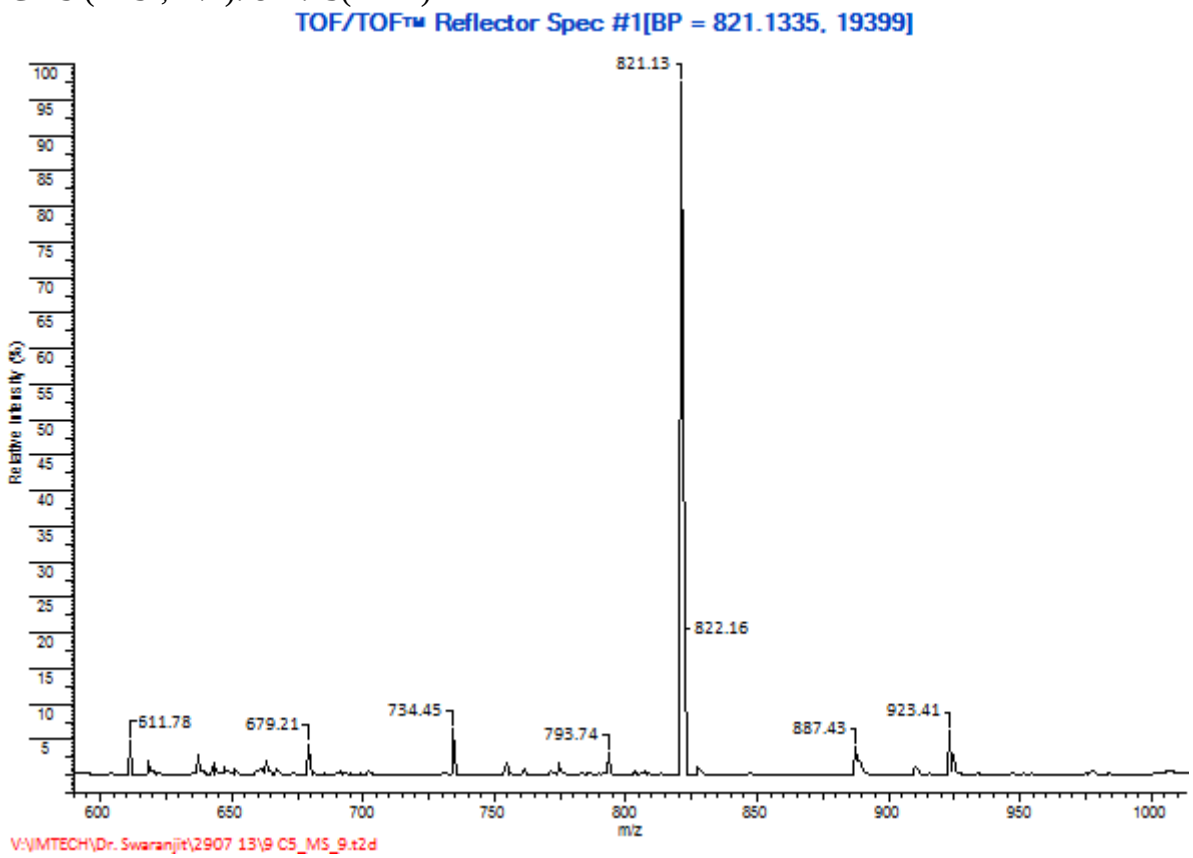

Figure 4.48: Chemical structure, HPLC chromatogram, and Mass spectra of peptidomimetic molecule **3e**

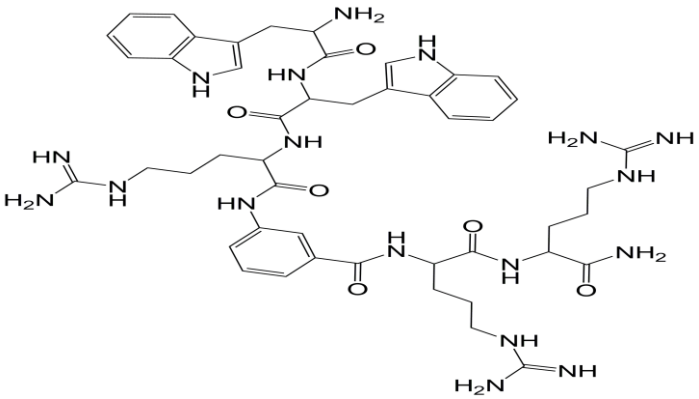

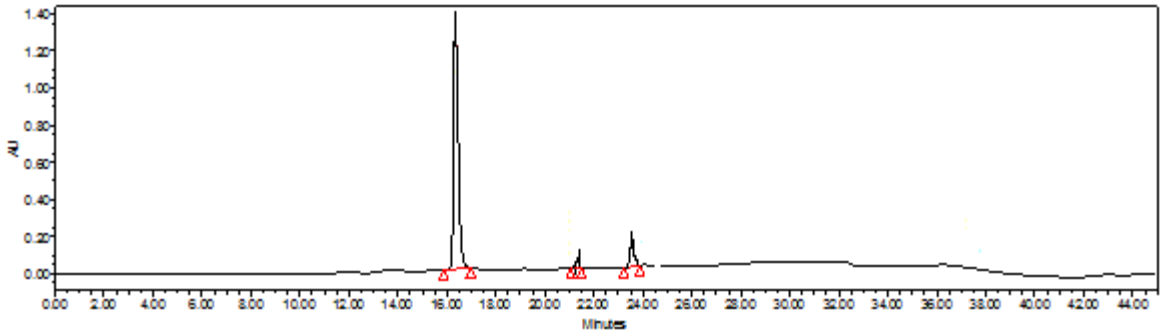

	Name	Retention Time	Area	% Area	Height	RT Ratio
1		16.48	18615730	97.59	1417432	
2		21.30	6752	0.33	1367	
3		23.52	22567	2.08	3256	

Molecular Weight: 976.53

LCMS (+ESI, m/z): 977.23 $(M+H)^+$

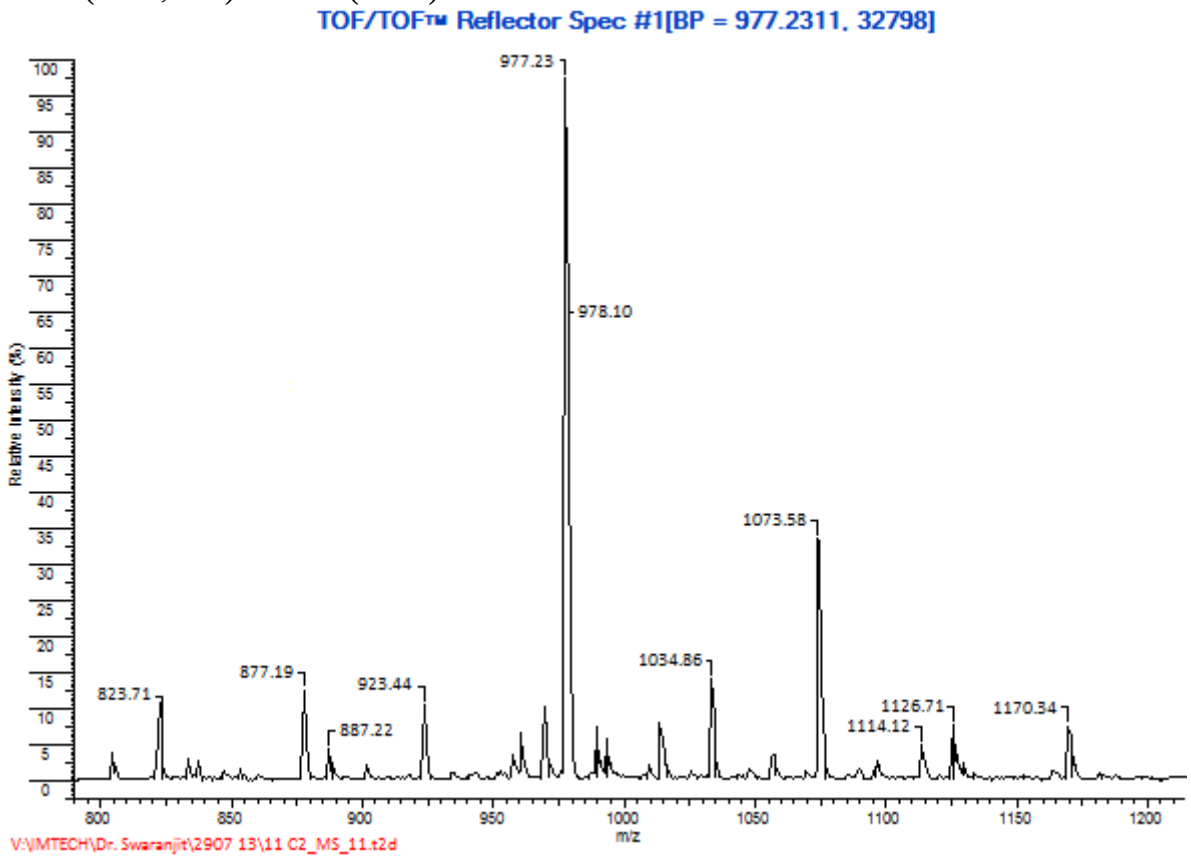

Figure 4.49: Chemical structure, HPLC chromatogram, and Mass spectra of peptidomimetic molecule **4a**

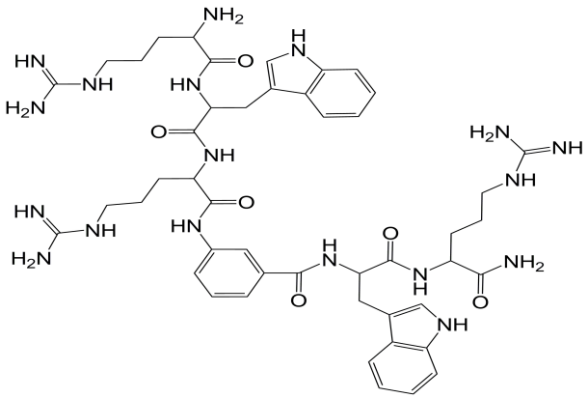

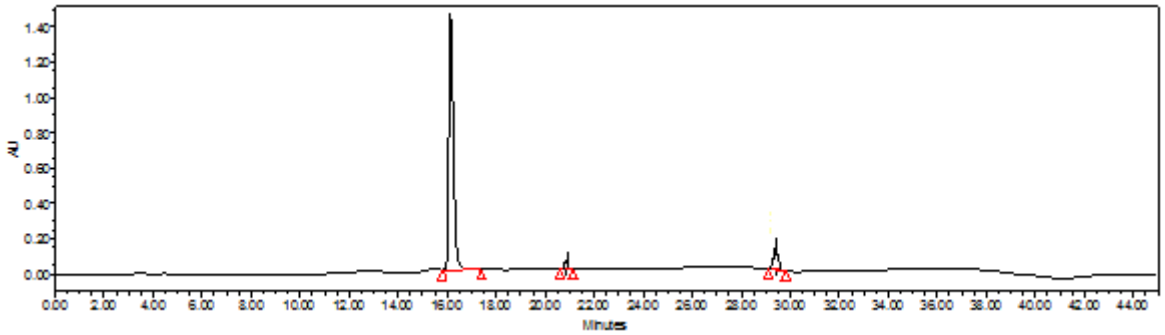

	Name	Retention Time	Area	% Area	Height	RT Ratio
1		16.37	21825388	97.19	1578732	
2		20.83	6005	0.48	2437	
3		29.46	24165	2.33	7721	

Molecular Weight: 976.53

LCMS (+ESI, m/z): 977.29 $(M+H)^+$

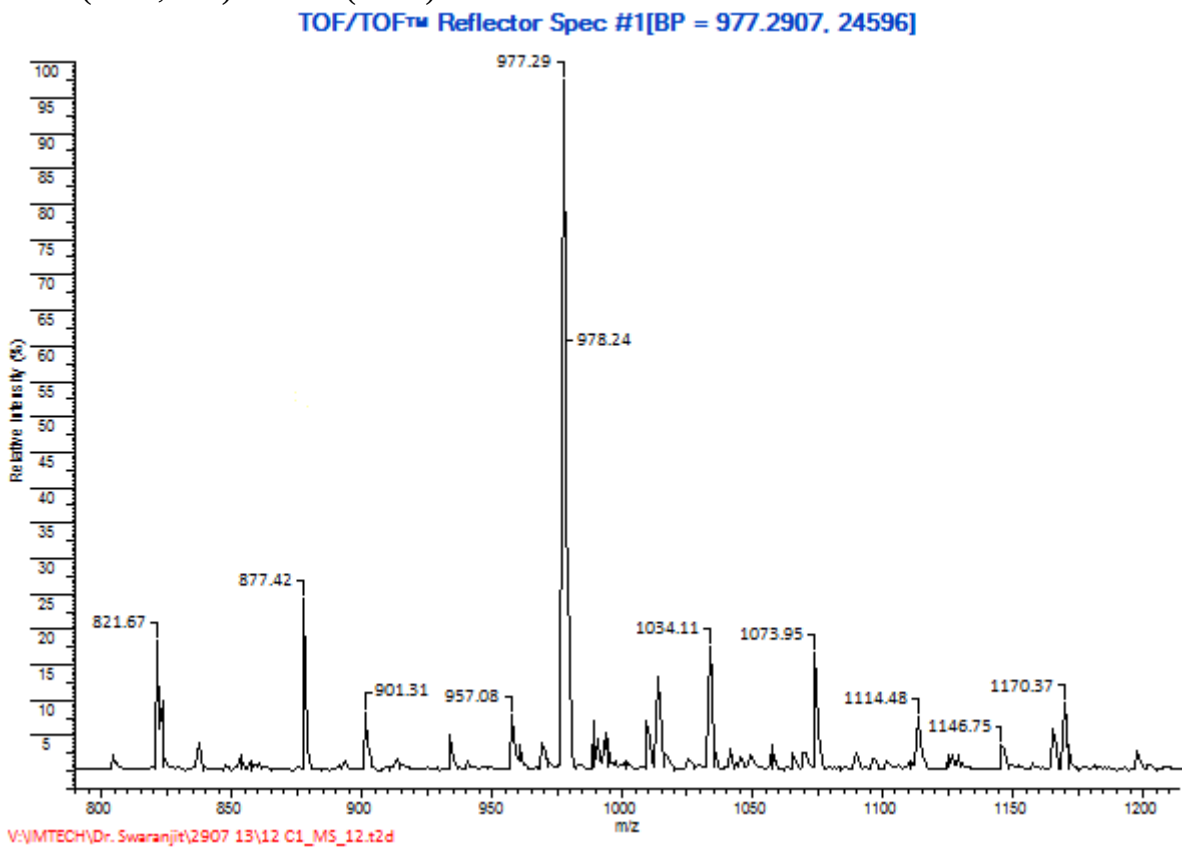

Figure 4.50: Chemical structure, HPLC chromatogram, and Mass spectra of peptidomimetic molecule **4b**

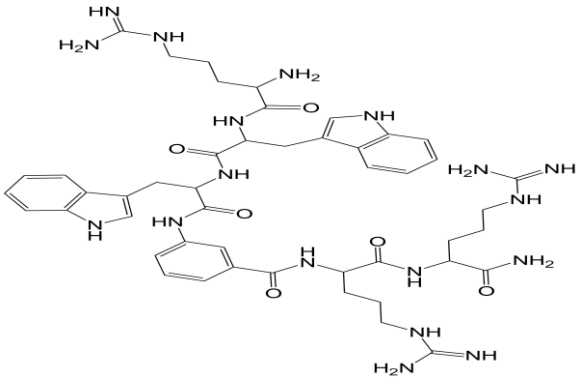

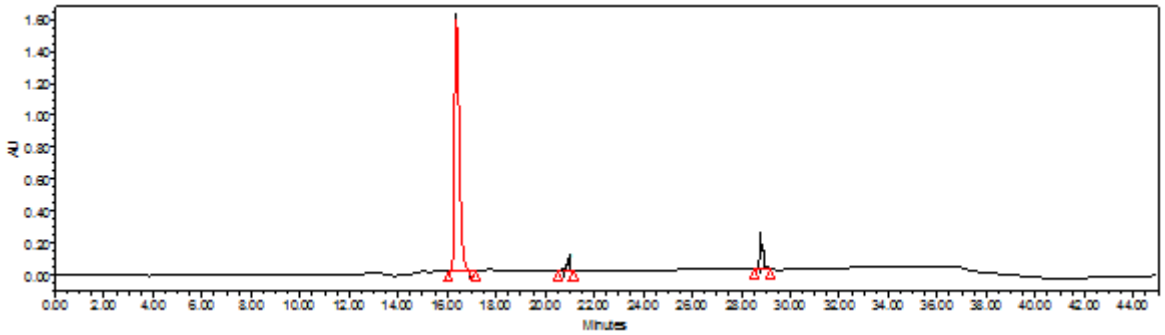

	Name	Retention Time	Area	% Area	Height	RT Ratio
1		16.52	30497798	98.34	1930654	
2		20.89	1866	0.29	1051	
3		29.96	13674	1.37	7856	

Molecular Weight: 976.53

LCMS (+ESI, m/z): 977.19 $(M+H)^+$

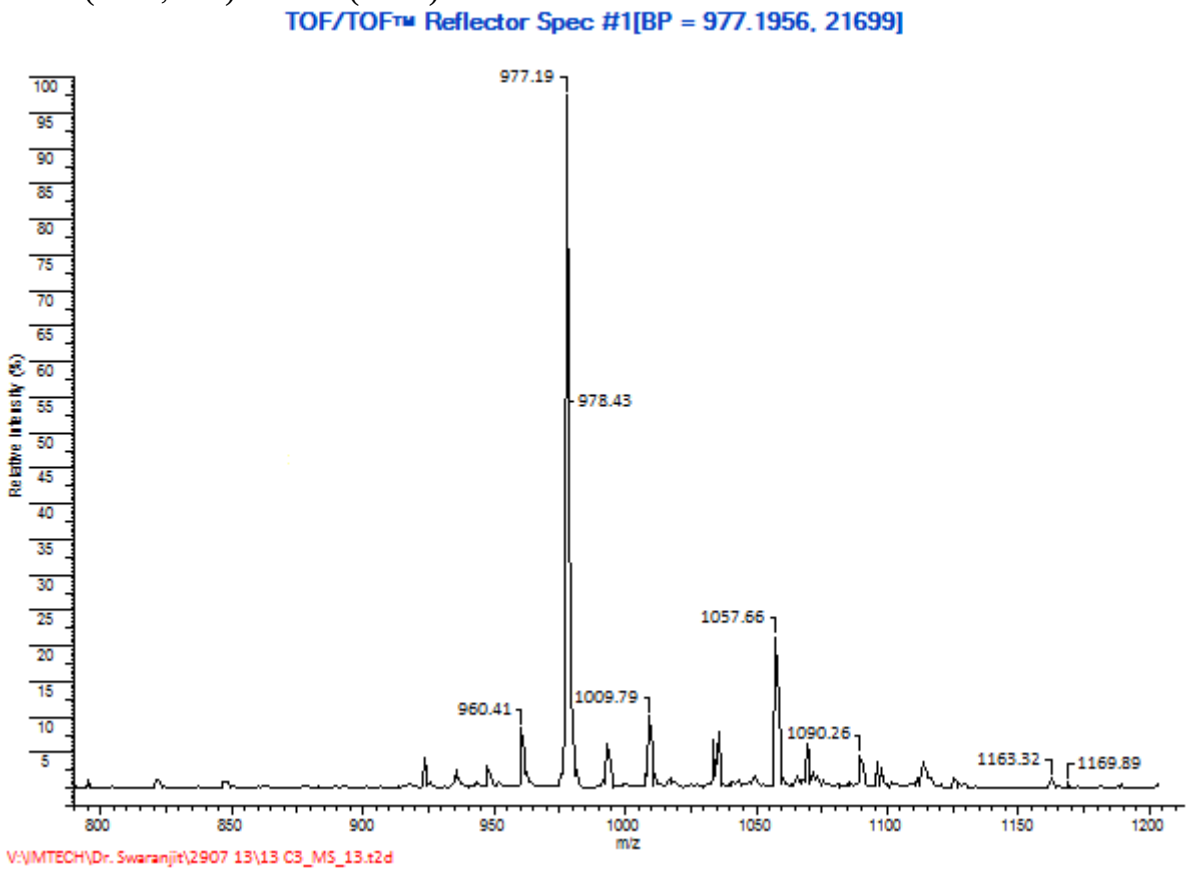

Figure 4.51: Chemical structure, HPLC chromatogram, and Mass spectra of peptidomimetic molecule **4c**

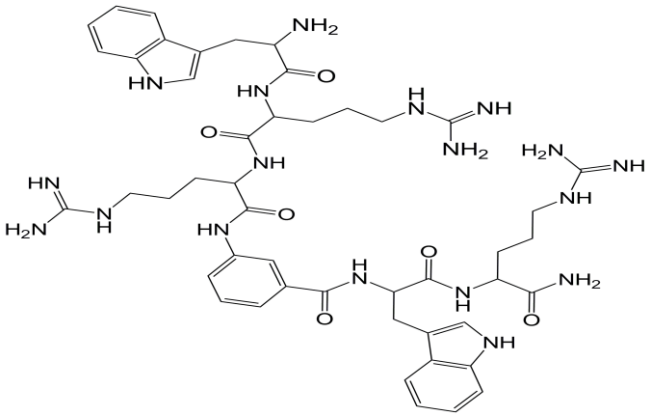

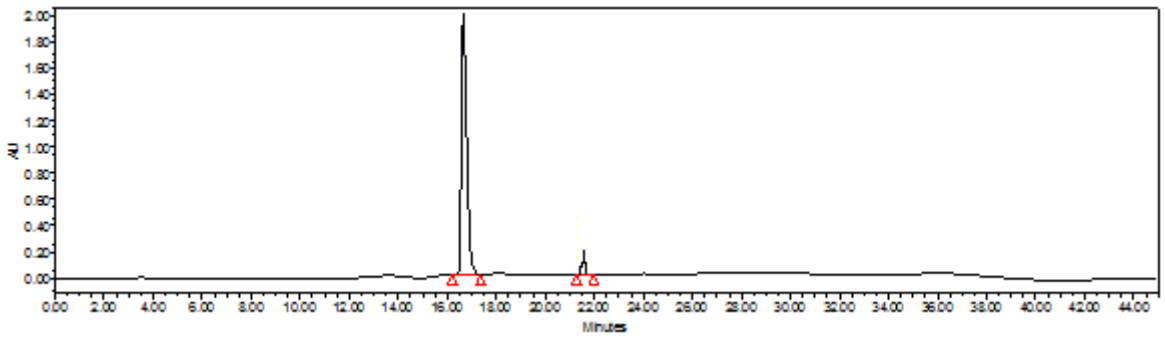

	Name	Retention Time	Area	% Area	Height	RT Ratio
1		16.87	30609984	98.40	2159736	
2		21.60	15703	1.60	6787	

Molecular Weight: 976.53

LCMS (+ESI, m/z): 977.27 $(M+H)^+$

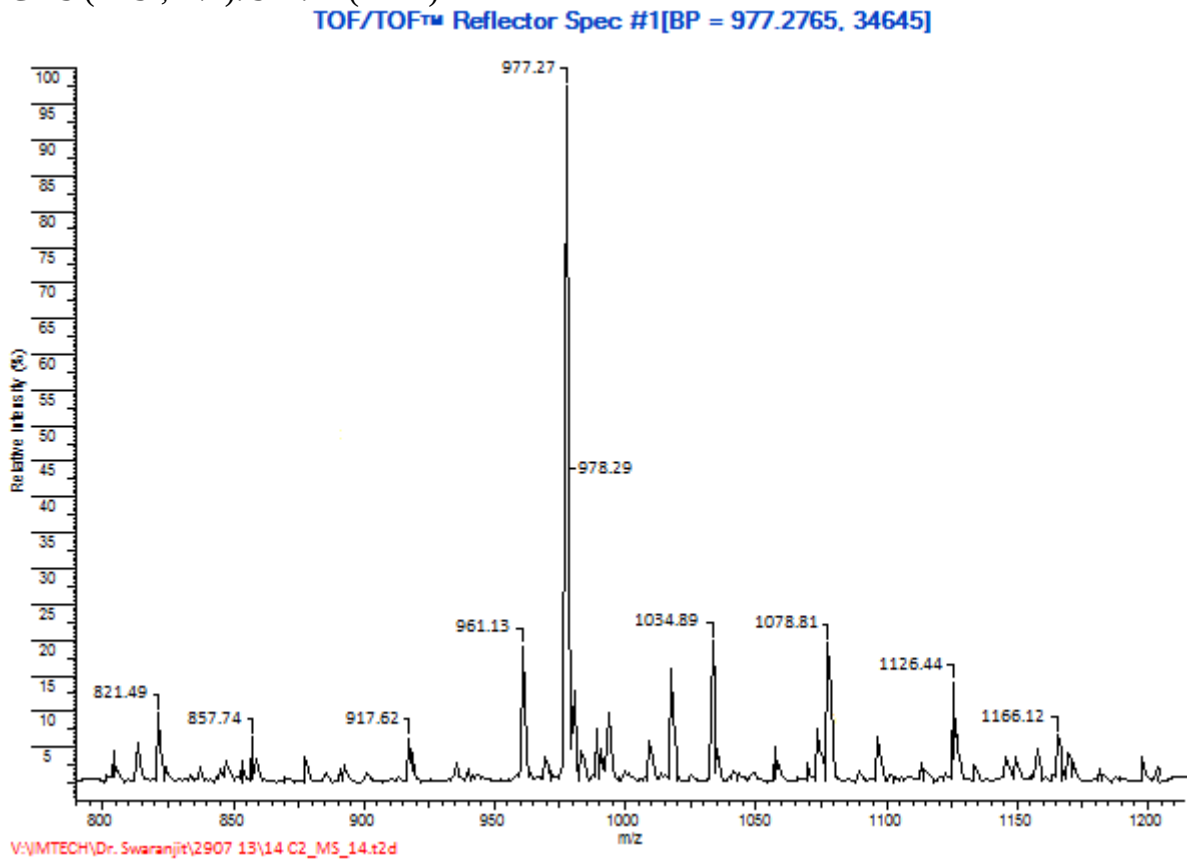

Figure 4.52: Chemical structure, HPLC chromatogram, and Mass spectra of peptidomimetic molecule **4d**

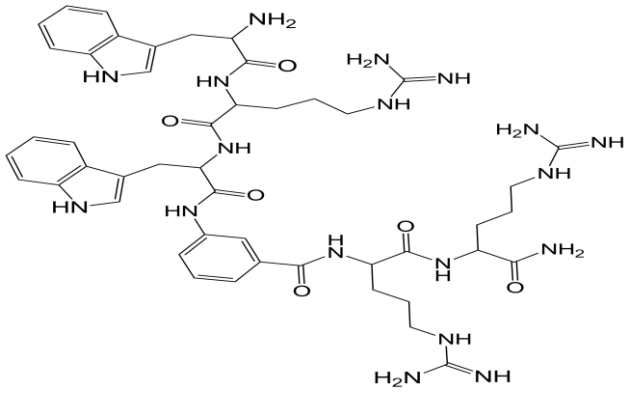

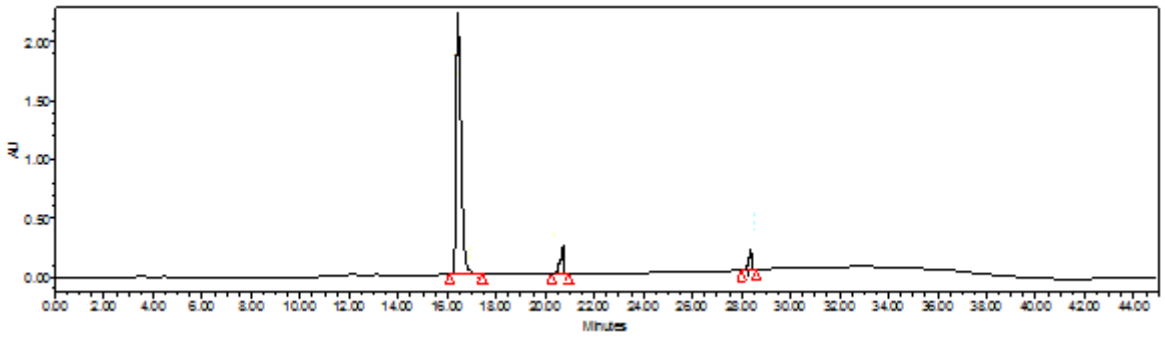

	Name	Retention Time	Area	% Area	Height	RT Ratio
1		16.23	31146215	97.83	1801974	
2		20.58	143716	1.31	7091	
3		28.41	41852	0.86	4320	

Molecular Weight: 976.53

LCMS (+ESI, m/z): 977.53 $(M+H)^+$

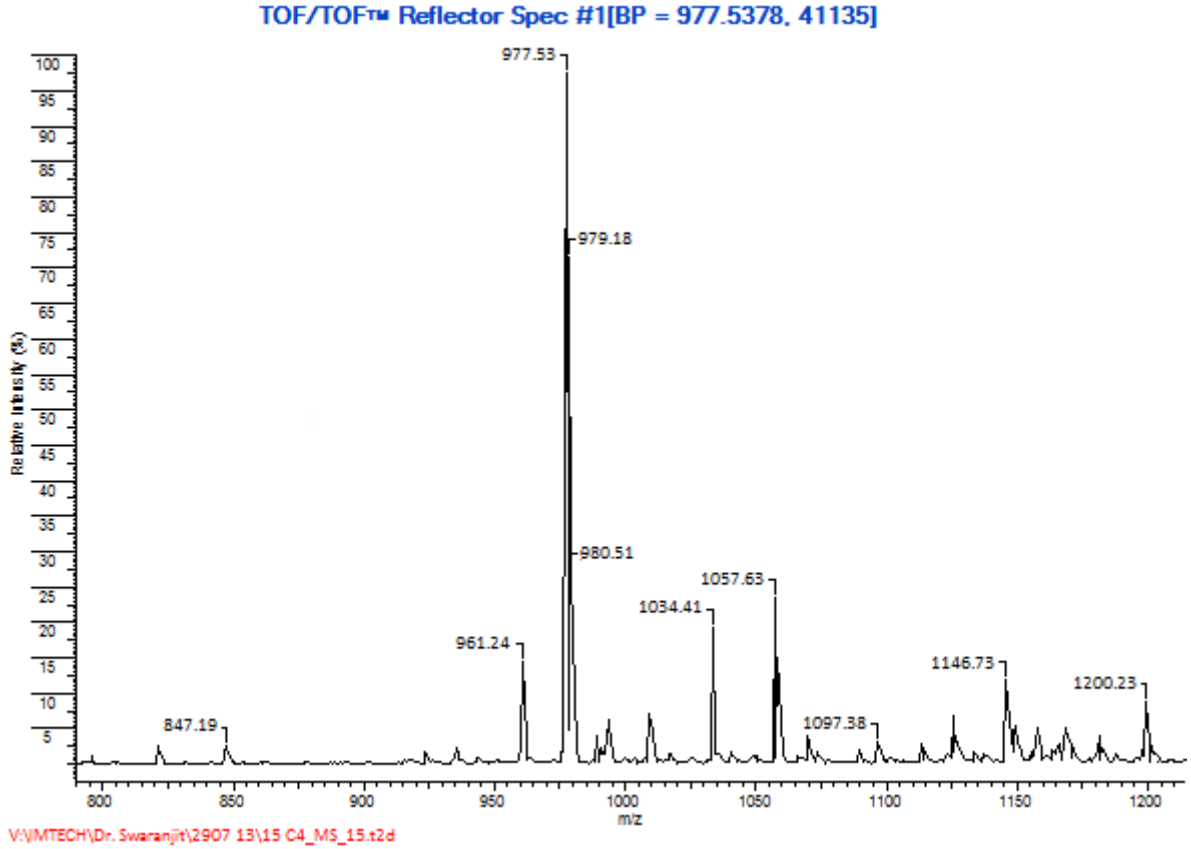

Figure 4.53: Chemical structure, HPLC chromatogram, and Mass spectra of peptidomimetic molecule **4e**

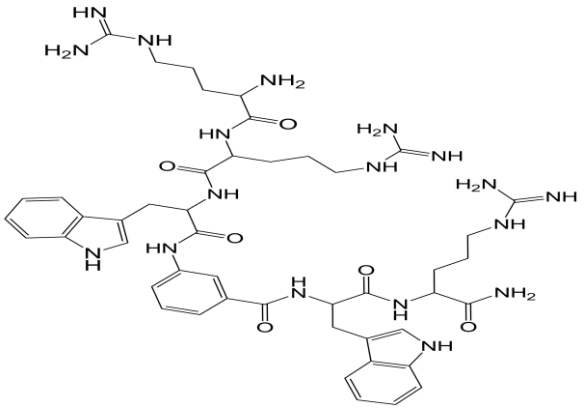

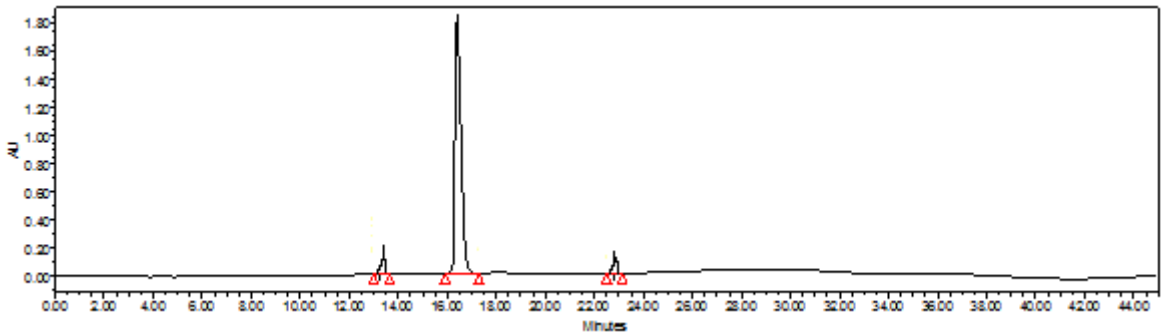

	Name	Retention Time	Area	% Area	Height	RT Ratio
1		13.46	27007	1.21	8212	
2		16.59	26774036	97.36	1471615	
3		22.99	29173	1.43	7694	

Molecular Weight: 976.53

LCMS (+ESI, m/z): 977.39 $(M+H)^+$

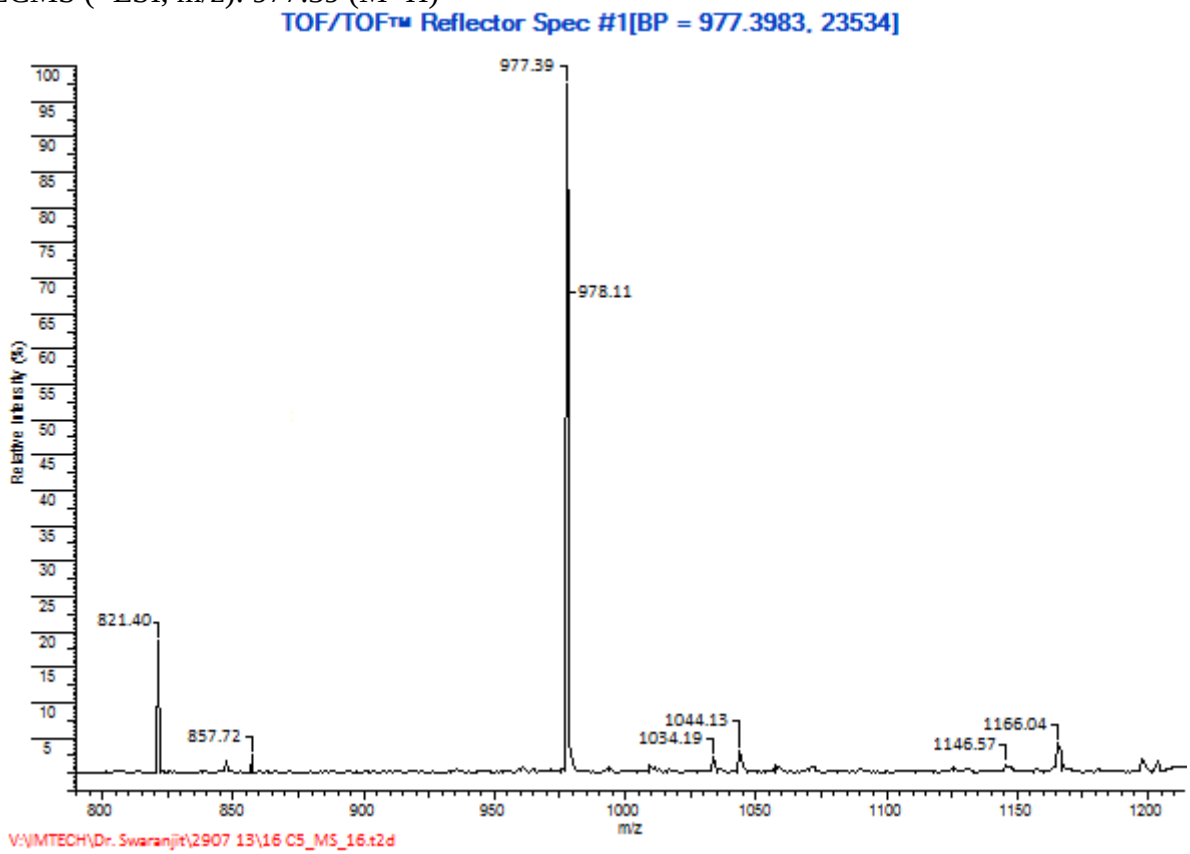

Figure 4.54: Chemical structure, HPLC chromatogram, and Mass spectra of peptidomimetic molecule **4f**

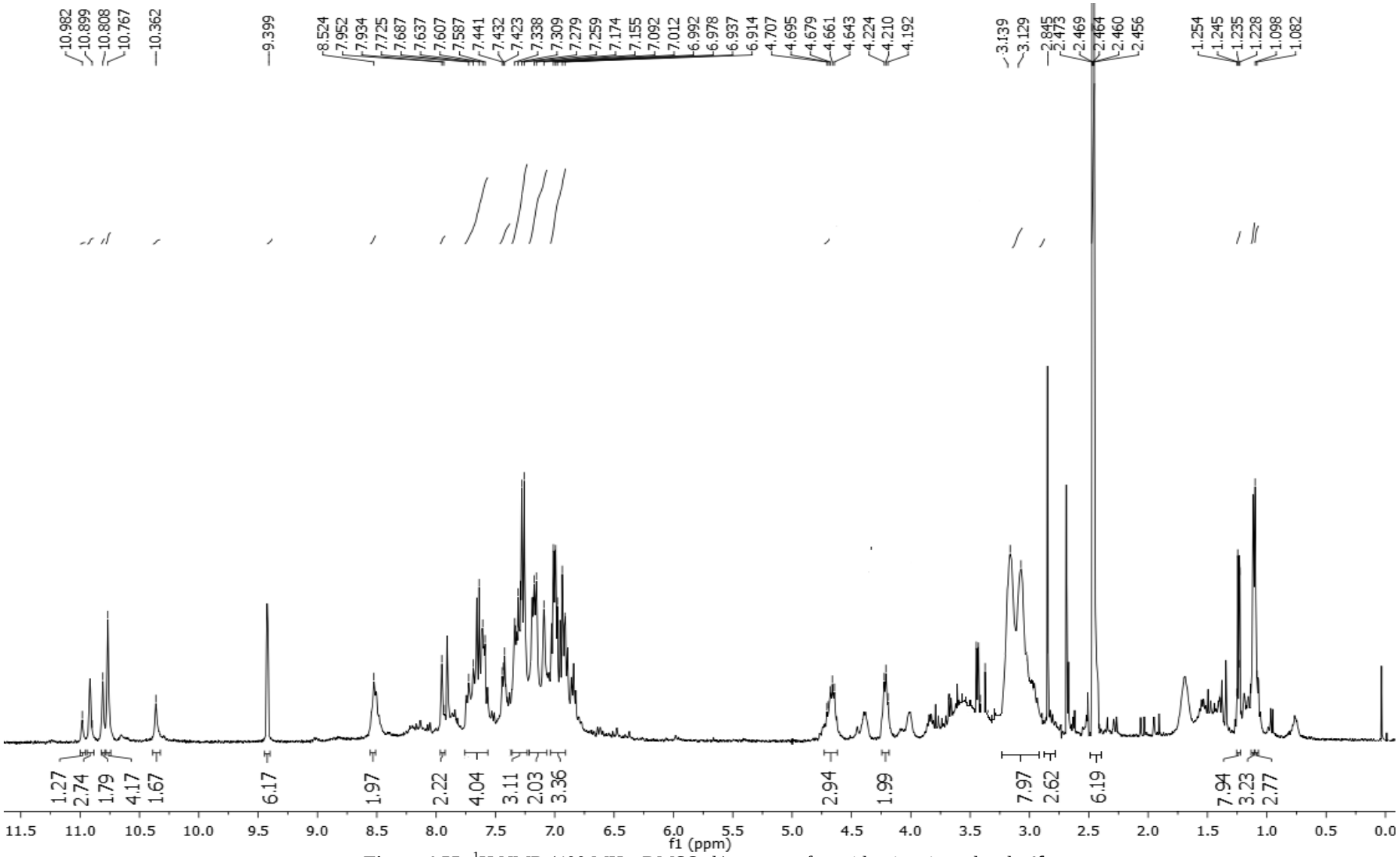

Figure 4.55: ^{1}H NMR (400 MHz, DMSO d_6) spectra of peptidomimetic molecule **4f**

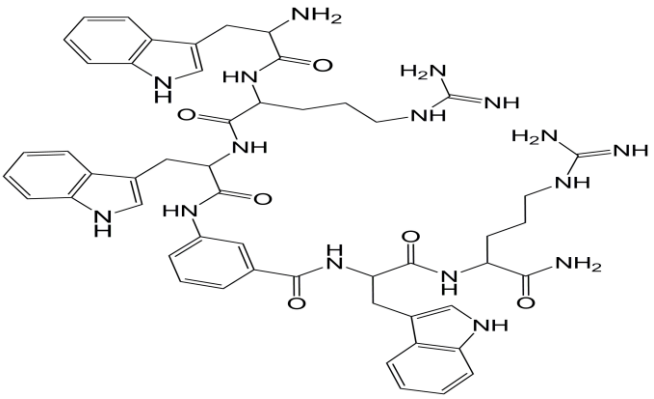

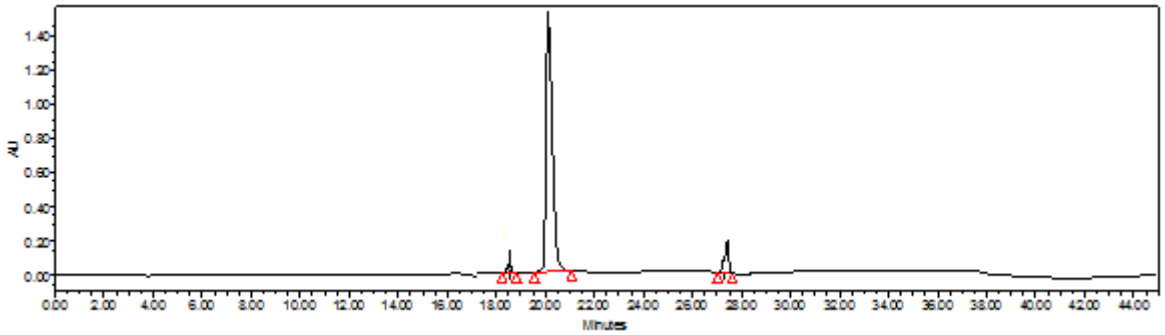

	Name	Retention Time	Area	% Area	Height	RT Ratio
1		18.51	2007	0.17	1212	
2		20.40	26774036	97.81	1471615	
3		27.23	17173	2.02	6694	

Molecular Weight: 1006.50

LCMS (+ESI, m/z): 1007.49 $(M+H)^+$

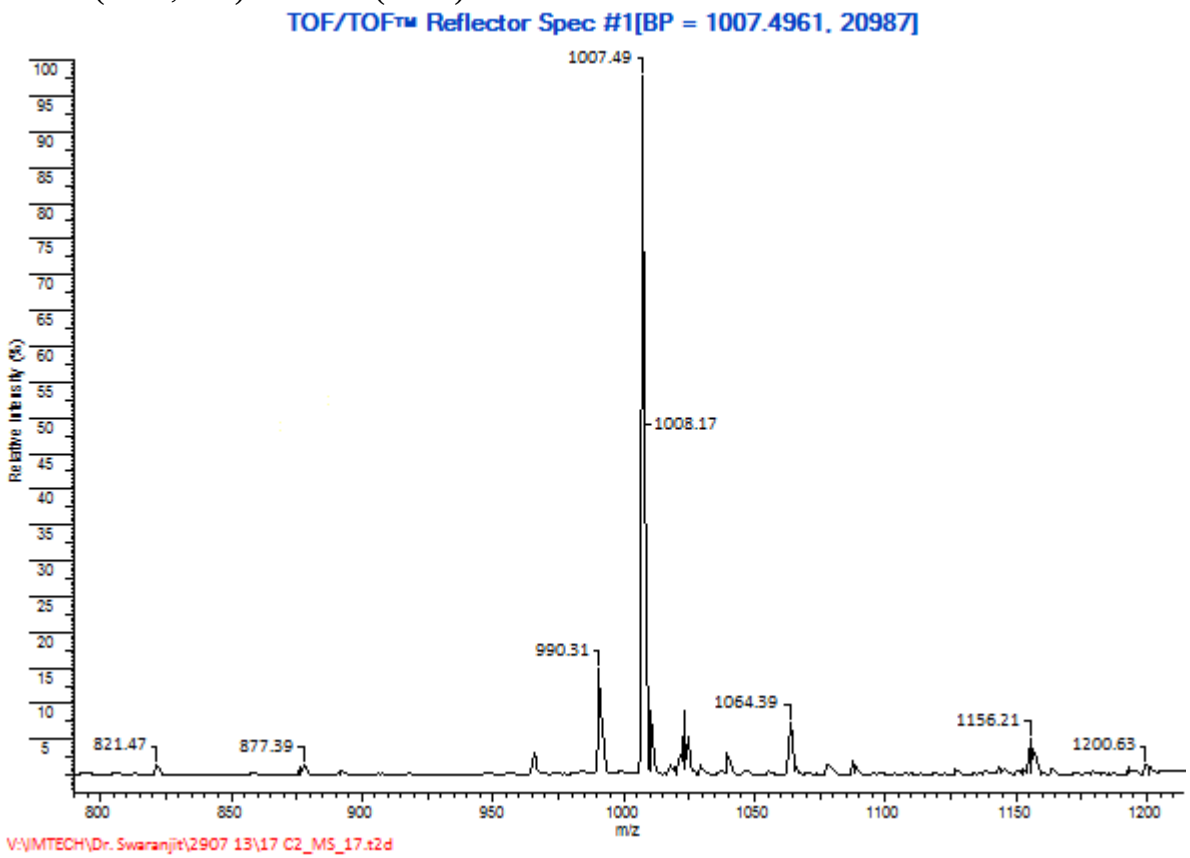

Figure 4.56: Chemical structure, HPLC chromatogram, and Mass spectra of peptidomimetic molecule **4g**

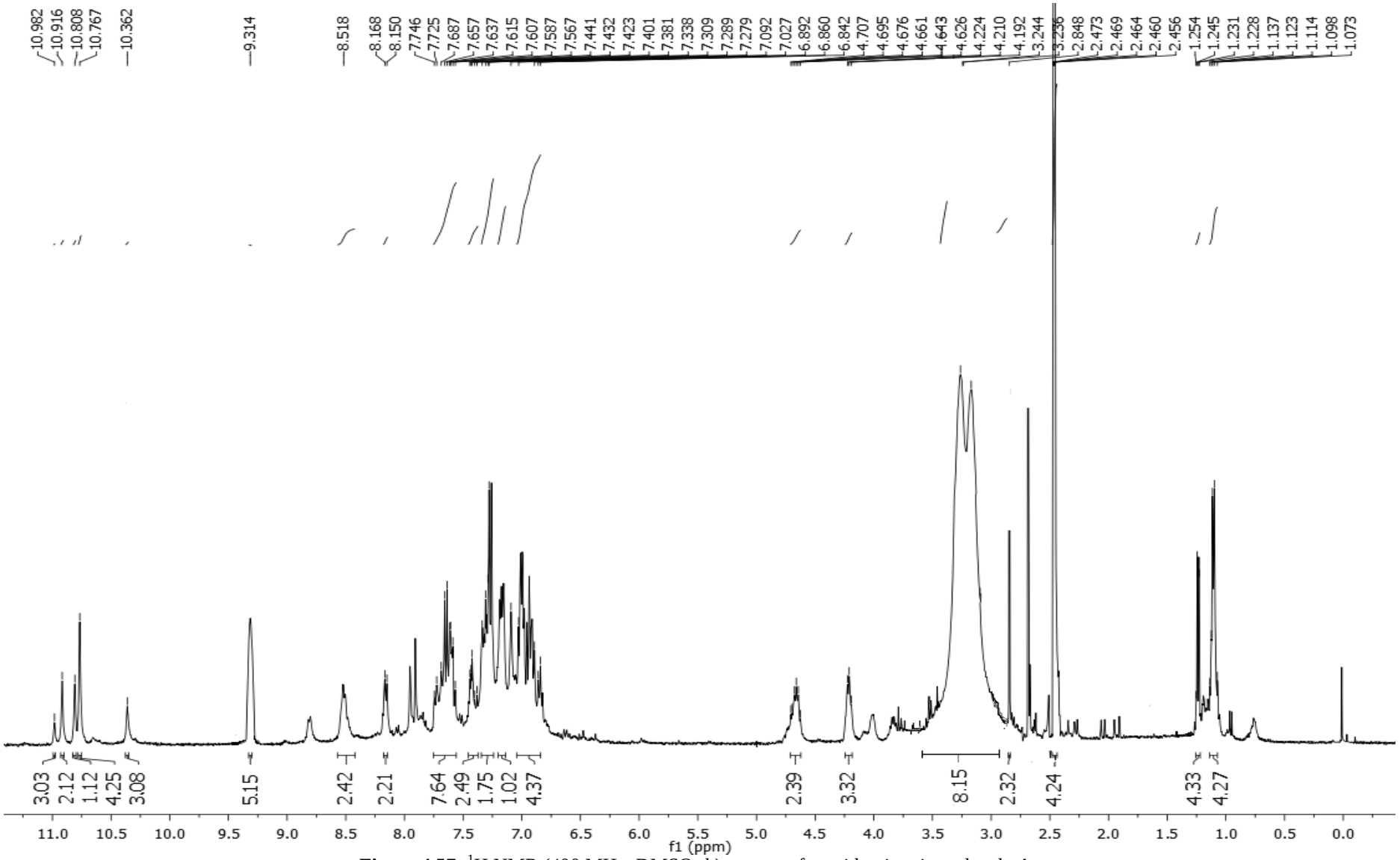

Figure 4.57: ^{1}H NMR (400 MHz, DMSO d_6) spectra of peptidomimetic molecule **4g**

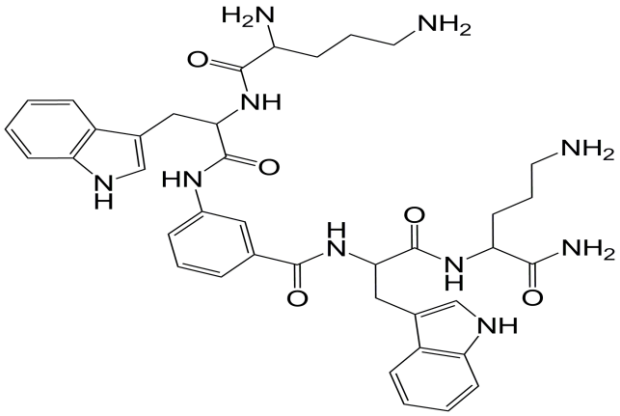

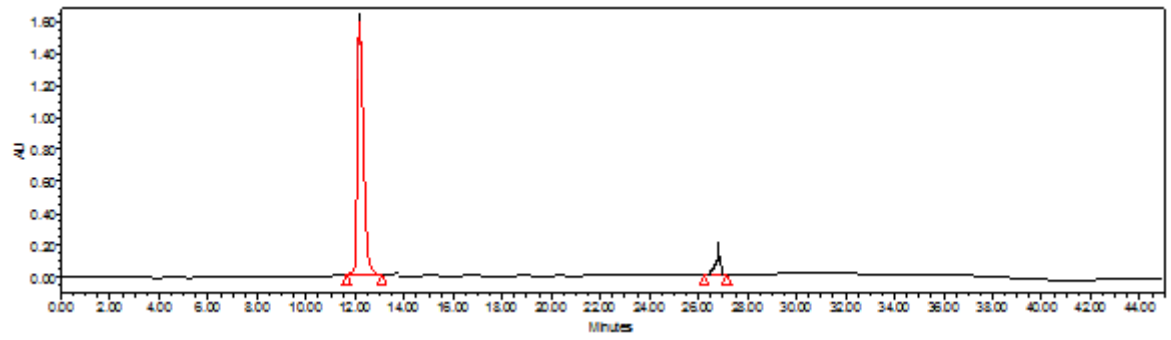

	Name	Retention Time	Area	% Area	Height	RT Ratio
1		12.32	17722012	98.66	1343634	
2		26.77	61835	1.34	6126	

Molecular Weight: 736.38

LCMS (+ESI, m/z): 737.18$(M+H)^+$

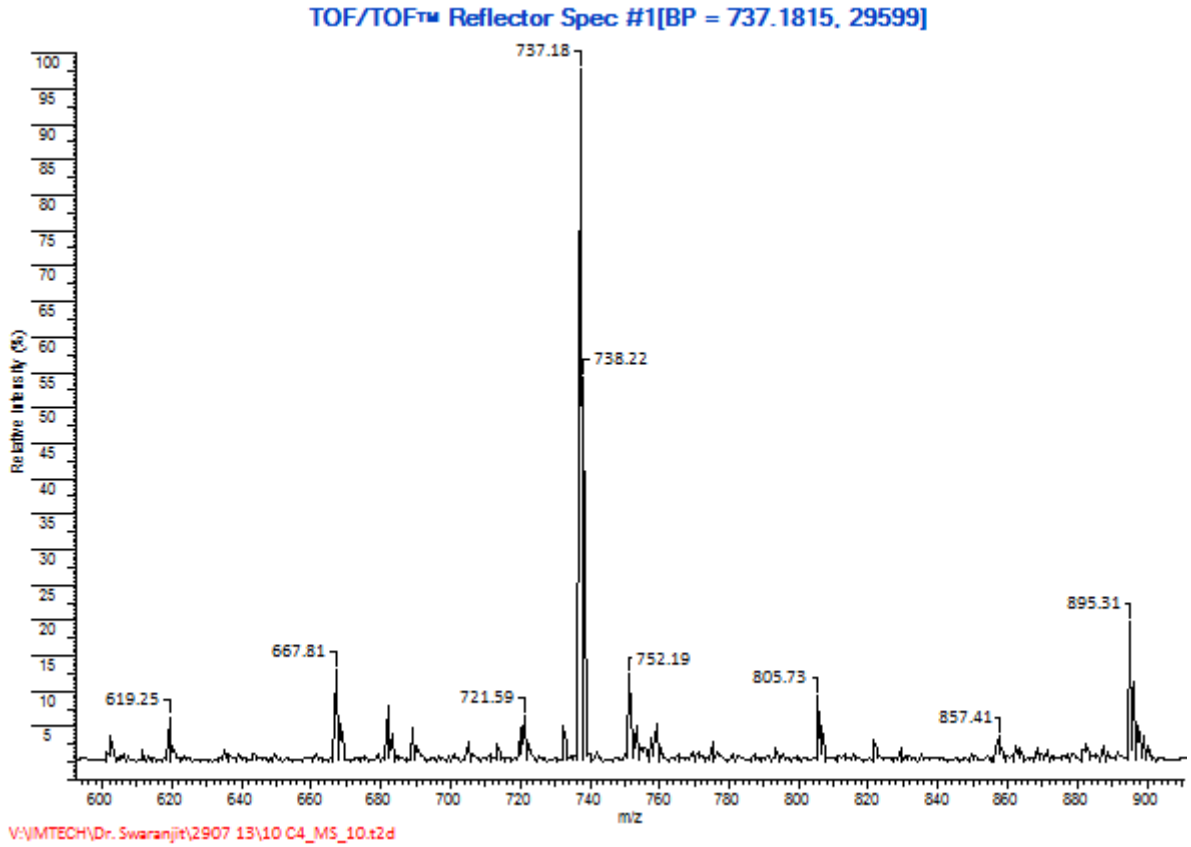

Figure 4.58: Chemical structure, HPLC chromatogram, and Mass spectra of peptidomimetic molecule **3f**

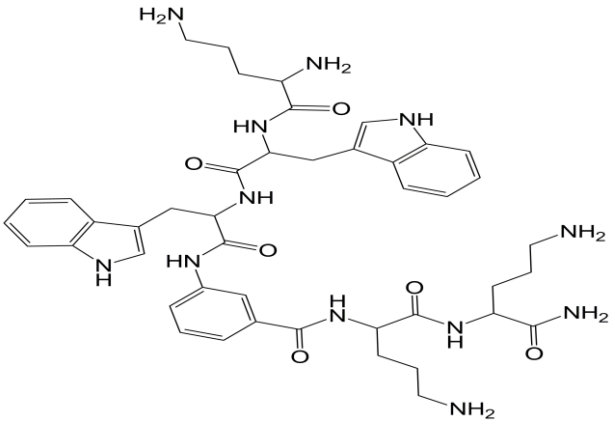

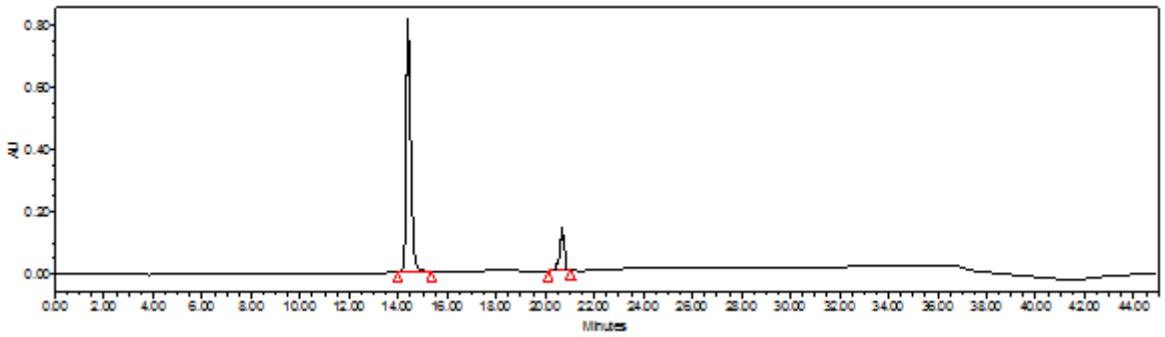

	Name	Retention Time	Area	% Area	Height	RT Ratio
1		14.70	27760910	96.29	1581458	
2		20.56	62938	3.71	11271	

Molecular Weight: 850.46

LCMS (+ESI, m/z): 851.47 $(M+H)^+$

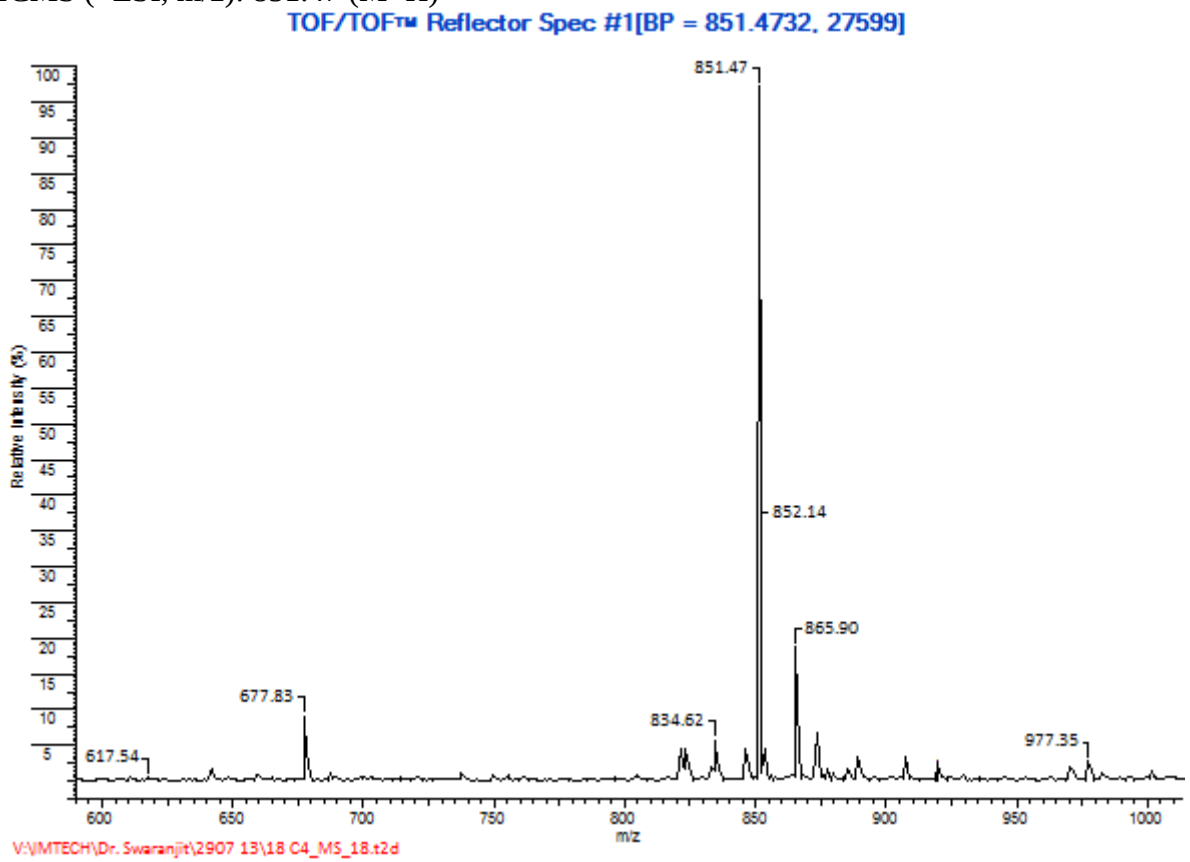

Figure 4.59: Chemical structure, HPLC chromatogram, and Mass spectra of peptidomimetic molecule **4h**

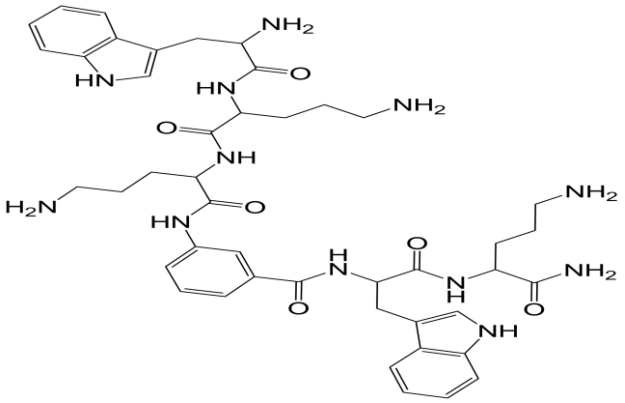

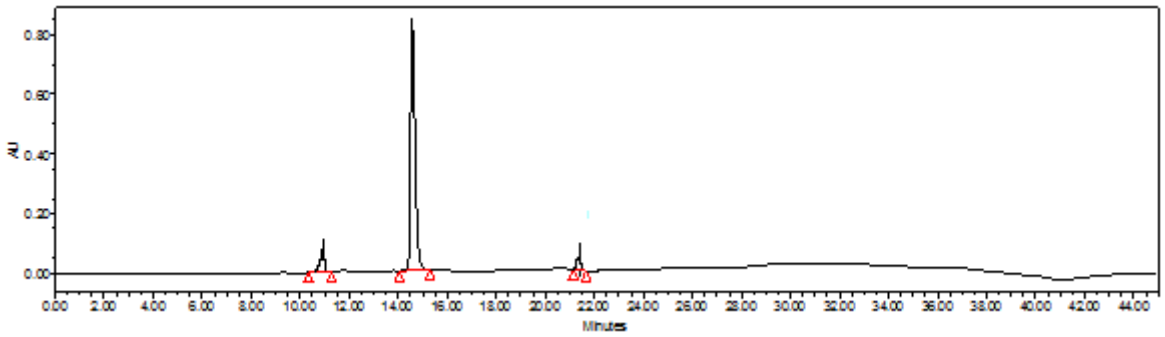

	Name	Retention Time	Area	% Area	Height	RT Ratio
1		10.63	27618	1.53	2155	
2		14.57	10857807	97.80	825758	
3		21.50	11012	0.67	3458	

Molecular Weight: 850.46

LCMS (+ESI, m/z): 851.32 $(M+H)^+$

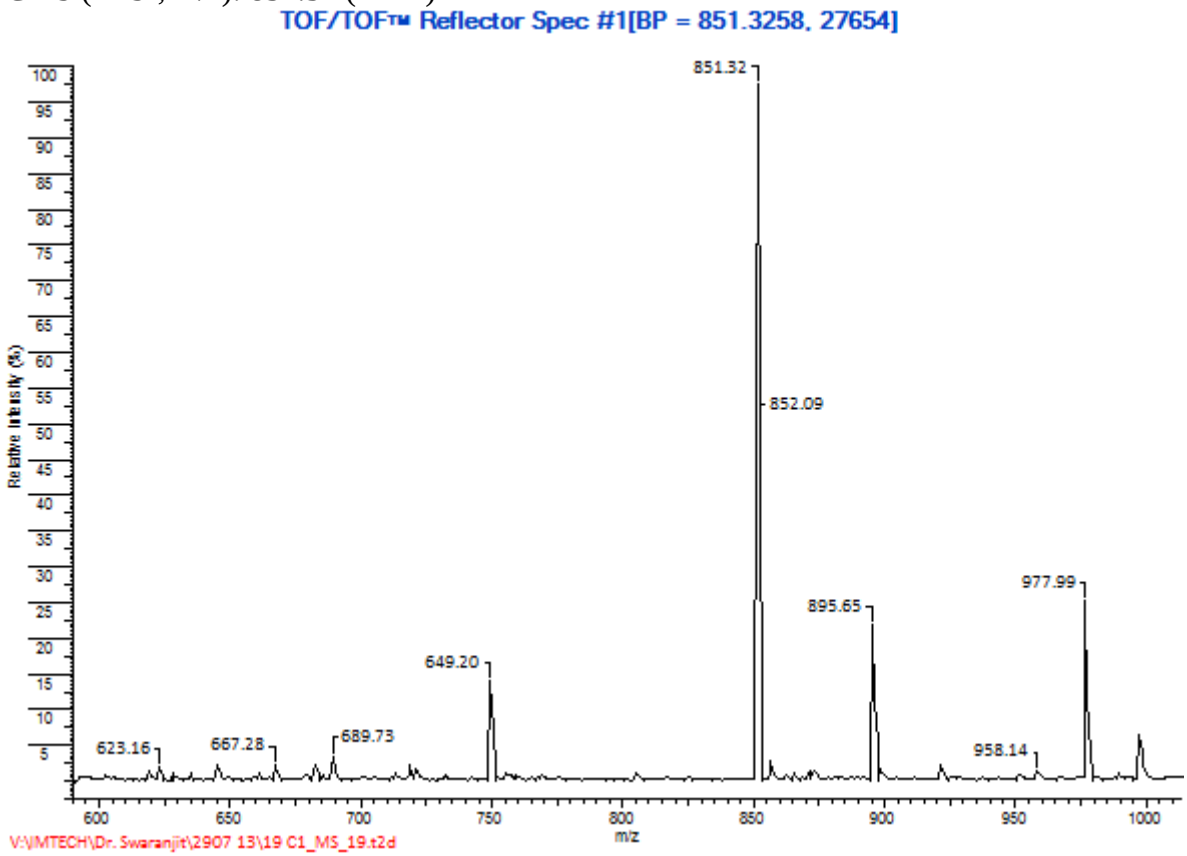

Figure 4.60: Chemical structure, HPLC chromatogram, and Mass spectra of peptidomimetic molecule **4i**

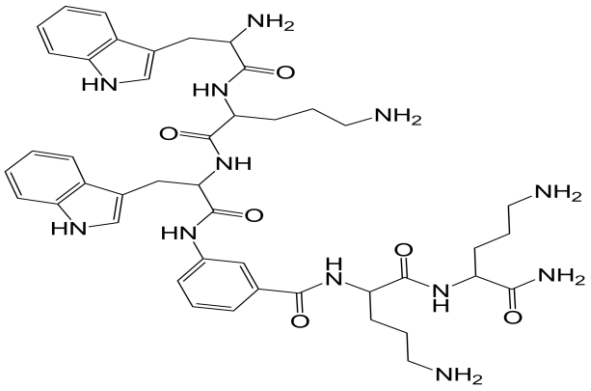

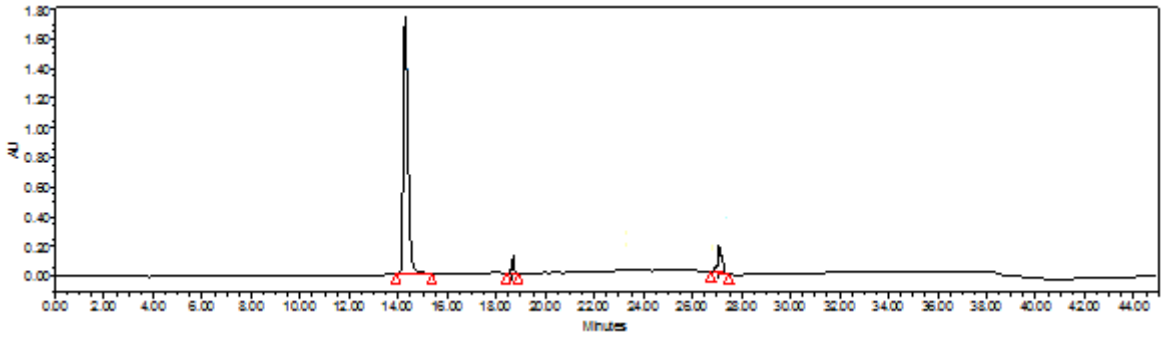

	Name	Retention Time	Area	% Area	Height	RT Ratio
1		14.66	22888546	98.69	1698372	
2		18.79	68441	0.19	2594	
3		27.12	262294	1.12	9919	

Molecular Weight: 850.46

LCMS (+ESI, m/z): 851.41 $(M+H)^+$

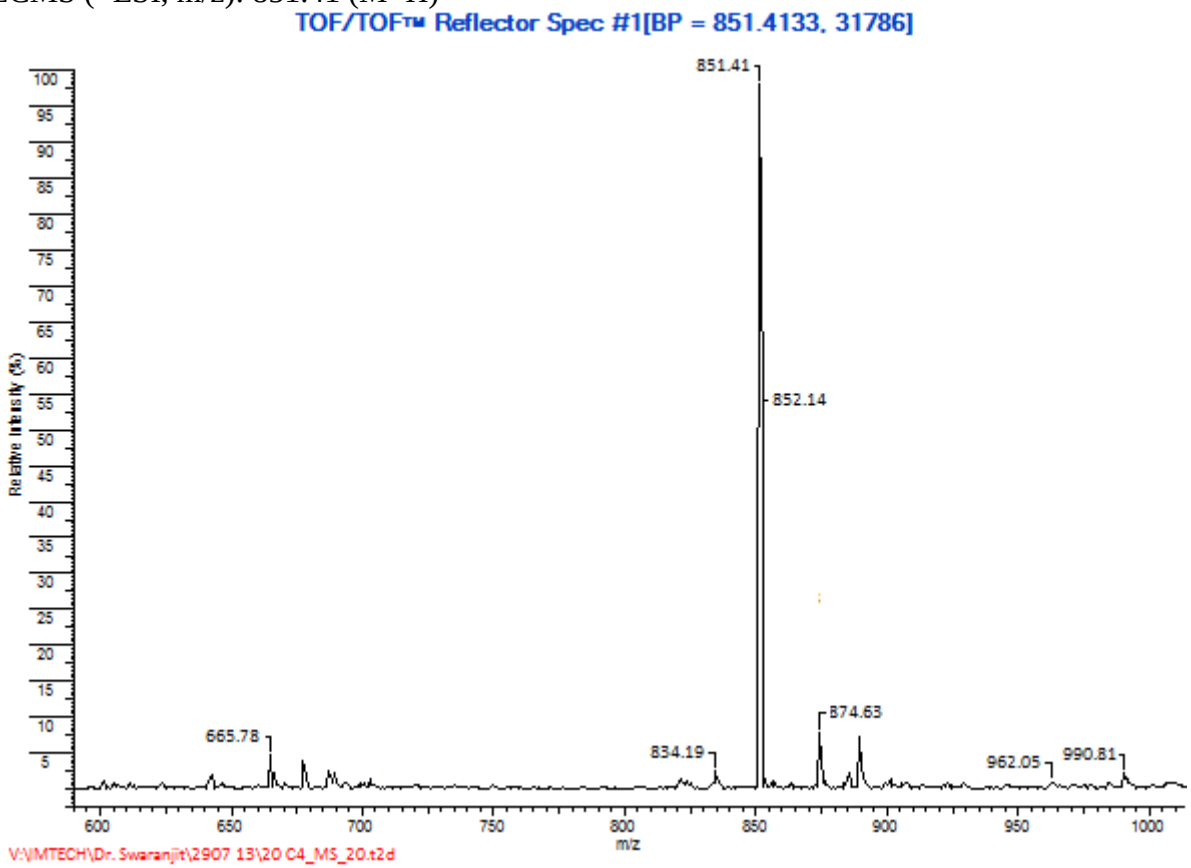

Figure 4.61: Chemical structure, HPLC chromatogram, and Mass spectra of peptidomimetic molecule **4j**

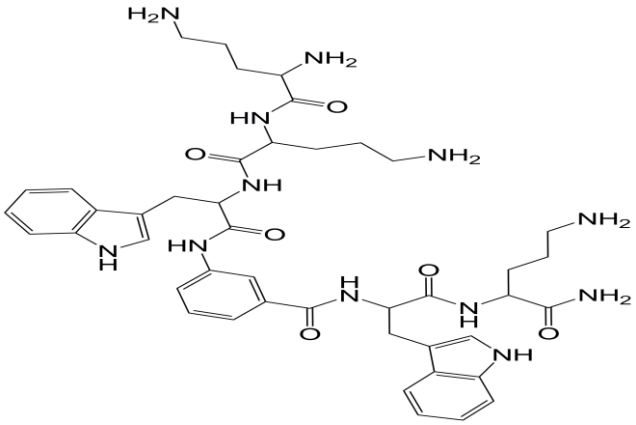

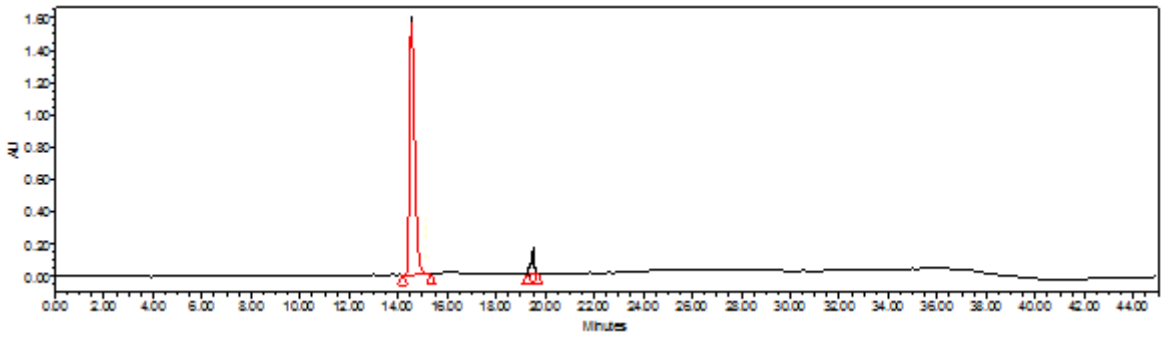

	Name	Retention Time	Area	% Area	Height	RT Ratio
1		14.70	22968159	98.97	1566209	
2		19.51	4698	1.03	1422	

Molecular Weight: 850.46

LCMS (+ESI, m/z): 851.34 $(M+H)^+$

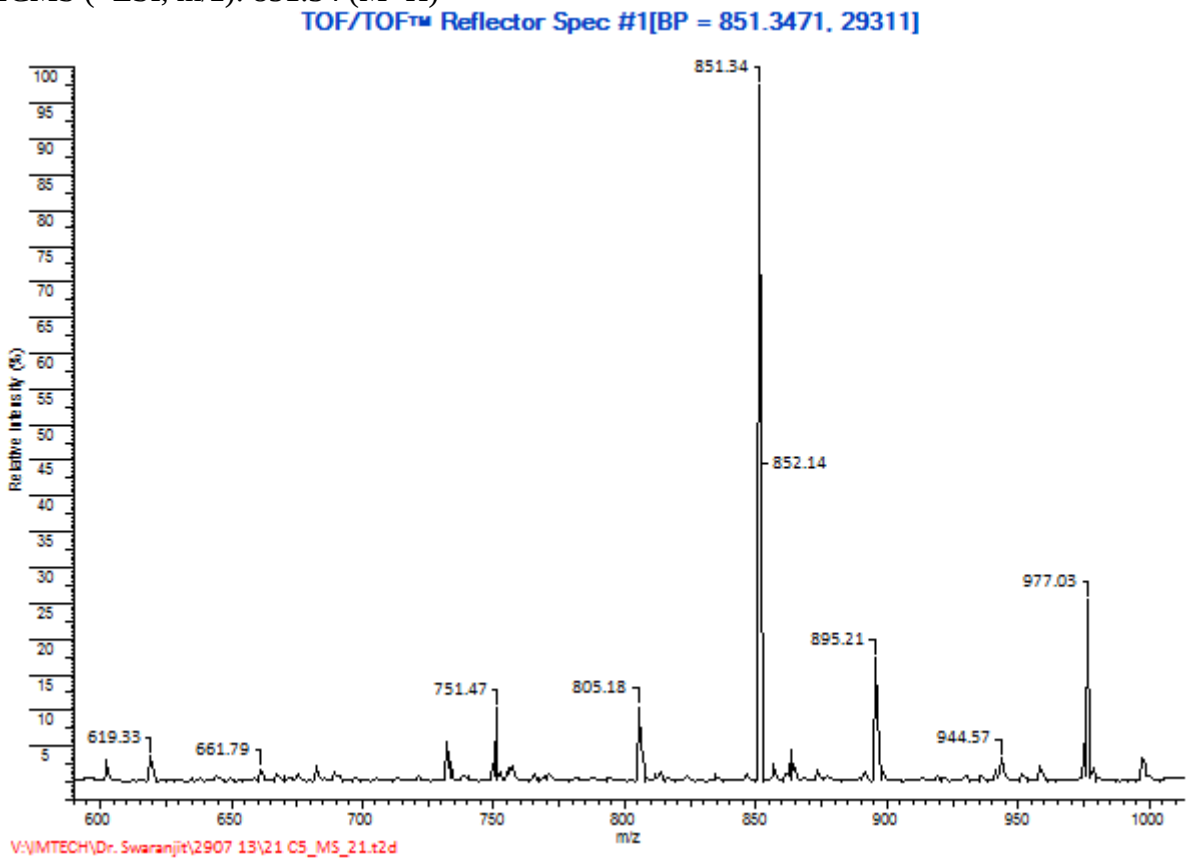

Figure 4.62: Chemical structure, HPLC chromatogram, and Mass spectra of peptidomimetic molecule **4k**

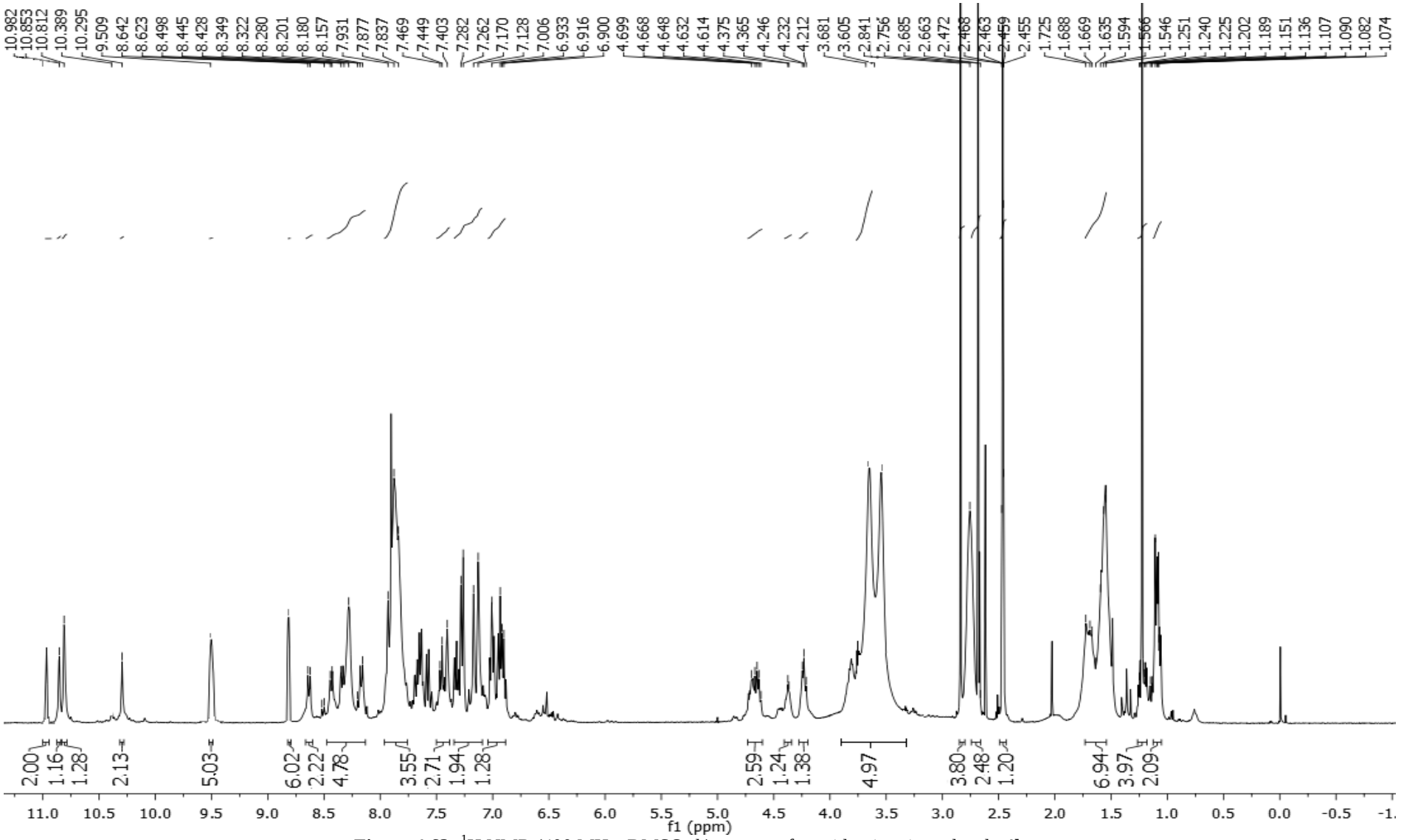

Figure 4.63: ^{1}H NMR (400 MHz, DMSO d_6) spectra of peptidomimetic molecule **4k**

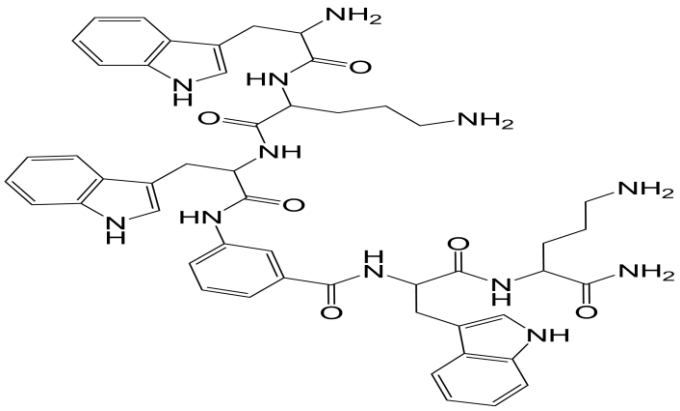

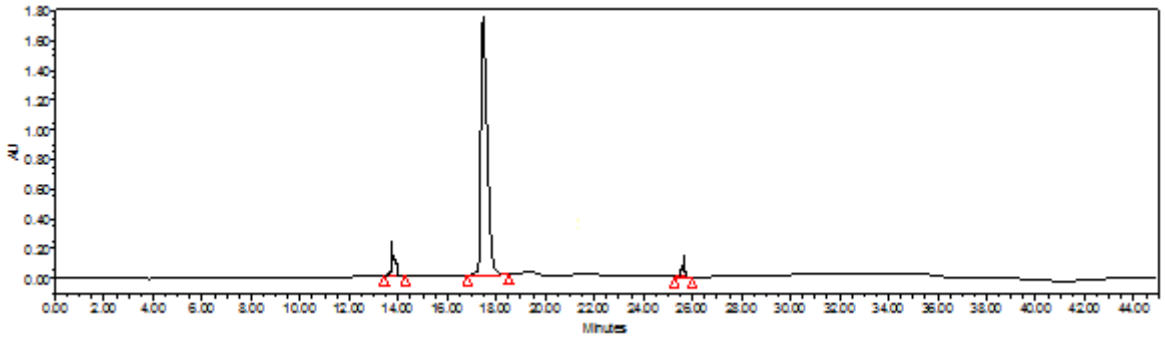

	Name	Retention Time	Area	% Area	Height	RT Ratio
1		13.92	23885	1.63	11204	
2		17.79	31425436	98.10	1700664	
3		25.64	7353	0.27	5488	

Molecular Weight: 922.46

LCMS (+ESI, m/z): 923.29$(M+H)^+$

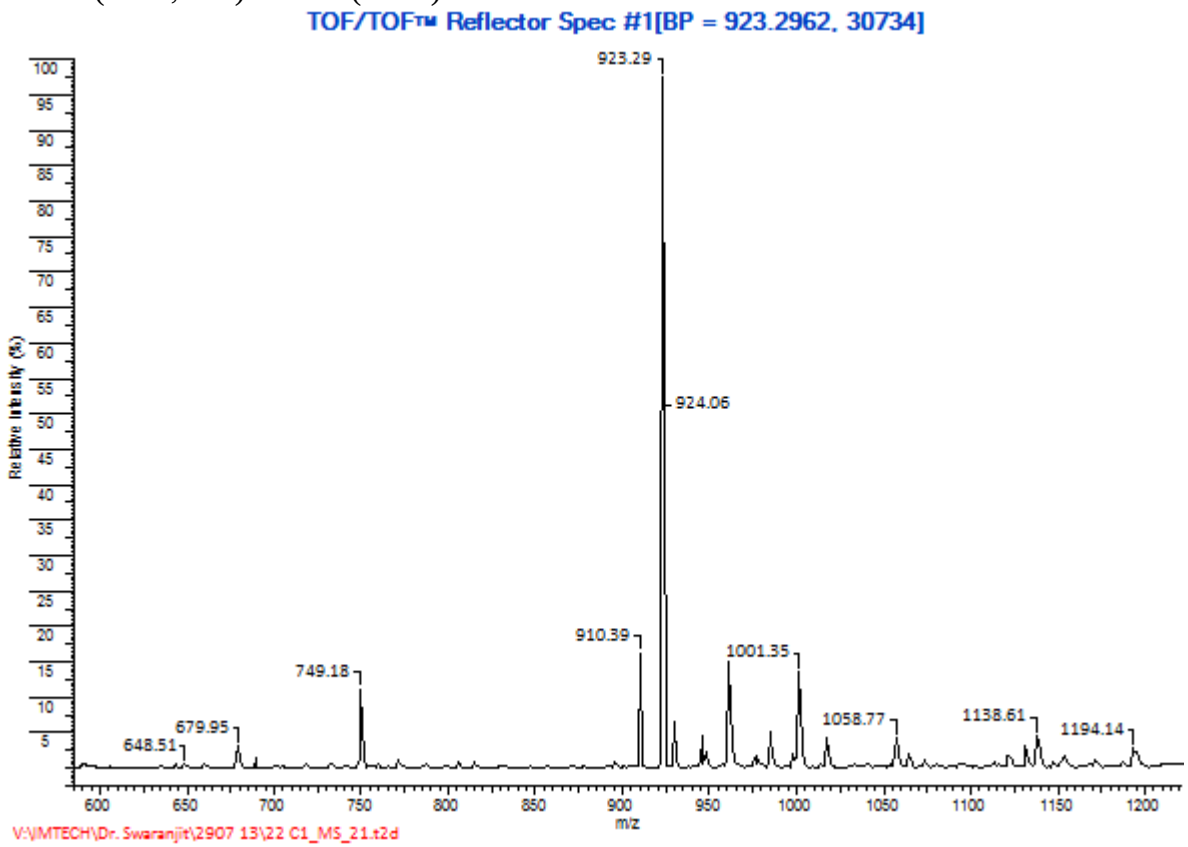

Figure 4.64: Chemical structure, HPLC chromatogram, and Mass spectra of peptidomimetic molecule **4l**

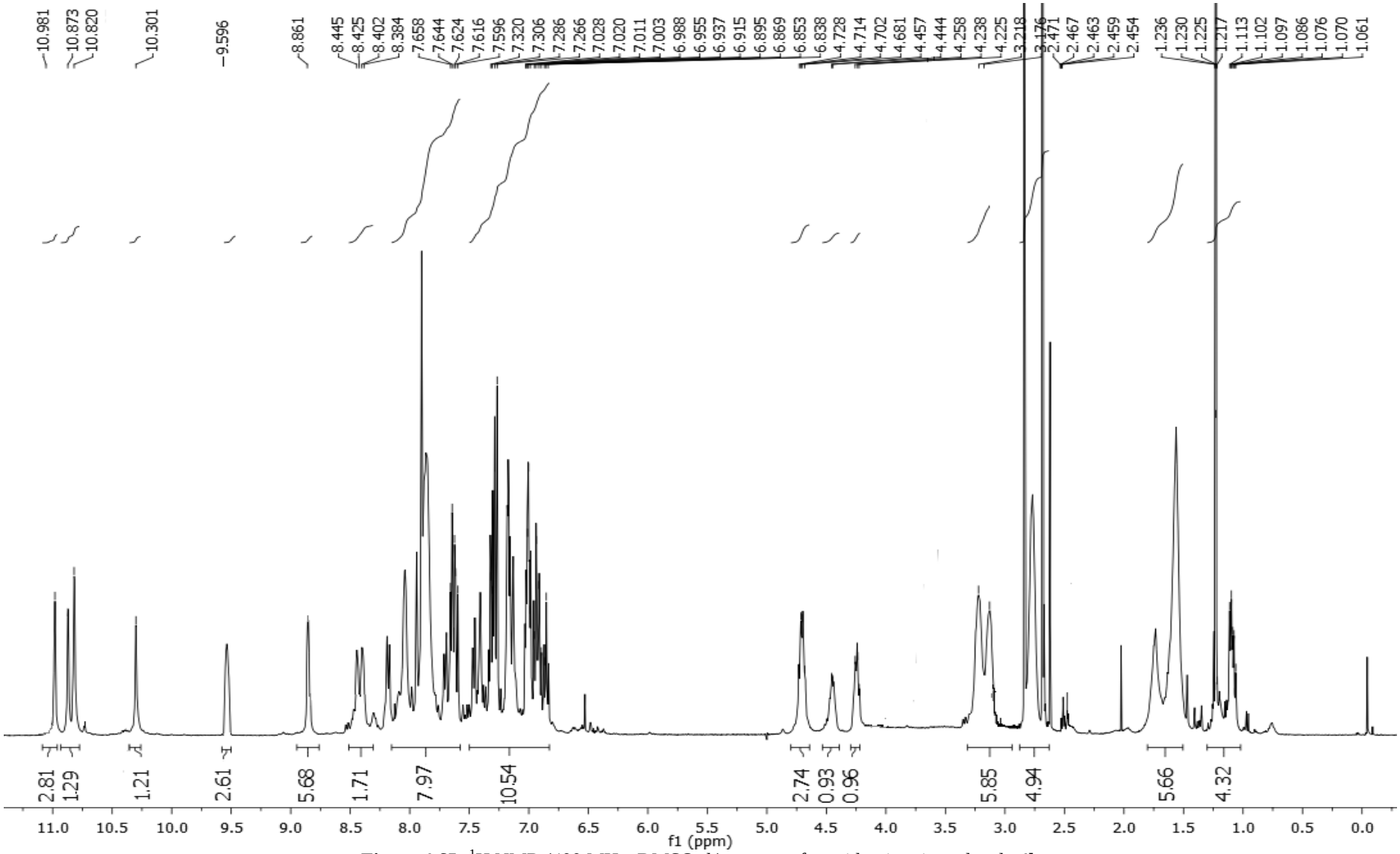

Figure 4.65: ^{1}H NMR (400 MHz, DMSO d_6) spectra of peptidomimetic molecule **4l**

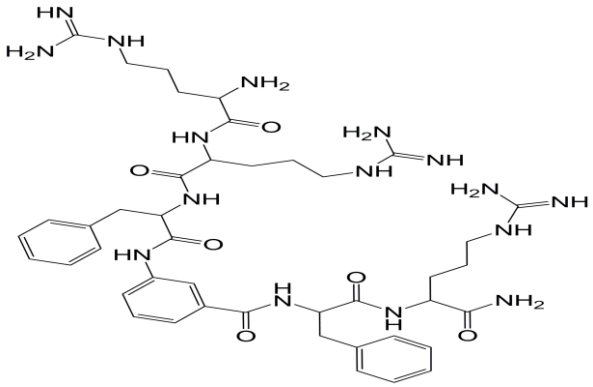

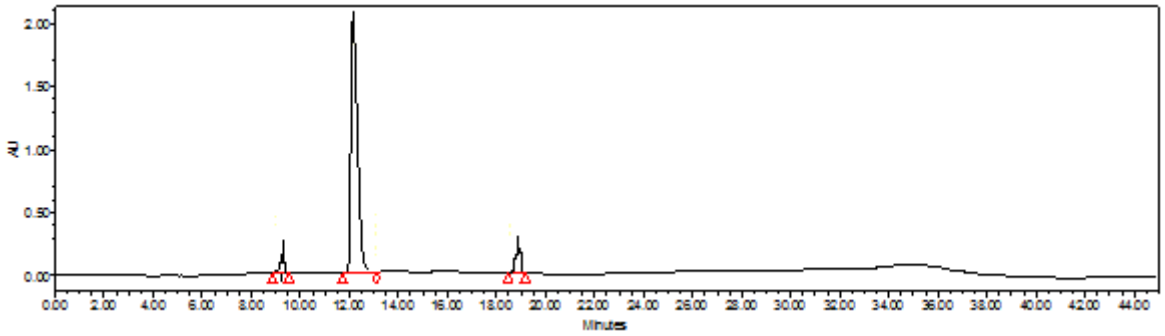

	Name	Retention Time	Area	% Area	Height	RT Ratio
1		9.27	14034	0.73	5813	
2		12.39	38198562	97.38	2009081	
3		18.90	26246	1.89	12938	

Molecular Weight: 898.50

LCMS (+ESI, m/z): 899.39$(M+H)^+$

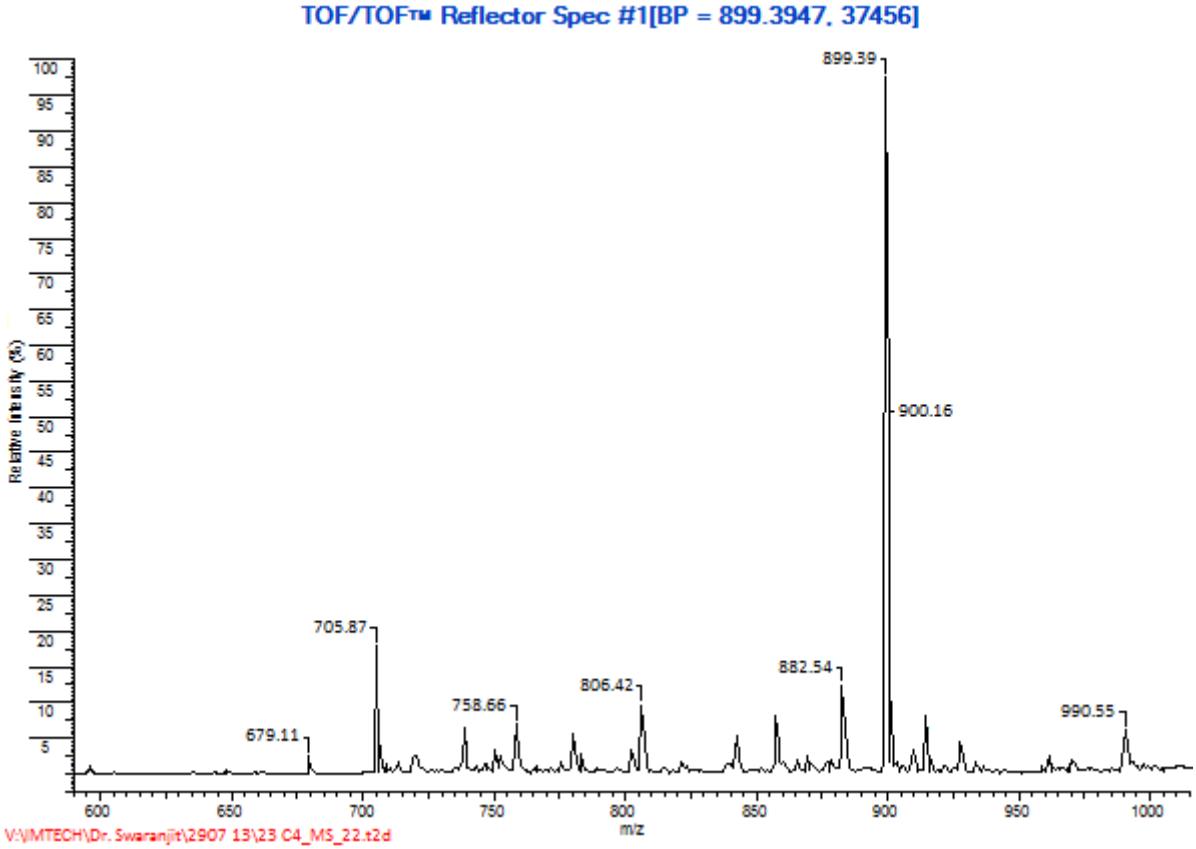

Figure 4.66: Chemical structure, HPLC chromatogram, and Mass spectra of peptidomimetic molecule **4m**

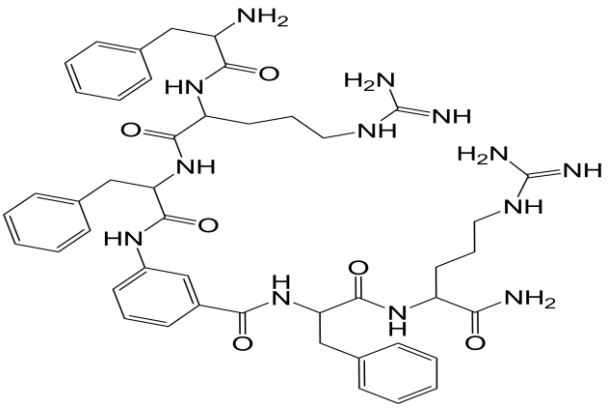

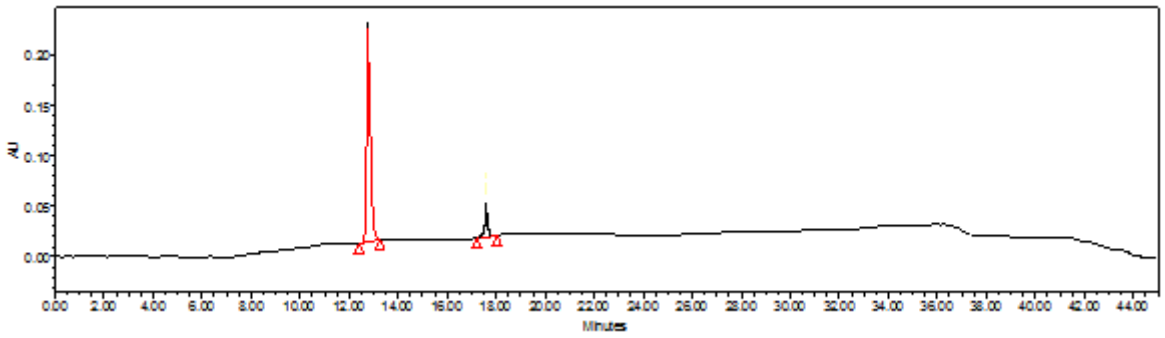

	Name	Retention Time	Area	% Area	Height	RT Ratio
1		12.87	2271127	98.06	211536	
2		18.61	14029	1.94	6197	

Molecular Weight: 889.47

LCMS (+ESI, m/z): 890.33 $(M+H)^+$

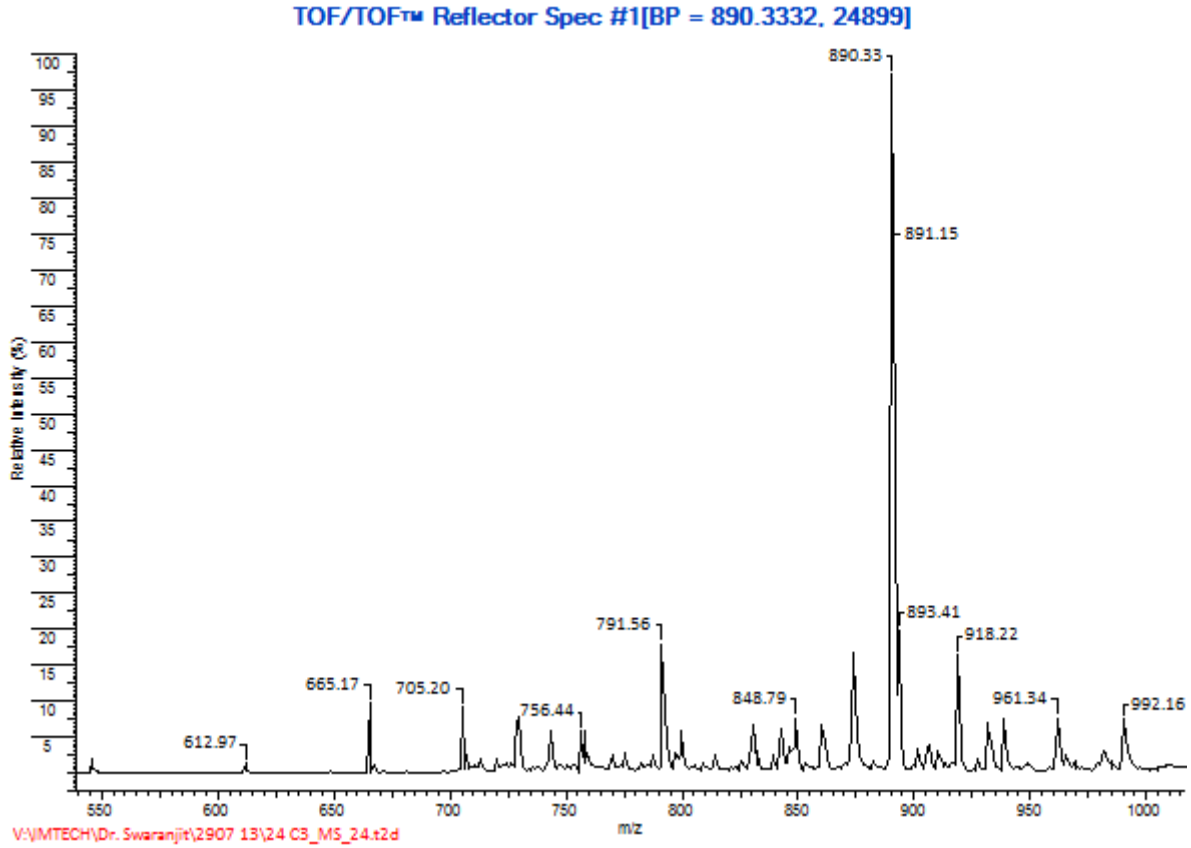

Figure 4.67: Chemical structure, HPLC chromatogram, and Mass spectra of peptidomimetic molecule **4n**

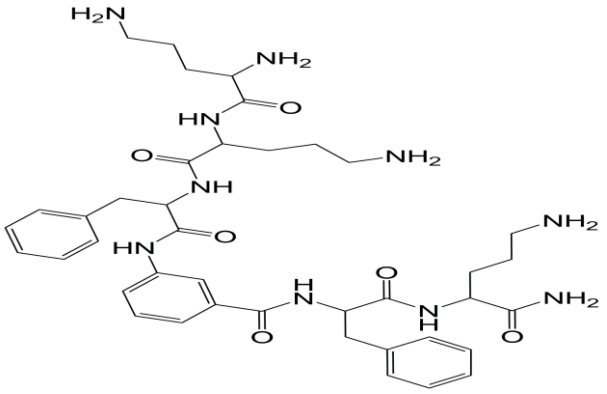

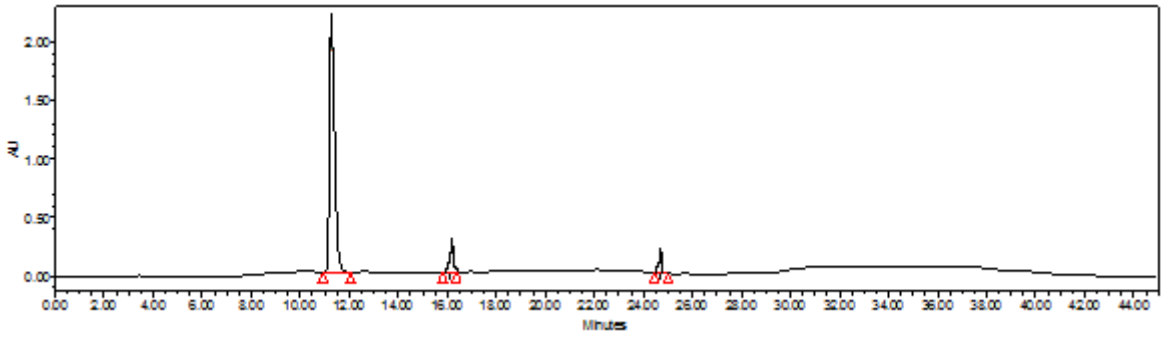

	Name	Retention Time	Area	% Area	Height	RT Ratio
1		11.39	32077516	97.87	2166548	
2		16.01	24754	1.20	7338	
3		24.72	11073	0.93	4321	

Molecular Weight: 772.44

LCMS (+ESI, m/z): 773.46$(M+H)^+$

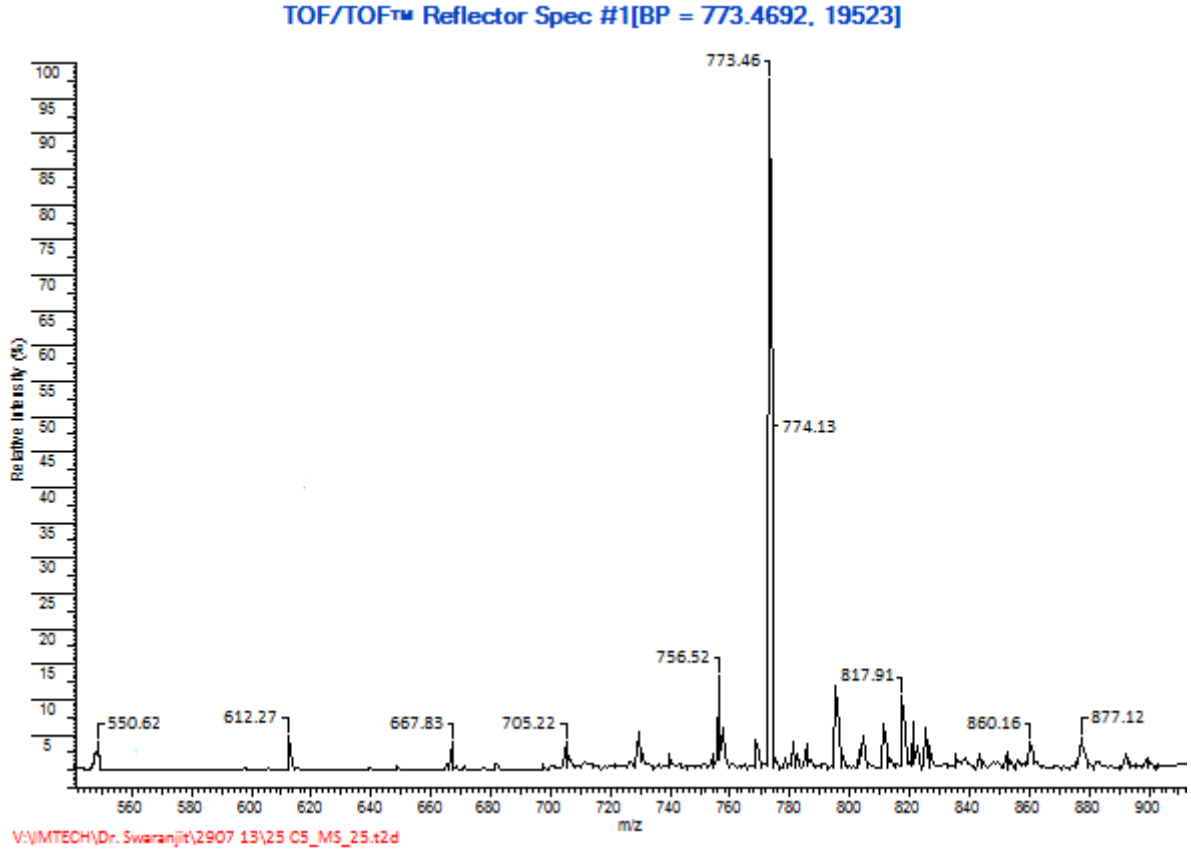

Figure 4.68: Chemical structure, HPLC chromatogram, and Mass spectra of peptidomimetic molecule **4o**

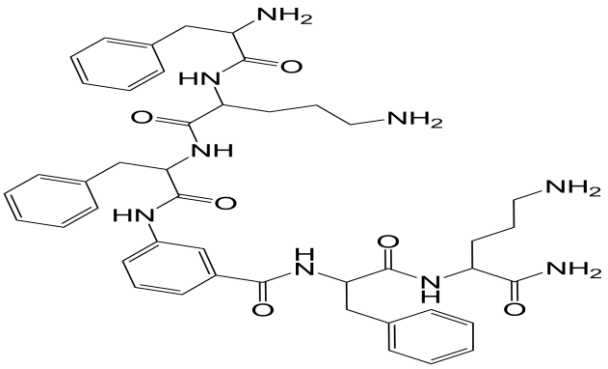

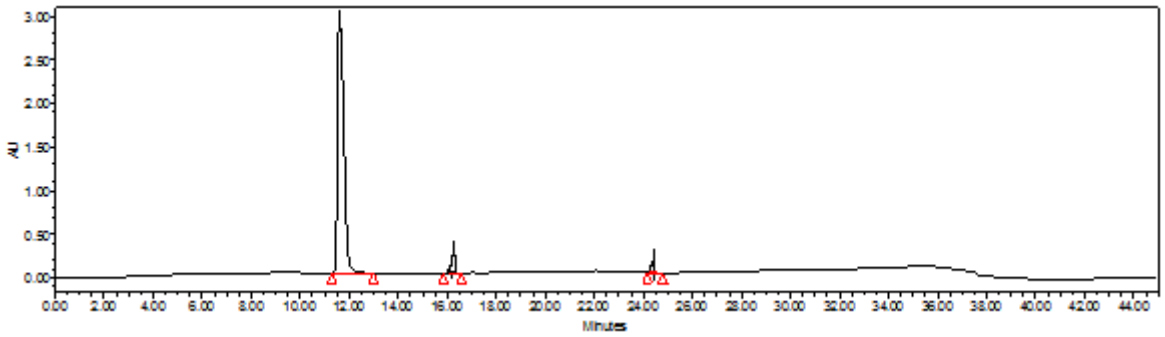

	Name	Retention Time	Area	% Area	Height	RT Ratio
1		11.97	53018630	98.75	2917009	
2		16.23	10240	1.09	3216	
3		24.48	6383	0.16	1837	

Molecular Weight: 805.43

LCMS (+ESI, m/z): 806.35$(M+H)^+$

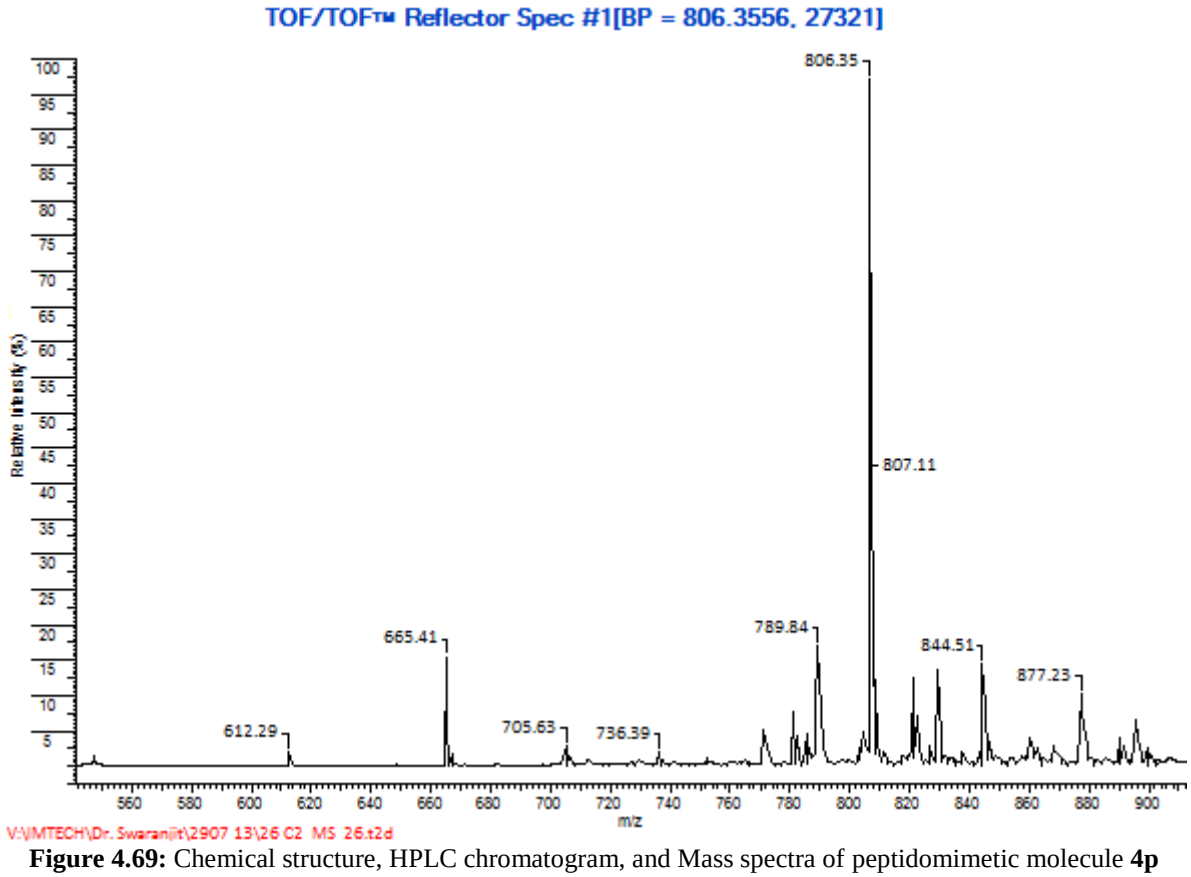

Figure 4.69: Chemical structure, HPLC chromatogram, and Mass spectra of peptidomimetic molecule **4p**

4.3. Biological evaluation

4.3.1. Antibacterial screening

4.3.1.1. Strains

Bacterial strains *Escherichia coli* (MTCC 723), *Pseudomonas aeruginosa* (MTCC 2295), *Staphylococcus aureus* (MTCC 3160), and *Bacillus subtilis* (MTCC 2763) were obtained from Microbial Type Culture Collection (MTCC) Chandigarh, India. Methicillin-resistant bacterial strains MRSA (ATCC BAA-1720) and MRSE (ATCC 51625) used in the present study were collected from Medicos laboratories, Chandigarh, India. Clinical isolates of bacterial strains used in the present study were collected from Post Graduate Institute of Medical Education and Research (PGIMER), Chandigarh, India and Government Medical College and Hospital (GMCH), Chandigarh, India. Twenty clinical isolates of ten different bacterial strains (one susceptible and one antibiotic resistant for each bacterial strain) were included in the study: *Staphylococcus aureus* (susceptible; PGI/DML03054), *Staphylococcus aureus* (Methicillin resistant; PGI/DML03149), *Staphylococcus epidermidis* (susceptible; GMCH/B0057), *Staphylococcus epidermidis* (Ampicillin resistant, GMCH/R-Amp008), *Streptococcus pneumoniae* (susceptible; PGI/DML02468), *Streptococcus pneumoniae* (Erythromycin resistant; PGI/DML02213), *Enterococcus faecium* (susceptible; GMCH/B0102), *Enterococcus faecium*(Penicillin resistant; GMCH/R-Pen003), *Enterococcus faecalis* (susceptible; GMCH/B0091), *Enterococcus faecalis* (Gentamicin resistant; GMCH/R-Gen011), *Escherichia coli* (susceptible; PGI/DML02250), *Escherichia Coli* (Imipenem resistant; PGI/DML02292), *Pseudomonas aeruginosa* (susceptible; PGI/DML02084), *Pseudomonas aeruginosa* (Streptomycin resistant; PGI/DML01991), *Klebsiella pneumonia* (susceptible; GMCH/B0127), *Klebsiella pneumonia* (Kanamycin resistant; GMCH/R-Kan006), *Acinetobacter baumannii* (susceptible; GMCH/B0083), *Acinetobacter baumannii* (Imipenem resistant; GMCH/R-Imi003), *Haemophilus influenzae* (susceptible; PGI/DML01751), *Haemophilus influenzae* (Ciprofloxacin resistant; PGI/DML01744). For experimental use each strain was streaked for single colony on Mueller-Hinton agar (MHA; HiMedia, Mumbai, India) plates and incubated at 37 °C overnight.

4.3.1.2. Method for MIC determination

Antimicrobial susceptibility testing was carried out using a modification of the Clinical Laboratory Standard Institute (CLSI) micro dilution broth assay [120]. Briefly, the inoculums were prepared from mid-logarithmic phase bacterial cultures. Each well of 96-well polypropylene microtiter plate (SIGMA) was inoculated with 90 μL of approximately 10^5 CFU/mL of bacterial suspension per mL of MHB. Then 10 μL of serially diluted peptides in 0.001% acetic acid and 0.2% BSA (SIGMA) over concentration ranging from 0.7-100 μg/mL was added to the wells of microtiter plate. The microtiter plates were incubated overnight with agitation at 37 °C and absorbance was read at 600 nm after 18 h. Cultures (approximately 10^5 CFU/ mL) without peptide were used as positive control. Uninoculated MHB was used as negative control. The tests were carried out in triplicate. The minimum inhibitory concentration (MIC) is defined as the lowest concentration of test compound that completely inhibits growth.

4.3.2. Antifungal screening

4.3.2.1. Strains

Fungal strains *Candida albicans,* (ATCC24433), *Aspergillus fumigates* (ATCC 42203), *Aspergillus niger* (ATCC 64028), and *Cryptococcus neoformans* (ATCC 2344) were obtained from Microbial Type Culture Collection (MTCC) Chandigarh, India. Clinical isolates of fungi used to carry out the screening of lipopeptides were collected from the Indira Gandhi Medical College (IGMC), Shimla, India. Eight clinical isolates of four different fungi were included in the study: *Aspergillus fumigatus* (susceptible; IGMC/LM6/0319), *Aspergillus fumigatus* (Fluconazole resistant; IGMC/LM1/0336), *Aspergillus niger* (susceptible; IGMC/LM1/084), *Aspergillus niger* (Itraconazole resistant; IGMC/LM1/0121), *Candida albicans* (susceptible; IGMC/LM7/0099), *Candida albicans* (Fluconazole resistant; IGMC/LM7/0129), *Cryptococcus neoformans* (susceptible; IGMC/LM3/0163), *Cryptococcus neoformans* (Ketoconazole resistant; IGMC/LM3/0198).

4.3.2.2. Method for MIC determination

The antifungal activity of the lipopeptides was measured using the conditions of the National Committee for Clinical Laboratory Standards (NCCLS) document M27-A [121,122]. The lipopeptides were examined in sterile 96-well plates (BD Falcon Microtest tissue culture plate) in a final volume of 200 μL as follows: 100 μL of a suspension containing fungi at a concentration of 2.5×10^3 CFU/mL in Roswell Park Memorial Institute (RPMI)

1640 medium (with L-glutamine, without glucose and $NaHCO_3$, buffered to pH 7.0 with 0.165 mol MOPS) was added to 100 µL of water containing the lipopeptides in serial 2-fold dilutions. The fungi were incubated for 24 h (*Aspergillus fumigatus* and *Aspergillus niger*) or 48-72 h (*Candida albicans* and *Cryptococcus neoformans*) at 37 °C in a new brunswick scientific incubator shaker. Growth inhibition was determined by measuring the absorbance at 600 nm in a microplate autoreader (Bio-Rad, India). The anti-fungal activity is expressed as the MIC, the concentration at which no growth was observed.

4.3.3. Cytotoxicity study

4.3.3.1. Hemolytic assay

Hemolytic activity of all synthesized molecules was determined using fresh isolated hRBCs as described in literature [123]. The hRBCs were centrifuged for 15 min to remove the buffy coat and washed three times with phosphate buffer saline (35 mmol phosphate buffer, 150 mmol NaCl pH 7.2). 100 µL of the hRBC suspended 4% (v/v) in PBS was plated into sterilized 96-well plates and then 100 µL solution of the test compound (serial two fold dilution in PBS) was added to each well. The plates were incubated for 1 h at 37 °C without agitation and centrifuged at 1000g for 5 min. Aliquots (100 µL) of the supernatant were transferred to 96-well plates, where hemoglobin release was monitored using microtiter plate reader (Bio-Rad, India) by measuring the absorbance at 540 nm. Percent hemolysis was calculated by the following formula:

%age hemolysis = $100 \times [(A - A_0)/(A_t - A_0)]$

Where, A represents absorbance of peptide sample at 540 nm and A_0 and A_t represent zero percent and 100% hemolysis determined in PBS and 1% Triton X-100, respectively.

4.3.3.2. Cytotoxicity against human keratinocytes (HaCaT cells)

4.3.3.2.1. Propagation of HaCaT cell culture

HaCaT cells (Human keratinocytes) were obtained from National Centre for Cancer Science (NCCS), Pune and grown as a monolayer in DMEM supplemented with 10% FBS (Fetal Bovine Serum), 100 µg/mL streptomycin and 100 units/mL penicillin. Cells were incubated at 37 °C in an atmosphere of 5% CO_2.

4.3.3.2.2. MTT assay

The cell viability of HaCaT cells was assessed by the MTT colorimetric assay, which is based on the reduction of MTT by the mitochondrial succinate dehydrogenase of intact cells to a purple formazan product. Briefly, cells were incubated in 96-well microtiter plates

for 24 h at 37 °C in a 5% CO_2 incubator. Following the addition of the test peptidomimetics, the plates were incubated for an additional 24 h. Control wells contained medium alone. Three replicate wells were used at each point in the experiments. After 24 h incubation, MTT solution (5 mg/mL in phosphate-buffered saline) was added and incubated for another 4 h. The resulting MTT/formazan product was dissolved by 100 µL of isopropanol and the plates were gently shaken to solubilize the formed formazan. The amount of formazan was determined by measuring the absorbance (OD) at 570 nm using a Bio-Rad 550 enzyme-linked immunosorbent assay (ELISA) microplate reader [124].

Cell survival was calculated as the percentage MTT inhibition as follows:

% growth inhibition = 100 − (mean OD of individual test group/ mean OD of each control group) ×100.

4.3.4. Bactericidal kinetic study

The time course of bacterial killing was studied by the exposure of *S. aureus* (MTCC 3160) and *E. coli* (MTCC 723) cultures (2×10^7 CFU/mL) to lead molecules at 4 × MIC in MHB. Aliquots were removed at a fixed time interval (30 min, 60 min, 90 min, 120 min, 180 min, and 240 min), diluted up to 10^8, plated on the MHA plate and CFU were counted after 24 h incubation at 37 °C. Untreated bacterial culture was used as a control. Data were obtained from two independent experiments performed in triplicate.

4.3.5. Membrane interaction study using membrane models

4.3.5.1. Preparation of calcein encapsulated liposomes

Large unilamellar vesicles (LUVs) were prepared by using extrusion method [125]. Briefly, two different compositions of lipids were prepared: PC/PE/PI/ergosterol (5:2.5:2.5:1, w/w) and PE/PG (7:3, w/w), which mimic the outer surface of the plasma membrane of fungi and bacteria, respectively. These lipid mixtures were dissolved in chloroform/methanol (2:1, v/v) in a 250 mL round bottom flask. The solvents were removed under a stream of nitrogen and the lipid film obtained was lyophilized overnight to remove any trace of solvent. The thin lipid film was rehydrated with calcein containing buffer comprising 70 mmol calcein, 150 mmol NaCl, and 0.1 mmol EDTA and adjusted to pH 7.4 by the addition of a few drops of sodium hydroxide solution (1 mol). The liposome suspension obtained after rehydration was frozen and thawed for five cycles and extruded 15 times through two stacked polycarbonate filters (100 nm pore size). The free calcein was removed by passing the liposome suspension through a Sephadex G-50 column and eluting with a buffer containing 10 mmol Tris-HCl

(150 mmol NaCl, 0.1 mmol EDTA). After passing the liposome through Sephadex G-50, liposome diameter was measured by dynamic light scattering using a Zetasizer Nano ZS (Malvern Instruments, India). Average diameter of LUVs was found to be in the range of 110-130 nm.

4.3.5.2. Calcein dye leakage assay

We investigated the membrane perturbation effect of lead molecules by measuring the calcein dye leakage from bacterial and fungal membrane mimicking LUVs. Induced leakage of calcein from the LUVs was monitored by measuring the fluorescence intensity at an excitation wavelength of 490 nm and an emission wavelength of 520 nm on a Fluoromax 4 (spex) spectrofluorometer. Aliquots of liposome suspension were then diluted in calcein free buffer (150 mmol NaCl, 0.1 mmol EDTA) to a final concentration of 40 μmol lipid and incubated for 5 min with different concentrations of the test compound. Calcein release from LUVs was assessed every minute for the first 20 min of the experiment and after onward measurement was taken at the interval of 10 min. The fluorescence intensity corresponding to 100% calcein release was determined by the addition of a 10% solution (w/v) of Triton X-100. The apparent percentage of dye leakage was calculated using the following formula:

$$\% \text{ Dye leakage} = 100 \times [(F - F_0)/ (F_t - F_0)]$$

Where F is the intensity measured at a given concentration of peptidomimetic, F_0 is the intensity of the liposomes (background), and F_t is the intensity after lysis by Triton X-100.

4.3.6. Fluorescence microscopy

In order to shed light on bactericidal mechanism of newly designed peptidomimetics fluorescence microscopy assay with DAPI (4',6-Diamidino-2-phenylindole dihydrochloride) and PI (Propidium iodide) as fluorophores was performed by treating *E. coli* and *S. aureus* cells. In this double staining method we can easily visualize and differentiate viable cells from the dead cells. DAPI as a double stranded DNA binding dye, stains all bacterial cells irrespective of their viability. Whereas PI is capable of passing through only damaged cell membranes and intercalates with the nucleic acids of injured and dead cells to form a bright red fluorescent complex. The cells were first stained with DAPI and then with PI. Bacterial cells were grown until they reached mid-logarithmic phase (2×10^6 cells) and then they were incubated with the peptidomimetics at the concentration of 4 × MIC for 2 h. Then the cells were pelleted by centrifugation at 3000g for 15 min in an eppendorf microcentrifuge. The supernatant was then decanted and the cells were washed with PBS several times and then

incubated with PI (5 μg/mL) in the dark for 15 min at 0 ^{o}C. The excess PI was removed by washing the cells with PBS several times. Then the cells were incubated with DAPI (10 μg/mL) for 15 min in dark at 0 ^{o}C. The DAPI solution was removed and cells were washed with PBS several times. Controls were performed following the exact same procedure for bacteria without the treatment with peptidomimetics. The bacterial cells were then examined by using the Nikon eclipse T*i* microscope with an oil-immersion objective (60×).

4.3.7. Microscopic visualization

4.3.7.1. Scanning Electron Microscopy (SEM)

Surface disruption effect of lead molecules on microbial cells was visualized using SEM. Bacterial culture of *E. coli* (MTCC 0723) and *S. aureus* (MTCC 3160) were suspended at 1 × 10^6 CFU/mL in 10 mmol PBS, pH 7.4 supplemented with 100 mmol NaCl. A 100 μL suspension containing *A. fumigatus* (ATCC 42203) at a concentration of 2 × 10^3 CFU/mL in PDB media was prepared from 2-3 days mature culture. For treatment bacterial and fungal cells were incubated with LP16 and LP24 at 37 °C respectively. Control was run in the absence of test compound. After 30 min the microbial cells were fixed with an equal volume of 4% glutaraldehyde in 0.2 mol Na-cacodylate buffer, pH 7.4, for 3 h at 4 °C followed by dehydration with a graded series of ethanol and dried the sample in HMDS (hexamethyldisilazane). The coating was done with gold approximately 20 nm thicknesses and observed under scanning electron microscope (Leo 435 VP).

4.3.7.2. Transmission Electron Microscopy (TEM)

Morphological changes of *E. coli* (MTCC 0723), *S. aureus* (MTCC 3160) and *A. fumigatus* (ATCC 42203) upon the treatment with lead molecules were analyzed using TEM. Bacterial culture of *E. coli* and *S. aureus* at 1 × 10^6 CFU/mL in MHB media were incubated with or without (control) the test compound dissolved in PBS at MIC and 4 × MIC for 30 min. After incubation with test compound a drop containing the bacteria was placed on to glow discharged carbon-coated copper grids for 1 min. The grids were rinsed in the same buffer, and stained with 1% uranyl acetate. Similarly, samples containing *A. fumigatus* (2.5 × 10^7 CFU/mL) were incubated with test compound dissolved in PBS at 4 × MIC for 30 min. Controls were run in the absence of test compound. A drop containing the fungi was deposited on to a carbon-coated grid and negatively stained with 1% uranyl acetate. Electron micrographs were then recorded using FEI Morgagni 268(D) operated at 70 kV.

4.3.8. DNA binding study

4.3.8.1. Isolation of bacterial plasmid DNA

Plasmid DNA was extracted from *E. coli* (PGI/DML02292) with some modification of the method used by Sambrook and Russell (2001). In brief, overnight grown culture of *E. coli* (10 mL) was treated with 5.0 ml cell lysis buffer mixed well and incubated for 1 h at 37 °C. After incubation, 50 µL of proteinase K was added to a final concentration of 100 µg/mL and mixed well. Later, it was incubated at 50 °C for 3 h in a water bath with intermittent shaking. An equal volume of phenol: chloroform: isoamyl alcohol (PCI) in 25:24:1 ratio was added to the above solution and mixed for 1 min. The tube was centrifuged at 3000g for 10 min at room temperature (RT), and the upper aq. phase was collected in a clean centrifuged tube. The aq. phase was once more treated with an equal volume of PCI and then once with an equal volume of chloroform:isoamyl alcohol (24:1). The upper aq. phase was finally collected after centrifugation at 3000g for 10 min at RT. To the aq. phase, one tenth volume of 3 mol sodium acetate, pH 5.2 was added, and DNA was precipitated by adding an equal volume of ice-cold isopropanol and incubating it at 4 °C overnight. The DNA pellet was obtained by centrifugation at 4000g for 15 min at RT. The pellet was washed once in 70% ethanol and centrifuged at 12000 rpm for 8 min. The DNA pellet settled at the bottom of the tube and was air dried by placing the tube open for 2-3 min. Finally, the DNA pellet was re suspended in 30-50 µL of nuclease-free water and stored at -20°C. The concentration and purity of isolated DNA was determined using thermo scientific nanodrop 2000 spectrophotometer.

4.3.8.2. Gel retardation assay

In order to determine the affinity of lead molecules towards DNA we performed gel retardation experiments [126]. Native lipo-antibiotic polymyxin B was included in the study as standard. Briefly, 100 ng of the plasmid DNA isolated from *E. coli* PGI/DML02292 was mixed with increasing amounts of peptide in 20 µL of binding buffer (5% glycerol, 10 mmol Tris-HCl, pH 8.0, 1 mmol EDTA, 1 mmol dithiothreitol, 20 mmol KCl, and 50 µg/mL BSA). Reaction mixtures were incubated at room temperature for 1 h. Subsequently, 4 µL of native loading buffer was added (10% Ficoll 400, 10 mmol Tris-HCl, pH 7.5, 50 mmol EDTA, 0.25% bromophenol blue, and 0.25% xylene cyanol), and a 20 µL aliquot subjected to 1% agarose gel electrophoresis in 0.5 × Tris borate-EDTA buffer (45 mmol Tris-borate and 1 mmol EDTA, pH 8.0).

4.3.9. Resistance development study [124]

We have determined the potential of susceptible as well as drug resistant pathogens to develop resistance against our most potent molecules. The initial MIC value of test compounds and standard antibiotics (ciprofloxacin, polymyxin B and daptomycin) against bacterial strains was obtained as described above. Serial passage and MICs determination were performed in 96 well microtiter plate containing peptidomimetics, each over a range of doubling dilution concentrations. After the incubation period 18 h the entire content of the triplicate wells with a concentration of test compound permitting visible growth were then used to prepare the bacterial dilution (approximately 2×10^6 CFU/mL) for the successive exposure. The experiment was repeated for 16 days. As a positive control, parallel cultures were exposed to two fold dilutions of the standard antibiotic (ciprofloxacin, polymyxin B and daptomycin).

4.3.10. Stability study

4.3.10.1. Proteolytic digestion assay

The stability testing of lead molecules against trypsin and α-chymotrypsin were conducted using a modified version of earlier reported protocol [112]. Briefly, each test sample was dissolved in a 0.1 mol NH_4HCO_3 buffer (pH 8.2) to a final concentration of 1 mg/mL. The enzymes (trypsin and α-chymotrypsin) solutions were prepared by dissolving 1 mg of enzyme to 50 mL of 0.1 mol NH_4HCO_3 buffer (pH 8.2). The test sample solution (150 µL), enzyme solution (150 µL), and 0.1 mol NH_4HCO_3 buffer (1200 µL) were combined and incubated at 37 ºC. Samples of 15 µL were collected at different time intervals, and 100 µL 10% (v/v) formic acid was added to stop the enzyme activity. For every test, a negative control without enzyme was incubated to ensure that whether the degradation was due to the enzyme or other factors. Quantitative analyses of remaining amount of the test samples were performed on RP-HPLC using a C18 waters column (Spherisorb®, ODS2, 5 µm, 4.6 mm × 250 mm) at room temperature. Solvents used in this method were: Solvent A, purified water with 0.05% TFA, and solvent B, HPLC grade acetonitrile with 0.05% TFA. The gradient chosen for separation started with an isocratic elution with 95% A and 5% B for 2 min, then a linear gradient to 40% A and 60% B after 3 min. The gradient was increased linearly to 10% A and 90% B after 10 min and was kept isocratic for 2 min. Flow speed was maintained at 0.2 mL/min for all set of experiments.

4.3.10.2. Plasma stability study

In vitro stability studies of most potent molecules were performed by using RP-HPLC [108]. A stock solution of test sample (1 mg/mL) was made by dissolving in water. Freshly collected heparinized blood plasma (1 mL) was added with 50 µL of peptidomimetic stock solution and incubated at 37 °C. Dilution of the human plasma was made in such a way that renders the proteolytic enzymes the limiting factor; enable a linear degradation of the peptidomimetics. After different time intervals (30 min, 1 h, 2 h, 6 h, 12 h, 24 h) 100 µL of the reaction solution was removed and added to 200 µL of 95% ethanol for precipitation of plasma proteins. The cloudy reaction sample is cooled at 4 ºC for 15 min and then centrifuge (18,000g) for 2 min to pellet the precipitated proteins. The clear supernatant was then analyzed using RP-HPLC on a 5 µm, 20 mm × 250 mm, Spherisorb® C18 column with UV detection at 280 nm.

CHAPTER 5.
RESULTS AND OBSERVATIONS

5.1. Short lipopeptides

5.1.1. Design and synthesis

We designed a library of short lipopeptide molecules by conjugating hydrophobic alkyl tails to N-terminal of cationic peptides. The unnatural amino acid "Ornithine" was chosen to represent the charged moiety as it would improve stability of lipopeptides in intended bioenvironment [114]. In addition, recently Habets *et al.* reported that pathogen resistant to AMPs (composed of genetically coded amino acid residues *viz* lysine, arginine, tryptophan etc.) shows cross resistance to innate immunity peptide (human-neutrophil-defensin-1; HNP-1) [128]. Therefore, we designed lipopeptide molecules by incorporating non-natural amino acid residue (Ornithine) to circumvent the long term risks associated with use of peptide based therapeutic agents.

Most native AMPs are composed of ≈12 to 50 amino acids residues, whereas naturally isolated antimicrobial lipopeptides are usually characterized by a small cyclic peptidic moiety composed of six to seven amino acids attached to a specific aliphatic chain [76,129]. In case of AMPs, their net positive charge, amphipathic conformation, and size were found to be important properties for biological functions [24]. Consequently, we synthesized short lipopeptide molecules by conjugating aliphatic moiety on N-terminus of totally cationic peptidic residue in order to provide structural amphipathicity. To determine the minimum requirement of charge and hydrophobic bulk in this novel class of antimicrobial agents, we undertook the synthesis by varying both charge unit (Orn_1-Orn_5) and hydrophobic tail (C8-C18). We synthesized a library of 30 short lipopeptide molecules (Scheme 1).

5.1.2. Antibacterial activity

The lipopeptides were screened against representative Gram-positive and Gram-negative bacteria including methicillin-resistant bacterial strains (MRSA & MRSE) which commonly cause nosocomial infections. Lipopeptides with single Orn residue and small aliphatic tail (C8 & C10) proved to be inactive as antimicrobials with MIC > 100 μg/mL (Table 5.1). Lipopeptides with Orn residues ranging from 2 to 5 units and aliphatic chain length from C12-C18 showed improved antimicrobial activity. Among the synthesized

molecules, lipopeptides composed of three Orn residues with N-terminus myristic acid (LP16) showed potent activity with MIC values of 1.5 µg/mL for *E. coli*, *P. aeruginosa*, *S. aureus*, and 6.25 µg/mL for *B. subtilis*. In addition, LP16 has good antimicrobial activity against drug resistant bacterial strains with MICs 6.25 µg/mL and 12.5 µg/mL against MRSE and MRSA, respectively (Table 5.1).

Selected lipopeptides were tested against susceptible as well as drug resistant clinical isolates of bacteria to uncover any unexpected selectivity between susceptible and drug resistant isolates. LP16 exhibits potent antibacterial activity against most of the tested Gram-positive and Gram-negative clinical isolates with MICs in the range of 1.5-4.5 µg/mL which compares favourably with the MICs of daptomycin and polymyxin B, the native lipopeptides available in the market. Antibacterial activity of LP16 against resistant strain of *E. coli* and *K. pneumoniae* was a bit higher with a MIC value of 5.5 µg/mL. Close examination of activity results of lipopeptides composed of 3 ornithine residues (LP16, LP17, and LP18) revealed that with the increase in length of aliphatic tail, activity was decreased against most of the tested bacteria. Exceptionally, LP18 killed susceptible *Streptococcus pneumoniae* at 2.5 µg/mL whereas 4.5 µg/mL of LP16 was required to inhibit the growth of susceptible *Streptococcus pneumoniae*. Furthermore, in case of lipopeptides composed of 4 and 5 ornithine residues no improvement in antibacterial activity was observed. Antibacterial activity results of lipopeptides against clinical isolates of Gram positive and Gram-negative bacterial strains are summarized in table 5.2 and 5.3, respectively.

Close examination of activity results revealed that lipopeptides are having same pattern of antimicrobial activity against clinical isolates of bacteria. Collectively, outcomes of antibacterial activity indicate that the balance of hydrophobicity and cationic charge appears to be critical for antimicrobial activity. It was interesting to note that all synthesized lipopeptides exhibits a broad antibacterial activity spectrum with insignificant difference between MIC values against susceptible and drug resistant isolates.

Table 5.1: Antibacterial activity of short lipopeptides

Lipopeptide designation	Minimum inhibitory concentration (μg/mL)					
	E. coli	*P. aeruginosa*	*S. aureus*	*B. subtilis*	MRSA	MRSE
LP01	>100	>100	>100	>100	>100	>100
LP02	>100	>100	>100	>100	>100	>100
LP03	100	50	100	>100	>100	>100
LP04	>100	>100	>100	>100	>100	>100
LP05	>100	>100	100	>100	>100	>100
LP06	>100	>100	>100	>100	>100	>100
LP07	>100	>100	>100	>100	>100	>100
LP08	>100	>100	>100	>100	>100	>100
LP09	50	50	>100	100	100	>100
LP10	6.25	3.1	25	50	50	100
LP11	12.5	6.25	3.1	12.5	12.5	25
LP12	25	25	12.5	50	25	25
LP13	>100	>100	100	100	>100	>100
LP14	>100	50	50	>100	100	>100
LP15	25	3.1	3.1	>100	12.5	12.5
LP16	1.5	1.5	1.5	6.25	12.5	6.25
LP17	6.25	3.1	6.25	12.5	25	12.5
LP18	12.5	6.25	6.25	12.5	12.5	12.5
LP19	>100	100	25	>100	100	100
LP20	50	25	25	>100	50	100
LP21	3.1	1.5	6.25	25	12.5	6.25
LP22	3.1	3.1	3.1	25	6.25	6.25
LP23	1.5	1.5	3.1	6.25	25	12.5
LP24	12.5	12.5	6.25	6.25	25	12.5
LP25	>100	>100	100	>100	>100	>100
LP26	100	50	50	100	>100	>100
LP27	6.25	6.25	12.5	50	12.5	12.5
LP28	3.1	6.25	12.5	12.5	6.25	12.5
LP29	6.25	12.5	6.25	12.5	12.5	25
LP30	12.5	12.5	12.5	25	25	12.5
Ciprofloxacin	0.7	0.3	0.15	0.7	-	-
Tetracycline	0.3	0.7	0.3	0.15	-	-
Vancomycin	-	-	-	-	1.5	2

Table 5.2: Antibacterial activity of short lipopeptides against clinical isolates of Gram-positive bacteria

Microbial strain	Resistant antibiotic	Minimum inhibitory concentration (µg/mL)									
		LP16	LP17	LP18	LP22	LP23	LP24	LP28	LP29	LP30	Daptomycin
Staphylococcus aureus (PGI/DML03054)	-	2.5	5	6.2	4.5	3.1	5	10	7.5	6.2	0.7
Staphylococcus aureus (PGI/DML03149)	Methicillin	3.1	4.5	5.5	5	4.5	7.5	12.5	10	10.5	1.25
Staphylococcus epidermidis (GMCH/B0057)	-	3.5	4	7.5	3.5	2.5	5.5	7.5	3.1	4.5	0.5
Staphylococcus epidermidis (GMCH/R-Amp008)	Ampicillin	3.1	5.5	5	4.25	2	5	12.5	7.5	10.5	1.5
Streptococcus pneumoniae (PGI/DML02468)	-	4.5	3.1	2.5	5.5	2.5	4	3.5	3.1	2.5	1.25
Streptococcus pneumoniae (PGI/DML02213)	Erythromycin	4.2	3.5	5	7.5	10.5	12.5	12.5	7.5	10	1.5
Enterococcus faecium (GMCH/B0102)	-	3.5	3	4.5	4	3.5	7.5	3.1	3	6.2	2
Enterococcus faecium (GMCH/R-Pen003)	Penicillin	3.1	5	7.5	5.5	3.5	12.5	6.21	7.5	12.5	2.5
Enterococcus faecalis (GMCH/B0091)	-	1.5	3.1	2.5	2	3.5	3.1	1.5	2	4.5	1.75
Enterococcus faecalis (GMCH/R-Gen011)	Gentamicin	4.5	5	6.25	3.5	7.5	10	10.5	12.5	15	1.5

Table 5.3: Antibacterial activity of short lipopeptides against clinical isolates of Gram-negative bacteria

Microbial strain	Resistant antibiotic	Minimum inhibitory concentration (µg/mL)									
		LP16	LP17	LP18	LP22	LP23	LP24	LP28	LP29	LP30	Polymyxin B
Escherichia coli (PGI/DML02250)	-	2	5.5	10	2.5	2	7.5	2.5	1.5	5	0.5
Escherichia Coli (PGI/DML02292)	Imipenem	5.5	6.25	7.5	10	12.5	7.5	6.25	5	7.5	0.75
Pseudomonas aeruginosa (PGI/DML02084)	-	1.5	2.5	1.5	3.1	3	4.5	1.5	2	2.5	0.12
Pseudomonas aeruginosa (PGI/DML01991)	Streptomycin	2.25	3.1	4.5	3	6.25	2	4.25	6.5	5	0.5
Klebsiella pneumoniae (GMCH/B0127)	-	4	3.5	3.5	4.5	2	3.5	6.2	2.5	4	2
Klebsiella pneumoniae (GMCH/R-Kan006)	Kanamycin	5.5	3.1	7.5	6.25	5.5	8	7.5	10	12.5	2.75
Acinetobacter baumannii (GMCH/B0083)	-	2.5	4	6.5	5	6.5	10	8.25	12.5	10	0.7
Acinetobacter baumannii (GMCH/R-Imi003)	Imipenem	3.25	5.5	4.5	5.5	10	12.5	6.5	9.5	7.5	0.7
Haemophilus influenzae (PGI/DML01751)	-	4.5	5	10	12.5	7.5	8	12.5	10	10	1.5
Haemophilus influenzae (PGI/DML01744)	Ciprofloxacin	3.1	5.5	7.5	10	12.5	12.5	15.5	12.5	15	2.25

5.1.3. Antifungal activity

Lipopeptides with comparatively bulky aliphatic tail were found to be more active towards fungal strains. Lipopeptide molecules synthesized by conjugating capric acid and caprylic acid displayed no antifungal potential at all. Similarly, moderate antifungal activity was observed for N-terminus lauric acid conjugated lipopeptides. The highest anti-fungal activity was observed for palmitic acid (LP17, LP23, and LP29) and stearic acid (LP18, LP24, and LP30) conjugated lipopeptides with MIC values in range of 1.5-6.25 µg/mL against all tested strains (Table 5.4).

Lipopeptides showed promising antifungal activity against initially tested strains, were subjected to further antifungal screening against a large panel of susceptible as well as drug resistant clinical isolates of fungi. Same as that of earlier antifungal activity results, maximum activity was observed in case of lipopeptides composed of N-terminal palmitic acid or stearic acid aliphatic tail. In particular, LP24 and LP30 displayed antifungal activity with a MIC values in the range of 1.5-3.5 µg/mL against all tested strains. However, lipopeptides bearing a myristic acid alky tail (LP16, LP22, and LP28) were found to be moderately active towards all tested fungal strains. Antifungal activity results of lipopeptides against susceptible and drug resistant clinical isolates are summarized in table 5.5 and 5.6, respectively.

Table 5.4: Antifungal activity of short lipopeptides

Lipopeptide designation	Minimum inhibitory concentration (µg/mL)			
	C. albicans	*A. fumigatus*	*A. niger*	*C. neoformans*
LP01	>100	>100	>100	>100
LP02	>100	>100	>100	>100
LP03	>100	>100	>100	>100
LP04	>100	>100	>100	>100
LP05	>100	>100	>100	>100
LP06	>100	>100	>100	>100
LP07	>100	>100	>100	>100
LP08	>100	100	>100	>100
LP09	50	50	100	50
LP10	25	12.5	25	25
LP11	6.25	6.25	12.5	6.25
LP12	12.5	6.25	12.5	25
LP13	>100	>100	>100	>100
LP14	100	50	50	100
LP15	12.5	12.5	6.25	25
LP16	6.25	3.1	6.25	12.5
LP17	3.1	3.1	1.5	6.25
LP18	6.25	1.5	3.1	6.25
LP19	>100	>100	>100	>100
LP20	>100	50	100	100
LP21	6.25	6.25	12.5	12.5
LP22	6.25	3.1	6.25	12.5
LP23	3.1	1.5	6.25	3.1
LP24	3.1	1.5	1.5	6.25
LP25	>100	>100	>100	>100
LP26	100	50	50	>100
LP27	12.5	12.5	12.5	25
LP28	6.25	3.1	6.25	6.25
LP29	6.25	1.5	1.5	6.25
LP30	3.1	3.1	1.5	3.1
Amphotericin B	0.3	0.3	0.15	0.7

Table 5.5: Antifungal activity of short lipopeptides against susceptible clinical isolates

Lipopeptide designation	Minimum inhibitory concentration (µg/mL)			
	A. fumigatus	*A. niger*	*C. albicans*	*C. neoformans*
LP16	10	7.5	12.5	7.5
LP17	8	6.25	5.5	5
LP18	5.5	4	5	4.5
LP22	6	5	10	7
LP23	3	3.25	5.5	4
LP24	1.5	2	3	2
LP28	5	3.5	3	4.5
LP29	2.5	2	2.25	3
LP30	2	2.5	2	2
Amphotericin B	0.5	0.5	0.3	0.5

Table 5.6: Antifungal activity of short lipopeptides against resistant clinical isolates

Lipopeptide designation	Minimum inhibitory concentration (µg/mL)			
	A. fumigatus	*A. niger*	*C. albicans*	*C. neoformans*
LP16	12.5	10.5	12	20
LP17	7.5	6.25	10.5	6.25
LP18	6.25	3.5	5.5	5.5
LP22	7.5	7.25	10.5	5
LP23	5.5	4.5	6.25	3.25
LP24	2.5	3	3.1	2.5
LP28	4.5	5	6.5	5
LP29	3.2	4.5	3	3.5
LP30	2.5	3.5	3	3.1
Amphotericin B	0.7	1.25	0.7	0.5

[a]Drugs against which the clinical isolates were found to be resistant were Fluconazole, Itraconazole, and Ketoconazole.

5.1.4. Cytotoxicity

Hemolytic activity of the short lipopeptides was studied as a measure of toxicity against human erythrocytes. Lipopeptide molecules with bulky fatty acid chain (16 and 18 carbon atoms long) showed higher affinity towards hRBC as compared to the lipopeptides with small fatty acid chain (8 to 14 carbon atoms long), suggesting a relationship between hydrophobicity and selectivity. As compared to native lipopeptides all synthesized short lipopeptides showed high selectivity index. Selectivity ratio (SR) measures the ratio of hemolytic activity to antimicrobial activity, which we defined as $HC_{50}/MIC_{E.c.}$ and $HC_{50}/MIC_{S.a}$ (Table 5.7). A high SR value indicates that compound possesses good selectivity profile. Among the complete library of compounds minimum selectivity ratio (SR = 20) was observed in case of lipopeptides with long aliphatic tail (LP24 and LP30). The most potent antibacterial lipopeptide (LP16) showed significant selectivity ratio (SR = 500; Table 5.7). These values indicate that lipopeptides were able to kill microbes without exerting significant lytic activity toward mammalian erythrocytes.

Table 5.7: Cytotoxicity of short lipopeptides against human red blood cells (hRBCs)

Code	[a]HC_{50} (µg/mL)	Selectivity		Code	[a]HC_{50} (µg/mL)	Selectivity	
		$HC_{50}/MIC_{E.c.}$	$HC_{50}/MIC_{S.a}$			$HC_{50}/MIC_{E.c.}$	$HC_{50}/MIC_{S.a}$
LP01	-	-	-	LP16	750	500	500
LP02	-	-	-	LP17	750	120	120
LP03	-	-	-	LP18	500	40	80
LP04	-	-	-	LP19	>1000	-	-
LP05	-	-	-	LP20	500	10	20
LP06	-	-	-	LP21	500	161.2	80
LP07	>1000	-	-	LP22	500	161.2	161.2
LP08	>1000	-	-	LP23	500	333.3	161.2
LP09	750	15	-	LP24	250	20	40
LP10	750	120	30	LP25	1000	-	-
LP11	500	40	161.29	LP26	750	7.5	15
LP12	500	20	40	LP27	500	80	40
LP13	>1000	-	-	LP28	500	161.2	40
LP14	1000	-	-	LP29	250	40	40
LP15	1000	40	322.5	LP30	250	20	20

[a]HC_{50} is the concentrations of lipopeptides at which 50% hemolysis was observed.

MTT assay results of lipopeptides against human keratinocytes (HaCaT calls) further revealed their selectivity towards microbial cells. More than 80% cell survival was observed among all lipopeptides at 100 µg/mL. It was interesting to note that at a high concentration of 500 µg/mL, only 35% of HaCaT cell viability was compromised. In particular, LP16 at 100 µg/mL showed almost no toxicity (92% cell viability), while at 500 µg/mL, only around 25% of HaCaT cell viability was compromised. In case of LP24, 82% cell viability was observed at 100 µg/mL and which was decreased to 67% at 500 µg/mL (Figure 5.1). The outcomes of MTT assay further confirm the selective killing action of lipopeptides towards microbes as compared to mammalian cells.

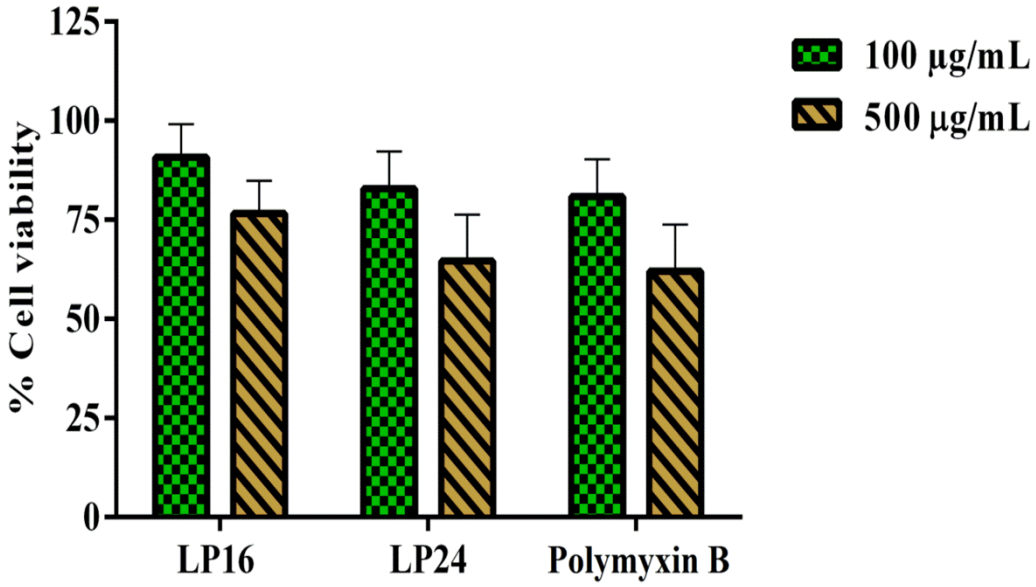

Figure 5.1: Toxicity evaluation of lipopeptides using MTT assay. Percentage viability of cells (HaCaT) upon treatment with different concentrations of LP16, LP24 and polymyxin B. The results represent the data (mean ± SD) obtained from two independent experiments performed in triplicate

5.1.5. Bactericidal kinetics

Viability of exponentially growing *E. coli* and *S. aureus* as representative Gram-negative and Gram-positive bacterial strains was checked against most potent lipopeptides (LP16 and LP23) by time-kill assay. The time kill curves of LP16 and LP23 against *S. aureus* and *E. coli* are shown in Figure 5.2. With a rapid bactericidal kinetics both LP16 and LP23 were able to completely eradicate 10^7 CFU/mL of *S. aureus* at 2 × MIC over a period of 3 h. In accordance with MIC data lipopeptides (LP16 and LP23) exhibited rapid killing rate against *E. coli* and showed complete killing action within 2 h.

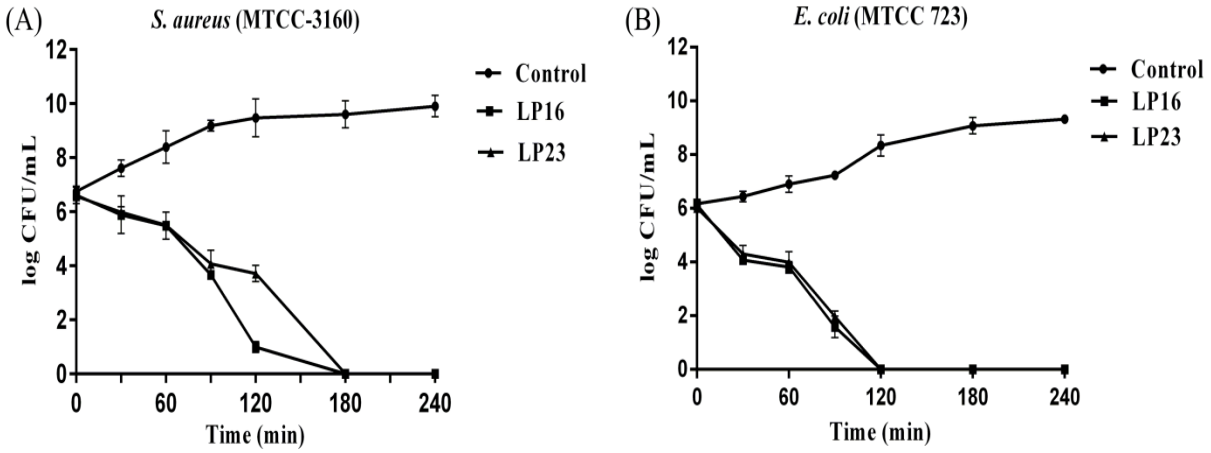

Figure 5.2: Bactericidal kinetics of lipopeptides (LP16 and LP23) against *S. aureus* (A) and *E. coli* (B). Data obtained are from two independent experiments performed in triplicate

5.1.6. Biomembrane interaction study using artificial membranes

The membrane perturbation effects of lipopeptides (LP16 and LP24) were investigated by measuring the calcein dye release from bacterial membrane mimicking LUVs. Lipopeptides, LP16 and LP24, caused a rapid increase in the fluorescent intensity at a concentration level of 1:50 lipopeptide:lipid molar ratio, leading to a 51% and 43% of dye leakage, respectively. At highest used experimental concentration (1:10 lipopeptide:lipid molar ratio), the percentage of calcein leakage for LP16 and LP24 was found to be 91% and 79%, respectively (Figure 5.3). The results of calcein dye leakage experiment also supported the activity results as LP16 exhibited higher potency as compared to LP24. Lipopeptides possesses potent activity towards all tested bacterial strains without any significant discrimination between Gram-positive and Gram-negative bacterial strains, which further indicates the membrane disruption action of lipopeptides. In addition, outcomes of the calcein dye leakage experiments suggested that both LP16 and LP24 damage bacterial membrane mimicking liposomes in a concentration dependent manner.

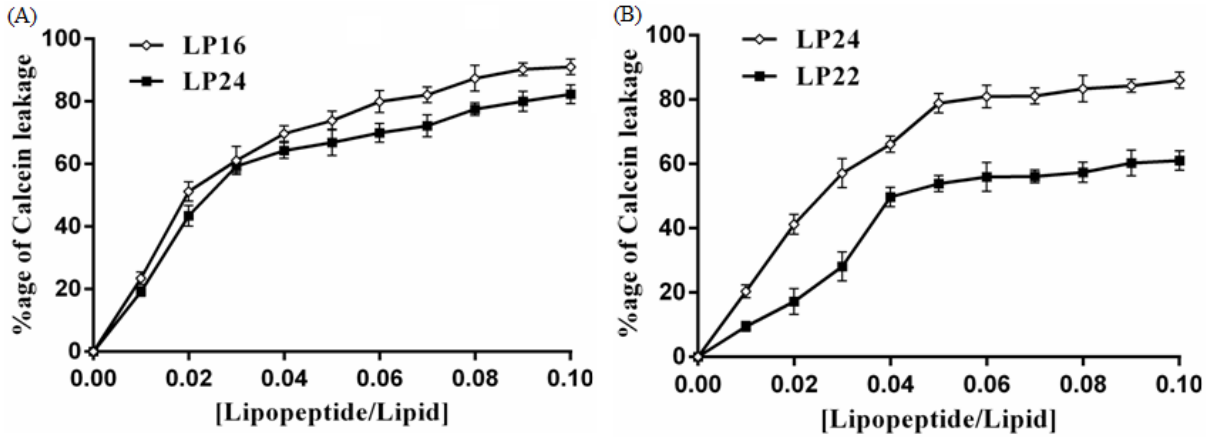

Figure 5.3: Concentration-dependent calcein dye leakage effect of lipopeptides (A) when LP16 and LP24 incubated with bacterial membrane mimicking LUVs (B) when LP24 and LP22 incubated with fungal membrane mimicking LUVs

We investigated the membrane perturbation effect of most potent lipopeptide (LP24) by measuring the calcein dye leakage from fungal membrane mimicking LUVs. To determine the role of the aliphatic tail in the membrane interaction potential of lipopeptides, we included lipopeptide bearing myristic acid as hydrophobic tail (LP22) in the study. After the comparative analysis of the leakage profile of lipopeptide LP24 and LP22, it was observed that LP24 caused a rapid increase in calcein leakage leading to a 41% at a low lipopeptide concentration (1:50 lipopeptide:lipid molar ratio) and thereafter increased gradually up to 86% at a maximum concentration tested (1:10 lipopeptide:lipid molar ratio). For LP22, 17% of dye leakage was observed at a 1:50 lipopeptide:lipid molar ratio and which was reached to 60% at a highest used experimental concentration (1:10 lipopeptide:lipid molar ratio). Calcein leakage data end in plateaus for both tested lipopeptides. The dose-response curves of lipopeptide induced calcein release are shown in figure 5.3.

5.1.7. Surface disruption effect of lead lipopeptide in intact bacterial cells

After knowing the membrane disruption effect of lipopeptides, we further confirmed the mechanism of action by visualizing the effects on intact bacterial (*E. coli* and *S. aureus*) and fungal (*A. fumigatus*) cells. In SEM images we visualized that untreated (control; Figure 5.4 A1-A3) microbial cells exhibited bright and smooth surface, whereas morphological alterations like surface blebs were spotted on the surface of lipopeptide treated cells (Figure 5.4 B1-B3). We also studied the surface effect of lipopeptides by transmission electron microscopy (TEM). In comparison to untreated controls (Figure 5.4 C1-C3) easily distinguishable disruption of cell structures was observed in case of treated microbial cells

(Figure 5.4 D1-D3). Taken together, the data from SEM and TEM studies indicated that lipopeptides (LP16 and LP24) exhibit antimicrobial effects by membrane perturbation.

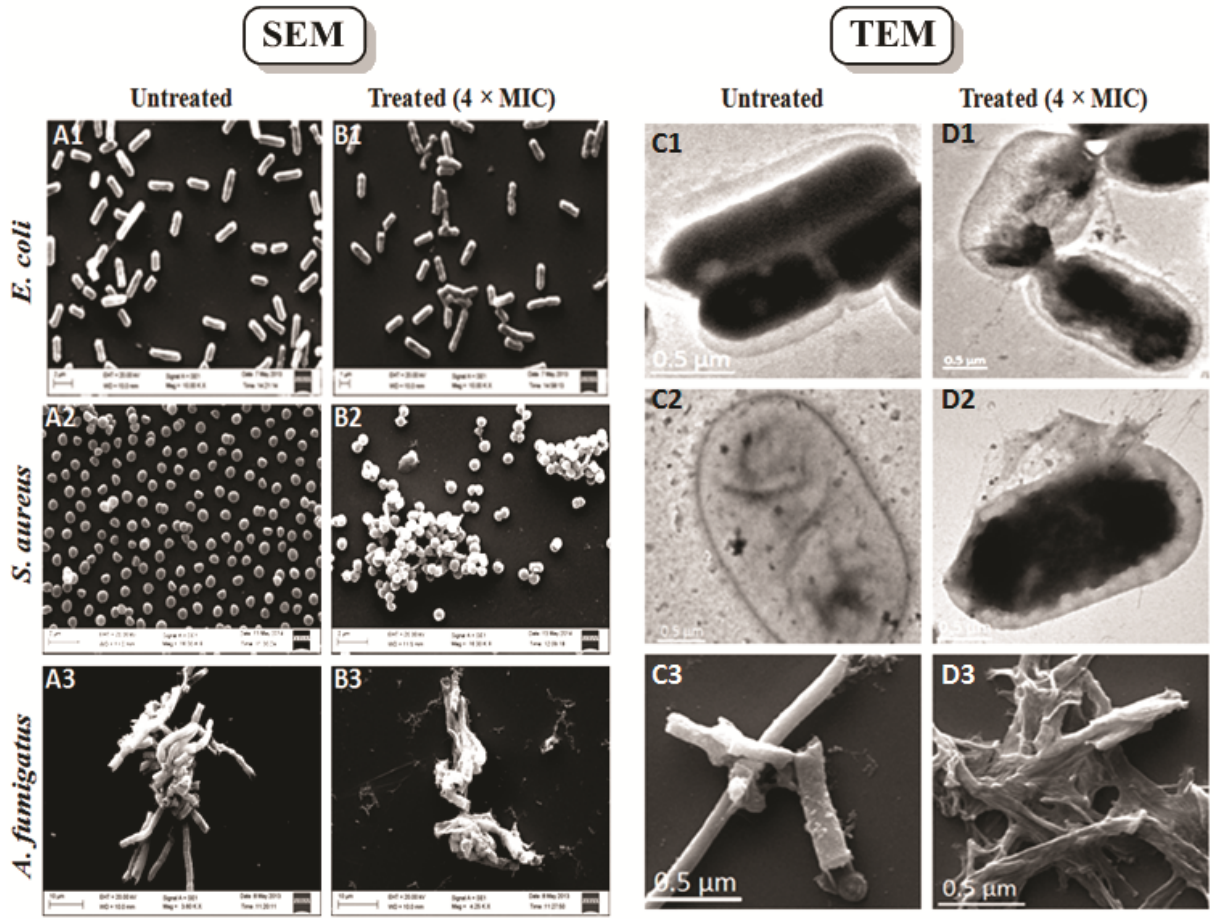

Figure 5.4: Scanning electron microscopic (SEM) and Transmission electron microscopic (TEM) images of bacteria (*E. coli* MTCC 0723 and *S. aureus* MTCC 3160) and fungi (*A. fumigatus* ATCC 42203) treated with LP16 and LP24 respectively

5.1.8. DNA binding assay

Native lipopeptide antibiotic polymyxin B is mainly active toward Gram-negative bacterial strains, which reflect the possibility of their intracellular effects. To determine the involvement of intracellular targets in the antibacterial action of lipopeptides, we assessed the DNA binding ability of LP16 and LP24. DNA complexation was not observed for LP16 and LP24 even at the highest used experimental concentration (12 µg/mL). Noticeably, polymyxin B showed DNA binding only at 12 µg/mL (Figure 5.5). These findings recommended a different mode of action for LP16 and LP24 as compared to polymyxin B and which might be due to the overall structural makeup of the molecule.

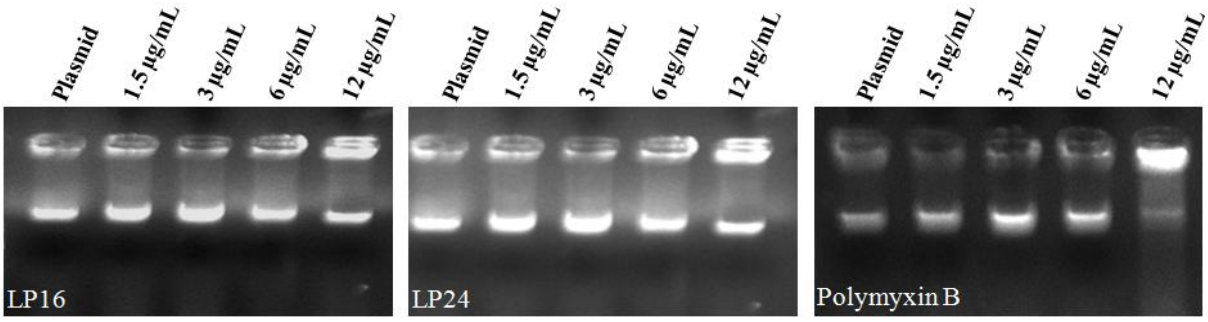

Figure 5.5: Gel retardation assay, binding was assayed by the inhibitory effect of LP16, LP24, and polymyxin B on the migration of plasmid DNA bands

5.1.9. Resistance development study

To further explore the therapeutic potential of LP16, a resistance development study was performed. The potential of susceptible as well as drug resistant Gram-positive (*S. aureus*) and Gram-negative (*E. coli*) bacteria to develop resistance was evaluated by serial passages of the bacterial cultures against LP16. Results from this study confirmed the low tendency of bacterial pathogens to develop resistance against LP16 and native lipopeptides (polymyxin B and daptomycin) in comparison to ciprofloxacin as there was an insignificant change in the MIC after 16 passages (Figure 5.6).

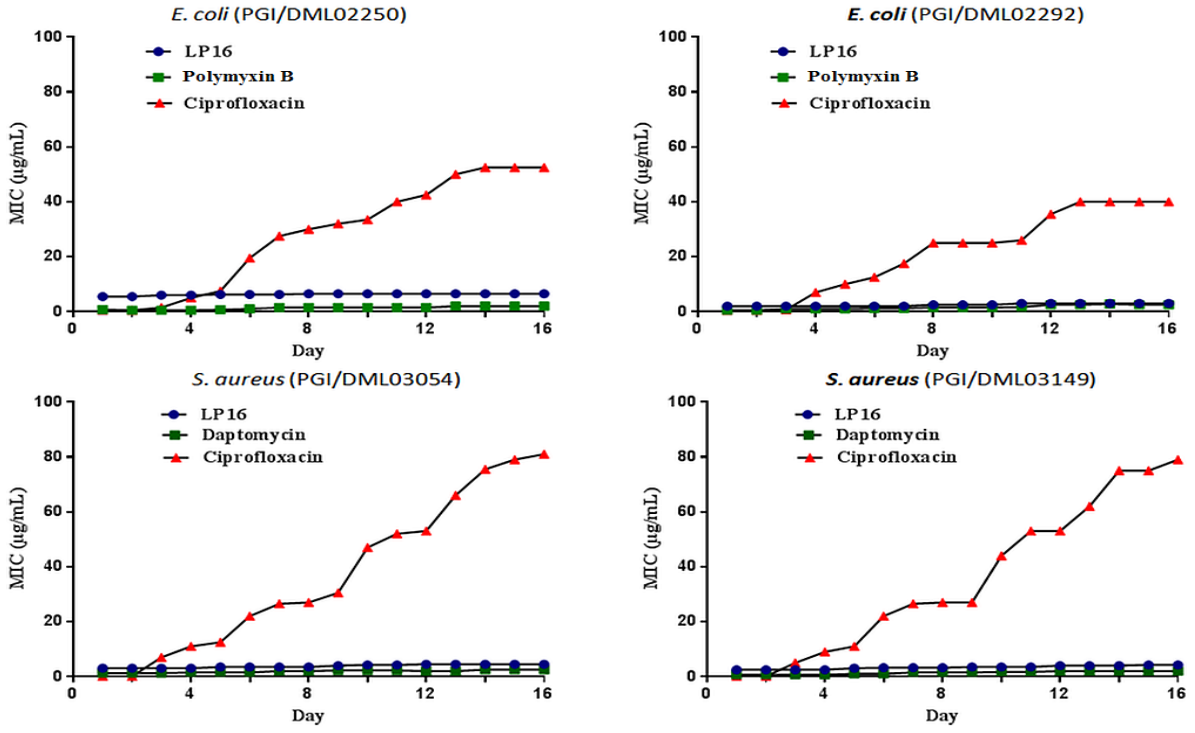

Figure 5.6: Evaluation of resistance development by susceptible as well as resistant clinical isolates of bacteria against LP16, polymyxin B and ciprofloxacin. (A) Susceptible *E. coli* PGI/DML02250; (B) Imipenem resistant *E. coli* PGI/DML02292; (C) Susceptible *S. aureus* PGI/DML03054; (D) Methicillin resistant *S. aureus* PGI/DML03149

5.1.10. Evaluation of the proteolytic stability of LP16

To determine the stability imparted to lipopeptides by ornithine residue, we conducted *in vitro* stability study of LP16 against trypsin. LP16 displayed no sign of degradation when incubated with trypsin over a period of 24 h, as the area of the peak corresponding to LP16 (RT-13.08 min.) did not change significantly (Figure 5.7). Proteolytic stability of LP16 was further confirmed by assessing stability in human blood plasma. It was interesting to note that LP16 was found stable in plasma even after 24 h of incubation (Figure 5.8).

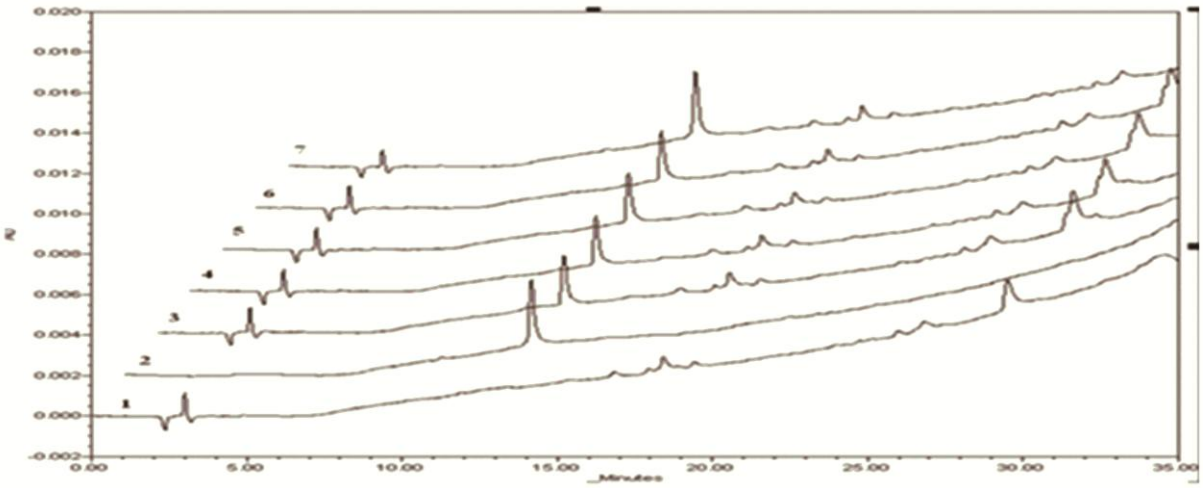

Figure 5.7: Tryptic stability study of LP16. Trypsin in buffer (chromatogram 1); LP16 in buffer (chromatogram 2); LP16 incubated with trypsin for 30 minutes (chromatogram 3); LP16 incubated for 1 h (chromatogram 4); LP16 incubated for 4 h (chromatogram 5); LP16 incubated for 12 h (chromatogram 6); LP16 incubated for 24 h (chromatogram 7).

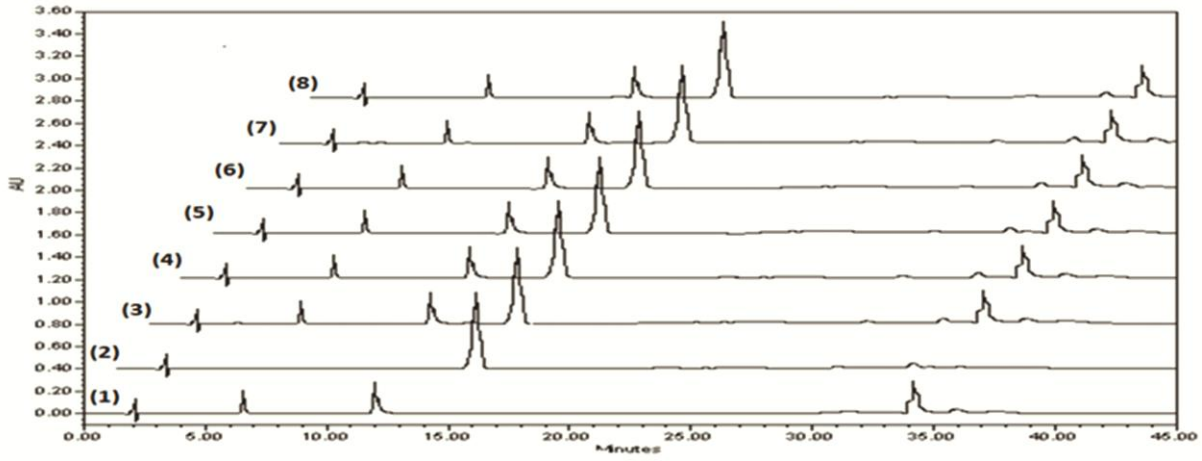

Figure 5.8: Stability study of LP16 in human blood plasma. Human blood Plasma in buffer (chromatogram 1); LP16 in buffer (chromatogram 2); LP16 incubated with blood plasma for 30 minutes (chromatogram 3); LP16 incubated with blood plasma for 1 h (chromatogram 4); LP16 incubated with blood plasma for 2 h (chromatogram 5); LP16 incubated with blood plasma for 6 h (chromatogram 6); LP16 incubated with blood plasma for12 h (chromatogram 7); LP16 incubated with blood plasma for 24 h (chromatogram 8).

5.2. Small cationic peptidomimetics

5.2.1. Design and synthesis

It is well documented that biological activity of native AMPs is depending on their secondary structure as well as net content of cationic charge and hydrophobicity [25,27]. Native AMPs and synthetically designed peptidomimetic templates comprised of genetically coded amino acid residues can be susceptible to proteolytic degradation [108,112,130,131]. Backbone modification is one of the synthetic approaches used to design peptidase immune peptidomimetics [112,131]. Consequently, incorporation of a suitable moiety in the peptide backbone which provides a specific turn and subsequently induces molecular amphipathicity may result into the improvement of antimicrobial activity as well as stability. Accordingly, we designed a series of small cationic peptidomimetics by incorporating constrained aromatic amino acid (3-ABA) which could mimic essential structural features of AMPs and endow with proteolytic stability in such a way that optimum therapeutic index may possibly be achieved.

Initially, a library of small cationic peptidomimetics (**1a, 2a-2c, 3a-3e, 4a-4g**) was synthesized by incorporating 3-amino benzoic acid (3-ABA) as peptidomimetic element (Scheme 2). Arginine (Arg) and Tryptophan (Trp) amino acid residues were used to provide cationic charge and hydrophobic bulkiness respectively. Peptidomimetic molecules **1a, 2a-2c, 3a-3e, 4a-4g** were synthesized by varying the sequence of charged (Arg) and hydrophobic (Trp) amino acid residues on both sides of 3-ABA. Further peptidomimetic molecules (**3f** and **4h-4l**) were synthesized by replacing Arg with non-proteogenic cationic amino acid ornithine (Orn) in the most active and moderately active molecules (**3e** and **4c-4g**; Scheme 3). Structural modification was done by the substituting bulky hydrophobic residue Trp with Phe (**4m-4p**) among the most active molecules (**4f**, **4g, 4k** and **4l**; Scheme 4). Finally, linear analogues (**5a-5d**) of most active peptidomimetic sequences (**4f**, **4g, 4k,** and **4l**) were synthesized for comparative analysis of antibacterial potential (Scheme 5).

5.2.2. Antibacterial activity

A closer examination of activity results revealed the predominantly anti-staphylococcal action of newly designed peptidomimetics. Peptidomimetic molecules **1a, 2a-2c, 3a-3d** composed of 3, 4, and 5 amino acid residues, virtually showed no antibacterial activity. In some cases moderate activity was observed with the exception of the molecule **3e** that exhibited MIC values of 12.5, 10, and 12.5 µg/mL against *S. aureus*, MRSA, and MRSE respectively. The peptidomimetic molecule **3e** was also active against *E. coli* and *P. aeruginosa*, although the MIC values were considerably higher in comparison to their activity against various strains of *S. aureus* (Table 5.8). Peptidomimetic molecules (**4a-4g**) with 6 amino acid residues displayed higher antibacterial activity against both Gram-positive and Gram-negative bacteria in comparison to peptidomimetic sequences with tri, tetra and penta amino acid residues. Most active peptidomimetic molecule **4g** displayed maximum potency with MIC values in the range of 5-5.5 µg/mL against *S. aureus*, MRSA, and MRSE. It was interesting to note that **4g** showed comparable activity against Gram-negative bacteria also with MIC values of 7.5 and 12.5 µg/mL against *E. coli* and *P. aeruginosa* respectively. Moreover, peptidomimetic molecule **4f** with 6 amino acid residues was found to be active against Gram-positive as well as Gram-negative bacteria. Same pattern of activity was observed in the case of **4l** which exhibited MIC values in the range of 5-6.25 µg/mL against *S. aureus*, MRSA, and MRSE. Peptidomimetic molecule **4l** was found to have somewhat low activity against Gram-negative bacteria with MICs 20 and 15.5 µg/mL against *E. coli* and *P. aeruginosa* respectively. Further, peptidomimetic molecules having phenylalanine as hydrophobic residue (**4m-4p**) showed insignificant lytic action against all screened bacterial strains. It was interesting to note that the linear analogues (**5a-5d**) of most active sequences showed poor antibacterial activity. Consequently, these activity results reflect the potential of our novel approach for designing small cationic peptidomimetics. The antibacterial activity results of small cationic peptidomimetics are summarized in table 5.8.

Table 5.8: Antibacterial activity of small cationic peptidomimetics

Code	[a]Sequence	Minimum inhibitory concentration (µg/mL)					
		E. coli	*P. aeruginosa*	*S. aureus*	*B. subtilis*	MRSA	MRSE
1a	W-3ABA-R-NH_2	>200	>200	>200	>200	>200	>200
2a	WW-3ABA-R-NH_2	150	170	120	150	200	>200
2b	RW-3ABA-R-NH_2	70	75	50	100	60	70
2c	WR-3ABA-R-NH_2	200	>200	150	200	150	200
3a	WW-3ABA-RR-NH_2	120	125	50	70	50	75
3b	RW-3ABA-RR-NH_2	100	75	70	100	75	75
3c	WR-3ABA-RR-NH_2	>200	>200	100	170	120	100
3d	WR-3ABA-WR-NH_2	150	120	60	75	50	75
3e	RW-3ABA-WR-NH_2	40	50	12.5	50	10	12.5
4a	WWR-3ABA-RR-NH_2	75	100	50	70	50	50
4b	RWR-3ABA-WR-NH_2	120	120	50	125	40	50
4c	RWW-3ABA-RR-NH_2	70	75	25	75	25	25
4d	WRR-3ABA-WR-NH_2	50	50	15	70	12.5	10
4e	WRW-3ABA-RR-NH_2	60	70	25	40	25	25
4f	RRW-3ABA-WR-NH_2	17.5	25	6.25	25	5	6.25
4g	WRW-3ABA-WR-NH_2	7.5	12.5	5	20	5.5	5
3f	OW-3ABA-WO-NH_2	50	40	17.5	50	20	15
4h	OWW-3ABA-OO-NH_2	100	100	50	100	50	50
4i	WOO-3ABA-WO-NH_2	75	100	40	75	50	40
4j	WOW-3ABA-OO-NH_2	70	75	25	40	25	20
4k	OOW-3ABA-WO-NH_2	40	50	7.5	40	10.25	12.5
4l	WOW-3ABA-WO-NH_2	20	15.5	6.25	25	5	6.25
4m	RRF-3ABA-FR- NH_2	>200	>200	150	200	150	170
4n	FRF-3ABA-FR- NH_2	>200	>200	120	150	125	120
4o	OOF-3ABA-FO- NH_2	>200	>200	>200	>200	>200	>200
4p	FOF-3ABA-FO- NH_2	>200	>200	150	>200	>200	>200
5a	RRWWR-NH_2	75	100	25	70	25	20
5b	WRWWR-NH_2	40	70	15	50	17.5	20
5c	OOWWO-NH_2	120	150	70	100	100	100
5d	WOWWO-NH_2	70	150	50	120	50	70
	Ciprofloxacin	0.7	0.3	0.15	0.7	-	-
	Vancomycin	-	-	-	-	1.5	2

[a]Amino acids are represented by their one letter denotation.

5.2.3. Cytotoxicity

To evaluate the selectivity of peptidomimetics towards bacterial cells over mammalian cells, their hemolytic activity against human red blood cells (hRBCs) was measured (Table 1). Typically, the hemolytic effect was assessed by measuring the concentration of peptidomimetics required for 50% (HC_{50}) and 10% hemolysis (HC_{10}) of hRBCs. Maximum hemolysis determined by HC_{10} was detected for **4g** at 80 µg/mL. Other peptidomimetic sequences caused 10% hemolysis at concentration above 100 µg/mL. Therefore, overall outcomes of hemolytic assay revealed that all synthesized peptidomimetics do not readily induce lysis of hRBCs. Furthermore, selectivity ratio (SR) was calculated by dividing HC_{50} values against human RBC and the MICs against *S. aureus*. The maximum selectivity was observed for one of the lead peptidomimetic molecule **4l** (SR = 62.4) followed by **4g** (SR = 62; Table 1). It was interesting to observe, that peptidomimetics with 3-ABA scaffold (**4f**, **4g, 4k,** and **4l**) displayed higher selectivity in comparison to linear peptides (**5a-5d**) as summarized in table 5.9.

Table 5.9: Cytotoxicity of small cationic peptidomimetics against human red blood cells (hRBCs)

Code	[a]HC_{10} (µg/mL)	[a]HC_{50} (µg/mL)	[b]Selectivity ($HC_{50}/MIC_{S.a}$)	Code	[a]HC_{10} (µg/mL)	[a]HC_{50} (µg/mL)	[b]Selectivity ($HC_{50}/MIC_{S.a}$)
1a	400	>500	-	4g	80	310	62
2a	100	240	2	3f	190	>500	>28.57
2b	205	500	10	4h	150	440	8.8
2c	300	>500	>3.3	4i	170	500	12.5
3a	150	400	8	4j	175	450	18
3b	350	>500	>7.14	4k	120	450	60
3c	325	>500	>5	4l	100	390	62.4
3d	220	400	6.66	4m	130	375	2.5
3e	250	410	32.8	4n	125	310	2.58
4a	200	380	7.6	4o	210	490	-
4b	210	400	8	4p	180	400	2.66
4c	255	420	16.8	5a	90	240	9.6
4d	190	380	25.33	5b	60	200	13.33
4e	140	370	14.8	5c	100	310	4.42
4f	100	355	56.8	5d	65	225	4.5

[a]HC_{10} and HC_{50} are the concentrations in µg/mL of peptidomimetic molecule at which 10% or 50% hemolysis was observed.
[b]Selectivity is calculated based on HC_{50}/the MIC of *S. aureus*.

Furthermore cytotoxicity of lead peptidomimetics (**4g** and **4l**) and their linear analogues (**5b** and **5d**) against HaCaT cells was assessed by using MTT assay. The results of MTT assay showed that tested molecules (**4g**, **4l, 5b, and 5d**) caused decrease in cell viability in a concentration dependent manner (Figure 5.9). However, **5b** and **5d** were found to be comparatively higher toxic toward HaCaT cells.

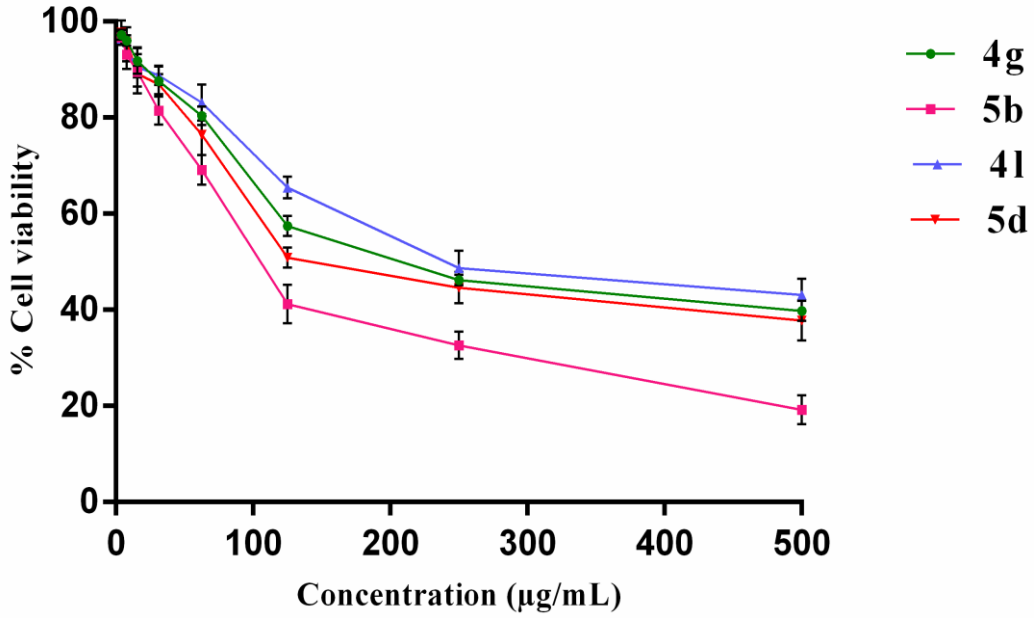

Figure 5.9: Concentration-dependent effect of lead peptidomimetics (**4g** and **4l**) and linear peptides (**5b** and **5d**) on cell viability of HaCaT cells determined by MTT assay. The results represent the data (mean ± SD) obtained from two independent experiments performed in triplicate.

5.2.4. Bactericidal kinetic assay

Bactericidal kinetic study results demonstrated the rapid killing effect of lead peptidomimetics (**4g** and **4l**). Compound **4g** and **4l** at 4 × MIC decrease the burden of both *S. aureus* and *E. coli* from 10^6 CFU/mL to nearly10^3 CFU/mL with in 30 min. The bactericidal kinetic curves of **4g** and **4l** against *S. aureus* and *E. coli* are shown in Figure 5.10A and 5.10B respectively.

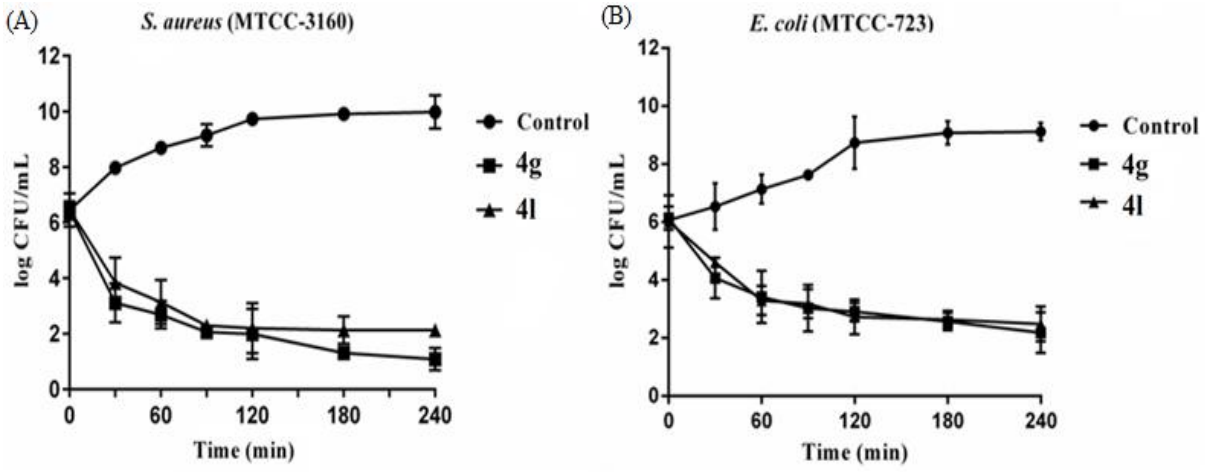

Figure 5.10: Bactericidal kinetics of lead cationic peptidomimetics (**4g** & **4l**) against *S. aureus* (A) and *E. coli* (B). The data obtained are from two independent experiments performed in triplicate

5.2.5. Calcein dye leakage

In order to explore the bactericidal mechanism of the newly designed peptidomimetics, we performed calcein dye leakage experiment by using vesicles of various lipid compositions. When calcein encapsulated bacterial membrane mimic large unilamellar vesicles (LUVs) were treated with most potent molecule **4g** and **4l**, resulting into breakage of the liposomal shell thereby leading to outburst of calcein into the aqueous environment, which was determined by measuring the fluorescence signal intensity on spectrofluorometer. Induced calcein dye leakage was measured at peptidomimetic concentrations of 5, 7.5, 10, 12.5, and 15 µg/mL at different time intervals (Figure 5.11). Fluorescent dye leakage experiment results showed that **4g** induces dye leakage in concentration dependent manner, as 47% of dye was released at highest experimental concentration (15 µg/mL) after approx. 20 min and 19% dye was released at lowest concentration (5 µg/mL) after nearly 50 min. In an analogous manner to **4g**, **4l** also induces dye leakage in dose dependent manner as 23% leakage was observed after 90 min at 5 µg/mL that increased to 48% at concentration of 15 µg/mL after the same time interval (Figure 5.11). While in case of mammalian membrane mimic liposomes negligible amount of dye leakage was observed even at maximum used experimental concentration (15 µg/mL) of both **4g** and **4l**. Therefore, results of dye leakage experiment support the activity results as **4g** exhibits higher MIC values against all tested strains of bacteria in comparison to **4l**. The calcein dye leakage experiment indicated that, the biological activity of these peptidomimetics is dependent on their ability to permeate target membranes, same as that of AMPs.

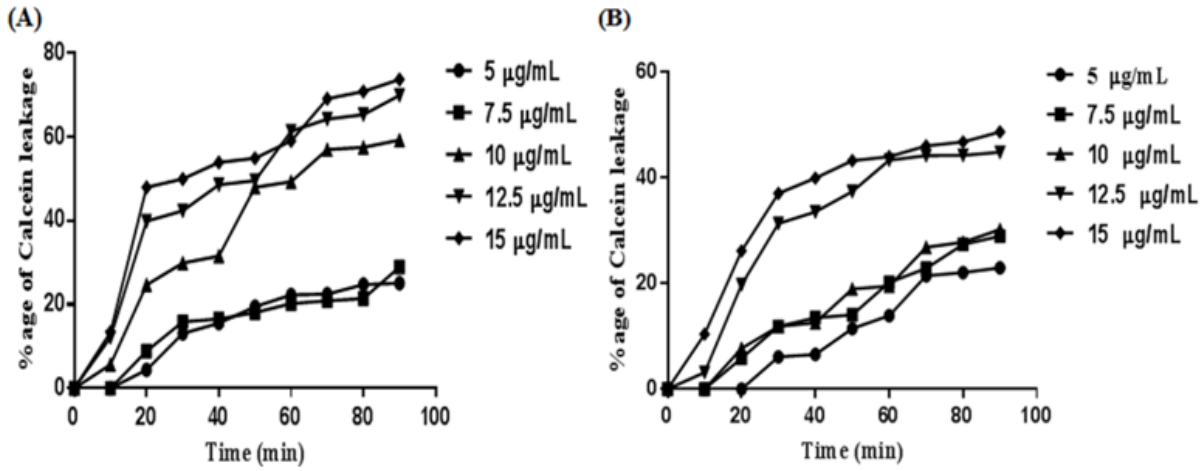

Figure 5.11: Concentration-dependent leakage of calcein dye from negatively charged [DPPC/DPPG (7:3, w/w)] LUVs measured after 5 min of incubation of cationic peptidomimetics **4g** (A) and **4l** (B) at different concentrations with LUVs

5.2.6. Fluorescence microscopy

To further investigate the mechanism involved in antibacterial activity of newly designed peptidomimetics, the ability of two most potent sequences **4g** and **4l** to cause membrane damage was assessed by fluorescence microscopy (Figure 6). The effect of active sequences on both Gram-negative (*E. coli*) and Gram-positive (*S. aureus*) bacteria was studied by a double staining method with DAPI (4',6-diamidino-2-phenylindole) and PI (propidium iodide). In the first step bacterial strains (*E. coli* and *S. aureus*) were incubated with **4g** and **4l** for 2 h after that cells were stained with DAPI, which stains all bacterial cells in blue irrespective of their viability and PI, which penetrates only injured or dead cells with compromised membranes. In control (without initial treatment with peptidomimetics), both *E. coli* and *S. aureus* showed blue fluorescence with DAPI, while negligible number of cells had red fluorescence with PI. On the other hand in case of treated *E. coli* and *S. aureus* cells, stronger red fluorescence was observed with PI (Figure 5.12). Comparatively intense red fluorescence was observed for *S. aureus*, suggesting their significant membrane damage, which fully supports our activity results. These results collectively indicate that compound **4g** and **4I** effectively arrest bacterial growth, via a membrane disruption mechanism similar to most of the native AMPs.

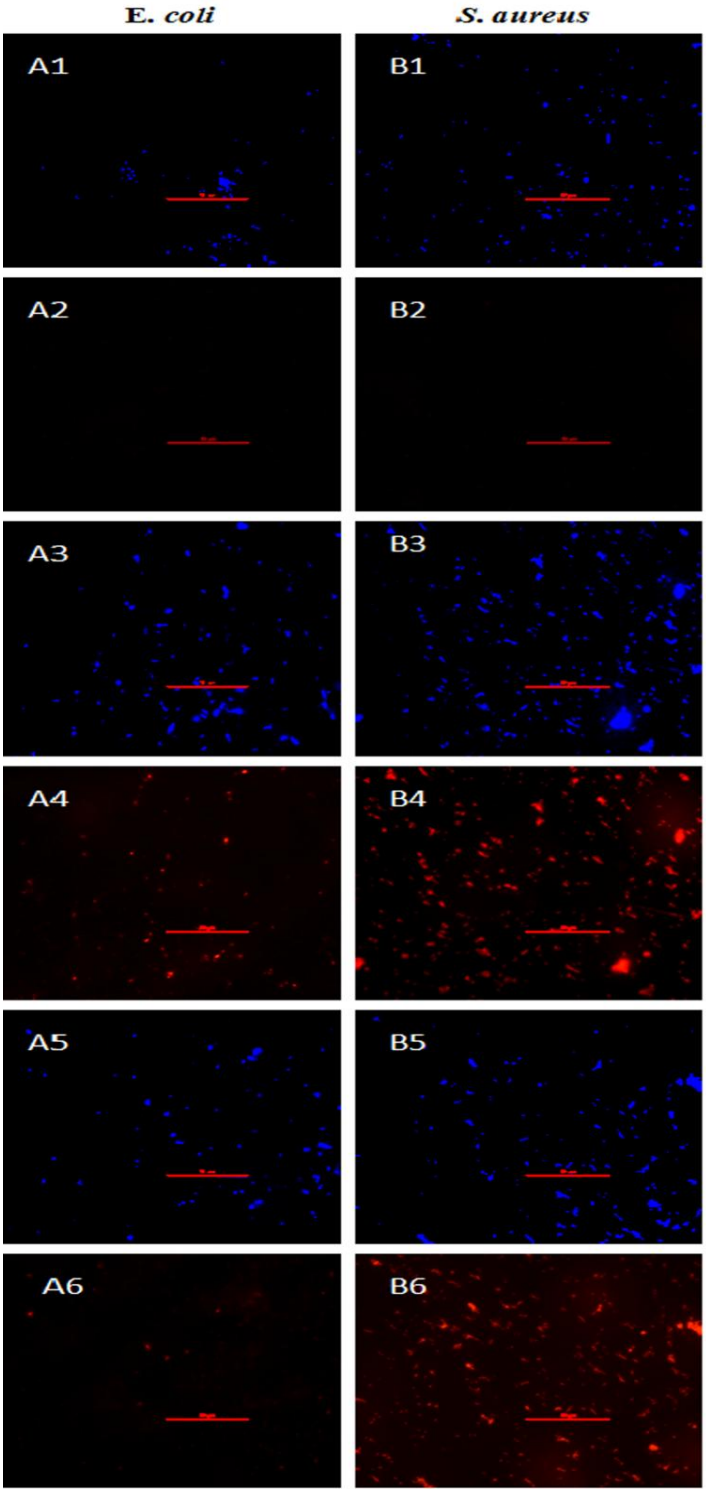

Figure 5.12: Fluorescence micrographs of *E. coli* and *S. aureus* treated with **4g** and **4l** (4 × MIC) for 2 h: (A1-A6) *E. coli*; (A1) control, no treatment, DAPI stained; (A2) control, no treatment, PI stained; (A3) **4g** treatment, DAPI stained; (A4) **4g** treatment, PI stained; (A5) **4l** treatment, DAPI stained; (A6) **4l** treatment, PI stained. (B1-B6) *S. aureus*; (B1) control, no treatment, DAPI stained; (B2) control, no treatment, PI stained; (B3) **4g** treatment, DAPI stained; (B4) **4g** treatment, PI stained; (B5) **4l** treatment, DAPI stained; (B6) **4l** treatment, PI stained

5.2.7. Resistance study

The potential of susceptible pathogenic *S. aureus* as well as MRSA to develop resistance was evaluated by serial passages of the bacterial cultures against representative peptidomimetic sequences (**4g** and **4l**). The new MIC values were determined every 24 h after propagation of bacterial cultures with fresh media and serially diluted concentrations of peptidomimetics (**4g** and **4l**). To make comparative analysis, parallel cultures were exposed to 2-fold dilutions of the antibiotic ciprofloxacin as a positive control. The experiment was repeated for 16 days. Results in figure 5.13 show the low propensity of bacterial pathogens to develop resistance against **4g** and **4l** as there was almost no change in the MIC after 16 passages.

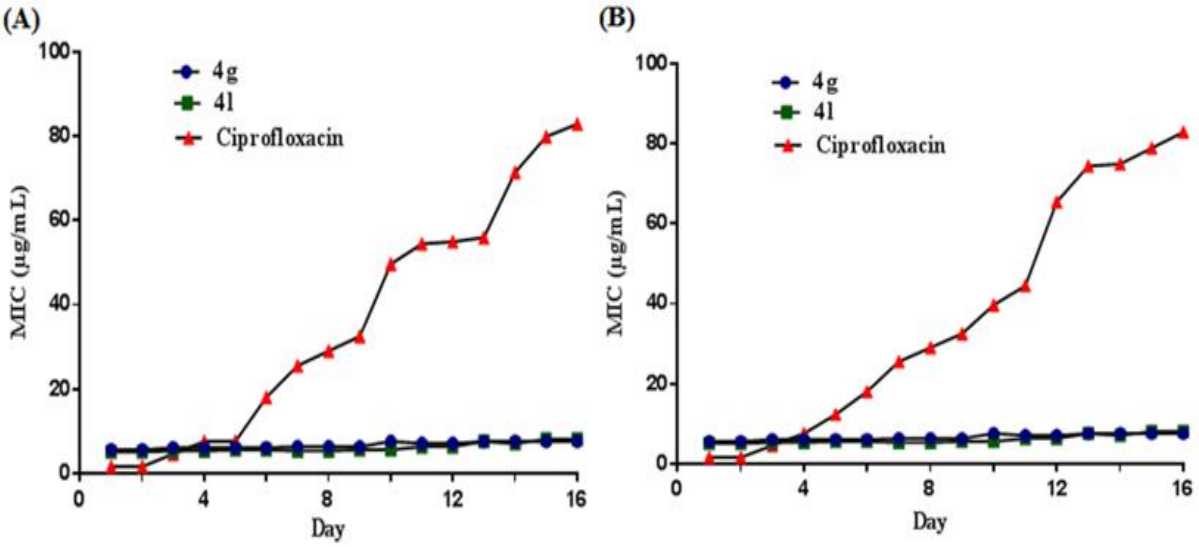

Figure 5.13: Evaluation of resistance development against lead peptidomimetics **4g** and **4l** in bacterial strains (A) *S. aureus* (MTCC 3160) and (B) Methicillin resistant *S. aureus* (MRSA, ATCC BBA-1720)

5.2.8. Proteolytic stability

To assess the proteolytic stability of lead peptidomimetics, we carried out trypsin and α-chymotrypsin digestion assay. **4g** was found stable against trypsin when incubated for 36 h and after that it was slowly degraded with approximately 65% of the peptidomimetic remaining after 4 days (Figure 5.14A). However, linear peptide sequence (**5b**) showed higher susceptibility towards trypsin as only 21% of the peptide remaining after 4 days. Noticeably, a negligible amount of tryptic degradation was observed for **4l**. In addition, linear peptide **5d** was also showed good stability with nearly 82% of the parent peptide remaining after 4 days. Peptidomimetics **4g** and **4l** were seemingly completely stable against proteolytic degradation by α-chymotrypsin for 24 h, and after that slow degradation was observed with nearly 70% of the peptidomimetics were still intact after 4 days (Figure 5.14B). On the other hand, linear

peptides (**5b** and **5d**) were gradually degraded when incubated with α-chymotrypsin and only 44% of the intact peptides remaining after 4 days.

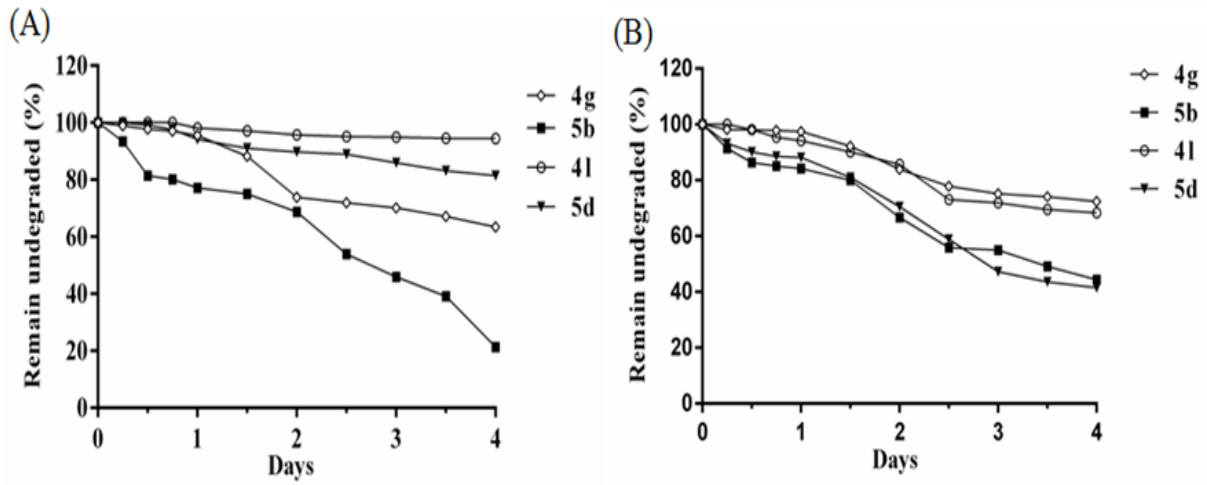

Figure 5.14: In vitro proteolytic digestion assay of lead peptidomimetics (**4g** and **4l**) and linear peptides (**5b** and **5d**) against trypsin (A) and α-chymotrypsin (B). Percentage of the remaining test sample was measured using analytical RP-HPLC

5.2.9. Plasma stability study

To further ensure the stability of lead peptidomimetics **4g** and **4l**, we conducted their stability study in human blood plasma. **4g** was not degraded when incubated in plasma for 1 h and minute degradation (6.58%) was observed after 2 h incubation in plasma. It was interesting to note that further degradation of **4g** did not take place even after 24 h incubation in plasma as no extra peak was observed (Figure 5.15). On the other hand, no sign of degradation was detected for **4l** even after 24 h incubation in plasma (Figure 5.15).

To determine the effectiveness of our novel synthetic approach regarding proteolytic stability we also carried out the plasma stability study of linear peptides (**5b** and **5d**). Minute degradation (5.31%) of **5b** was detected after 30 min incubation and it was further increased (11.79%) when incubated for 1 h in plasma. No more enzymatic degradation of **5b** was takes place when incubated in plasma for 12 h and 18% of **5b** was degraded when incubated in plasma for 24 h (Figure 5.15). Small amount of enzymatic degradation (4.72%) was detected for **5d** after 30 min incubation in plasma and it was no more degraded when incubated in plasma for 24 h (Figure 5.15).

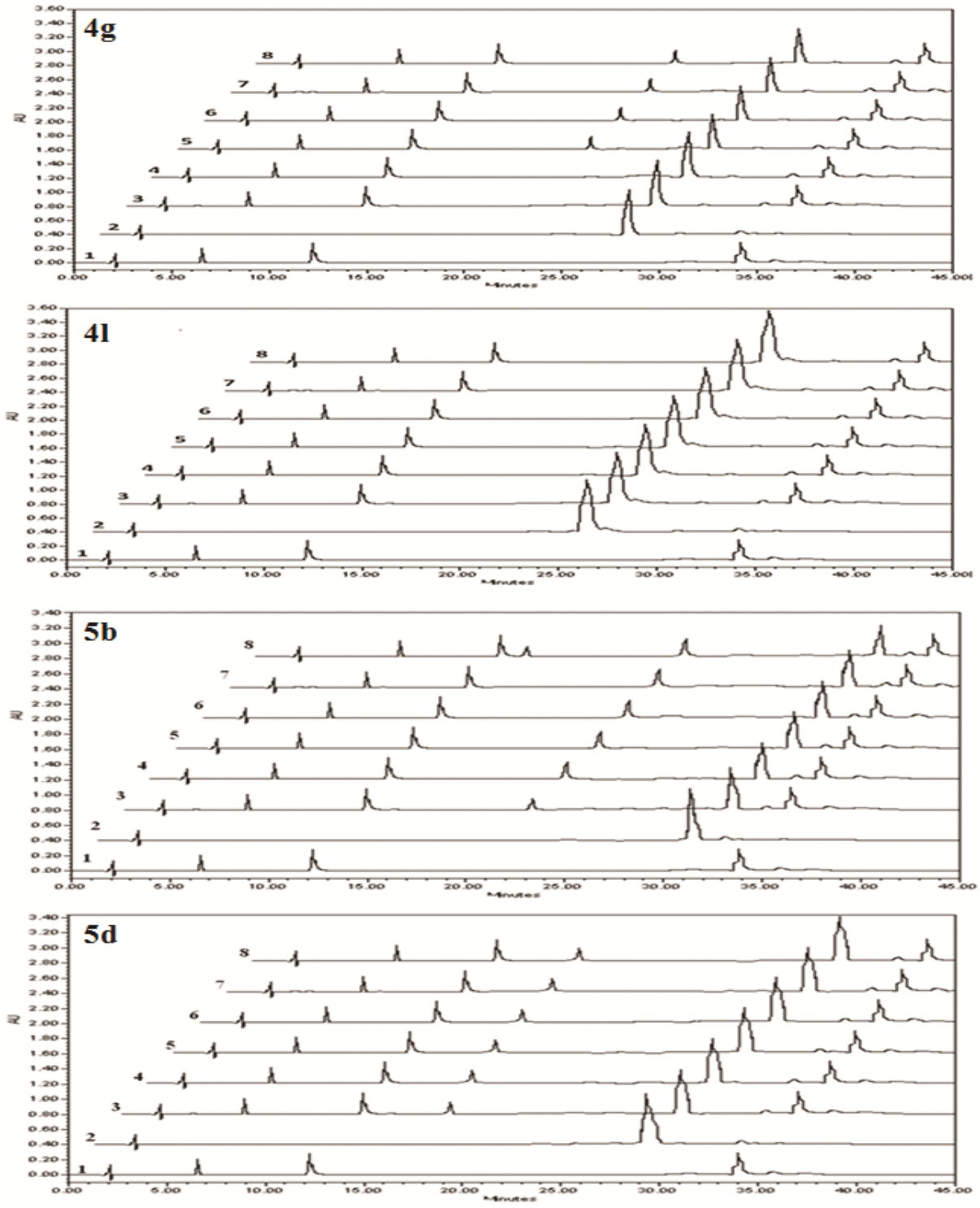

Figure 5.15: Plasma stability study of lead peptidomimetics (**4g** and **4l**) and linear peptide sequences (**5b** a **5d**). Human blood Plasma in buffer (chromatogram 1); test sample in buffer (chromatogram 2); test sample incubated with blood plasma for 30 minutes (chromatogram 3); test sample incubated with blood plasma for 1 h. (chromatogram 4); test sample incubated with blood plasma for 2 h. (chromatogram 5); test sample incubated with blood plasma for 6 h. (chromatogram 6); test sample incubated with blood plasma for12 h. (chromatogram 7); test sample incubated with blood plasma for 24 h. (chromatogram 8). The chromatograms have been offset by one minute relative to one another along the horizontal axis so that peaks can be observed

CHAPTER 6.
DISCUSSION

6.1. Short lipopeptides

Most of the naturally occurring lipopeptides are having a complex structural framework [75], which might be responsible for their non-cell selectivity. Consequently, we designed a library of short cationic lipopeptides. Structurally, these short lipopeptides partially mimic alkylated ammonium salts (native metabolites); which are toxic to all type of cells [81]. On the contrary, lipopeptides reported here possess broad-spectrum of antimicrobial activity against drug resistant clinical isolates with no hemolytic effects. Importantly, in contrast to most of the native lipopeptides which are active either against bacteria or fungi alone, number of short lipopeptides synthesized here are highly potent against both bacteria and fungi. Numerous studies showed that threshold of charge and hydrophobicity of the peptidic chain is crucial for the biological function of AMPs [96-98]. Accordingly, we systematically investigated the effect of both charge and hydrophobic bulk on lytic activity of short lipopeptides and explored the minimum requirement of cationic charge and lipophilic bulk among this novel class of anti-infectives.

Lipopeptide molecules with minimum three Orn residues (LP13-LP18) showed significant antimicrobial activity. This facilitated the use of MIC values of these lipopeptides against bacterial (*S. aureus* and *E. coli*) and fungal strain (*C. albicans*) to determine the effect of length of aliphatic tail on lytic activity. Analyzing the antimicrobial activity of six lipopeptides with hydrophobic tail varying from 8 to 18 carbon atoms showed that bulky hydrophobic tail improved the activity against both bacteria and fungi, as it was evident by decrease in MIC values with increase in aliphatic chain length (Figure 6.1). This indicates that lipophilicity of the alkyl tail is highly important for interaction with microbial membranes. Lipopeptide bearing N-terminus myristic acid aliphatic tail (LP16) was found to be most potent against tested bacterial strains and there was no further enhancement in antibacterial activity with increase in hydrophobic bulk (LP17 and LP18). In accordance with the earlier findings, lipopeptides with bulky hydrophobic tail (LP17 and LP18) exhibited better antifungal activity in contrast to their low hydrophobic counterparts (LP13-LP15). Lipopeptides with comparatively small aliphatic tail (LP13-LP15) showed no lytic effect against both bacteria and fungi, probably due to the low hydrophobicity, which lead to less

optimal hydrophobic interaction towards microbial membrane (Figure 6.1). However, with the increase in the length of aliphatic tail, the ability of lipopeptides to discriminate between fungal and mammalian cell membrane was compromised to some extent, as it was evident by observing maximum hemolysis and low percentage of human keratinocytes (HaCaT cells) viability for stearic acid conjugated lipopeptides (LP18, LP24, and LP30). Thus, it seems that, the increased hydrophobic bulk of lipopeptides drives them toward zwitterionic membranes, which mimic the membrane of fungi and mammalian cells.

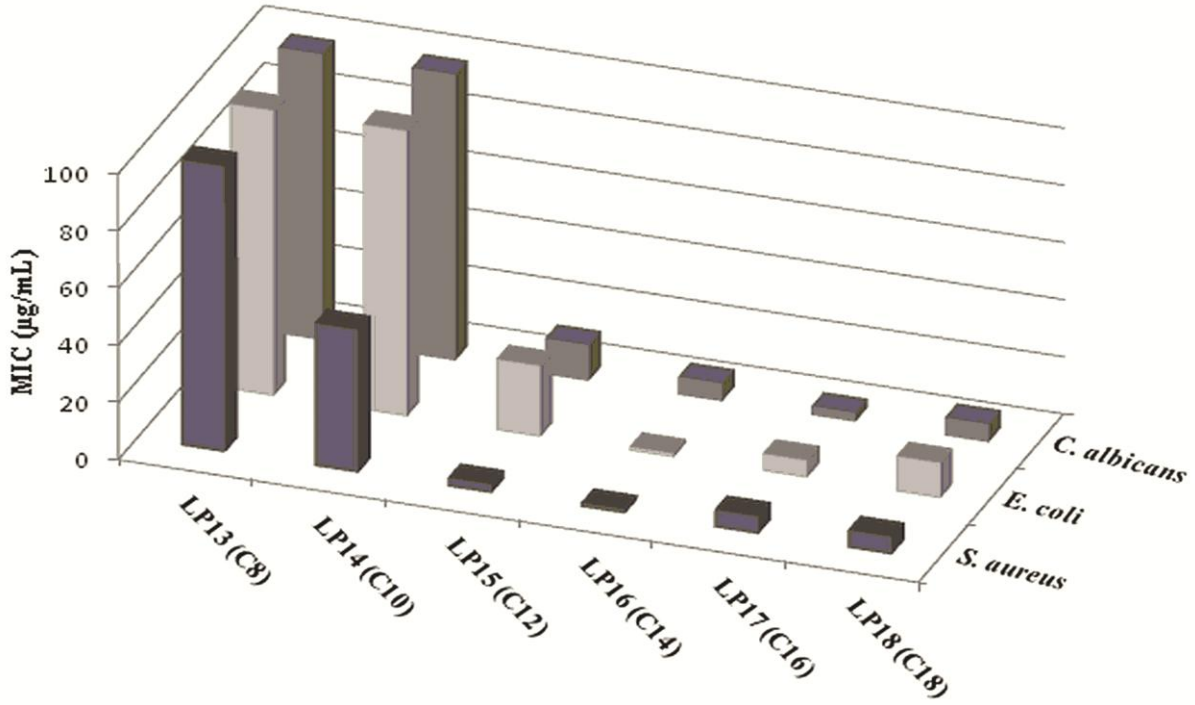

Figure 6.1: Effect of aliphatic chain length of short cationic lipopeptides on antimicrobial activity

The effect of cationic charge content on antimicrobial activity was assessed by comparing the MIC values of lipopeptides with cationic charge residues (Ornithine) ranging from1 to 5 units and a common myristic acid tail (LP04, LP10, LP16, LP22, and LP28) against bacterial (*S. aureus* and *E. coli*) and fungal strains (*C. albicans*). Closer examination of the activity results showed that lipopeptide with single Orn residue (LP04) was inactive against complete panel of tested microbial strains, while incorporation of one more cationic charge residue resulted into lipopeptide (LP10) with moderate antimicrobial activity. Lipopeptide with three Orn residues (LP16) exhibited maximum antimicrobial activity and further increment in cationic charge content of lipopeptide molecules (LP22 and LP28) did not improve antimicrobial activity (Figure 6.2). Based on these outcomes, we concluded that three cationic charge residues are sufficient for lytic activity of lipopeptide molecules.

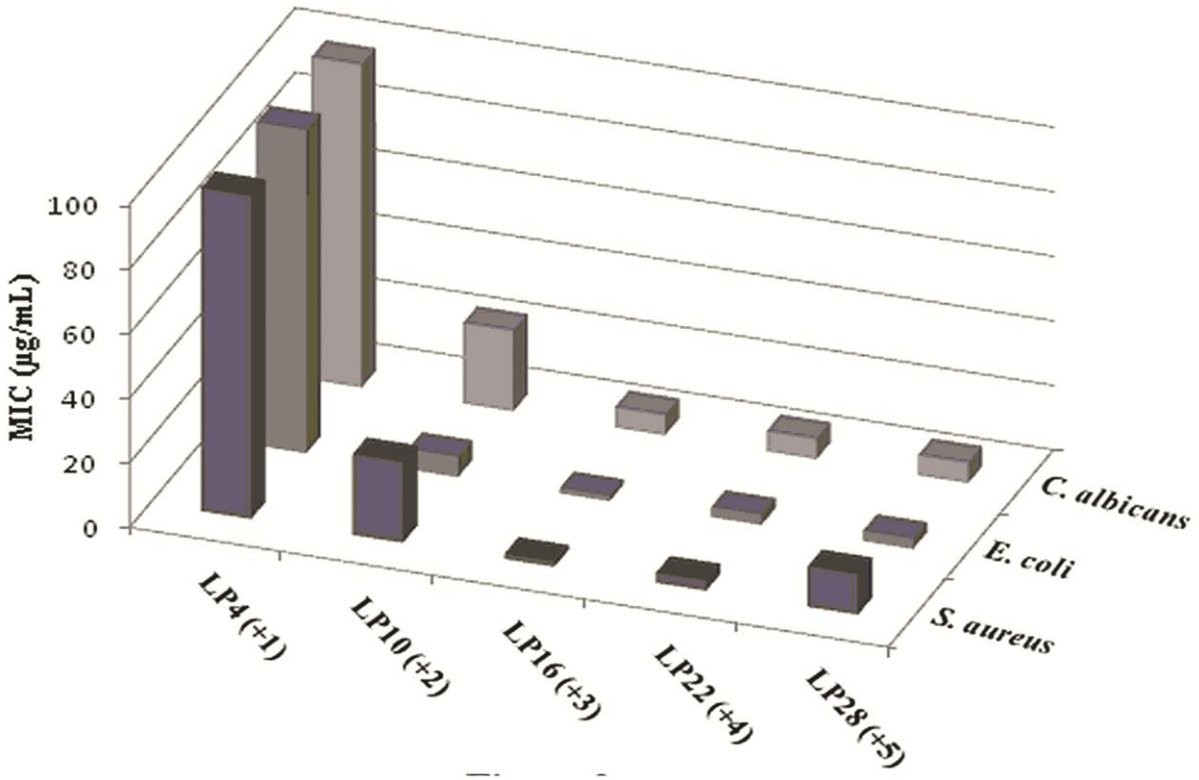

Figure 6.2: Effect of cationic charge of short cationic lipopeptides on antimicrobial activity

Proteolytic degradation is one of the biggest hurdles in the development of peptide based therapeutics. With aim to provide enzymatic stability in intended bioenvironment, we synthesized lipopeptide molecules by incorporating non-proteogenic cationic amino acid ornithine. It is well documented that trypsin cleaves α-peptides adjacent to positively charged residues (lysine or arginine) [132]. Thus, the high stability of LP16 against tryptic degradation and in human blood plasma might be due to the presence of ornithine.

Mechanistically, these evolutionary lipidated peptide templates have been shown to exert their antimicrobial action via inhibiting the biosynthesis of cell wall components [133] or by membrane lysis [134]. In order to get insight into the membrane interaction behaviour of short lipopeptides, calcein dye leakage experiments were carried out using bacterial and fungal membrane mimicking liposome system (LUVs). Calcein is a water soluble relatively large molecule and its release from LUVs is assumed to involve the formation of pores and/or disruption of the surface of LUVs. In accordance to the antibacterial activity results LP16 caused the maximum release of calcein dye from bacterial membrane mimicking LUVs. In case of fungal membrane mimicking LUVs, lipopeptide LP24 induced the release of encapsulated fluorescent dye at lower concentration level whereas for moderately active lipopeptide LP22, a higher concentration threshold was required to induce dye leakage. Thus,

in agreement with earlier literature as well as our activity and selectivity results these outcomes are indicative of the comparatively higher affinity of bulky aliphatic tail conjugated lipopeptide (LP24) toward zwitterionic fungal membrane. Usually, pathogens are unable to develop resistance against membrane active agents. On similar lines, even drug resistant pathogens were not able to develop resistance against LP16, which highlight the clinical applicability of short lipopeptides as novel anti-infective agents. Collectively, this study paves the way to develop a new class of structurally small cationic antimicrobial lipopeptides which are active against wide range of clinically relevant strains.

6.2. Small cationic peptidomimetics

The inherent properties of AMPs (responsible for antimicrobial action), coupled to their poor *in vivo* activity, led to the search for synthetic mimics of AMPs that would improve anti-infective properties while potentially eliminating the problems associated with druggability of native antimicrobial peptide templates. Earlier, number of research groups have designed synthetic mimics of naturally occurring AMPs and explore their potential as future antibiotics [96,108]. In an attempt to find the pharmacophore of short antimicrobial peptidomimetics, we have synthesized a new series of small cationic peptidomimetics by incorporating 3-ABA as peptidomimetic element. Strom *et al.* have previously documented that a specific content of both cationic charge and lipophilic bulk is required to design potent synthetic mimics of AMPs [96]. Accordingly, we undertook the synthesis of peptidomimetic molecules by varying number as well as sequence of both cationic and hydrophobic residues. The first series of peptidomimetic molecules was synthesized by using arginine (Arg) and tryptophan (Trp) to represent the properties of cationic charge and hydrophobic bulk respectively. We preferred arginine (Arg) over lysine because it behaves like charged moiety under all physiological conditions and also guanidine group would exhibits higher electrostatic interaction with the negatively charged phospholipids of bacterial cell membrane [96,123]. The selection of Trp was based on the presumption that the indole nucleus would be inserted into the membrane with the hydrophobic part interacting with the hydrophobic portion of the bilayer and the amine function interacting more closely with the polar head-groups of the membrane [135].

The activity results showed that peptidomimetic molecules were in general more potent against *S. aureus* and their resistant strains (MRSA and MRSE) than other bacterial strains (*B. subtilis*, *E. coli*, and *P. aeruginosa*) used in the study. These outcomes point out

their anti-staphylococcal behaviour which is in agreement with previous reports [96,108]. The activity results revealed a strong correlation between antibacterial potency and overall structural amphipathicity of peptidomimetics. This can be illustrated by observing highest antibacterial activity in case of **4g** and **4l** which are having amphipathic structure. 3D view of the structural framework of lead peptidomimetics (**4g** and **4l)** and linear peptides (**5b** and **5d**) is shown in Figure 6.3. This structure-activity relationship was further confirmed by observing bacterial killing effect of **3e**, the only penta peptidomimetic having amphipathic structural framework. The presence of hydrophobic structural motif composed of 3-ABA flanked by Trp residues is another common structural feature of active peptidomimetic molecules (**4f, 4g, 4k,** and **4l**; Figure 6.4). Wessolswski *et al.* have already reported that small Arg-Trp rich AMPs with three adjacent aromatic residues display high bactericidal action [136]. In this way this could be another reason for the efficient antibacterial potency of newly designed peptidomimetics.

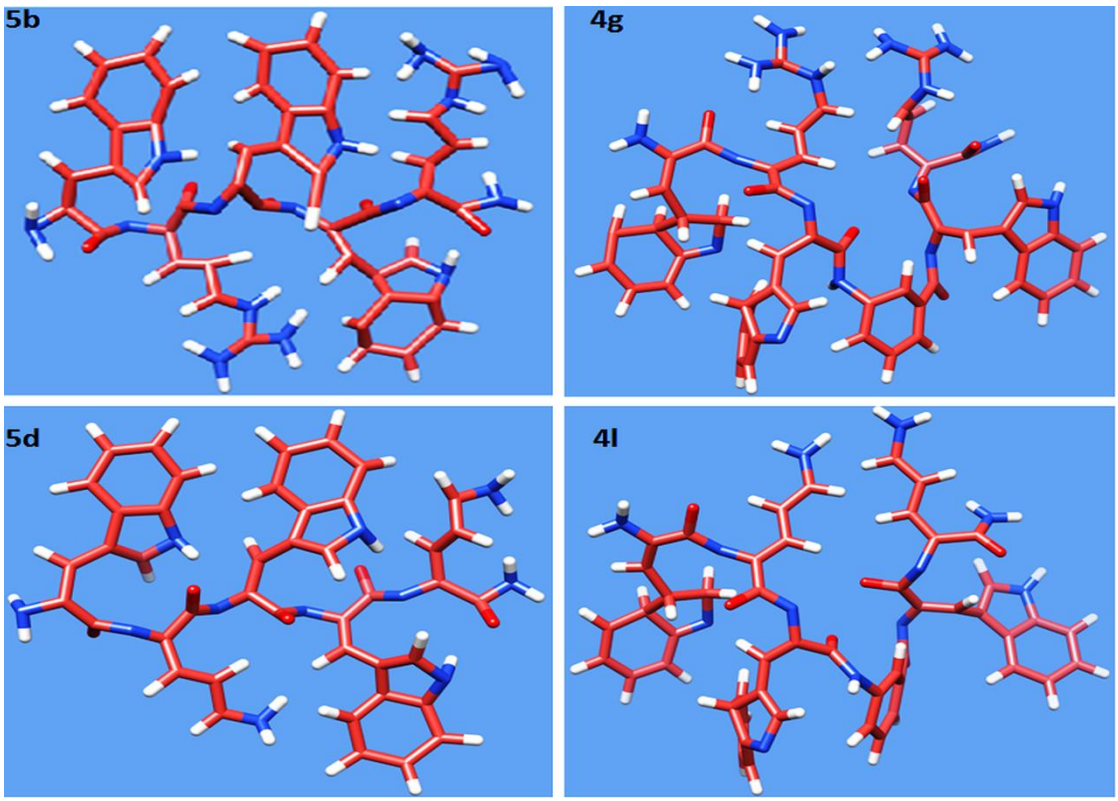

Figure 6.3: 3D structural view of the lowest energy conformers of lead peptidomimetics (**4g** and **4l**) and linear peptides (**5b** and **5d**). Structural optimization experiments were conducted by using UCSF CHIMERA version 1.4

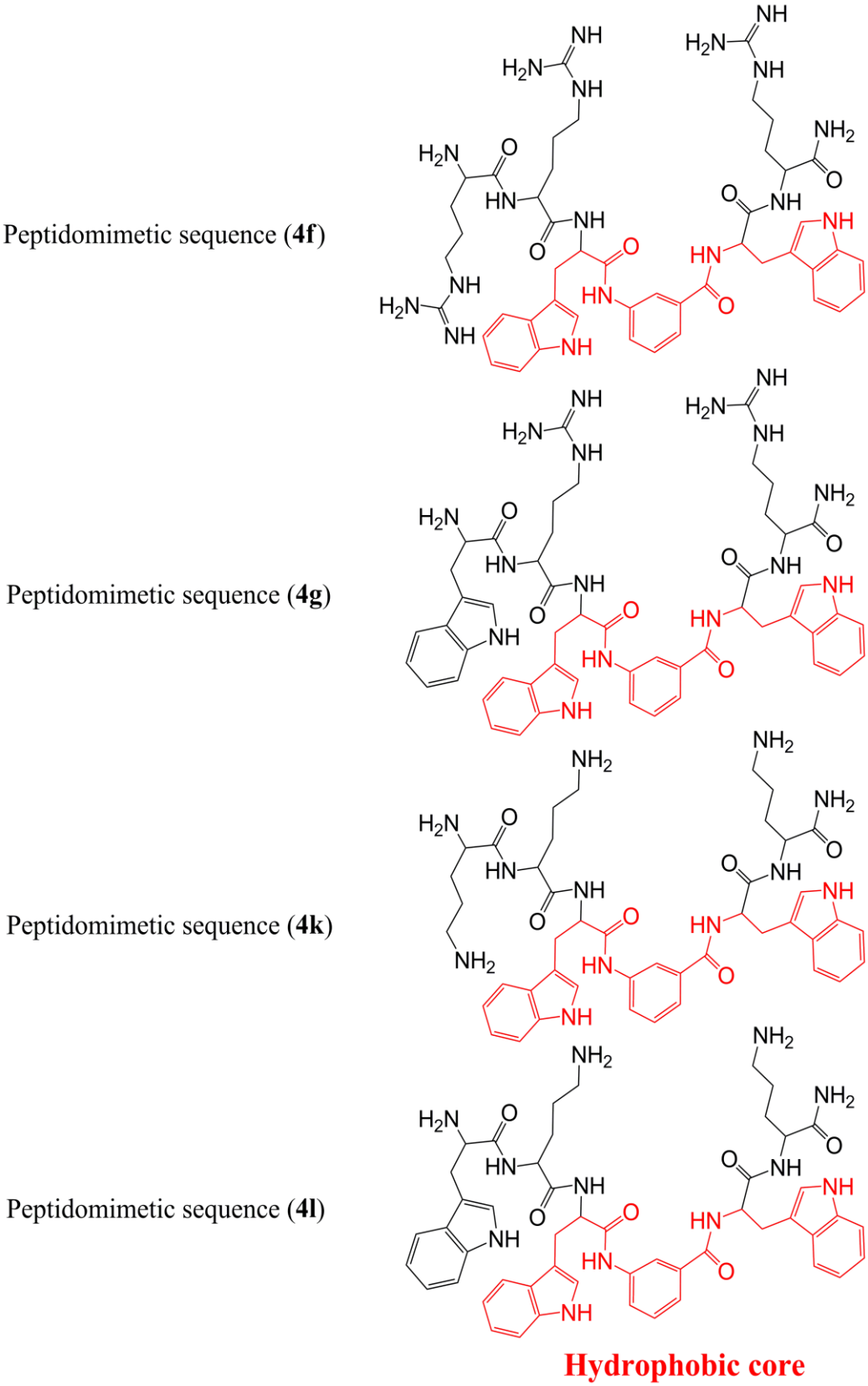

Figure 6.4: Chemical structure of active peptidomimetic sequences (**4f**, **4g, 4k,** and **4l**) having a hydrophobic core as common structural feature

The presence of both naturally occurring amino acid residues (Arg and Trp) in peptidomimetic sequences could render them substrates for proteolytic enzymes. The results from the stability study on lead peptidomimetic **4g** and linear peptide **5b** were rather striking. **4g** showed low susceptibility toward proteolytic degradation as compared to **5b**. The high stability of **4g** might be due to the presence of 3-ABA as it is the only structural difference between both test molecules.

Further synthesis of cationic peptidomimetics was carried out by replacing Arg with cationic non-genetically coded amino acid Orn (**3f** and **4h-4l**) among initially synthesized peptidomimetic sequences which show some antibacterial potential (**3e** and **4c-4g**). This structural modification would be able to improve the proteolytic stability of peptidomimetic molecules in intended bioenvironment as Orn is not a well known substrate for proteolytic enzymes. Activity results of peptidomimetics **3f**, **4h-4l** showed that there is no significant loss of antibacterial potency besides lead peptidomimetic **4l** was found to be stable against proteolytic degradation. Although, the linear peptide (**5d**) was degraded when incubated with proteolytic enzymes and human blood plasma. Consequently, we concluded that in addition to the replacement of Arg with Orn, backbone modification by incorporation of 3-ABA also could renders **4l** immune against proteolytic degradation. Finally, to determine whether the indole nucleus of Trp is responsible for activity, compounds **4m**, **4n**, **4o** and **4p** were synthesized by replacing Trp with phenylalanine (Phe) in compounds **4f, 4g, 4k** and **4l**. Activity results showed that replacement of tryptophan with phenylalanine was not fruitful as peptidomimetics **4m**, **4n**, **4o** and **4p** were inactive against all screened bacterial strains.

To determine the effectiveness of this novel structural framework of small cationic peptidomimetics, linear analogues (**5a-5d**) of most potent peptidomimetics (**4f, 4g**, **4k** and **4l**) were also synthesized. Surprisingly, peptidomimetics **4f** and **4g** synthesized by incorporating 3-ABA displayed 3-4 fold of improvements in activity against *S. aureus*, MRSA, and MRSE in comparison to their linear analogues **5a** and **5b**. In similar fashion, peptidomimetics having Orn as cationic residue (**4k** and **4l**) required nearly 8-10 fold of less concentration in comparison to their linear analogues (**5c** and **5d**) to completely eradicate the growth of *S. aureus*, MRSA, and MRSE. Therefore, the results demonstrated that this novel design principle may facilitates the development of new potent antibacterial peptidomimetics as well as in some cases may also boost up the activity profile of already designed small peptidomimetic molecules.

We performed hemolytic assay by quantifying 50% (HC_{50}) as well as 10% hemolysis (HC_{10}) against hRBCs as a measurement of toxicity. In general, lengthy peptidomimetic derivatives (**4a-4p**) were found more hemolytic than smaller peptidomimetic derivatives (**1a**, **2a-2c**, and **3a-3f**). Thus, it seems that, as the hydrophobic bulk of peptidomimetic derivatives increases, their ability to discriminate between anionic bacterial surface and zwitterionic mammalian membrane decreases. These outcomes were in accordance with Kondejewski *et al*., who explored the correlation between hydrophobicity and hemolytic activity [137]. Moreover, our novel structural model was found to be effective in terms of selectivity also as the lead peptidomimetics with 3-ABA scaffold (**4f**, **4g**, **4k**, and **4l**) displayed low hemolytic activity as compared to peptide sequences without 3-ABA (**5a-5d**). The MTT assay results further confirmed the comparatively lower cytotoxic behaviour of lead peptidomimetics (**4g** and **4l**) towards mammalian cells.

In comparison to the conventional antibiotics, AMPs are having fast bacterial killing kinetics [106,138]. To determine whether this ability is also inherent to newly designed peptidomimetics reported here, the viability of exponentially growing *S. aureus* and *E. coli* was checked against most potent peptidomimetics (**4g** and **4l**) by time-kill assay. Kinetic study results demonstrated the rapid bactericidal effect since **4g** and **4l** at 4 × MIC killed most of the bacterial cells of both *S. aureus* and *E. coli* within 30 min. The rapid bactericidal effect is usually observed among most of the membrane active AMPs. Thus, rapid bacterial killing effect of lead peptidomimetics (**4g** and **4l**) suggest that their antibacterial action might be mediated through permeabilization of the bacterial membrane.

Membrane disruption is generally considered as the plausible mode of action for most of the naturally occurring AMPs and synthetically designed small cationic antimicrobial peptidomimetics [139-141]. In order to assess membrane interaction behaviour of the designed peptidomimetics, we performed calcein dye leakage experiment by designing negatively charged and zwitterionic calcein encapsulated liposomes which mimics the outer surface of bacterial and mammalian cell membranes respectively. When lead peptidomimetics (**4g** and **4l**) were treated with negatively charged vesicles, we observed a sharp increase in fluorescent intensity due to the efflux of calcein dye from liposome system. In this way, we conclude that association of lead peptidomimetics with bacterial membrane mimic liposomes renders them calcein permeable due to destabilization of the vesicle bilayer. Therefore, results of calcein dye leakage experiment show the membranolytic action of lead peptidomimetics. This is not the case when peptidomimetics were treated with zwitterionic liposome system

which indicated the low affinity of peptidomimetic molecules toward mammalian cells. The membrane disruption effect of **4g** and **4l** was further confirmed by fluorescence microscopy. In fluorescent micrographs intense DAPI as well as PI staining was observed in case of both *E. coli* and *S. aureus* after treatment with **4g** and **4l**. On the other hand, untreated bacterial cells stain with DAPI but not with PI. The results further demonstrated the membrane leakage effect of lead peptidomimetics.

The efficacy of conventionally used antibiotics in treating infections caused by drug resistant pathogens has been diminished as a result of pathogens ability to switch on to an alternate metabolic pathway. It has already been reported that low propensity of resistance development was observed in case of therapeutics that kill bacteria by targeting call membrane [139,71]. Therefore, we have determined the potential of susceptible pathogenic *S. aureus* as well as MRSA, a clinically relevant drug resistant bacteria pathogen, to develop drug resistance against most potent sequences **4g** and **4l**. The insignificant increase in MIC values of **4g** and **4l** indicating the inability of both, susceptible as well as methicillin resistant, *S. aureus* to develop resistance against them. Thus, the lead obtained from present study could be optimized for therapeutic use against drug resistant bacterial strains.

CHAPTER 7.
CONCLUSION AND OUTLOOK

7.1. Conclusion

Research work depicted in this thesis deals with the structure based designing, synthesis and antimicrobial evaluation of short lipopeptides and small cationic peptidomimetics. We successfully designed and synthesized a library of 30 short lipopeptide molecules (LP01-LP30) by incorporating non-proteogenic amino acid residue ornithine. Most of the synthesized lipopeptides showed potent, broad-spectrum activity against fungi and a series of Gram-positive and Gram-negative bacteria, including resistant clinical isolates. In particular, LP16 exhibit maximum activity against most of the tested bacterial strains with MICs in the range of 1.5-6.25 μg/mL. LP24 was found to be most effective against fungal strains with MIC ≤ 6.25 μg/mL. Structure activity relationship (SAR) study of short lipopeptides suggested that, 3 ornithine residues and 14 carbon atoms long aliphatic tail (myristic acid) is the minimum structural requirement for antimicrobial activity. All synthesized lipopeptides demonstrated excellent safety profile against hRBCs (HC_{50} > 250 μg/mL). Plasma stability study and trypsin digestion assay results revealed the high proteolytic stability of lead molecule (LP16). Presence of non-proteogenic amino acid ornithine could be the reason for the proteolytic stability. Moreover, pathogens (susceptible as well as resistant) were not able to elicit resistance against LP16 even after 16 repeated exposures. The biophysical (calcein dye leakage assay) and microscopic (SEM & TEM) evidences demonstrated the predominant membranolytic action of lead molecules.

We also designed and synthesized a library of 26 small cationic peptidomimetics (**1a**, **2a**-**2c**, **3a**-**3e**, **4a**-**4p**) by incorporating 3-ABA as peptidomimetic element. Antibacterial activity results point out the predominant anti-staphylococcal action of the peptidomimetic molecules. Two peptidomimetic molecules (**4g** and **4l**) displayed maximum activity against *S. aureus*, MRSA, and MRSE with MICs in the range of 5-6.25 μg/mL. Notably, our novel structural model has resulted in the identification of potent antibacterial peptidomimetics that exhibit higher activity as compared to peptide sequences without 3-ABA (**5a**-**5d**). Newly designed peptidomimetic templates were found to be selective toward bacteria relative to eukaryotic red blood cells. *In vitro* stability study results of lead peptidomimetics (**4g** and **4l)** and linear peptide sequences (**5b** and **5d**) collectively demonstrated that the incorporation of

ornithine as well as 3-ABA could render the peptide sequences immune against proteolytic enzymes. Resistance development study revealed the low propensity of pathogens to develop resistance against our most potent peptidomimetic molecules (**4g** and **4l**). Based on the outcomes of calcein dye leakage and fluorescent microscopy experiments we propose that lead peptidomimetics (**4g** and **4l)** are more prone to membrane damage mode of action.

7.2. Outlook

From our research work, lipopeptides LP16 and LP24 were found to be most promising antibacterial and antifungal agents, respectively. In addition to that lead peptidomimetics (**4g** and **4l**) were also showed excellent therapeutic properties like proteolytic stability, low propensity of resistance development, and membrane disruption action. The antimicrobial potential of representative peptidomimetic molecules can be improved by applying different synthetic approaches like N- and C-terminal capping and incorporation of unusual amino acid derivatives. Besides, incorporation of constrained γ-amino acid residue (3-ABA) as a turn motif among the linear peptidomimetic sequences like β-peptides and peptoids may result into the improvement of therapeutic potential.

In particular, the small molecular size (Mol. Wt. = 740.53) of lead lipopeptides as compared to native lipo-antibiotics *viz.* polymyxin B (Mol. Wt. = 1553.46) as well as the presence of non genetically coded amino acid residue (ornithine) not only contribute to biological activity but may also contribute to improved pharmacokinetics. Furthermore, stability of LP16 in human blood plasma reflects its biocompatibility. Hence, further studies to assess *in vivo* antimicrobial potential can be an encouraging step toward the development of short lipopeptides as next generation antibiotics.

CHAPTER 8.
REFERENCES

1. Hancock R.E., *"The end of an era?"*, Nat. Rev. Drug. Discov., vol. 6, pp. 28, Jan. 2007.

2. Mullard A., *"2011 FDA drug approvals"*, Nat. Rev. Drug Discov., vol. 11, pp. 91-94, 2012.

3. Keller M., Blench M., Tolentino H., Freifeld C.C., Mandl K.D., Mawudeku A., Eysenbach G., Brownstein J.S., *"Use of unstructured event-based reports for global infectious disease surveillance"*, Emerg. Infect. Dis., vol. 15, pp. 689-695, May 2009.

4. Arias C.A., Murray B.E., *"Antibiotic-resistant bugs in the 21st century-a clinical super-challenge"*, N. Engl. J. Med., vol. 360, pp. 439-443, Jan. 2009.

5. Livermore D.M., *"Has the era of untreatable infections arrived?"* J. Antimicrob. Chemother., vol. 64, pp. i29-i36, Sep. 2009.

6. Klevens R.M., Morrison M.A., Nadle J., Petit S., Gershman K., Ray S., Harrison L.H., Lynfield R., Dumyati G., Townes J.M., Craig A.S., Zell E.R., Fosheim G.E., McDougal L.K., Carey R.B., Fridkin S.K., *"Invasive methicillin-resistant Staphylococcus aureus infections in the United States"*, JAMA., vol. 298, pp. 1763-1771, Oct. 2007.

7. de Oliveira J.M., Lisboa Lde B., *"Hospital-acquired infections due to gram-negative bacteria"*, N. Engl. J. Med., vol. 363, pp. 1482-3, Oct. 2010.

8. Falagas M.E**.,** Bliziotis I.A**,** Kasiakou S.K**,** Samonis G**,** Athanassopoulou P, Michalopoulos A., *"Outcome of infections due to pandrug-resistant (PDR) Gram-negative bacteria"*, BMC Infect. Dis., vol. 5, pp. 24, April 2005.

9. Wilson J., Elgohari S., Livermore D.M., Cookson B., Johnson A., Lamagni T., Chronias A., Sheridan E., *"Trends among pathogens reported as causing bacteraemia in England, 2004-2008"* Clin. Microbiol. Infect., vol. 17, pp. 451-458, 2010.

10. Kumarasamy K.K., Toleman M.A., Walsh T.R., Bagaria J., Butt F., Balakrishnan R., Chaudhary U., Doumith M., Giske C.G., Irfan S., Krishnan P., Kumar A.V., Maharjan Sunil, Mushtaq S., Noorie T., Paterson D.L., Pearson A., Perry C., Pike R., Rao B., Ray U., Sarma J.B., Sharma M., Sheridan E., Thirunarayan M.A., Turton J., Upadhyay S., Warner M., Welfare W., Livermore D.M, Woodford N., *"Emergence of a new antibiotic resistance mechanism in India, Pakistan, and the UK: a molecular, biological, and epidemiological study"*, Lancet Infect. Dis., vol. 10, pp. 597-602, 2010.

11. Bajwa S.J., Kulshrestha A. *"Fungal infections in intensive care unit: challenges in diagnosis and management"*, Ann. Med. Health Sci. Res., vol. 3, pp. 238-44, Apr. 2013.

12. Marukutira T, Huprikar S, Azie N, Quan S., Meier-Kriesche H., Horn D.L., *"Clinical characteristics and outcomes in 303 HIV-infected patients with invasive fungal infections: data from the Prospective Antifungal Therapy Alliance registry, a multicenter, observational study"*, HIV AIDS (Auckl), vol. 6**,** pp. 39-47, 2014.

13. Mikolajewska A, Schwartz S, Ruhnke M., *"Antifungal treatment strategies in patients with haematological diseases or cancer: from prophylaxis to empirical, pre-emptive and targeted therapy"*, Mycoses, vol. 55 pp. 2-16, Jan. 2012.

14. Schieffelin J.S., Garcia-Diaz J.B., Loss G.E., Beckman E.N., Keller R.A., Staffeld-Coit C., Garces J.C., Pankey G.A., *"Phaeohyphomycosis fungal infections in solid organ transplant recipients: clinical presentation, pathology, and treatment"* Transpl. Infect. Dis., vol. 16, pp. 270-278, Apr. 2014.

15. Petrikkos G, Skiada A., *"Recent advances in antifungal chemotherapy"* Int. J. Antimicrob. Agents, vol. 30, pp. 108-117, Aug. 2007.

16. Sundriyal S, Sharma RK, Jain R. *"Current advances in antifungal targets and drug development"*, Curr. Med. Chem., vol. 13: pp. 1321-35, 2006.

17. Loeffler J., Stevens D.A., *"Antifungal drug resistance"* Clin. Infect. Dis. Vol. 15, pp. 36 (Suppl 1): S31-41, Jan. 2003.

18. Albericio F., Kruger H.G., *"Therapeutic peptides"* Future Med. Chem., vol. 4, pp. 1527-1531, Aug. 2012.

19. Corey G.R., Stryjewski M.E., Weyenberg W., Yasothan U., Kirkpatrick P., *"Telavancin"*, Nat. Rev. Drug Discovery, vol. 8, pp. 929-930, Dec. 2009.

20. Boucher H.W., Talbot G.H., Bradley J.S., Edwards J.E., Gilbert D., Rice L.B., Scheld M., Spellberg B., Bartlett J., *"Bad Bugs, no drugs: No ESKAPE! An Update from the Infectious Diseases Society of America"* Clin. Infect. Dis., vol. 48, pp. 1-12, Jan. 2009.

21. Peet N.P., *"Drug resistance: a growing problem"*, Drug Discov. Today, vol. 15, pp. 583-586, 2010.

22. Collier R., *"Drug development cost estimates hard to swallow"* CMAJ, vol. 180, pp. 279-280, 2009.

23. Toke O., *"Antimicrobial peptides: New candidates in the fight against bacterial infections"*, Biopolymers, vol. 80, pp. 717-735, 2005.

24. Jenssen H., Hamill P., Hancock R.E., *"Peptide antimicrobial agents"* Clin. Microbiol. Rev., vol. 19, pp. 491-511, Jul. 2006.

25. Zasloff M., *"Antimicrobial peptides of multicellular organisms"* Nature, vol. 415, pp. 389-395, Jan. 2002.

26. Brogden K.A., Ackermann M., McCray P.B., Tack B.F., *"Antimicrobial peptides in animals and their role in host defences"*, Int. J. Antimicrob. Agents, vol. 22, pp. 465-478, Nov. 2003.

27. Yeung A.T., Gellatly S.L., Hancock R.E., *"Multifunctional cationic host defence peptides and their clinical applications"*, Cell Mol. Life Sci., vol. 68, pp. 2161-2176, 2011.

28. Cederlund A., Gudmundsson G.H., Agerberth B., *"Antimicrobial peptides important in innate immunity"*, FEBS J., vol. 278, pp. 3942-3951, Oct. 2011.

29. Selsted M.E., Ouellette A.J., *"Mammalian defensins in the antimicrobial immune response"*, Nat. Immunol., vol. 6, pp. 551-557, Jun. 2005.

30. Hancock, R.E.W., *"Cationic peptides: effectors in innate immunity and novel antimicrobials"*, Lancet Infect. Dis., vol. 1, pp. 156-164, Oct. 2001.

31. Mookherjee N., Hancock R.E., *"Cationic host defence peptides: innate immune regulatory peptides as a novel approach for treating infections"* Cell. Mol. Life Sci., vol. 64, pp. 922-933, Apr. 2007.

32. Schroder J.M., *"Epithelial peptide antibiotics"*, Biochem. Pharmacol., vol. 57, pp. 121-134, Jan. 1999.

33. Bowdish D.M., Davidson D.J., Hancock R.E., *"Immunomodulatory properties of defensins and cathelicidins"* Curr. Top Microbiol. Immunol., vol. 306, pp. 27-66, 2006.

34. Hancock R.E., Lehrer R., *"Cationic peptides: a new source of antibiotics"*, Trends Biotechnol., vol. 16, pp. 82-88, Feb. 1998.

35. Giuliani A., Pirri G., Nicoletto S.F., *"Antimicrobial peptides: an overview of a promising class of therapeutics"*, Cent. Eur. J. Biol., vol. 2, pp. 1-33, 2007.

36. Giangaspero A., Sandri L., Tossi A., *"Amphipathic α helical antimicrobial peptides"*, Eur. J. Biochem., vol. 268, pp. 5589-5600, 2001.

37. Lai R., Liu H., Lee W.H., Zhang Y., *"An anionic antimicrobial peptide from toad Bombina maxima"*, Biochem. Biophys. Res. Comm., vol. 295, pp. 796-799, Jul. 2002.

38. Yeaman M.R., Yount N.Y., *"Mechanisms of antimicrobial peptide action and resistance"*, Pharmacol. Rev., vol. 55, pp. 27-55, 2003.

39. Matsuzaki K., *"Why and how are peptide-lipid interactions utilized for self-defense? Magainins and tachyplesins as archetypes"*, *Biochim. Biophys. Acta*, vol. 1462, pp. 1-10, Dec. 1999.

40. Brodgen K.A., *"Antimicrobial peptides: pore formers or metabolic inhibitors in bacteria?"*, Nat. Rev. Microbiol., vol. 3, pp. 238-250, Mar. 2005.

41. Yang L., Mishra A., Purdy K., Som A., Tew G.N., Wong G.C.L., *"Synthetic antimicrobial oligomers induce a composition-dependent topological transition in membranes"*, J. Am. Chem. Soc., vol. 129, pp. 12141-12147, 2007.

42. Wimley W., Hristova K., *"Antimicrobial peptides: successes, challenges and unanswered questions"*, J. Membr. Biol., vol. 239, pp. 27-34, 2011.

43. Stromstedt A.A., Ringstad L., Schmidtchen A., Malmsten M., *"Interaction between amphiphilic peptides and phospholipid membranes"*, Curr. Opin. Colloid Interface Sci., vol. 15, pp. 467-478, 2010.

44. Shai Y., Oren Z., *"From "carpet" mechanism to de-novo designed diastereomeric cell-selective antimicrobial peptides"*, Peptides, vol. 22, pp. 1629-1641, 2001.

45. Sanderson J.M., *"Peptide-lipids interactions: insights and perspectives"*, Org. Biomol. Chem., vol. 3, pp. 201-212, 2005.

46. Sitaram N., Nagaraj R., *"Interaction of antimicrobial peptides with biological and model membranes: structural and charge requirements for activity"*, Biochim. Biophys. Acta, vol. 1462, pp. 29-54, Dec. 1999.

47. Sanderson J.M., *"Peptide-lipids interactions: insights and perspectives"*, Org. Biomol. Chem., vol.3, pp. 201-212, 2005.

48. Pouny Y., Rapaport D., Mor A., Nicolas P., Shai Y., *"Interaction of antimicrobial dermaseptin and its fluorescently labeled analogues with phospholipid membranes"* Biochemistry, vol. 31, pp. 12416-12423, 1992.

49. Ghosh J.K., Shaool D., Guillaud P., Ciceron L., Mazier D., Kustanovich I., Shai Y., Mor A., *"Selective cytotoxicity of dermaseptin S3 toward intraerythrocytic Plasmodium falciparum and the underlying molecular basis"*, J. Biol. Chem.**,** vol. 272, pp. 31609-31616, 1997.

50. Gazit E., Boman A., Boman H.G., Shai Y., *"Interaction of the mammalian antibacterial peptide cecropin P1 with phospholipid vesicles"*, Biochemistry, vol. 34, pp. 11479-11488, 1995.

51. Oren Z., Lerman J.C., Gudmundsson G.H., Agerberth B., Shai Y., *"Structure and organization of the human antimicrobial peptide LL-37 in phospholipid membranes: relevance to the molecular basis for its non-cell-selective activity"*, Biochem. J. vol. 341, pp. 501-513, 1999.

52. Ehrenstein G., Lecar H., *"Electrically gated ionic channels in lipid bilayers"* Q. Rev. Biophys. Vol. 10, pp. 1-34, 1977.

53. Mangoni M.L., *"Host-defense peptides: from biology to therapeutic strategies"*, Cell. Mol. Life Sci., vol. 68, pp. 2157-2159, 2011.

54. Ludtke S.J., He K., Heller W.T., Harroun T.A., Yang L., Huang H.W., *"Membrane pores induced by magainin"*, Biochemistry, vol. 35, pp. 13723-13728, 1996.

55. Matsuzaki K., Murase O., Fujii N., Miyajima M., *An antimicrobial peptide, magainin 2, induced rapid flip-flop of phospholipids coupled with pore formation and peptide translocation"*, Biochemistry, vol. 35, pp. 11361-11368, 1996.

56. Heller W.T., Waring A.J., Lehrer R.I., Huang H.W., *"Multiple states of betasheet peptide protegrin in lipid bilayers"*, Biochemistry, vol. 37, pp. 17331-17338, 1998.

57. Yang L., Harroun T.A., Weiss T.M., Ding L., Huang H.W., "Barrel-stave model or toroidal model? A case study on melittin pores", Biophys. J., vol. 81, pp. 1475-1485, 2001.

58. Park C.B., Kim H.S., Kim S.C., "Mechanism of action of the antimicrobial peptide buforin II: buforin II kills microorganisms by penetrating the cell membrane and inhibiting cellular functions", Biochem. Biophys. Res. Commun. vol. 244, pp. 253-257, 1998.

59. Xiong Y.Q., Bayer A.S., Yeaman M.R., "Inhibition of intracellular macromolecular synthesis in *Staphylococcus aureus* by thrombin-induced platelet microbicidal proteins", J. Infect. Dis., vol. 186, pp. 668-677, 2002.

60. Kragol G., Lovas S., Varadi G., Condie B.A., Hoffmann R., Otvos L., *"The antibacterial peptide pyrrhocoricin inhibits the ATPase actions of DnaK and prevents chaperone-assisted protein folding"*, Biochem., vol. 40, pp. 3016-3026, 2001.

61. Subbalakshmi C., Sitaram N., *"Mechanism of antimicrobial action of indolicidin"*, FEMS Microbiol. Lett., vol. 160, pp. 91-96, 1998.

62. Carlsson A., Engstrom P., Palva E.T., Bennich H., *"Attacin, an antibacterial protein from Hyalophora cecropia, inhibits synthesis of outer membrane proteins in*

Escherichia coli by interfering with omp gene transcription", Infect. Immun., vol. 59, pp. 3040-3045, 1991.

63. Oh J.T., Cajal Y., Skowronska E.M., Belkin S., Chen J., Van Dyk T.K., Sasse M., Jain M.K., *"Cationic peptide antimicrobials induce selective transcription of micF and osmY in Escherichia coli "*, Biochim. Biophys. Acta, vol. 1463, pp. 43-54, Jan. 2000.

64. Yount N.Y., Bayer A.S., Xiong Y.Q., Yeaman M.R., "Advances in antimicrobial peptide immunobiology", Biopolymers, vol. 84, pp 435-458, 2006.

65. Gunn J.S., Tamayo D., Portillo A.C., "*Mechanism of bacterial resistance to antimicrobial peptides*", In D.A. Devine and Hancock R.E.W., ed.; Cambridge university press NY, 2004.

66. Nizet V., "*Antimicrobial peptide resistance mechanisms of human bacterial pathogens*" Curr. Issues Mol. Biol., vol. 8, pp 11-26. Jan. 2006.

67. Giacometti A., Cirioni O., Barchiesi F., Scalise G., *"In-vitro activity and killing effect of polycationic peptides on methicillin-resistant Staphylococcus aureus and interactions with clinically used antibiotics"*, Diagn. Microbiol. Infect. Dis., vol. 38, pp. 115-118, 2000.

68. Ganz T., *"Defensins and host defense"*, Science, vol. 286, pp. 420-421, 1999.

69. Gallo R.L., Ono M., Povsic T., Page C., Eriksson E., Klagsbrun M., Bernfield M., *"Syndecans, cell surface heparan sulfate proteoglycans, are induced by a proline-rich antimicrobial peptide from wounds"*, Proc. Natl. Acad. Sci. U.S.A., vol. 91(23), pp. 11035-11039, Nov. 1994.

70. Mor A., *"Peptide-based antibiotics: A potential answer to raging antimicrobial resistance"*, Drug Dev. Res., vol. 50, pp. 440-447, 2000.

71. Perron G.G., Zasloff M., Bell G., "Experimental evolution of resistance to an antimicrobial peptide", Proc. Biol. Sci., vol. 273, pp. 251-256, 2006.

72. Haynie S.L., Crum G.A., Doele B.A., *"Antimicrobial activities of amphiphilic peptides covalently bonded to a water-insoluble resin"*, Antimicrob. Agents Chemother., vol. 39, pp. 301-307, 1995.

73. Balkovec J.M., *"Lipopeptide antifungal agents"*, Expert Opin. Invest. Drugs., vol. 3, pp. 65-82, 1994.

74. De Lucca A.J., Walsh T.J., "Antifungal peptides: novel therapeutic compounds against emerging pathogens", Antimicrob. Agents Chemother., vol. 43, pp. 1-11, 1999.

75. Raaijmakers J.M., De Bruijn I., De Kock M.J., *"Cyclic lipopeptide production by plant-associated Pseudomonas spp.: diversity, activity, biosynthesis, and regulation"*, Mol. Plant Microbe. Interact., vol. 19, 699-710, 2006.

76. Straus S.K., Hancock R.E., *"Mode of action of the new antibiotic for Gram-positive pathogens daptomycin: comparison with cationic antimicrobial peptides and lipopeptides"*, Biochim. Biophys. Acta, vol. 1758, pp. 1215-1223, Sep. 2006.

77. Jung D., Rozek A., Okon M., Hancock R.E., *"Structural transitions as determinants of the action of the calcium-dependent antibiotic daptomycine"*, Chem. Biol., vol. 11, pp. 949-957, Jul. 2004.

78. Epand R.M., *"Biophysical studies of lipopeptide-membrane interactions"*, Biopolymers, vol. 43, pp. 15-24, 1997.

79. Toniolo C., Crisma M., Formaggio F., Peggion C., Epand R.F., Epand R.M., *"Lipopeptaibols, a novel family of membrane active, antimicrobial peptides"*, Cell. Mol. Life Sci., vol. 58, pp. 1179-1188, Aug. 2001.

80. Avrahami D., Shai Y., *"Bestowing antifungal and antibacterial activities by lipophilic acid conjugation to D,L-amino acid-containing antimicrobial peptides: a plausible mode of action"*, Biochemistry, vol. 42, pp. 14946-14956, Dec. 2003.

81. Makovitzki A., Avrahami D., Shai Y., *"Ultrashort antibacterial and antifungal lipopeptides"*, Proc. Natl. Acad. Sci. U.S.A., vol. 103, pp. 15997-16002, Oct. 2006.

82. Thevissen K., Terras F.R., Broekaert W.F., *"Permeabilization of fungal membranes by plant defensins inhibits fungal growth"*, Appl. Environ. Microbiol., vol. 65, pp. 5451-5458, Dec. 1999.

83. Hobden C., Teevan C., Jones L., O'Shea P., *"Hydrophobic properties of the cell surface of Candida albicans: a role in aggregation"*, Microbiology, vol. 141 (Part 8), pp. 1875-1881, Aug. 1995.

84. Ahlstrom B., Chelminska-Bertilsson M., Thompson R.A., Edebo L., *"Submicellar complexes may initiate the fungicidal effects of cationic amphiphilic compounds on Candida albicans"*, Antimicrob. Agents Chemother., vol. 41, pp. 544-550, Mar. 1997.

85. Straus S.K, Hancock R.E., *"Mode of action of the new antibiotic for Gram-positive pathogens daptomycin: Comparison with cationic antimicrobial peptides and lipopeptides"*, Biochim. Biophys. Acta, vol. 1758, pp. 1215-23, Sep. 2006.

86. Makovitzki A., Baram J., Shai Y., *"Antimicrobial lipopolypeptides composed of palmitoyl di- and tricationic peptides: in vitro and in vivo activities, self-assembly to*

nanostructures, and a plausible mode of action", Biochemistry, vol. 47, pp. 10630-10636, Oct. 2008.

87. Letscher-Bru V., Herbrecht R., *"Caspofungin: the first representative of a new antifungal class"*, J. Antimicrob. Chemother., vol. 51, pp. 513-521, Mar. 2003.

88. Giuliani A., Pirri G., Bozzi A., Di Giulio A., Aschi M., Rinaldi A.C., "Antimicrobial peptides: natural templates for synthetic membrane-active compounds", Cell. Mol. Life Sci., vol. 65, pp. 2450-2460, Aug. 2008.

89. Shalev D.E., Rotems S., Fish A., Mor A., *"Consequences of N-acylation on structure and membrane binding properties of dermaseptin derivative K4–S4-(1–13)"*, J. Biol. Chem., vol. 281, pp. 9432-9438, Apr. 2006.

90. Avrahami D., Shai Y., *"Conjugation of a magainin analogue with lipophilic acids controls hydrophobicity, solution assembly, and cell selectivity"*, Biochemistry, vol. 41, pp. 2254-2263, Feb. 2002.

91. Malina A., Shai Y., *"Conjugation of fatty acids with different lengths modulates the antibacterial and antifungal activity of a cationic biologically inactive peptide"*, Biochem. J., vol. 390, pp. 695-702, Sep. 2005.

92. Arnusch C.J., Ulm H., Josten M., Shadkchan Y., Osherov N., Sahl H.G., Shai Y., *"Ultrashort peptide bioconjugates are exclusively antifungal agents and synergize with cyclodextrin and amphotericin B"*, Antimicrob. Agents Chemother., vol. 56, pp. 1-9, Jan. 2012.

93. Arnusch C.J., Albada H.B., Van Vaardegem M., Liskamp R.M.J., Sahl H.G., Shadkchan Y., Osherov N., Shai Y., *"Trivalent ultrashort lipopeptides are potent pH dependent antifungal agents"*, J. Med. Chem., vol. 55, pp. 1296-1302, Feb. 2012.

94. Laverty G., McLaughlin M., Shaw C., Gorman S.P., Gilmore B.F., *"Antimicrobial activity of short, synthetic cationic lipopeptides"*, Chem. Biol. Drug Des., vol. 75, pp. 563-569, Jun. 2010.

95. Haug B.E., Stensen W., Stiberg T., Svendsen J.S., *"Bulky nonproteinogenic amino acids permit the design of very small and effective cationic antibacterial peptides"*, J. Med. Chem., vol. 47, pp. 4159-4162, Aug. 2004.

96. Strøm M.B., Haug B.E., Skar M.L., Stensen W., Stiberg T., Svendsen J.S., *"The pharmacophore of short cationic antibacterial peptides"*, J. Med. Chem., vol. 46, pp. 1567-1570, Apr. 2003.

97. Tomita M., Takase M., Bellamy W., Shimamura S., *"A review: The active peptide of lactoferrin"*, Acta Paediatr. Jpn., vol. 36, pp. 585-591, Oct. 1994.

98. Rekdal Ø., Andersen J., Vorland L.H., Svendsen J.S., *"Construction and synthesis of lactoferricin derivatives with enhanced antibacterial activity"*, J. Peptide Sci., vol. 5, pp. 32-45, 1999.

99. Haug B.E., Svendsen J.S., *"The role of tryptophan in the antibacterial activity of a 15-residue bovine lactoferricin peptide"*, J. Peptide Sci., vol. 7, pp. 190-196, Apr. 2001.

100. Strøm M.B., Rekdal Ø., Svendsen J.S., *"Antibacterial activity of 15-residues lactoferricin derivatives"*, J. Peptide Res., vol. 56, pp. 265-274, Nov. 2000.

101. Bikshapathy E., Sitaram N., Nagaraj R., *"Effect of introducing p-fluorophenylalanine and multiple tryptophan residues in a 13-residue antibacterial peptide"*, Protein Pep. Lett., vol. 6, pp. 67-71, 1999.

102. Wu M., Hancock R.E.W., *"Improved derivatives of bactenecin, a cyclic dodecameric antimicrobial cationic peptide"*, Antimicrob. Agents Chemother., vol. 43, pp. 1274-1276, May 1999.

103. Lawyer C., Pai S., Watabe M., Borgia P., Mashimo T., Eagleton L., Watabe K., *"Antimicrobial activity of a 13 amino acid tryptophan-rich peptide derived from a putative porcine precursor protein of a novel family of antibacterial peptides"*, FEBS Lett., vol. 390, pp. 95-98, Jul. 1996.

104. Selsted M.E., Novotny M.J., Morris W.L., Tang Y.Q., Smith W., Cullor J.S., *"Indolicidin, a novel bactericidal tridecapeptide amide from neutrophils"*, J. Biol. Chem., vol. 267, pp. 4292-4295, Mar. 1992.

105. Schiffer M., Chang C.H., Stevens F.J., *"The functions of tryptophan residues in membrane proteins"*, Protein Eng., vol. 5, pp. 213-214, Apr.1992.

106. Findlaya B., Zhanelb G.G., Schweizer F., *"Cationic amphiphiles: A new generation of antimicrobials inspired by the natural antimicrobial peptide scaffold"*, Antimicrob. Agents Chemother., vol. 54, pp. 4049-4058, Oct. 2010.

107. Fjell C.D., Jenssen H., Hilpert K., Cheung W.A., Pante N., Hancock R.E., Cherkasov A., *"Identification of novel antibacterial peptides by chemoinformatics and machine learning*", J. Med. Chem., vol. 52, pp. 2006-2015, Apr. 2009.

108. Haug B.E., Stensen W., Kalaaji M., Rekdal Y., Svendsen J.S., *"Synthetic antimicrobial peptidomimetics with therapeutic potential"*, J. Med. Chem., vol. 51, pp. 4306-4314, Jul. 2008.

109. Gime´nez D., Andreu C., Olmo M.D., Varea T., Diaz D., Asensio G., *"The introduction of fluorine atoms or trifluoromethyl groups in short cationic peptides enhances their antimicrobial activity"*, Bioorg. Med. Chem., vol. 14, pp. 6971-6978, Oct. 2006.

110. Sharma R.K., Reddy R.P., Tegge W., Jain R., *"Discovery of Trp-His and His-Arg analogues as new structural classes of short antimicrobial peptides"*, J. Med. Chem., vol. 52, pp. 7421-7431, Dec. 2009.

111. Svenson J., Stensen W., Brandsdal B.O., Haug B.E., Monrad J., Svendsen J.S., *"Antimicrobial peptides with stability toward tryptic degradation"*, Biochemistry, vol. 47, pp. 3777-3788, Mar. 2008.

112. Karstad R., Isaksen G., Brandsdal B.O., Svendsen J.S., Svenson J., *"Unnatural amino acid side chains as S1, S1', and S2' probes yield cationic antimicrobial peptides with stability toward chymotryptic degradation"*, J. Med. Chem., vol. 53, pp. 5558-5566, Aug. 2010.

113. Isaksson J., Brandsdal B.O., Engqvist M., Flaten G.E., Svendsen J.S.M., Stensen W.A., *"Synthetic antimicrobial peptidomimetic (LTX 109): stereochemical impact on membrane disruption"*, J. Med. Chem., vol. 54, pp. 5786-5795, Aug. 2011.

114. Bisht G.S., Rawat D.S., Kumar A., Kumar R., Pasha S., *"Antimicrobial activity of rationally designed amino terminal modified peptides"*, Bioorg. Med. Chem. Lett., vol. 17, pp. 4343-4346, Aug. 2007.

115. Srinivasulu G., Ramana Rao M.H.V., Kiran Kumar S., Kunwar A.C., *"β-Hairpin peptides containing 3-amino benzoic acid, a constrained γ-amino acid"*, Arkivoc, pp. 69-86, 2004.

116. Ramana Rao M.H.V., Kiran Kumar S., Kunwar A.C., *"Formation of β-hairpins in L-Pro-Gly containing peptides facilitated by 3-amino benzoic acid"*, Tetrahedron Lett., vol. 44, pp. 7369-7372, 2003.

117. Lundya F.T., Nelson J., Lockhart D., Greer B., Harriott P., Marley J.J., *"Antimicrobial activity of truncated α-defensin (human neutrophil peptide (HNP)-1) analogues without disulphide bridges"*, Mol. Immunol., vol. 45, pp. 190-193, Jan. 2008.

118. Lengyel G.A., Eddinger G.A., Horne W.S., *"Introduction of cyclically constrained γ-residues stabilizes an α-peptide hairpin in aqueous solution"*, Org. Lett., vol. 15, pp. 944-947, Feb. 2013.

119. Merrifield R.B., *"Solid phase synthesis"*, Science vol. 232, pp. 341-347, Apr. 1986.

120. Wikler M.A., Low D.E., Cockerill F.R., Sheehan D.J., Craig W.A., Tenover F.C., Dudley M.N., *"Methods for dilution antimicrobial susceptibility tests for bacteria that grow aerobically: approved standard-seventh edition"*, CLSI (formerly NCCLS), M7-A7, 2006.

121. Clinical and Laboratory Standards Institute, *"Reference method for broth dilution antifungal susceptibility testing of filamentous fungi"*, Approved standard 2nd ed., M38-A2; Clinical and Laboratory Standards Institute: Wayne, PA, 2008.

122. Clinical and Laboratory Standards Institute, *"Reference method for broth dilution antifungal susceptibility testing of yeasts"*, Approved standard M27-A3; Clinical and Laboratory Standards Institute: Wayne, PA, 2008.

123. Hansen T., Alst T., Havelkova M., Strøm M.B., *"Antimicrobial activity of small β-peptidomimetics based on the pharmacophore model of short cationic antimicrobial peptides"*, J. Med. Chem., vol. 53, pp. 595-606, Jan. 2010.

124. Denizot F., Lang R., *"Rapid colorimetric assay for cell growth and survival. Modifications to the tetrazolium dye procedure giving improved sensitivity and reliability"*, J. Immunol. Methods, vol. 89, pp. 271-277, May 1986.

125. Zhang L., Rozek A., Hancock R.E.W., *"Interaction of cationic antimicrobial peptides with model membranes"*, J. Biol. Chem., vol. 276, pp. 35714-35722, Sep. 2001.

126. Joshi S., Bisht G.S., Rawat D.S., Kumar A., Kumar R., Maiti S., Pasha S., *"Interaction studies of novel cell selective antimicrobial peptides with model membranes and E. coli ATCC 11775"*, Biochim. Biophys. Acta, vol. 1798, pp. 1864-1875, Oct. 2010.

127. Niu Y., Padhee S., Wu H., Bai G., Harrington L., Burda W.N., Shaw L.N., Cao C., Cai J., *"Identification of gamma-Aapeptides with potent and broad-spectrum antimicrobial activity"*, Chem. Commun. (Cambridge, U. K.), vol. 47, pp. 12197-12199, Nov. 2011.

128. Habets M.G., Brockhurst M.A., *"Therapeutic antimicrobial peptides may compromise natural immunity"*, Biol. Lett., vol. 8, pp. 416-418, Jun. 2012.

129. Jerala R., *"Synthetic lipopeptides: a novel class of anti-infectives"*, Expert Opin. Invest. Drugs, vol. 16, pp. 1159-1169, Aug. 2007.

130. Scott R.W., DeGrado W.F., Tew G.N., *"De novo designed synthetic mimics of antimicrobial peptides"*, Curr. Opin. Biotechnol., vol. 19, pp. 620-627, Dec. 2008.

131. Svenson J., Stensen W., Brandsdal B.O., Haug B.E., Monrad J., Svendsen J.S., *"Antimicrobial peptides with stability toward tryptic degradation"*, Biochemistry, vol. 47, pp. 3777-3788, Mar. 2008.

132. Porter E.A., Weisblum B., Gellman S.H., *"Mimicry of host-defense peptides by unnatural oligomers: antimicrobial β-Peptides"*, J. Am. Chem. Soc., vol. 124, pp. 7324-7330, Jun. 2002.

133. Debono M., Gordee R.S., *"Antibiotics that inhibit fungal cell wall development"*, Annu. Rev. Microbiol., vol. 48, pp. 471-97, 1994.

134. Maget-Dana R., Ptak M., *"Interactions of surfactin with membrane models"*, Biophys. J., vol. 68, pp. 1937-43, May 1995.

135. Lohan S., Bisht G.S., *"Small cationic antimicrobial peptidomimetics: emerging candidate for the development of potential anti-infective agents"*, Curr. Pharm. Des. Vol. 19, pp. 5809-5823, 2013.

136. Wessolowski A., Bienert M., Dathe M., *"Antimicrobial activity of arginine- and tryptophan-rich hexapeptides: the effects of aromatic clusters, D-amino acid substitution and cyclization"*, J. Pept. Res., vol. 64 pp. 159-169, Oct. 2004.

137. Kondejewski L.H., Lee D.L., Jelokhani-Niaraki M., Farmer S.W., Hancock R.E.W., Hodges R.S., *"Optimization of microbial specificity in cyclic peptides by modulation of hydrophobicity within a defined structural framework"*, J. Biol. Chem., vol. 277, pp. 67-74, Jan. 2002.

138. Auvynet C., Rosenstein Y., *"Multifunctional host defense peptides: Antimicrobial peptides, the small yet big players in innate and adaptive immunity"*, FEBS J., vol. 276, pp. 6497-6508, Nov. 2009.

139. Wimley W.C., *"Describing the mechanism of antimicrobial peptide action with the interfacial activity model"*, ACS Chem. Biol., vol. 5, pp. 905-917, Oct. 2010.

140. Ahn M., Murugan R.N., Jacob d B., Hyun J.K., Cheong C., Hwang E., Park H.N., Seo J.H., Srinivasrao G., Lee K.S., Shin d S.Y., Bang J.K., *"Discovery of novel histidine-derived lipo-amino acids: Applied in the synthesis of ultra-short antimicrobial peptidomimetics having potent antimicrobial activity, salt resistance and protease stability"*, Eur. J. Med. Chem., vol. 68, pp. 10-18, Oct. 2013.

141. Murugan R.N., Jacob B., Kim E.H., Ahn M., Sohn H., Seo J.H., Cheong C., Hyun J.K., Lee K.S., Shin b S.Y., Bang J.K., *"Non hemolytic short peptidomimetics as a new class of potent and broad-spectrum antimicrobial agents"*, Bioorg. Med. Chem. Lett., vol. 23 pp. 4633-4636, Aug. 2013.

Publications:

1. Sandeep Lohan, Swaranjit Singh Cameotra, Gopal Singh Bisht. Antibacterial evaluation of structurally amphipathic, membrane active small cationic peptidomimetics: Synthesized by incorporating 3-amino benzoic acid as peptidomimetic element. ***Eur. J. Med. Chem.*** 2014, 83, 102-115. (Impact factor-3.49)
2. Sandeep Lohan, Jitender Monga, Swaranjit Singh Cameotra, Gopal Singh Bisht. In vitro and in vivo Antibacterial Evaluation and Mechanistic Study of Ornithine Based Small Cationic Lipopeptides against Antibiotic Resistant Clinical Isolates. ***Eur. J. Med. Chem.*** DOI: 10.1016/j.ejmech.2014.06.039. (Impact factor-3.49)
3. Sandeep Lohan, Arneesh Kalanta, Praveen Sonkusre, Swaranjit Singh Cameotra, Gopal Singh Bisht. Development of novel membrane active lipidated peptidomimetics active against drug resistant clinical isolates. ***Bioorg Med. Chem***. 2014, 22, 4544-4552. (Impact factor-2.9)
4. Sandeep Lohan, Swaranjit Singh Cameotra, Gopal Singh Bisht. Systematic study of non-natural short lipopeptides as broad-spectrum antimicrobial agents. ***Chem. Biol. Drug Des.*** 2013, 82(5), 557-566. (Impact factor-2.46)
5. Sandeep Lohan, Gopal Singh Bisht. Small cationic antimicrobial peptidomimetics: Emerging candidate for the development of potential anti-infective agents. ***Curr. Pharm. des.*** 2013, 19(32), 5809-5823. (Impact factor-3.31)
6. Sandeep Lohan, Gopal Singh Bisht. Recent approaches in design of peptidomimetic for antimicrobial drug discovery research. ***Mini Rev. Med. Chem.*** 2013, 13(7), 1073-1088. (Impact factor-2.86)
7. Sandeep Lohan, Jitender Monga, Chetan Singh Chauhan, Gopal Singh Bisht. *In Vitro* and *In Vivo* Evaluation of Small Cationic Abiotic Lipopeptides as Novel Antifungal Agents. ***Chem. Biol. Drug Des.*** 2015 (Impact factor-2.46)

Patent filed:

- Gopal Singh Bisht and Sandeep Lohan. "Non-Natural Short Cationic Antimicrobial Lipopeptides" IN Patent 1161/DEL/2014.

Conference:

- Sandeep Lohan and Gopal Singh Bisht. Design and Synthesis of Small Lipopeptides as Broad-Spectrum Antimicrobial Agents. 7^{th} Annual Convention of ABAP & International Conference (Oct, 2013, Delhi university, New Delhi, India).